"SYNTHESIS, CHARACTERIZATION, ELECTROCHEMICAL AND ANTITUMOUR STUDIES OF METAL CHELATES OF SCHIFF BASES DERIVED FROM CURCUMINOID ANALOGUES"

Thesis Submitted to the Faculty of Science,

*University of Calicut in partial fulfillment of the requirements for the Degree of **Doctor of Philosophy** in Chemistry*

By

RAINA JOSE CHERAPPANATH

DEPARTMENT OF CHEMISTRY

CHRIST COLLEGE (AUTONOMOUS)

UNIVERSITY OF CALICUT

IRINJALAKUDA, THRISSUR, KERALA – 680125, INDIA

MARCH 2018

CERTIFICATE

This is to certify that the thesis entitled "Synthesis, Characterization, Electrochemical and Antitumour Studies of metal chelates of Schiff bases derived from curcuminoid analogues" is an authentic record of the research work carried out by RAINA JOSE CHERAPPANATH, under my supervision in partial fulfillment of the requirements for the Degree of Doctor of Philosophy in Chemistry of the University of Calicut, and further that no part thereof has been presented before for any other Degree.

Dr. JOHN .V. D

(Supervising Teacher)

Institutional Animal Ethical Committee
(Reg. No. 149/PO/Rc/S/1999/CPCSEA)
Amala Cancer Research Centre

RESEARCH DIRECTOR &   AMALANAGAR - 680 555, THRISSUR
CHAIRMAN, IAEC   : DR. RAMADASAN KUTTAN, Ph.D.   KERALA, INDIA
                                                                    21.06.2017

Ref :   Date:

CERTIFICATE

The Institutional Animal Ethics Committee of Amala Cancer Research Centre (No.149/PO/Rc/S/1999/CPCSEA) unanimously approved the animal experiments of the Ph.D. Thesis work of **Raina Jose Cherappanath**, Research Scholar, Christ College, Irinjalakuda, entitled **"Metal Chelates of Curcuminoid Analogues And Their Biological Applications"** (Approval No.ACRC/IAEC/17-01[2]) carried out under the guidance of Dr. Ramadasan Kuttan.

Dr. Jose Padikkala, Ph.D.

Secretary, IAEC

SECRETARY
Institutional Animal Ethical Committee
Reg. No. 149/1999/CPCSEA
Amala Cancer Research Centre

DECLARATION

I, RAINA JOSE CHERAPPANATH hereby declare that the thesis, entitled "Synthesis, Characterization, Electrochemical and Antitumour Studies of metal chelates of Schiff bases derived from curcuminoid analogues" submitted to the University of Calicut, in partial fulfillment of the requirements for the Degree of Doctor of Philosophy in Chemistry, is an authentic record of the research work carried out by me under the supervision and guidance of Dr. John. V. D, Associate Professor (Rtd), Department of Chemistry, Christ College, Irinjalakuda, Kerala and further that no part thereof has been presented before for any other Degree.

RAINA JOSE CHERAPPANATH

ACKNOWLEDGEMENT

Joseph for their enthusiastic support, constructive guidance that made me confident in taking up the challenging field of research.

A word of thanks to the spirit of truth for the providential care bestowed on me during the investigation.

.

<div align="right">

RAINA JOSE CHERAPPANATH

</div>

DEDICATED

TO

MY FAMILY

PREFACE

Schiff bases and their metal complexes have been largely explored because of their varied range of applications including catalysts, medicine, crystal engineering and as anti-corrosion agent. Schiff bases possess these varied properties due to their synthetic flexibility, selectivity and the sensitivity towards the central metal atom along with the structural similarities with natural biological compounds and also due to the presence of azomethine or imine group. Schiff bases derived from 1,7 diaryl heptanoids (curcuminoids) possess many enhanced properties that showed by curcumins. Structurally curcuminoids are 1,7- diaryl heptanoids .They are a group of naturally occurring 1,3 – diketones in which diketo function is directly attached to olefinic groups. The Schiff bases derived from the aryl azo derivatives of curcuminoids contain aromatic rings, electron donating centers like nitrogen, oxygen atoms and the azomethine linkage which all make it ideally suited to act as corrosion inhibitors and biologically active compounds. Literature review has revealed the enhanced corrosion inhibition efficiency of Schiff bases with more number of electron donating centers and aromatic moieties. Their structure is ideally suited to act as chelating ligands towards a variety of metals and to form complexes similar to diketones. Curcuminoids have been reported to possess a wide spectrum of biological actions such as anti-inflammatory, antioxidant, anticancer, antidiabetic, antiallergic, antiviral, antiprotozoal, antibacterial and antifungal activities. The utility of curcumin is limited by its colour, lack of water solubility and relatively low invivo bioavailability. Literature review has revealed the enhanced biochemical activities of Schiff bases derived from curcuminoids and their metal complexes especially as cytotoxic, agents. The present study is mainly on the synthesis and characterization of a series of Schiff bases derived from the aryl azo derivatives of curcuminoid analogues (1,7-diaryl heptanoids) and their metal complexes with Cu(II) ,Zn(II) and Ni(II). The anti-corrosive activities and antitumour activities of the synthesized Schiff

base compounds and their metal complexes were also studied. The thesis is divided into four parts.

Part I. Introduction

Schiff bases played an important role in development of coordination chemistry and were involved as vital point in the development of corrosion inhibitors and inorganic biochemistry. The Schiff bases derived from synthetic curcuminoid analogues with chemical modifications of curcumin have been studied intensively to identify compounds with similar or enhanced properties of curcumin. Ten Schiff bases derived from the aryl azo derivatives of curcuminoid analogues were synthesized in the present work. In the synthesized compounds the phenyl ring part in natural curcumin has been modified and also introduced new azomethine linkage. The phenyl ring part has been substituted with heterocyclic rings, polynuclear rings, substituted polynuclear rings, trisubstituted and disubstituted phenyl rings with substituents different from that of natural curcumin. The structural and spectral properties were studied by UV, IR, ^{1}H NMR,^{13}C NMR,2D-COSY NMR, Mass Spectral techniques etc. Research in the field of coordination chemistry of Schiff bases has gained considerable momentum in recent years. Schiff bases with more number of electron rich centers are found to possess high corrosion inhibition efficiency. So the electrochemical studies were performed to investigate the corrosion inhibition efficiency of the five synthesized Schiff bases. It has also been revealed that the biological significance of the Schiff base molecules is enhanced by complex formation with metal ions. Schiff bases are excellent chelating ligands which can bind with metal ions to form stable metal complexes. Metal complexation of these Schiff bases has led to effective changes in their biological activities including antitumour activity. In the present investigation transition metal ions namely Cu^{2+}, Zn^{2+} and Ni^{2+}were complexed with the synthesized Schiff bases. The

biological activities investigated include the cytotoxic activity and the antitumour activity of synthesized compounds.

Part II. Literature Review

This part includes the review of literature related with the anticorrosive and biological studies of Schiff bases and its metal chelates. The corrosion inhibition property of Schiff bases against mild steel corrosion and studies about the different Schiff base inhibitors are well said. The biological activities of Schiff bases like anti-inflammatory, antioxidant, anti-bacterial, antiviral, antitumour activity etc. are discussed in this part. The clinical activities of the curcuminoids from which Schiff bases have been derived have also discussed. The importance of Schiff bases derived from curcuminoid analogues and the metal complexes as biologically significant agents have been well established. Studies related with the cytotoxic nature of curcuminoid analogues and their metal chelates also have been extensively discussed in this part. The enhanced pharmacological significance of the compounds due to complexation has also been revealed in this part. This part explains the necessity of synthesis of Schiff bases of 1,7 diaryl heptanoids (curcumin analogues) and their metal chelates and their anticorrosive and biological significance.

Part III. Materials, Methods and Experimental techniques

This part is a general description on various chemicals and methods employed, instruments used and various experimental techniques. The methods used for the synthesis of Schiff bases, their transition metal chelates and purification of compounds is given. Various spectral techniques involved in characterization of the compounds have been explained. The corrosion studies carried out include weight loss method and electrochemical methods like electrochemical impedance spectra and Tafel polarization techniques. Materials and techniques used in the studies are detailed. The biological studies conducted include Invitro cytotoxic study, Invivo antitumour study and effect of compounds on solid tumour. Materials, cell lines, animals, chemicals, methods etc. employed in the studies are given.

Part IV. Synthesis, Characterization, Electrochemical and Antitumour studies of metal chelates of Schiff bases derived from curcuminoid analogues

This part is divided into three chapters.

Chapter I. The chapter deals with the Synthesis and Characterization of Schiff bases and their Transition metal chelates.

Section I: Synthesis and characterization of Schiff bases derived from aryl azo derivative of 1,7-bis(thiophen-2-yl)-hepta-1,6-diene-3,5-dione and 1,7-bis(3 methyl thiophen-2-yl)-hepta-1,6-diene-3,5-dione with ethylene diamine; [TEDTDH] 1a and [MTEDTDH] 1b. They were characterized by UV, IR, ^{1}H NMR, ^{13}C NMR, 2D COSY and Mass spectral techniques.

Synthesized Transition metal chelates of 1a and 1b with Cu(II), Zn(II) and Ni(II) and were also characterized by various spectral techniques.

Section II: Synthesis and characterization of Schiff base ligands derived from aryl azo derivatives of 1,7-bis(2-methyl phenyl)-hepta-1,6-diene-3,5-dione and 1,7-bis(2-hydroxy

phenyl)-hepta-1,6-diene-3,5-dione with ethylene diamine ; [MEDTDH] 2a and [HEDTDH] 2b.They were characterised by various spectral techniques.

Synthesis and Characterization of Transition metal chelates of 2a and 2b with Cu(II), Zn(II) and Ni(II).The synthesized metal chelates were also characterized by various spectral techniques

Section III: Synthesis and characterization of Schiff bases derived from aryl azo derivatives of 1,7-bis(aryl)hepta-1,6-diene-3,5-diones with di & trisubstituted phenyl ring and ethylene diamine [EHEDTDH] 3a, [DHEDTDH] 3b and [TMEDTDH] 3c. The synthesized Schiff bases were characterised by various spectral techniques

Synthesized Transition metal chelates of Schiff bases 3a, 3b and 3c with Cu(II),Zn(II) and Ni(II).and used various spectral techniques for characterization.

Section IV: Synthesis and characterization of Schiff bases derived from aryl azo derivatives of curcuminoid analogues with naphthyl and substituted naphthyl rings and ethylene diamine [NEDTDH] 4a, [MNEDTDH] 4b and [HNEDTDH] 4c. Various spectral techniques were used for their characterization.

Synthesis and Characterization of Transition metal chelates of 4a, 4b and 4c with Cu(II),Zn(II) and Ni(II).They were also characterized by various spectral techniques

Chapter II. This chapter deals with the corrosion studies of Schiff bases

Section I: Corrosion inhibition studies of Schiff bases TEDTDH, DHEDTDH, NEDTDH, HEDTDH, and TMEDTDH on mild steel in 1M hydrochloric acid medium.

The corrosion inhibition studies were carried out using Weight loss method, Electrochemical impedance spectra and Potentiodynamic polarisation techniques. The surface morphology was studied using SEM, EDX and AFM analysis.

Section II: Corrosion inhibition studies of Schiff bases TEDTDH, DHEDTDH, NEDTDH, HEDTDH, and TMEDTDH on mild steel in 0.5M sulphuric acid medium.

The corrosion inhibition investigation of the Schiff bases was carried out using Weight loss method, Electrochemical impedance spectra and Potentiodynamic polarisation techniques. The surface morphology was studied using SEM, EDX and AFM analysis.

Chapter III. This chapter deals with the biological studies of Schiff bases

Section I: Antitumour studies of bis(1,7-di(thiophen-2-yl)-4-(phenyl-hydrazono)-hepta-1,6-diene-3,5-dione)ethylenediimine and bis(1,7-di(3-methyl thiophen-2-yl)-4-(phenyl-hydrazono)-hepta-1,6-diene-3,5-dione)ethylenediimine and the transition metal chelates. The studies include invitro cytotoxic study of Schiff base ligands and their metal complexes [Cu(II), Zn(II) and Ni(II)] by Trypan blue dye exclusion method towards DLA and EAC cell lines. *In vivo* antitumour studies were conducted in mice with the ligands 1a and 1b and their Cu(II) complexes. The effect of ligands 1a and 1b and their copper complexes on solid tumour development in mice were also studied

Section II: Antitumour studies of bis(1,7-di(2-methyl phenyl)-4-(phenyl-hydrazono)-hepta-1,6-diene-3,5-dione)ethylenediimine and bis(1,7-di(2-hydroxy phenyl)-4-(phenyl-hydrazono)-hepta-1,6-diene-3,5-dione)ethylenediimine and the transition metal chelates. The studies include invitro cytotoxic study of Schiff base ligands and their metal complexes [Cu(II),Zn(II) and Ni(II)]by Trypan blue dye exclusion method. *In vivo* antitumour studies were conducted in mice with the ligand bis(1,7-di(2-hydroxy phenyl)-4-(phenyl-hydrazono)-hepta-1,6-diene-3,5-dione)ethylenediimine (**2b**) and its Cu(II) & Ni(II) complexes. The ligands 2a and 2b and their copper complexes were used to find the effect on solid tumour development in mice.

Section III: Cytotoxic and Antitumour studies of bis(1,7-di(3-ethoxy-4-hydroxy phenyl)-4-(phenyl-hydrazono)-hepta-1,6-diene-3,5-dione)ethylenediimine (3a), bis(1,7-di(2,4-dihydroxy phenyl)-4-(phenyl-hydrazono)-hepta-1,6-diene-3,5-dione)ethylenediimine (3b) and bis(1,7-di(3,4,5-tri methoxy phenyl)-4-(phenyl-hydrazono)-hepta-1,6diene-3,5-dione)ethylenediimine (3c) and the transition metal chelates. The studies include invitro cytotoxic study of ligands and their metal complexes [Cu(II),Zn(II) and Ni(II)] by Trypan blue dye exclusion method towards DLA and EAC cell lines. *In vivo* antitumour studies were conducted in mice with the ligands bis(1,7-di(3-ethoxy-4hydroxy phenyl)-4-(phenyl-hydrazono)-hepta-1,6-diene-3,5-dione)ethylenediimine and bis(1,7-di(3,4,5-tri methoxy phenyl)-4-(phenyl-hydrazono)-hepta-1,6-diene-3,5-dione)ethylenediimine and their Cu(II) complexes. The ligand 3c and its copper complex were used to find the effect on solid tumour development in mice

Section IV: Cytotoxic and Antitumour studies of Schiff bases derived from the aryl azo derivative of curcuminoid analogues with substituted naphthyl rings and their transition metal chelates. The studies include invitro cytotoxic study of ligands and their metal complexes [Cu(II), Zn(II) and Ni(II)] by Trypan blue dye exclusion method towards DLA and EAC cell lines. *In vivo* antitumour studies were conducted in mice with the ligands bis(1,7-di(2 - methoxy naphthyl)-4-(phenyl-hydrazono)-hepta- 1,6-diene-3,5-dione) ethylenediimine (4b) and bis(1,7-di(2-hydroxy naphthyl)- 4 - (phenyl - hydrazono) – hepta - 1, 6 – diene - 3, 5 - dione) ethylenediimine (4c) and their Cu(II) complexes

ABBREVIATIONS

EDX	––	Energy Dispersive X-ray
SEM	––	Scanning Electron Microscope
CPF	––	Controlled Permeability Formwork
CPE	––	Constant Phase Element
EIS	––	Electrochemical Impedance Spectroscopy
OCP	––	Open Circuit Potential
DMC	––	Demethoxy curcumin
BDMC	––	BisDemethoxy curcumin
SIM	––	Selected ion monitoring
PBS	––	Phosphate Buffered Saline
SAR	––	Structure Activity Relationship
DMSO	––	Dimethyl Sulphoxide
EAC	––	Ehrlich Ascites Carcinoma
COSY	––	Correlation Spectroscopy
DLA	––	Daltons Lymphoma Ascites
ILS	––	Increase in life span

CONTENTS

PART-I

GENERAL INTRODUCTION

GENERAL INTRODUCTION

Schiff bases refers to the compounds that carry azomethine (R-CH=NR') or imine $R_2C=NR'$ (R' $\neq$ H) functional group and which is named after Hugo Schiff. The term Schiff base is generally applied to the compounds when they are being used as ligands to form coordination complexes with different metal ions. Such complexes do exist naturally but a greater part of Schiff bases are synthetic and have a variety of applications.

Schiff bases can be synthesized by the nucleophilic addition of an aromatic or aliphatic amine and carbonyl compound[1] , resulting in the formation of a hemiaminal, followed by the dehydration to yield an imine. Schiff bases commonly acts as enzymatic intermediates. The metabolism of the amino acids and fructose 1,6-bisphosphate aldolase enzyme catalyzed reaction during glycolysis and are examples in which the substrate forms a Schiff base with the enzyme. Schiff bases are important ligands in coordination chemistry as it exhibits pi-acceptor properties due to the presence of basic imine nitrogen. Schiff bases and their metal complexes have been largely explored because of their varied range of applications including catalysts [2], medicine[3,4], , crystal engineering[5] and as anti-corrosion agent[6]. Schiff bases have been reported to show a variety of biological activities like antifungal[7], antibacterial[8], clinical and herbicidal activities by virtue of the azomethine linkage. Furthermore, Schiff bases also act as cytotoxic agents[9], pigments, dyes[10] and polymer stabilizers[10]. Schiff bases are researched widely due to their synthetic flexibility, selectivity and the sensitivity towards the central metal atom along with

the structural similarities with natural biological compounds and also due to the presence of azomethine or imine group[11]

Schiff base organics are extensively studied as corrosion inhibitors against mild steel corrosion in acidic medium. Most of the efficient corrosion inhibitors are the organic compounds containing sulphur, nitrogen and phosphorus atoms in their structure[12,13]. Heteroatoms like nitrogen, oxygen and sulphur are capable of forming coordinate covalent bond with metal atom owing to the lone pair of electrons present in them and thus acting as corrosion inhibitor. Molecules with pi-bonds also normally show good inhibitive properties due to the interaction of the orbital with the metal surface. Schiff base compounds with general formula R-CH=NR' have both the above mentioned features, along with their structure which may then give rise to potential inhibitors.

In the recent years, the organic compounds with Schiff bases as integral part of their structures, have gained much attention because of unique biological properties exhibited by such compounds. Schiff base compounds have increased prominence in the pharmaceutical and medical fields due to a broad spectrum of biological functions such as analgesic[3], anti-inflammatory[14], anticonvulsant[15] , antimicrobial[8], antitubercular[16] , antioxidant[2] ,anticancer[9,4] , anthelmintic[7] and so forth. Schiff bases are considered as a very important class of organic compounds because of their ability to form complexes with transition metal ions and of their pharmacological properties[16]. Transition metal complexes containing Schiff bases have been of great interest over the last years, largely because of its various applications in biological processes and potential applications in designing new therapeutic agents. But still there is need to explore intensively the biological properties and the corrosion inhibition efficiencies of Schiff bases

Curcuminoids and Schiff bases derived from curcuminoid Analogues

Curcumin is a natural polyphenolic compound which is responsible for the yellow colour of the turmeric. Turmeric (Curcuma longa) a traditional Indian medicinal plant, is a perennial herb of ginger family, Zingaberacea[17]. The rhizome of this plant which is also referred to as the "root" is the most valuable part of the plant. It is used as colouring agent for food and textiles, as dietary spice and for a wide variety of medicinal purposes. Turmeric is widely used in traditional Indian medicine to cure anorexia, biliary disorders, diabetic wounds, cough, rheumatism, hepatic disorders and sinusitis. Turmeric contains three different kinds of curcuminoids namely curcumin, demethoxy curcumin and bisdemethoxy curcumin. Structurally they are linear 1, 7-diaryl- 1,6-heptadiene-3,5-diones which exist in rapid equilibrium with its tautomeric enol form. Among these, Curcumin (diferuloyl methane) makes up approximately 90% of the curcuminoid content in turmeric. Vogel in 1842 isolated curcuminoids from turmeric[18] and the structure of curcumin was first explained by Lampe and Milobedeska in 1910.

Most of the medicinal activities related with curcumin are due to its ability to suppress inflammation. Curcumin has been shown to be very effective in acute as well as chronic models of inflammation. Laboratory studies have identified a number of different molecules involved in inflammation that are inhibited by curcumin including, lipooxygenase, phospholipase, leukotrienes, cyclooxygenase COX-2, prostaglandins, thromboxane, collagenase, nitric oxide, hyaluronidase, elastase, interferon-inducible protein, MCP-1, tumour necrosis factor, and interleukin-12[17] (Nita Chainani-wu etal 2003). The anticarcinogenic activity of curcumin can also be attributed to its direct antioxidant and free radical scavenging properties as well as its ability to indirectly increase glutathione levels, thereby assisting in detoxification of mutagens and carcinogens. The antioxidant activity of curcumin could be mediated through antioxidant enzymes such as catalase, superoxide dismutase, and glutathione peroxidase. The administration of curcumin through the diet suppresses the development of chemically induced cancers. On the other side, curcumin is limited in its medicinal efficacy due to its poor water solubility and its low absorption level in the gastrointestinal tract. The low bioavailability of the curcumin is a major concern and can be improved by the use of structural analogues of curcumin. A wide range of curcumin derivatives were synthesized in order to overcome the pharmacokinetics limitations, preserving the same safety profile[19].

Generally Schiff bases are reported to have greater solubility and greater bioavailability. A large number of Schiff bases of curcuminoid analogues were synthesized and their biological activities were reported earlier. Schiff bases derived from curcuminoid analogues are found to show much more anti-cancer

efficiency than other Schiff bases. The soluble nature of Schiff bases makes it more advantageous in anti-corrosive studies and anti tumour studies.

In the present study, we synthesized Schiff bases derived from aryl azo derivatives of ten curcuminoid analogues and their different metal complexes. The Pabon method was used for synthesizing 1, 7-diaryl- 1,6-heptadiene-3,5-diones. Different aromatic aldehydes were condensed with acetyl acetone and B_2O_3 in presence of n-butyl amine and tri(sec-butyl)borate. The Schiff bases of the synthesized curcuminoid analogues were prepared by treating them with benzene diazonium salt at $0^{o}C$ and then condensing with ethylene diamine. The structural and spectral properties of the series of Schiff bases of curcumin analogues were studied by UV, IR, ^{1}H NMR, ^{13}C NMR, Mass Spectral techniques etc. Spectral analysis established that the newly synthesized Schiff bases derived from aryl azo derivatives of 1,7-diaryl heptanoids exist in the imine hydrazone form.

The anticorrosive nature of the newly synthesized Schiff bases were investigated using weight loss method, potentiodynamic polarization studies and electrochemical impedance spectroscopy techniques. The surface analysis of the mild steel used for corrosion analysis was done using Atomic Force Microscopy, SEM analysis and EDX spectra.

Biological activities investigated in the present work include cytotoxic activity and antitumour nature against DLA and EAC cells of Schiff bases of aryl azo derivatives of curcumin analogues.

Applications of Schiff bases as corrosion inhibitors

Corrosion

Corrosion usually refers to the destructive and accidental attack of a metal, which is an electrochemical process and generally begins at the surface. The term corrosion originates from the Latin word *corrodere* meaning gnawing to pieces. Metallic corrosion affects the national economy and also creates an impact on the environment. Most of the industries employ metals or their ores (such as mild steel, aluminum, copper and zinc) in the construction of their installations. In most of the cases, these metals used are exposed to aggressive medium and are susceptible to corrosion. Corrosion can be defined in general terms or in specific terms depending upon the perspective from which it is defined. In general corrosion is defined as an electrochemical process which involves degradation of materials in a corrosive environment. During corrosion the dissolution of metal occurs at anode, generating metal ions and electrons. These electrons move to the cathode via an electronic path through the metal, simultaneously the positive ions move from anode to the cathode by ionic current path. The positively charged ions get reduced by these electrons at cathode. Thus in the metal during corrosion a closed electrical circuit is functioning. The general corrosion accounts for the greatest loss of metal on a tonnage basis. The material loss per unit area in unit time (i.e. the rate of anode and cathode reactions) is defined as the corrosion rate[20].

In nature, most metals occur in a chemically combined state known as ore. All metals (except noble metals) exist in nature as their oxides, hydroxides, carbonates, silicates, sulphates etc., which are thermodynamically more stable low-energy states[21]. The pure metals in their elemental form are extracted from these ores after supplying a large amount of energy. Thermodynamically, as a result of this

metallurgical process, metals attain higher energy levels, decrease in their entropies occur and they become more unstable. This arises as the driving force behind corrosion. It is a natural tendency to go back to a state of lower energy, to a combined state. The metals with higher oxidation state exhibit a tendency to recombine with the elements present in the environment for attaining a stable state with a decrease in free energy.

The most commonly used structural metals are iron and steel. Steel is an alloy with elements C, Mn, Si, S, and P. The corrosion of steel reinforcement is seen in marine structures, chemical manufacturing plants, bridge decks, parking structures and other structures exposed to chlorides. The consequent extensive study on factors contributing to steel corrosion has increased our understanding of corrosion, especially regarding the role of chloride ions. Corrosion in industries is often commenced by industrial processes like acid wash, pickling, etching and others. The corrosion of a metal or an alloy can be determined either by direct weight loss measurements in a given environment or via measuring the changes in physical, electrical, or electrochemical properties with time. The cost of replacing metals affected with corrosion is often extortionate and economically unacceptable.

Therefore, industries have adopted several methods to prevent corrosion of metals such as anodic/cathodic protection, painting, galvanizing and electroplating. In this scenario, the application of corrosion inhibitors has proven to be one of the most efficient methods.

Factors Affecting Corrosion

The extent of corrosion mainly depends on the nature of the metal, nature of the corroding environment and nature of the electrolyte. The purity of the metal, the passivity, the position of metal in the galvanic series, the nature of oxide film on the metal surface, the flow rate of the electrolyte, the concentration of aggressive ions in the electrolyte all plays important role in corrosion. The secondary factors affecting the outcome of the corrosion reaction are temperature, pH, associated fluid dynamics, concentrations of dissolved oxygen and dissolved salt. Another factor causing the corrosion of metals and alloys is acid rain, which is usually caused by the industrial burning of fuels containing sulphur and nitrogen oxides.

Corrosion Prevention Methods

Different techniques are there to slow down the corrosion damage to metallic structures which are exposed to the acids, weather, sea water, or other corrosive environments. Selecting a material which does not corrode in the actual environment is the most important criteria. When changing the material is not possible, changing the environment to prevent transport of oxygen and water to the metal surface often using corrosion inhibitors is the next most reasonable prevention method. Surface treatments like painting, plating and cathodic protection are the common techniques used to prevent corrosion.

Applied Coatings

Corrosion can be prevented by coating the metal with paint, oil, grease, varnish or with non-corrosive metals. Different methods are there for coating the metal with non-corrosive metal like galvanizing, tinning, electroplating, anodizing and alloying.

Reactive coatings

The electrochemical reactions on surfaces of metals can be prevented by coating corrosion inhibitor chemicals on metal surface which form an electrically insulating/chemically impermeable coating on the exposed areas. Chemicals like phosphates, chromates, salts in hard water, polyaniline, a wide range of long chain organic molecules with ionic end groups which resemble surfactants and other conducting polymers are using for this. The advantage of this reactive coating method is that it makes the metal less sensitive to scratches or defects in the coating and there is also a possibility of adding extra inhibitors whenever the bare surface gets exposed. Recent studies have shown that the Zinc chromate and other anti-corrosive, anti-rust primer agents are highly toxic and carcinogenic.

Bio-film coatings

The application of bacterial films of certain species on the metal surface in highly corrosive environment is a recent method of corrosion inhibition. The corrosion resistance of the metal is increased outstandingly in this method. Interestingly, it is reported that mild steel corrosion due to sulphate-reducing bacteria can be prevented by the use of antimicrobial biofilms[22]

Galvanizing

This method is commonly used to protect iron or steel from corrosion. Galvanization is a process of giving a thin coating of zinc on iron by dipping it in molten zinc.

Electroplating

Electroplating is done to cover one metal with a more active metal to prevent from corrosion. A thin layer of metal is deposited on the substrate metal in an electrolytic bath which is a solution of salt of metal to be deposited and water. Silver plated spoons, gold plated jewellery are examples.

Anodizing

Anodizing is the process of changing an anode into a cathode by bringing a more active anode in contact with it. The electrochemical conditions during anodizing must be adjusted such that a strong film of oxide, harder than the usual surface forms over copper and aluminium. Due to the resilient nature, it must be cleaned frequently to prevent edge staining.

Controlled permeability formwork (CPF)

This is a method of preventing corrosion of the reinforcement, by naturally improving the strength of the cover, during concrete placement. The effects of abrasion, frost, chlorides and carbonation can be lessened with this method[22].

Cathodic Protection

Cathodic protection is the most effective method among corrosion preventive measures used for reinforced concretes. Two types of cathodic protection are sacrificial anode protection and impressed current cathodic protection. Metal

anodes are introduced to the electrolytic environment, to sacrifice themselves (corrode) in order to protect the cathode. Metals that have the most negative electro-potential like zinc, aluminium or magnesium are generally used as sacrificial anodes and the current flows from anode to cathode. Sacrificial anode attached to the hull of a ship is a case of sacrificial protection. Impressed current cathodic protection is used in case of large structures. High silicon cast iron is an example.

Impressed current cathodic protection (ICCP)

Impressed current cathodic protection is used in case of large structures. This method use anodes which are connected to a DC power source. Anodes for the ICCP are composed of several specialized materials systems which are solid rod and tubular in shape. These include high silicon cast iron, graphite and mixed metal oxide/ niobium coated /platinum coated titanium rod & wires[23].

Anodic protection

Anodic protection is the opposite of cathodic protection .Impressed anodic current is suitable for metals that show passivity (stainless steel). This type of protection is used in aggressive mediums, like solution of sulphuric acid.

Corrosion inhibitors

Corrosion inhibitors are chemicals that get adsorbed on metal surface and form a coating, often a passivation layer, thus inhibiting the access of the corrosive substance to the metal. The major industries where corrosion inhibitors used are petroleum refining, oil and gas exploration, chemical production and water treatment plants. This is a vital method of prevention of corrosion particularly in

hydrochloric acid and sulphuric acid mediums, which are used for the pickling of aluminium and electro-chemical etching. The protective inhibitor layer affects the anodic or cathodic polarization behaviour, decreases the diffusion of chloride and sulphate ions to the metal surface and thereby increases the resistance of the metal surface.

Numerous studies have been carried out in search of effective non-toxic green corrosion inhibitors. They usually comprise organic compounds containing functional group hetero atoms such as nitrogen, phosphorous, oxygen and sulphur. Heterocyclic compounds are reported as good corrosion inhibitors. The initial step in the corrosion inhibition of metals in acid solutions consists of adsorption of the inhibitor on the oxide free metal surface followed by retardation of cathodic and/or the anodic electrochemical corrosion reactions[24]. Hamdy and his coworkers reported that the inhibition of mild steel corrosion in hydrochloric acid solution can be effectively done by different triazole derivatives[25](Hamdy et al., 2007) and investigated the suitability of the use of the triazole based inhibitors in cooling systems. The recent works have shown that the compounds containing imidazoline group acts as good corrosion inhibitors than the amides[26].The high inhibition efficiency of the imidazoline group may be attributed to the presence of the iminic double bond (N=C) and the cyclic structure of the imidazoline. Reports revealed that quinoline and benzaldehyde derivatives, benzotriazoles and their derivatives, quaternary imidazoline derivative, alkaloids, pyridine bases, quaternary salts of benzenethiol, imidazole azo derivatives, derivatives of toluidenes and chloroanilines, triazoles, thiourea etc. possess clear inhibitory action.[27-28]

The inhibition efficiency of the Schiff base can be attributed to its molecular structure, presence of electronegative atoms (such as N, S and O), unsaturated

bonds, electronic properties as well as corrosive environment. The main two factors influencing the selection of an efficient corrosion inhibitor are the geometric and electronic properties of the compound. They are inter dependent of each other and therefore should be considered together while selecting a good inhibitor. Sometimes a molecule with less planar geometry but with more electron donor centres are preferred than a molecule with high planarity but with less electron donating atoms. Based on this Soliman et al; (2014) synthesized a new Schiff base compound 4-hydroxy-3-(3-phenyl-allylideneamino)-benzene sulphonic acid2-[2-(2-{2-[2-92-hydroxy-ethoxy)-ethoxyl]-ethoxy}-ethoxy)-ethoxy]-ethylether(PAAB) and studied its anticorrosive activity against 1.0M HCl and reported that this compound inhibited the corrosion in HCl environment[13].

The invention of new and improved green corrosion inhibitors has now become a challenging mission since corrosion is one among the key problems faced by many industrial, research and medical fields. Most of the well-known corrosion inhibitors are organic molecules, containing hetero atoms (electron donating centers) like oxygen, nitrogen, sulphur etc. These inhibitor molecules have electron donating centers which are able to form strong coordinate bond with metal surface. The presence of azomethine linkage along with the electron cloud on aromatic rings, presence of electronegative hetero atoms like oxygen, nitrogen, and sulphur in the Schiff base molecules make them efficient corrosion inhibitors. Even though the corrosion behaviour of various heterocyclic Schiff bases were studied earlier, the corrosion inhibition behaviour of Schiff bases derived from 1,7 diaryl heptanoids are scanty.

Inhibition properties of the 1,7 diaryl heptanoids (curcumin) based Schiff base may even help it to bind with the cancer cells to block its DNA from repair and thereby

functions as an anticancer drug, so that it can be used in medicinal field also as an anti-corrosive agent in the sterilization of medical endoscopes. The corrosion inhibition behavior of the compounds can be studied using weight loss method, electro chemical impedance spectra and potentiodynamic polarization techniques.

The present work comprises the investigation of the inhibition efficiency of five Schiff bases derived from curcuminoid analogues against mild steel corrosion in 1.0M HCl solution and 0.5M H_2SO_4 solution since no studies are reported on the anti-corrosive behaviour of these types of Schiff bases. The surface analysis of the mild steel used for corrosion studies was done using SEM, EDX and AFM analysis. The investigation of corrosion inhibition property of these compounds on mild steel is a subject of marked technological impact. The adsorption mechanism of these inhibitors on metal surface is studied by plotting different adsorption isotherms. Thermodynamic parameters like adsorption equilibrium constant (K) and free energy of adsorptions (ΔG^0) are also calculated from suitable adsorption isotherms. The corrosion inhibition efficiencies of the synthesized Schiff bases were also compared with that of parent compounds. The effect of temperature on the corrosion behaviour of the Schiff bases was evaluated to calculate the thermodynamic parameters such as activation energy, entropy and enthalpy.

Cancer chemo preventive effect of curcumin and Schiff bases derived from curcuminoid analogues

Cancer chemoprevention is defined as the use of natural or synthetic chemical agents to suppress, reverse or prevent carcinogenic advancement to cancer. Various dietary phytochemicals present in fruits and vegetables have been shown to possess a good cancer chemo preventive effect in both preclinical animal

models and human epidemiological studies[29] (Jong et al., 2013). Phytochemicals are biologically active nutritive chemical compounds present in plants and are responsible for the health promoting characteristics of various natural and functional foods. They have the ability to alter cell communication and DNA repair and to influence cells that can cause development of cancer and other diseases. These phytochemicals can prevent the initiation of carcinogenesis either by direct scavenging of reactive oxygen or nitrogen species or by the induction of cellular defense detoxifying/antioxidant agents. The curcumin, present in turmeric is a phytochemical substance which acts as a very effective agent in suppressing and blocking cancerous cells. Many attempts were made to study the cancer chemo preventive effect of turmeric against different types of tumours including stomach, and skin tumors induced by chemical carcinogens on animal systems. Animal models are an inevitable factor of cancer chemo preventive research. They provide an important path for identifying compounds which can be used effectively and safely in humans. They also give an information base for developing intervention trials in human beings. It was found that the inclusion of 5% curcumin in regular diet reduces the tumor incidence by 90%[30]. Curcumin has been shown to thwart the transformation, tumour initiation, tumour promotion, the invasion, angiogenesis and metastasis. Curcumin inhibits the proliferation of a wide variety of tumour cells, including B-cell and T-cell leukemia, epidermoid carcinoma, colon carcinoma and various breast carcinoma cells. This safe natural product mediates its effects through the modulation of several molecular targets including oncoproteins (c-Myc, Cyclin D1), tumour suppressor proteins (p53, p21WAF1), anti-apoptosis proteins (survivin, bcl-2) and transcription factors (NF-κB, β-catenin). The role of curcumin in inhibition of tumour cell proliferation and TPA

induced ODC activity and induction of phase II detoxification enzyme QR, shows that the anticarcinogenic effects of curcumin were contributed mainly by its antioxidant activity[31] (Tzeng-Horng et al., 2002). The antioxidant activity of the curcumin is attributed to the presence of β-diketone moiety, the phenolic hydroxyl and methoxyl groups and the conjugated double bonds of curcumin. Moreover, it has been shown that curcumin induces immuno-restoration in animal tumour systems, indicating that the inclusion of this natural product in therapeutic treatments against cancer should be beneficial for major proportion of cancer patients.

Recent works have shown that curcumin has a dose dependent chemopreventive effect in several animal tumour bioassay systems including intestinal[32],colon[33], esophageal[34],stomach and oral[35] carcinogenesis. It has been shown to reduce tumours induced by 7, 12 dimethyl benzaanthracene and benzapyrene[36,30] (Singh et al., 1998; Azuine and Bhide, 1992), on carcinogen-induced tumourogenesis in the fore stomach, tumour promotion induced by phorbol esters [37] (Huang et al., 1988) on mouse skin and N-ethyl-N′-nitro-N-nitrosoguanidine-induced duodenal tumours [33](Huang et al.,1994). Topical application of curcumin inhibits carcinogen induced DMBA-DNA adduct formation and the development of skin cancer. Curcumin also strongly inhibits proliferation and enhances apoptosis of HT-29 and HCT-15 human colon cancer cell lines[38] (Hanif et al., 1997). Dietary administration of curcumin enhances the activities of antioxidant and phase II-metabolizing enzymes involved in detoxification and production of reactive oxygen species. Very low rate of bowel tumour in Indians has been attributed to the practice of adding curcumin in Indian cuisines [39](Mohandas and Desai, 1999). Intake of synthetic curcumin through the diet during the promotion stage considerably inhibited the multiplicity

of invasive adenocarcinomas of the colon [40](Kawamori et al., 1999). Curcumin has been also demonstrated to induce apoptosis in prostate cancer cells [41] (Dorai et al.,2001).It has been shown to intervene the activities of a number of enzymes such as protein kinase C [42] (Liu et al., 1993), cyclooxygenase [43](Zhang et al., 1999), and protein tyrosine kinases [44] (Chen and Huang, 1998). Recently it has shown that curcumin is a potential candidate in the treatment of Head and neck squamous cell carcinoma (HNSCC) which is the sixth most common cancer worldwide[45] (Wilken et al., 2011).

 Snyder and co-workers have reviewed studies carried out by Mosely et al; on symmetrical 1,5-diaryl penta dienones which has indicated that without much loss in activity the active methylene group of curcumin can be substituted [46]. Li and co-workers have extended this work and included cyclohexanone and cyclopentanone analogues and studied their antibacterial properties against ampicillin-resistant bacteria indicating long chain substituents and hetero aryl substituents may boost the activity of the curcuminoids[47,48]. Recently the pyrazolic and the isoxaxolic analogues of curcumin have been shown to own good neuroprotective action[49]
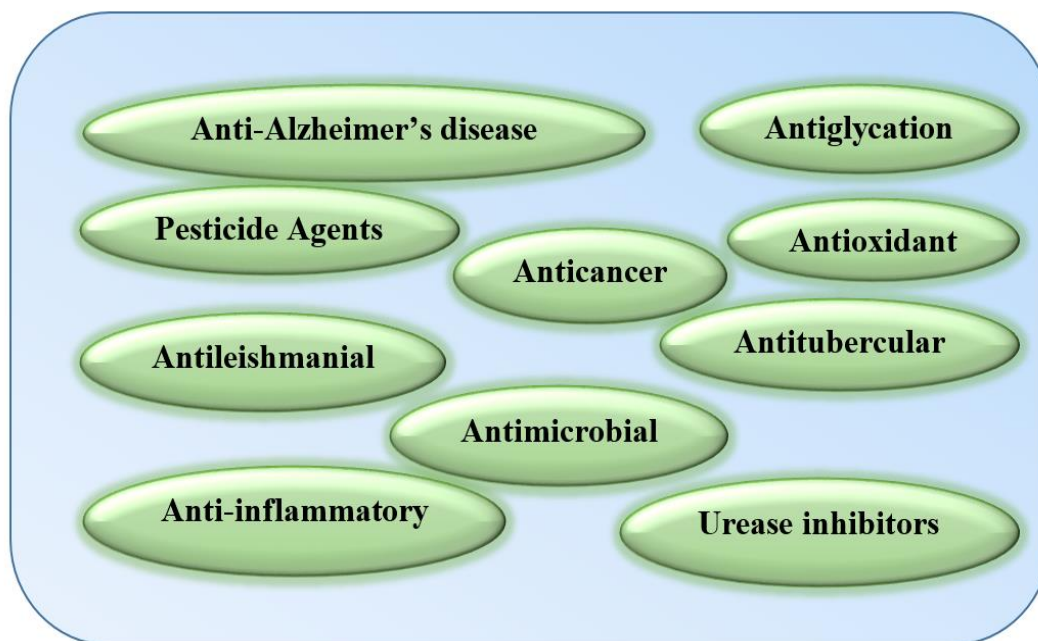
Bioactivities of Schiff bases

Studies showed that heterocyclic derivatives (Schiff bases) containing nitrogen and sulphur atoms serve as unique and versatile platforms for systematic drug design. M.Ahmed et al; 2016, synthesized twelve Schiff bases from curcumin scaffold having sulfonamide moiety successfully and their structures were confirmed by IR, ^{13}C NMR and ^{1}H NMR spectral techniques. All the Schiff base compounds were analyzed for their anti-inflammatory and antinociceptive activities in experimental animal models (Swiss albino mice) as well as against a panel of 12 microorganisms (gram positive, gram negative and fungi types). Among the tested compounds, Schiff base compound with isoxazole moiety showed highest anti-inflammatory and antinociceptive activities compared to standard drugs like diclofenac sodium and indomethacin[50] . Subhash padhye et al; synthesized the fluoro analogues of the Knoevenagel condensates of curcuminoids and their Schiff bases and found that substitution on curcumin structure does not introduce any major steric changes allowing recognition at the macromolecular sites and hence sustaining the enhanced the biological activities of the compounds. All the synthesized Schiff

bases acted as effective Proteasome Inhibitors and Apoptosis Inducers in Cancer Cells.[51].

Schiff bases of curcuminoid analogues have been demonstrated to induce anti-carcinogenic effect both invivo and invitro. Studies reported the anti-carcinogenic activity of Schiff bases of curcuminoid analogues against various cancer cell lines, including the multidrug-resistant ones. So in the present investigation, the antitumour activity against DLA and EAC cancer cell lines, of a series of Schiff bases derived from aryl azo derivatives of synthetic analogues of natural curcuminoids have been studied by invitro and invivo methods.

Metal chelates of curcuminoid analogues and Schiff bases

Curcuminoids form metal complexes in the same manner as 1,3-diketones do. The metal chelating abilities of curcuminoids is through the β diketo group which in turn forms new structural entities with modified biochemical activities. The curcuminoids and their metal complexes possess remarkable biochemical activities. The physicochemical features such as the planarity, hydrophobicity and size and nature of the ligand, as well as the coordination geometry of the metal complex all have important roles in determining the binding/intercalating mode of metal complexes to DNA. According to these findings, a large number of metal complexes has been and is still being experimented as anticancer drugs. Cobalt, copper, nickel and zinc are the various metal ions potentially and commonly used because of forming low molecular weight complexes and therefore, prove to be more advantageous against several diseases.

Curcuminoids are powerful chelating agents and can be used in therapy. Chelation therapy is a medical procedure that involves the administration of chelating agents to remove heavy metals from the body[52]. These ligands bind to heavy metals such as cadmium and lead, thereby reducing the toxicity of these heavy metals (Daniel Sheril et al., 2004)[53]. The brown colour observed when turmeric is mixed with slaked lime is due to the interaction between curcuminoids and Ca^{2+}ions. The biological activity of Cu^{2+},Ni^{2+},Co^{2+},Zn^{2+},Pd^{2+} metal complexes [54]of synthetic curcuminoids were reported and well established. Angulo and his coworkers synthesized and characterized 2:1 curcumin Hg(II) complex in 1986. In animal models Curcumin interaction with copper and iron[55] suggests one possible mechanism of action in Alzheimers disease. A.Valentini et al; reported heteroleptic Palladium (II) complex of curcumin shows antitumoural effects on human prostate cancer cells[56] . The Curcumin –Al(III)complexes[57] are very efficient in the treatment of Alzheimers disease. Yu Min Song et al synthesized rare earth complexes (Sm,Eu,Dy) of curcumin[58] and the metal complexes exhibited excellent antibacterial activity than that of curcumin analogues . A mononuclear 1:1 copper complex of curcumin was synthesized[59] and tested for its superoxide dismutase activity. The cytotoxic activity of synthesized Ruthenium-arene complexes of curcumin[60] were studied and are found to be very effective.

Copper is an important biometal which is needed for normal human metabolism and its imbalance leads to copper deficiency or copper excess diseases. Cu(II)complexes are ideal candidates for different pharmacological studies due to the presence of its biorelevent ligands[61,62]. The metal complexes have various roles in medicinal proceedings such as antimicrobial, antiviral, antiinflammatory, antitumor agents, enzyme inhibitors or chemical nucleases with reduced side

effects and it has distinct superoxide dismutase-(SOD-)mimetic activity[63]. DNA is a potent target of cytostatic drugs and the impact of copper compounds on DNA functionality is very important. The ability of the Cu(II) complexes to bind to DNA and to exhibit nuclease activity in the presence of a reducing agent is well established. Knoevenagel condensates of curcumin and their copper complexes are found to be more effective in inhibiting TNF-α induced NF-κB activation and proliferation of human leukemic KBM-5 cells[62].

Schiff bases of fluorinated curcumin and their corresponding copper complexes have been patented by Sarkar et al; 2011[Patent Number WO2011142795 A1]. The patent claims that the Schiff bases of curcuminoid analogues synthesized in this study have enhanced anticancer activity and bioavailability than curcumin and its previously known analogues. The water-soluble novel Schiff base compounds were not only found to be chemopreventive therapeutic agents against various cancer cell lines, but upon coadministration of this drug could also boost the potential of standard anticancer drugs like gemcitabine. Subhash Pandhye et al; 2009, studied inhibitory effects of twelve Schiff bases (derived from difluoro Knoevenagel condensates of curcumin) and their copper complexes on purified rabbit 26S proteasome, and analyzed the growth inhibition and induction of apoptosis in chemo resistant cell lines like pancreatic and colon cancer cell lines[51]. The copper complexes showed superior biological activity than their corresponding Schiff bases. The nitrogen and sulphur atoms play an important role in the coordination of metal atoms at the active centres of various metallobiomolecules. Metal complexes of chelating ligands containing N and S have attracted considerable attention because of their remarkable physicochemical properties and pronounced pharmacological and biological activities. These concerns have led to major

research efforts to discover new antitumour agents that could be used to combat cancerous tissues one of which are the Schiff bases of curcumin analogues have highly effective Pharmacophoric systems. Stable 1:1 complexes of transition metals can be prepared by refluxing stoichiometric amounts of Schiff bases derived from curcuminoid analogues and metal salts in suitable organic solvents for few hours, the precipitated complex can be separated and purified either by column chromatography and repeated crystallization. Based upon this, intensive effort have been undertaken in the present study to synthesize a series of Schiff bases of curcuminoid analogues and their metal complexes especially with biologically active metals like copper, nickel and zinc. Their structural characterization was done using different spectral techniques. The invitro cytotoxic activity and invivo antitumour activity of the synthesized transition metal complexes were also evaluated.

Hence the present study was undertaken with the following objectives:

1. Synthesis and structural characterization of Schiff bases derived from aryl azo derivatives of curcuminoid analogues.

2. Synthesis and structural characterization of transition metal complexes (Cu^{2+}, Zn^{2+} , Ni^{2+}) of synthetic Schiff bases derived from aryl azo derivatives of curcuminoid analogues.

3. To evaluate the corrosion inhibition behavior of a series of Schiff bases derived from aryl azo derivatives of synthetic curcuminoid analogues.

4. To evaluate the cytotoxicity and antitumour activity of a series of Schiff bases derived from aryl azo derivatives of synthetic analogues of natural   curcuminoids and their synthesized transition metal chelates.

PART II

REVIEW OF LITERATURE

INTRODUCTION

 Schiff bases played an important role in development of coordination chemistry and were involved as vital point in the development of optical materials and inorganic biochemistry. Schiff base derivatives in various processes promoted the researchers for designing of novel aryl/heterocyclic Schiff bases for development of innovative environmental-friendly technology. The first standard synthesis of Schiff bases reported by Hugo Schiff (1864)[64,65] includes the condensation of primary amines with carbonyl compounds [66] under azeotropic distillation. Till now literature have described many methods for the synthesis of imines[67].

General Reaction Scheme for the synthesis of Schiff bases
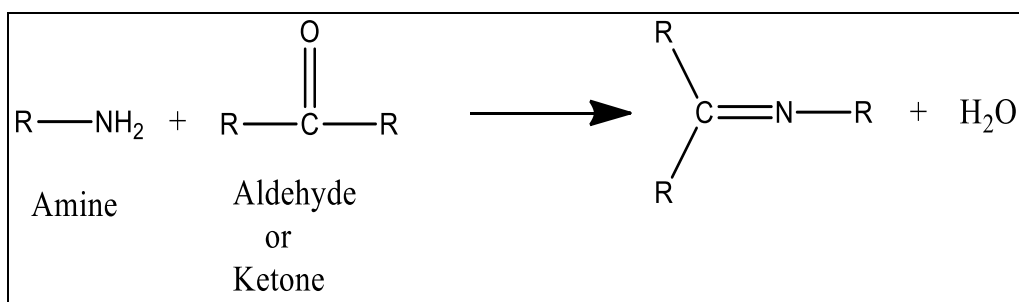
In the 1990s using typical dehydrating solvents like tetramethyl orthosilicate or trimethyl orthoformate an *in situ* method for water elimination instead of using molecular sieves were developed[68,69]. In 2004, Chakraborti et al. [70] explained that the efficiency of these methods can be increased by the use of highly electrophilic carbonyl compounds and strongly nucleophilic amines. They proposed the use of substances that function as Brönsted-Lowry or Lewis acids as an alternative, to activate the carbonyl group of aldehydes, to catalyse the nucleophilic attack by the

amines and to dehydrate it. Brönsted-Lowry or lewis acids used for the synthesis of Schiff bases include $TiCl_4$, $ZnCl_2$, $MgSO_4$-PPTS, alumina, $Ti(OR)_4$, $NaHCO_3$, H_2SO_4, $Mg(ClO_4)_2$, $MgSO_4$, H_3CCOOH, $Er(OTf)_3$, HCl, P_2O_5/Al_2O_3 [71,72]. In the past 10 years a number of innovations and novel techniques have been reported, including solvent-free/clay/microwave irradiation, K-10/microwave, solid-state synthesis, [bmim]BF_4 / molecular sieves, water suspension medium, infrared irradiation/no solvent, solvent-free/CaO/microwave, $NaHSO_4·SiO_2$ / microwave / solvent-free, and silica / ultrasound irradiation [73,74].

Xavier et al; synthesized four Schiff bases Salicylaldimine, Benzilimine, P-Toludine cinnamaldimine, P-Toludine benzilimine and studied their biological importance [75]. Bhupendra N. Ghose explained the synthesis of six new Schiff bases having the ONNO donor system from the condensation of biacetyl monoxime, benzil, o -vanillin, 9, 10-phenanthrenequinone, ethanolamine, 1,3diaminopropan-2-ol and ethylenediamine [76]. Zainab Hussain et al; followed the classical reaction for the synthesis of Schiff's bases in an ethanolic solution and glacial acetic acid as a catalyst and synthesized substituted sulfamethoxazole compounds [77].

Schiff bases and their derivatives possess many different applications in different levels. Anti-corrosive activity of Schiff bases is one among them. Schiff bases have been reported as effective corrosion inhibitors for mild steel and some other alloys in acidic media .The use of Schiff base inhibitors is one of the most vital processes in the field of prevention of corrosion and its control. Due to the presence of the azomethine linkage in the Schiff base molecules, they act as good corrosion inhibitors. Some Schiff base compounds have recently been reported as efficient corrosion inhibitors for different metals like mild steel, copper, aluminium and zinc in highly corrosive acid media [78,79]. The important part in the mechanistic aspect of

such inhibitors is the specific interaction between certain functionalities (nitrogen, oxygen, sulphur) in the inhibitors with the corrosion active centres on the metal surface. Schiff bases have been found to exhibit more inhibition efficiency than their parent amines[80].Multidentate Schiff bases shows greater corrosion inhibition efficiency than monodentate ones[81].Schiff bases of 1,7 di-aryl heptanoids are one among them.

Another important application of Schiff bases is in the bio-inorganic field. The development in the field of bio-inorganic chemistry has increased the interest in the Schiff base complexes, since it has been recognized that many of these complexes may function as models for biologically important species. Sham M. Sondhi et al; synthesized the Schiff bases by condensing 2-hydroxy naphthaldehyde with functionalized diamines and studied the anti-inflammatory analgesic and kinase (CDK-1, CDK-5 and GSK-3) inhibition activities which gave a good result[14]. Schiff base compounds have been used as synthons in the synthesis of a number of industrial and biologically active compounds such as formazans, 4-thiazolidinines, benzoxazines and so forth, via ring closure, cycloaddition, and replacement reactions. Neelima et al; explained the anti-tumour activities of Schiff base ligand 2,3–dihydro–1H–indolo–[2,3–b]–phenazin–4(5H)–ylidene)benzothiazole–2–amine and its Lanthanum metal complexes[82]. Ali et al;evaluated the antitumour activity of vanillin semicarbazone (VSC) against Ehrlich ascites carcinoma (EAC) cells in Swiss albino mice and found to be most potent anti tumour agent[4]. The active centers of cell constituents may be involved in the hydrogen bond formation with the nitrogen atom of azomethine group and interferes in the normal cell processes. Advances in this field will need study of the structure–activity relationships of the

Schiff bases as well as the mechanism of action of these biologically active compounds.   .

Studies enlightened that biological activity for metal complexes are greater than free organic ligands. Enhancement in the biological activity was seen by employment of transition metals into Schiff bases. Abu-dief et al; synthesized Schiff base complexes of Co(II), Ni(II), Cu(II) and Zn(II) incorporating indole -3-carboxaldehyde and m-aminobenzoic acid and screened by disc diffusion method. The activity order of the synthesized compounds were found to be : Cu(II) > Co(II) > Ni(II) > Zn(II) > Ligand[10]. The enhanced activity of the metal complexes may be due to the impact of the metal ions on the normal cell membrane. Metal complexes have polar and nonpolar properties together which helps complexes for permeation to the cells and the tissues. In addition, chelation may increase or suppress the biochemical activity of bioactive species[83] (Nair et al., 2012).

Curcuminoids and Schiff bases of curcuminoid analogues

The Indian subcontinent is gifted with rich and diverse indigenous health traditions which is matched with an equally rich and diverse plant genetic resources. With the dawn of modern techniques it has become possible to isolate and characterize the bioactive chemical compounds present in Medicinal plants.

Phytochemicals are the bioactive chemical compounds present in plants[84,85,86]. Phytochemicals belong to several classes of organic compounds such as terpenoids, flavanoids, sulphur containing compounds, carbonyl compounds, polyphenols etc. The medicinal and biological properties of these plants are mainly due to the presence of these types of compounds. Some of the main sources of the

naturally occurring carbonyl compounds are Curcuminoids (Turmeric), Piperine (Black pepper), Nomillin (citrus fruits), Cassumunin A (Indonesian medicinal ginger), Quercetin (cereal, grains), Ellagic acid (fruits, nuts), etc[87]. Among these naturally occurring carbonyl compounds, curcuminoids present in turmeric possess several interesting structural features and numerous practical applications. Turmeric (*Curcuma longa Linn*) has been used as a household remedy for various diseases in traditional Indian medicine [88,89,90,91,92,93] including cough, anorexia, hepatic disorders, wounds, rheumatism, chicken pox, sinusitis etc. .Its rhizome is used extensively for imparting flavour[94] and colour to foodstuffs in Asian countries. The powder obtained from the dried rhizomes of turmeric, is widely used for medicinal purposes (Srimal 1997). Turmeric contains moisture (9%), curcumin (5-6.6%), volatile oils (<3.5%), extraneous matter (<0.5%), calcium, potassium sesquiterpenoids, polysaccharides, protein, vitamins, etc.[95, 96, 97]. Turmeric is also a good source of α- linoleic acid and ω-3 fatty acids[98] (Goud et al; 1993).

Curcumin content present in turmeric comprises curcumin I (94 %),curcumin II (6%) and curcumin III (0.3%)[17] (Chainani – Wu et al; 2003) .Curcumin I and two related compounds curcumin II (demethoxy curcumin) (DMC) and curcumin III (bis demethoxy curcumin) (BDMC), are altogether known as curcuminoids. Among these curcumin I is the yellow colouring substance. The discovery of curcumin dates to around two centuries ago when Vogel and Pelletier [99] reported the isolation of "yellow colouring matter" from the rhizomes of turmeric and named it "curcumin". In 1842, Vogel obtained a pure preparation of curcumin but did not report its formula. Milobedzka and Lampe first identified the chemical structure of curcumin in 1910 [100, 101]. Through intensive chemical derivatization

they established the identity of curcumin as diferuloyl methane or 1,7 – bis (4-hydroxy -3 - methoxy phenyl)1,6- heptadiene – 3,5 – dione .The established structures of Curcumin-I, Curcumin-II and Curcumin-III are given below.

The three different forms of curcumin present in turmeric

Curcumin
(Curcumin I)

Demethoxycurcumin
(Curcumin II)

Bis-demethoxycurcumin
(Curcumin III)
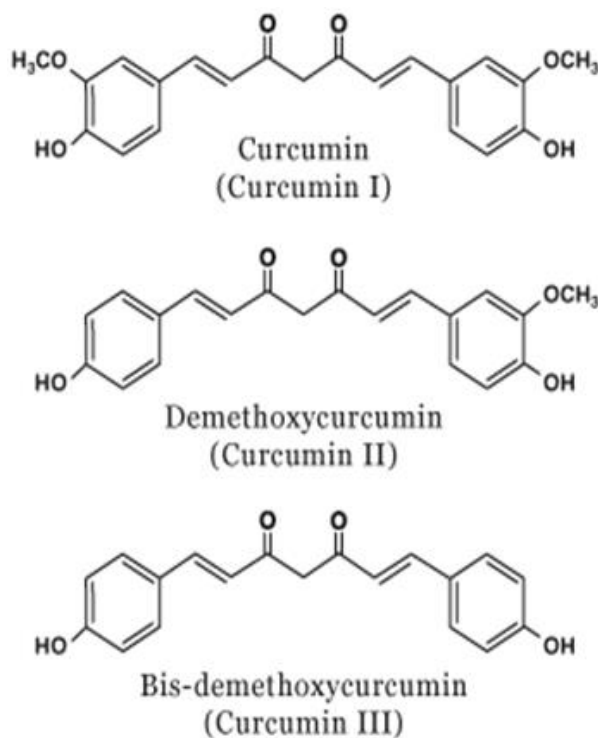
The therapeutic activity of curcumin is mainly attributed to its chemical structure and very unique physical, chemical, and biological properties[53, 102, 103]. It is a diferuloyl methane molecule comprising two ferulic acid residues joined by a methylene bridge. Curcumin has three important functionalities: an aromatic o-methoxy phenolic group, an α, β-unsaturated β-diketo moiety and a seven carbon linker[100].

CURCUMIN health benefits:
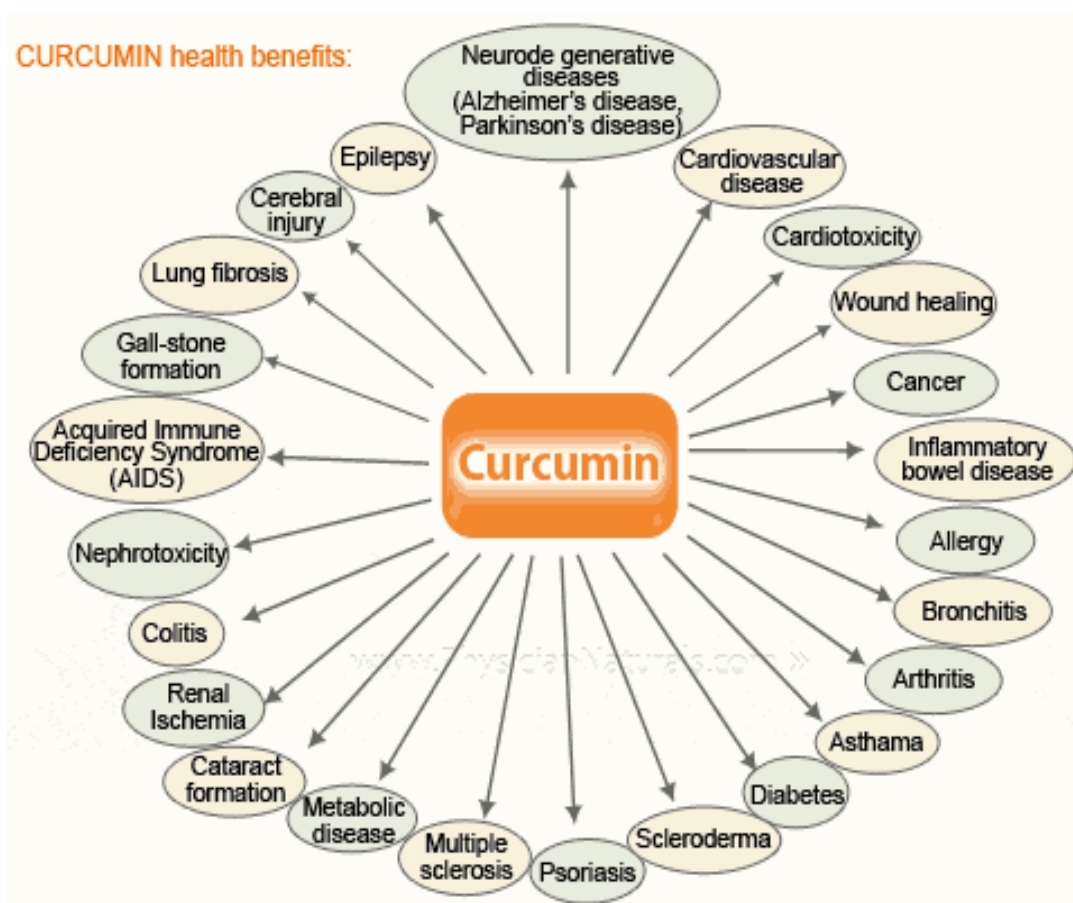
V.Lampe (1918)[104] reported the first synthesis of curcuminoids from the chloride of carbomethoxy ferulic acid and acetoacetate. The first industrial synthesis was later developed by pavolini (1937). Later Pabon et al; [105] established a modified simple procedure for its synthesis. The active methylene group of acetyl acetone was blocked with boric anhydride and made it to react with Vanillin and the product formation took place via Knoevenagel condensation. Boron based reagents such as boric acid, boron oxide act as Lewis acids with the β diketone system and decreases the nucleophilicity of the C-3 position. The two terminal methyl groups then undergo aldol condensation with two Vanillin molecules. And the hydrolysis of the intermediate formed in acid medium results in the formation of curcumin.

Synthesis of curcumin by the general method proposed by Pabon
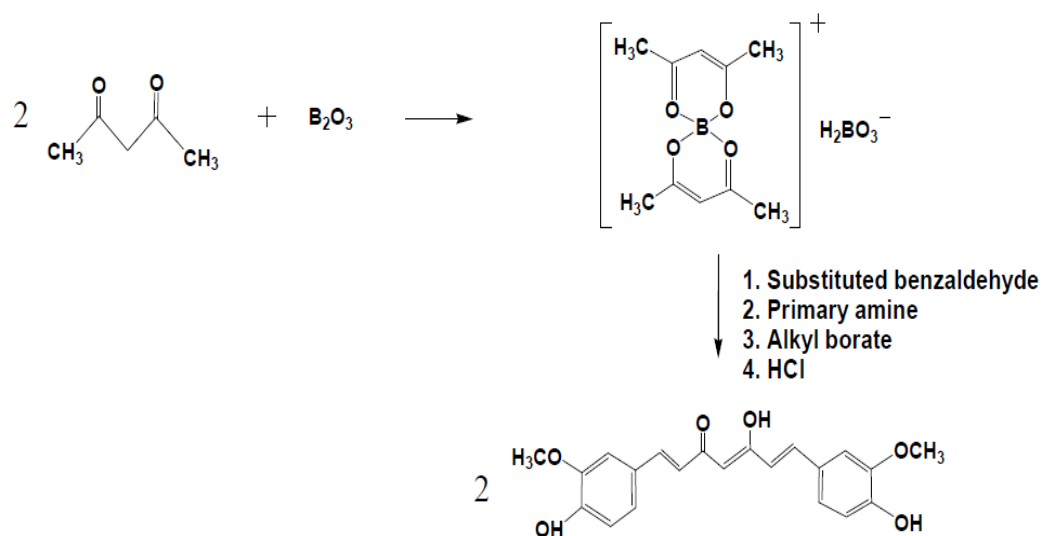
A new efficient and environmental friendly procedure for the synthesis of a series of salicylaldehyde-based schiff bases under microwave irradiation was described by Sunitha Bhagath et al; 2013[106]. Joseph et al; [62]synthesized 2-aminobenzothiazole derivatives by the condensation of knoevengal condensate acetoacetanilide (obtained from substituted benzaldehydes and acetoacetanilide) and 2-aminobenzothiazole. Ahmed et al; synthesized Schiff bases of benzenes sulfonamides bearing curcumin scaffold and investigated their pharmacological effects[107]. Padhey et al,[51]treated di fluoro analogues of curcumin with different hydrazides/amines to yield corresponding bis-Schiff base ligands.

Arene diazonium salts can be coupled with many active methylene and methine compounds to form compounds containing imine $R_2C=NR'$ (R' $\neq$ H) groups. The diketo group in the curcuminoids will make the methylene group least acidic and the diazonium salt can easily attack the active methylene group. Krishnan kutty and his coworkers synthesized the aryl azo derivatives by the coupling of benzene diazonium salt with β-diketones[108]. After destroying the excess nitrous acid with

urea the benzene diazonium salt prepared was added drop by drop to a solution of the β- diketone (0.01 mol in 15 ml ethanol) kept below 0 ^{o}C with constant stirring. Using sodium acetate the pH of the solution was maintained around 6 (mild acidic condition). The acid concentration must be controlled because the diazonium salt will get protonated at highly acidic medium and hence becomes non-nucleophile, equilibrium will be pulled to the left and imine formation will not occur. Therefore, many aryl azo compound synthesis reactions are best carried out at mild acidic pH.

Fadda et al; 2009[109], coupled the diazonium salt of some aromatic amines with curcuminoids in a view to synthesis new azodisperse dyes to investigate the possibility of finding some new azodyes which are capable of dyeing different types of fibers and have expected wide range of biological activity. Diazonium salts undergoes a coupling reaction with the curcumin to give the respective 4-arylazo derivatives.

Sayudevi P et al; synthesized Schiff bases by the condensation of aryl azo derivatives of acetyl acetone and ethylene diamine. Zang, Q et al; used several common heteroaromatic rings such as indole, imidazole, pyrazole and benzimidazole to replace the OH groups of curcumin and attempted to develop potent cytotoxic anticancer drug[110]. They analyzed that hetero aromatic substituent shows more cytotoxic activity than simple aromatic systems.

Applications of Schiff bases

Schiff bases as anticorrosive agents

 Schiff bases are very important in corrosion studies as they act as very good corrosion inhibitors. It is very interesting to note that several commercial inhibitors contain aldehydes and amines but apparently because of the presence of >C=N

bond in them, this makes Schiff bases function more resourcefully as corrosion inhibitors.

Saha et al; in order to evaluate the effect of the functional group present in the ligand towards corrosion inhibition performances, synthesized three Schiff-base molecules namely,(*E*)-4-((2-(2,4-dinitrophenyl)-hydrazono)-methyl)-pyridine,(*E*)-4-(2-(pyridin-4-ylmethylene)-hydrazinyl)-benzonitrile and (*E*)-4-((2-(2,4-dinitrophenyl)-hydrazono)-methyl)-phenol and studied the corrosion inhibition behavior on mild steel in 1.0M HCl medium[111]. And all the three Schiff bases exhibited good anticorrosive activity. The weight loss method and the electrochemical results showed that the inhibitors impart high resistance towards charge transfer across the metal–electrolyte interface and behaved as strong inhibitors. Ahamad et al; synthesized four Schiff base corrosion inhibitors namely N'-(phenylmethylene) isonicohydrazide(INHB), N'-(2-hydroxy bezylidene) isonicohydrazide(INHS), N'-(furan-2-ylmethylene) isonicohydrazide(INHF), and N'-(phenylallylidene) isonicohydrazide(INHC) and investigated their inhibition effect on corrosion of mild steel in HCl solutions and also studied by varying temperature and immersion time[112]. Among these INHC showed 99.5 percentage efficiency. The mechanism of adsorption of inhibitors on mild steel was explained as one which involve complex interactions; both physical and chemical adsorptions.

H.El-lateef et al;2014 synthesized three Schiff bases Sodium 3-[{[1-carboxy-3-(methylthio) propyl] imino} methyl]-4- hydroxybenzenesulfonate (SI) and Sodium 3-{[(1-carboxy-2-phenylethyl) imino] methyl}-4-hydroxybenzenesulfonate (SII) and studied the effect of Schiff bases on the corrosion of mild steel in 1.0 M HCl solution at 50ºC and the mechanism of inhibition was studied using

electrochemical techniques. The connection between the inhibition efficiency of studied Schiff bases and the quantum chemical parameters (such as energies of HOMO, LUMO and dipole moment) have been also analysed[113]. The different analysis showed that, inhibition efficiencies of the imines increase with the inhibitor concentration. Adsorption of these studied inhibitors follows Langmuir adsorption isotherm.

Bedair et al; synthesized three novel Schiff bases named as 17-hydroxy-3, 6, 9, 12, 15 –penta - oxa - hepta – decyl 3 - (4 - (dimethylamino) benzylideneamino) - 4-hydroxybenzenesulfonate,17-hydroxy-3,6,9,12,15-pentaoxaheptadecyl4-hydroxy-3-(pyridin-2-ylmethyleneamino)benzenesulfonate, and 17-hydroxy-3,6,9,12,15-pentaoxaheptadecyl4-hydroxy-3-(2-hydroxy benzylidene amino) benzene sulfonate abbreviated as S1, S2 and S3 respectively. [114]They studied the corrosion inhibition effect of the synthesized compounds on steel in 1.0 M HCl and used analysis methods such as weight loss method, Electrochemical Impedance, potentiodynamic polarization techniques and computational studies. The experimental results revealed that these Schiff base molecules inhibited the corrosion reaction in 1.0 M HCl solution. Polarization curves revealed that the inhibitors are mixed-type inhibitors. A good correlation was observed between the experimental results and quantum chemical parameters of the Schiff base molecules. Molecular dynamic simulation revealed that these inhibitors were adsorbed strongly on the metal surface.

Gddotokmen et al; studied the inhibition efficiency of 3,4-diaminobenzonitrile against steel corrosion, using different techniques like electrochemical impedance spectroscopy, potentiodynamic polarization measurements and solution assay analysis. The corrosion rate was determined using different methods and apparent

derived Stern-Geary coefficient (B) from solution assay analysis and compared with value obtained from Tafel plots. In presence of inhibitor, the difference in the values from different methods becomes negligible. When the anodic dissolution kinetics begins to be governed by strongly adsorbed inhibitor, resistance against charge transfer process becomes the most important and results from different routes becomes closer[115].

Schiff bases as corrosion inhibitors on mild steel

Mild steel is a significant alloy because of its wide range of applications in industrial field for many mechanical and structural purposes. As widely used in engineering fabrications, mild steel is much susceptible to attack by various corrosion agents among which aggressive acids like hydrochloric acid and sulphuric acid are the most common. These acids have been used for drilling purposes, pickling baths and also in descaling processes.

Corrosion of mild steel and its alloys in acid media and the inhibitors used for that has been largely studied. Mild steel is largely affected in the pH range 4 to 11 but moderately resistant to attack by alkaline medium. Organic molecules having hetero atoms are found to be very efficient corrosion inhibitors for the mild steel. The researchers have reported the effect of some imine group containing compounds on corrosion of mild steel in various acid solutions.

Ahamad et al; [112]used weight loss, electrochemical measurements and quantum chemical calculations to study the corrosion inhibition efficiency of four Schiff bases namely, N0-(phenylmethylene) isonicotinohydrazide (INHB), N0-(2-hydroxybenzylidene) isonicotinohydrazide (INHS), N0-(fur- an-2-ylmethylene) isonicotinohydrazide (INHF) and N0-(3-phenyl- allylidene) isonicotinohydrazide

(INHC). All compounds exhibited >90% inhibition efficiency at their higher concentrations. The different thermodynamic parameters were calculated to study the mechanism of corrosion inhibition. The adsorption of the studied inhibitors on the mild steel follows Langmuir adsorption isotherm. Polarization studies revealed that all above inhibitors are mixed type. The quantum chemical parameters like electron affinity (EA) and molecular band gap (DEMBG) showed good correlation with good inhibition efficiencies.

Hosseini et al, [116]investigated the corrosion inhibition efficiency of three new Schiff bases, viz.,N,N-ethylen-bis (salicylidenimine) [S1],N,N-isopropylien-bis (salicylidenimine) [S2], andN-acetylacetone imine,N-(2-hydroxybenzophenone imine) ortho-phenylen [S3] on mild steel in $0.5MH_2SO_4$ using Tafel polarization method and electrochemical impedance spectroscopy (EIS). The three Schiff base molecules exhibited good inhibition efficiencies of ∼97–98% at its optimum concentration. The fraction of the mild steel surface covered by the inhibitor molecules was found to increase with inhibitor concentration. Of the three studied Schiff bases, the S2 showed better efficiency than the other two Schiff bases. The adsorption of the inhibitor on the metal surface followed Langmuir isotherm. Thermodynamic calculations indicated the adsorption to be physical adsorption.

Sadeghi et al; [81]synthesized and studied the inhibition efficiency of three multidentate Schiff base ligands (A = 3-(2-aminobenzylimino)-1-phenylbutan-1-one], B = 3 - [({o - [(E) - (o - Hydroxyphenyl) methyl- ideneamino] phenyl}methyl)imino]-1-phenyl-1-buten-1-ol, and C = 3-[({o-[(E)-(2-Hydroxy-1-naphthyl)methylideneamino]phenyl}methyl)imino]-1-phenyl-1-buten-1-ol on the corrosion of mild steel in 1 M hydrochloric acid using potentiodynamic polarization techniques and electrochemical impedance spectroscopy. The

efficiency of the corrosion inhibitors followed the order A < B < C. The adsorption of inhibitors obeyed Langmuir adsorption isotherm. The values of ΔG°_{ads} indicated that the process involves both chemisorption and physisorption .The effect of A, B and C on mild steel surface was also studied by quantum mechanical calculations.

Ansari et al;2013, [117]used gravimetric measurements, electrochemical impedance spectroscopy (EIS), potentiodynamic polarization and quantum chemical calculations to study inhibition effect of three bis-Schiff bases of isatin namely (2-methoxybenzylidene) hydrazono) indolin- 2-one (HZ-1), (2-hydroxybenzylidene) hydrazono) indolin-2-one (HZ-2) and (4-nitrobenzylidene) hydrazono) indolin-2-one (HZ-3) on mild steel corrosion in 1.0 M HCl .The values of activation energy, equilibrium constant, free energy of adsorption, activation enthalpy and activation entropy were calculated and discussed. The adsorption of inhibitors followed Langmuir's adsorption isotherm. SEM and EDX analysis confirmed the existence of protective inhibitor film on metal surface.

The reports of the corrosion inhibition nature of Schiff bases derived from 1,7-di aryl heptanoids are scanty. In medicinal field also, 1,7-di aryl heptanoids based corrosion inhibitors have a promising future that it can prevent the corrosion of different equipment that is inserting into the body.

Biological effects of Schiff bases

The synthesis, characterization and the SAR (structure activity relationship) of Schiff base compounds have been researched worldwide recently. The studies explained that the presence of a lone pair of electron in the sp^2 hybridized orbital of the nitrogen atom of the azomethine group is of biological and chemical importance. By virtue of hydrogen bonds formed between the active centers of cell

constituents and the sp^2 hybridized nitrogen atom of the azomethine linkage Schiff base molecules interfere in the normal cell processes [118].

In coordination chemistry, Schiff bases plays vital role in the design and development of novel compounds, having strong biological activities. The Schiff bases are the intermediates in many organic reactions and are more explored for their efficiency. The derivatives of Schiff bases have attracted the attention of researchers for exploring new methods for development of new environment-friendly technology[119]. In clinical field, Schiff bases are now drawing the attention of researchers due to chemotherapeutic functions. They are known to possess a wide variety of potent activities. Parveen and his co-workers have studied the interaction of the calf thymus (CT) DNA with a new asymmetric copper(II) N,N-ethane bridged N_2S_2 macrocycle[120].

Anu kajal et.al., 2013 synthesized a new series of fluoroquinolone C-3 heterocycles, that is, s-triazole Schiff 27and mannich bases derivatives of ofloxacin and evaluated their invitro antitumor activity with a a human leukocytoma cell line (HL60), murine leukemia cell line (L1210), and a Chinese hamster ovary cell line (CHO) using the MTT assay and saw a high potent activity for molecules containing free phenol group. Schiff base ligands have acted as useful synthetic models for iron-containing enzymes[121] [122]

The flouro analogues of Knovengal condensates of curcumin and their Schiff bases slows down the rapid metabolism of curcumin and in turn act as proteasome inhibitors and apoptosis inhibitors[51] (Subhash et al.,2009).

Joseph et al; synthesized novel Schiff bases derived from 2-aminobenzothiazole and Knoevenagel condensate of β-ketoanilides and characterized and studied its

anti-bacterial activity. The Schiff bases was found to be very effective[62]. The sulfonamides were conjugated with curcumin (β-diketones) to form Schiff bases via keto and enol linkage that could lead to better activity. Newly synthesized compounds were screened for in vitro antibacterial, antifungal and *in vivo* anti-inflammatory and antinociceptive activities (Ahmed M. et al; 2016)[50]. Several papers have reported the anti-carcinogenic activity of Schiff base of curcumin against various cancer cell lines. Schiff base derivatives of curcuminoid analogues have been shown to be promising leads for the design of more efficient antitumour agents. Some of the newly synthesized analogues were more effective than curcumin, whereas some exhibited similar activity.

Metal complexes of Schiff bases: biological effects

Coordination chemistry of transition metal Schiff base complexes possessing N, O, and S-donor atoms has received consideration over the past few decades, due to the imperative roles these compounds have played in a variety of biochemical procedures like halo peroxidation[123], insulin mimicking[124,125], fixation of nitrogen [126], inhibition of cancer growth, and prophylaxis against carcinogenesis[127,125].

Several Studies show that metal complexes of Schiff base are more potent than free organic ligand[128]. Lots of researchers reported that the complex formation of transition metals with Schiff bases increases its biological activity [129].

Yousif et al; synthesized a total of five new metal complex derivatives of 2N-salicylidene-5-(*p*-nitro phenyl)-1,3,4-thiadiazole, with the metal ions Co(II), Vo(II), Rh(III), Pd(II) and Au(III) in alcoholic medium[130]. Selwin et al; did the synthesis and characterization of Schiff base metal complexes from imidazole-2-carboxaldehyde with L-phenylalanine.[131]

Saghatforoush et al. [132] synthesized Fe(III) complexes with tetradentate Schiff base ligands pythsalHX ([5-X-N-(2-pyridylethylsulfanylethyl)salicylideneimine] (X = OMe, N2Ph, I, NO2)and characterized them by various methods like IR, NMR, UV etc. Morad et al. synthesized Ni(II) complex with salicylaldehyde and 2-amino benzoic acid and characterized it by various methods and also studied its antibacterial activity[133]. Boghaei [134] synthesized and investigated non-symmetrical tetradentate Schiff base complexes of Ni(II) and Cu(II) ions. .

Transition metal complexes of Schiff bases have been known to be one of the most promising, modifiable and comprehensively studied systems with applications in different fields like clinical and analytical fields[135,136].The antioxidants derived from metal Schiff base complexes have received wide attention for their ability to safeguard living systems and cells from impairment caused by free radicals or oxidative stress . DNA binding, scavenging potentials, cleavage potentials, and anticancer studies of Schiff base-ruthenium(III) complexes have been accounted for [137]. Amidino-Schiff base forms complexes with Cu (II) and Fe (II) and the complex act as a thrombin inhibitor[138].Salicylidiene anthranilic acid[139] possesses antiulcer activity and complexation behaviour with copper complexes, which show an increase in antiulcer activity. Kumar et al; 1995 [140]synthesized some Schiff bases and their metal complexes with metals Cu, Ni, Zn and Co from 2,4-dihydroxy- benzaldehyde, salicylaldehyde, L-alanine and glycine and found to possess antitumor activity and their of reactivity with metal complexes followed the order Ni>Cu>Zn>Co. Amino Schiff base compounds formed with aromatic and heterocyclic amine possess high order of activity against human tumour cell lines. Aryl-azo Schiff bases synthesized exhibit antitumour activity. Schiff base derived from indole-2-caboxaldehydes show inhibitor activities to KB cell lines.

Diorgano- tin (IV) Schiff base complexes show antitumor activities in vitro and inhibit interaction to BEL-7402 and K B HCT-8 tumour cell lines.

Zhang et al synthesized three transition metal coordination complexes $Cu(C_{18}H_{16}N_3O_2)_2 \cdot 2CH_3OH$, $Zn(C_{18}H_{16}N_3O_2)_2 \cdot 2CH_3CH_2OH$ and $Cd(C_{18}H_{16}N_3O_2)_2 \cdot 2CH_3OH$, derived from 2-acetylpyridine and l-tryptophan ($C_{18}H_{16}N_3 O_2$), and studied the antitumour activities of the three synthesized complexes on MDA-MB-231 breast cancer cells. The results show that all the three complexes inhibit the cellular proliferation. Moreover, $Cd(C_{18}H_{16}N_3O_2)_2 \cdot 2CH_3OH$ has the maximum anti-proliferative activity among the three complexes. In addition, the cadmium complex can inhibit proteasomal chymotrypsin type activity and also can bring apoptosis on human breast cancer (MDA-MB-231) cells and also has potential to be used as a proteasome inhibitor and anticancer agent (Zhang et al; 2012)[141]. Cu(II) complexes of Schiff bases derived from 2-aminobenzothiazole and Knoevenagel condensate of β-ketoanilides were found to be more effective in toxicity studies than corresponding ligands (Joseph et al;2014)[62]

The most exciting aspect of 'metal-Schiff bases derived from 1,7-di aryl heptanoids (curcuminoids)' complexes is that many of them show very diverse and promising health effects. First invention on anticancer effect of transition metal-curcumin complexes date back to the year 1998. Several transition metal complexes of curcuminoids have been successfully tested *invitro* and *invivo* for their antitumour effects. Among a series of metal complexes VO(IV), Co (II), Ni(II), Cu(II), Zn(II), the copper complexes turned out to exhibit highest selective cytotoxicity and also showed a significant reduction in the solid tumour volume in ascites tumour bearing mice[55] . Zn^{2+}-curcuminoid complexes displayed

anti- cancer, gastro protective and anti-depressant activities in rats. Anti-tumour activity has been testified for metal curcuminoid complexes of group 13 elements (Al, Ga and In), the first row transition metals (V, Fe, Zn, Cu) the second row transition metals (Ru, Pd) as wells as some rare earth metals. The Copper complexes presented enhanced anti tumour activity against three Human cancer cell lines namely HeLa(Cervical Cancer), MCF-T(breast cancer) and ASPC-1(Panceratic Carcinoma).

1,7-di aryl heptanoids (curcuminoids) are bioactive compounds with strong medicinal properties found in Turmeric. The present investigation is an attempt to prepare the Schiff bases derived from aryl azo derivatives of synthetic analogues of the active chemical component namely curcuminoids present in the herbaceous medicinal plant 'Turmeric'. Coordination chemistry of biologically efficient plant products has gained considerable attention in recent years. This is evident from the numerous experimental reports on medicinal and other aspects of metal complexes of curcuminoids and their allied derivatives. The main aim of this study is to synthesize, characterize and investigate the electrochemical and antitumour activities of transition metal complexes of a series of Schiff bases derived from aryl azo derivatives synthetic curcuminoid analogues.

PART III

MATERIALS, METHODS AND INSTRUMENTAL TECHNIQUES

This chapter deals with the materials, methods and instrumentation techniques used for the a)synthesis and characterization of the Schiff bases derived from aryl azo derivatives of synthetic curcuminoid analogues b) study of the corrosion inhibition behaviour of the newly synthesized Schiff bases on mild steel c) invivo and invitro anti tumour studies.

Synthesis and characterization of the Schiff bases derived from aryl azo derivative of synthetic curcuminoid analogues

The chemicals required were procured from Sigma Aldrich chemical suppliers and were of analytical reagent grade. Different aromatic aldehydes were used along with the 1,3-diketone and acetyl acetone. Metal salts used for the synthesis of complexes include copper (II) acetate monohydrate, nickel (II) acetate tetrahydrate and zinc(II) acetate. The commercial solvents taken were distilled and used for synthesis.

Synthesis of 1,7-di aryl-hepta-1,6diene-3,5-diones.

Acetyl acetone (0.005mol, 0.5g) and boric oxide (0.0035mol, 0.25g) was stirred about 1 hour to obtain acetyl acetone-boron complex. To the reaction mixture, the aldehyde (0.01mol) dissolved in dry ethyl acetate (7.5ml) and tri(sec-butyl) borate (0.02mol,5.4 ml) were added and stirred and the temperature was kept above $80^{o}C$. The reaction mixture was stirred and while stirring n-butyl amine (0.1ml dissolved in 1ml dry ethyl acetate) was added drop wise for about 40minutes. Stirring was continued for an additional period of ~ 4h and the mixture was kept aside overnight. Hot (~$60^{o}C$) HCl (0.4M, 7.5ml) was added and then the mixture was again stirred for ~ 1h. Two layers were separated and the top organic layer was extracted with 5ml ethyl acetate. The extracts were allowed to evaporate and the

residue material was stirred with Con.HCl (10ml) for ~1h. The solid product separated was washed with water and dried in vacuum. A mixture of 1,7-diaryl heptanoid and 6-aryl hexanoid was obtained. The products obtained were quantitatively separated by column chromatography using silica gel (60 – 120 mesh) as described below.

Separation and purification of 1,7-diaryl heptanoids

The solid product obtained above was dissolved in minimum quantity of ethyl acetate solvent and added to the column densely packed with silica gel. The eluting solvent used for separation was 1:5 (v/v) acetone: chloroform mixture. As the elution continues, two bands were developed in the column. The elution was then repeated by using 1:2 (v/v) mixture of acetone and chloroform as the eluent and collected in aliquots, checked by TLC and the extracts on removing the solvent in vacuum, yield 1,7-diaryl heptanoid in 65 – 70% yield. The isolated 1,7-diaryl heptanoids were recrystallized twice from hot benzene to get chromatographically pure material.

Synthesis of phenyl azo derivatives

The synthesized 1,7-diaryl heptanoids were coupled with benzene diazonium salt. Benzene diazonium salt (0.01 mol) was prepared as reported earlier[105]. Excess nitrous acid present in the diazonium salt was destroyed by adding urea to it and the diazonium salt solution was added drop by drop to a solution of the β-diketone (0.01 mol in 15ml methanol) kept below 0^0C with constant stirring. Sodium acetate was added to the mixture to keep the pH in the range of 6-7.The precipitated compound was filtered, washed with water and recrystallized from methanol to get chromatographically pure (TLC) material.

Synthesis of Schiff Bases

The Schiff bases were synthesized by the condensation of phenyl azo compounds with 1,2-diaminoethane (en) as follows. A methanolic solution of the 1,2-diaminoethane (0.01mol, 20ml) was added to an methanolic solution of the synthesized compound (0.02mol, 20ml). The solution was stirred using a magnetic stirrer for approximately 5 hours and evaporated at reduced pressure. The crystalline compound formed was filtered and recrystallized from hot methanol to get chromatographically (TLC) pure compound.

Synthesis of metal complexes with Cu(II),Zn(II), & Ni(II)

The Cu(II) complexes of the Schiff bases were prepared by adding a methanolic solution of copper(II) acetate (20 ml, 0.01mol) to a solution of Schiff base (20 ml, 0.01 mol) in methanol and refluxed gently for 3 hours. After reducing the volume to half, the solution was cooled to the room temperature. The precipitated complex was then filtered, washed with 1:1, methanol:water mixture and recrystallized from hot methanol. The Cu(II) complexes were synthesized and characterized.

The Zn(II) complexes were prepared by adding a methanolic solution of zinc(II)acetate (20ml,.01mol) to a solution of Schiff base (20ml,0.01mol) in methanol and refluxed gently for 3 hours. The precipitated complex was filtered, washed with 1:1, methanol: water mixture and recrystallized from hot methanol.

The Ni(II) complexes were prepared by adding a methanolic solution of nickel acetate (20ml,0.01mol) to a solution of curcuminoid analogue(20ml,0.01mol)in methanol and refluxed gently for 3 hours. The precipitated complex was filtered, washed with 1:1, methanol:water mixture and recrystallized from hot methanol

Characterization of the ligands and metal complexes:

The Schiff base ligands and metal complexes were characterized using various spectral and analytical techniques. The spectral techniques involve UV,IR,^{1}H NMR,^{13}C NMR, 2DCOSY NMR and Mass spectra. Elemental analysis of compounds synthesized were done to find C,H,N,S and metal percentages by Vario EL III analyzer. The analysis was carried out at STIC, CUSAT.

UV-Visible Spectra

The absorption in the UV-Vis region is dependent on the electronic structure of the absorbing species. The UV spectra are characterized by two parameters, the position of the absorption maxima at λ_{max} and intensity of band. Only two transitions $n \rightarrow \pi^*$ and $\pi \rightarrow \pi^*$ can be achieved by energies in the 200-800nm region. Molecules which contain π and nonbonding electrons are likely to absorb light in UV-Vis region. The important transitions observed in the spectrum of synthesized compounds were $n \rightarrow \pi^*$ and $\pi \rightarrow \pi^*$ transitions. Absorbance spectroscopy was performed on a Schimadzu UV-VIS -1601 spectrophotometer.

IR Spectra

IR spectra represent a unique reflection of the molecular structure of the compounds. IR spectroscopy is often used to identify molecular structures because functional groups give rise to characteristic bands in IR both in terms of intensity and position (frequency). Molecules experience a variety of vibrational motions which are the characteristic of their component atoms. The compounds absorb IR radiations that correspond to the energy of these vibrations. The IR spectra of synthesized compounds were characterized by bands corresponding to C=O, C=N,

NH, C=C phenyl, C=C alkenyl, CH=CH trans group vibrations etc. The observed position and intensity of these bands in the IR spectra helps us to identify the presence of hydrogen bonding, conjugation etc. in the compound. IR spectra of compounds were recorded on Perkin Elmer FTIR spectrophotometer.

^{1}H NMR Spectra

NMR spectroscopy is the research technique that exploits the magnetic properties of certain atomic nuclei. It is a definitive method to identify organic compounds and provides detailed information about the structure, dynamics and chemical environment of molecules. Different functional groups give distinguishable signals and same functional groups with different neighbouring substituents also give distinguishable signals. The position and nature of splitting of the NMR signals depends on the coordination and nature of substituents and extent of delocalization in the chelate ring. The position of functional groups like NH, alkenyl and aryl protons can be identified in the spectrum. The ^{1}H NMR spectra were recorded on a Varian 300 NMR spectrophotometer.

^{13}C NMR Spectra

The Carbon atoms present in a molecule could be probed by NMR in the same fashion as hydrogen atoms does. The ^{13}C NMR spectrum of an organic compound displays single sharp signal for each structurally distinct carbon atom present in a molecule. The ^{13}C chemical shifts are nearly 20 times greater than that for the chemical shift for protons and this together with the absence of splitting of signals make it more likely that each structurally and magnetically distinct carbon gives only a single peak. The carbon atoms can be easily identified. In ^{13}C NMR , chemical shifts lies in a range 0 to 220ppm. Saturated carbon atoms, carbonyl

carbon, CN carbon, alkenyl and aromatic carbon atoms can be identified from their positions in the ^{13}C spectra. The carbonyl carbon and CN carbon usually appears at the lowest field values and has the largest chemical shifts due to the electronegative oxygen and nitrogen attached to it which produces deshielding. The property anisotropy is responsible for the large chemical shifts of carbon atoms in the aromatic rings. The ^{13}C NMR spectra were recorded on a Bruker, AV 400 – AVANCE III NMR spectrophotometer.

2D COSY NMR

Correlation spectroscopy is one type of two dimensional NMR spectroscopy which is best known by its acronym,COSY.Two dimensional NMR spectra provide more information about a molecule than one dimensional NMR spectra.In two dimensional experiments,there are two coordinate axes representing ranges of chemical shifts.The signal is displayed as a function of each of these chemical shift ranges.The data are plotted as a grid, with two axes representing chemical shift ranges and third dimension constitutes the intensity of the observed signal.The result is a form of contour plot in which contour lines correspond to signal intensity.The two dimensional experiments include H-H correlation spectroscopy, COSY and heteronuclear correlation spectroscopy ,HETCOR. COSY NMR spectra were recorded using Bruker, AV 400-AVANCE III FT-NMR spectrophotometer

Mass Spectroscopy

Mass spectrometry is an important analytical tool that ionizes chemical compounds to generate ions or molecule fragments and measures their mass to charge ratio. The m/z value at which the molecular ion peak appears on the mass spectrum gives idea about the molecular mass of the molecule. Fragmentation of the molecular ion

produces fragment ions at m/z values corresponding to their individual masses. Mass spectra give indication about the molecular weight of a molecule and the fragmentation pattern of the molecule. Metal complexes of Schiff bases have been studied extensively by electron impact mass spectrometry. The FAB mass spectra were recorded on a Joel SX−102 mass spectrophotometer from CDRI, Lucknow, India.

C, H, N, S analysis

C, H, N, S analysis is very significant in studying the structure of organic moiety in metal complexes. A CHNS Analyzer is a scientific instrument which determines the elemental composition of a given sample. The analyzer uses the combustion process to break down substances into simple units, which are then quantified, usually by infrared spectroscopy. C, H, N, S analysis was done using Vario EL III analyzer. The metal percentage was also calculated using standard methods.

Corrosion studies

Conventional methods were employed for the analysis of corrosion inhibition capacity of the Schiff bases, like weight loss measurements and electrochemical measurements (Tafel polarization studies and electrochemical impedance spectroscopy). The preparation of metal specimens, aggressive solutions and different methods adopted for the evaluation of corrosion inhibition properties are explained in detail.

Metal specimens

For weight loss studies, the Mild Steel of the following composition was used for the studies (0.2% C, 1% Mn,.03% P,.02% S and rest Iron). Mild steel coupons of 1.5cmx1.5cmx.1mm were used (1 cm^2 exposed area).They were abraded with various grades of silicon carbide papers (120, 400, 600, 800, 1000, 1200 and 1400) to obtain well-polished surfaces as per ASTM standards. The exact surface area of the metal specimens was determined accurately using a vernier calipers and screw gage. Then the metal pieces were degreased with acetone, washed with distilled water, to remove the possible residues of polishing and dried in air and finally weighed. Specimens were immersed in aggressive solutions in the absence and presence of the inhibitor in various concentrations.

Test solutions

1.0M HCl and 0.5M H$_2$SO$_4$ solutions were prepared by diluting analytical grade acids with de-ionized water. Stock solutions of the Schiff base inhibitors were prepared with respective acids and diluted to various concentrations in the range 50ppm −150ppm. For weight loss studies, 50ml of acid solutions were used, but 100ml was taken for the electrochemical investigations.

Weight Loss Measurements

In weight loss studies, the MS surfaces were directly exposed to acidic environments for a particular period of time in the absence and presence of the inhibitors and then the weight loss of the metal pieces were measured from which the inhibition efficiencies were calculated. The experiments were carried out in blank acid solutions and in the test solutions containing inhibitor concentrations ranging from 50 ppm to 150ppm. Mild steel (MS) coupons of 1.5cm x1.5cm x1mm

were used. The pre-weighed coupons were suspended in different concentrations of inhibitor in acid solution at 28^0C using glass hooks in the absence and presence of inhibitor in aerated condition. Test coupons were taken out and reweighed after 24 hours. The difference between the initial and final weights of the coupons gave the weight loss. The reproducibility of the experiments was ensured by carrying out duplicate and the average values were reported

The values of corrosion rate (K), inhibition efficiency (η_w) and the degree of surface coverage (θ) for MS immersed in acid in the absence and presence of different concentrations of inhibitor can be obtained from the weight loss method. The corrosion rate (k) in mg $cm^{-2}h^{-1}$ was calculated by the following equation.

$$k = \frac{\Delta W}{S.t} \tag{1}$$

ΔW is the weight loss of coupon (mg), S is the total area of the coupon (cm^2) and t is the time of treatment (hrs.).The degree of surface coverage (θ) and the inhibition efficiency η_w [142,143,114] were calculated using the equation 2, 3 respectively.

$$(\theta) = \frac{K_o - K}{K_o} \tag{2}$$

$$\eta_w = \frac{K_o - K}{K_o} \times 100 \tag{3}$$

Where k_o and k are the values of the corrosion rate without and with inhibitor, respectively.

Adsorption isotherms

The inhibitory action (anti-corrosive activity) of Schiff bases is due to the adsorption of these molecules on the metal surface. The adsorption on the metal surface may be physical adsorption, chemical adsorption or a mixture of both. The mode of adsorption can be explained by considering the adsorption isotherms.

These isotherms can explain the interactions of the inhibitor molecules with the active sites on the MS surface. The most commonly studied adsorption isotherms are Langmiur, Freundlich, Temkin and Frumkin. The isotherms are represented as equations and the best fit isotherm is accepted with the aid of correlation coefficient (R^2).

Langmiur adsorption isotherm $\quad \frac{C}{\theta} = \frac{1}{K_{ads}} + C$ (4)

Freundlich adsorption isotherm $\theta = K_{ads}C$ (5)

Temkin adsorption isotherm $\quad e^{f\theta} = K_{ads}C$ (6)

Frumkin adsorption isotherm $\frac{\theta}{1-\theta}\exp(f\theta) = K_{ads}C$ (7)

where C is the concentration of the inhibitor molecule, θ is the fractional surface coverage, f is the molecular interaction parameter and K_{ads} is the adsorption equilibrium constant. Among the different isotherms studied, the one which has the highest correlation coefficient (R^2) value was taken for interpreting the mechanism of adsorption.

The K_{ads} and ΔG^o are related by the equation

$\Delta G^o = -RT \ln (55.5 K_{ads})$ (8)

Where 55.5 is the molar concentration of water, R is the universal gas constant and T is the temperature in kelvin.

Effect of temperature

The change of corrosion inhibition behavior of the Schiff base molecules with temperature was studied in the range 30-60^{0}C. The MS specimens for weight loss measurements were kept at different temperatures such as 30^{0}C, 40^{0}C, 50^{0}C and 60^{0}C on a thermostat for 24 hours in the presence and absence of Schiff bases in

acidic solution and the data obtained was tabulated and were utilized to calculate the thermodynamic parameters of corrosion such as activation energy (E_a), Arrhenius factor (A), enthalpy of corrosion (ΔH^*) and entropy of corrosion (ΔS^*).

The energy of activation can be calculated using the Arrhenius equation

$$K = A\,exp\left(-\frac{E_a}{RT}\right) \tag{9}$$

where K is the rate constant, A is the Arrhenius factor, E_a is the activation energy, R is the universal gas constant and T is the temperature in Kelvin scale. A plot of logK Vs 1000/T will give a straight line with a slope $-E_a/2.303R$ and intercept log A.

From the transition state theory[144], the enthalpy and entropy of activation (ΔH^*, ΔS^*) can be calculated as

$$K = \left(\frac{RT}{Nh}\right)\exp\left(\frac{\Delta S^*}{R}\right)\exp\left(\frac{-\Delta H^*}{RT}\right) \tag{10}$$

where, N is the Avogadro number and h is the Plancks constant. The graph of logarithmic form of this equation gives a straight line with a slope $-\Delta H/2.303R$ and intercept $log\frac{R}{Nh} + \frac{\Delta S}{2.303R}$, from which enthalpy of activation and entropy of activation can be calculated.

Electrochemical measurements

Electrochemical techniques are widely used for the study of corrosion of metals. These advanced techniques are very useful in investigating the corrosion rate and exploring the mechanism of corrosion and corrosion inhibition. One of the foremost advantages of electrochemical methods is that it requires a short measurement time and provides a fast and a mechanistic info about the corrosion. The electrochemical behaviour of the metal in the presence and absence of the

inhibitor can be investigated using electrochemical systems and thereby providing a mechanistic way to calculate the inhibitive efficiency of the various organic compounds in acidic environment[145,146]. The electrochemical corrosion measurement techniques most commonly used are electrochemical impedance spectroscopy (EIS) and polarization studies. Polarization studies are further categorized into Tafel polarization analysis and linear polarization resistance analysis. Metallic corrosion involves two processes, the anodic dissolution (oxidation) of the metal and the cathodic hydrogen evolution. Analysis of the charge transfer processes during electrode reactions give electrochemical parameters such as corrosion current density, corrosion potential, charge transfer resistance, cathodic and anodic slope values etc. These values will help to calculate the rate of corrosion, the mechanism of corrosion and inhibition efficiency of inhibitor molecules.

Electrochemical Impedance Spectroscopy

The behavior of the metal/solution interface was studied using electrochemical impedance spectroscopic technique. Electrochemical impedance spectroscopy (EIS) or AC impedance methods are widely employed in corrosion experiments in recent years as a sophisticated and accurate method[147,148,149,150,151,152]. Kinetic and mechanistic information on corrosion inhibition mechanism can be attained by impedance measurements. The system response offers information about the different reactions taking place at the metal solution interface. The recognition of dielectric and electric properties of components under investigation is made possible by the system. Electrochemical analysis can be done with the help of appropriate equivalent electrical circuits[153].

Electrochemical measurements were realized using Computer controlled Metrohm Autolab PGSTAT 50519. The EIS measurements were carried out using a classical three electrode corrosion cell. A three electrode system was used to determine the potential across electro chemical interface accurately .Saturated Calomel Electrode was used as the reference electrode and MS coupons with exposed surface area $1cm^2$ as the working electrode and the Platinum electrode was used as the counter electrode. 100ml of acid solutions with and without inhibitor were used for the studies. After keeping the solutions for 1hr for stabilizing OCP, the values were measured. Nova Software was used to collect the experimental data.
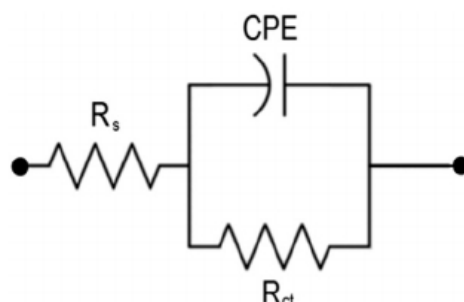
Fig. 1. Circuit diagram for EIS measurements (Randles circuit)

Electrochemical equivalent circuit model for the corrosion studies is shown in Fig.1.The Randles circuit is one of the simplest cell models. It is used to model corrosion processes. The R_{ct} is the charge transfer resistance and R_s is the solution resistance[154]. Modeling an electro chemical phenomenon with an ideal capacitor assumes that the surface under investigation is homogenous which normally not the case is. Since the interface is not ideal a constant phase element is used instead of pure capacitance. CPE is the constant Phase element. This non ideal behavior can be explained with the electrical double layer theory. There exists two capacitors in serial, one between the metal and outer Helm Holtz plane and another through the

Goupy Chapman diffuse layer and as a consequence a differential capacitance behavior occurs[115]. The impedance of the CPE could be expressed as[155,156,25].

$$Z_{CPE} = [Y_o(j\omega)^n]^{-1} \qquad (11)$$

Where Y_o is the admittance of an ideal capacitance, $j^2 = -1$ is the imaginary number, ω is the angular frequency and n is an empirical constant ranging from 0 to 1. The n values are connected to the deviation of ideal capacitance behavior. For ideal electrodes, the value of n is equal to one and for a pure resistor n is equal to zero. The inhibition efficiency was calculated using the following equation[157,158].

$$\eta_{EIS}\% = \frac{R'_{ct} - R_{ct}}{R'_{ct}} \times 100 \qquad (12)$$

where R_{ct} and R'_{ct} are the charge transfer at metal solution interface in the absence and presence of inhibitor respectively

Electrochemical impedance plots

Impedance measurements can be plotted using the Nyquist (Cole-Cole) plot, Bode plot and the impedance plot. The plot of the real part of impedance against the imaginary part gives a Nyquist plot. In the Nyquist plots a depressed single capacitive loop was obtained in each case i.e. the center of the each semicircle is depressed by an angle of $(1 - n) = 90°$. The solution resistance R_s(ohmic resistance), which is the resistance between the working electrode and the reference electrode, is given by the impedance (Z')value at high frequency side in the Nyquist plot. The frequency reaches a maximum value at the left most end of the semicircle, where the semicircle meets the x- axis. The frequency reaches its lowest value at the right end of the semicircle where the impedance of the system is the sum of R_s and R_{ct}.
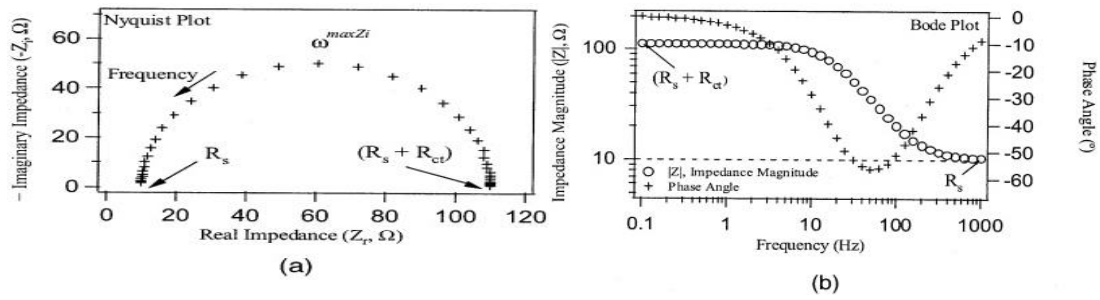
Fig. 2 Nyquist plot and Bode plots

In Bode plots, the impedance magnitude |Z| and phase angle θ are plotted on either y axis against frequency. |Z| can be obtained from equation $|Z| = \sqrt{Z'^2 + Z''^2}$.

The curve representing the |Z| against frequency called the impedance plot, will give the value of R_s and R_{ct}. The break point of this curve would lie on a straight line with a slope of -1. The value of C_{dl} is obtained on extrapolation to the y-axis (at f=1).

$$|Z| = \frac{1}{C_{dl}} \tag{13}$$

In the plot of θ versus f, the peak which corresponds to f ($θ^{max}$) shows the maximum phase shift and the C_{dl} can be evaluated from that. Frequency break points with each step are the characteristic of Bode and impedance plots. The Bode plot is a better alternative to the Nyquist plot as the problem with longer measurement time associated with low frequency can be evaded. This is the more complete way of presenting the data. The Bode plots show that the break point frequency shifted gradually to lower values as the concentration of the inhibitor increases. The Bode plots show a slightly broadened maximum which may account for the formation of a protective layer after 1hr of immersion time.

Potentiodynamic Polarization studies

Polarization method is a good technique when the potential of the working electrode is changed; that is polarized and measuring the current produced as a function of potential or time. Polarization may be of two types, activation polarization and concentration polarization, the former because of the resistance developed when electrical charge transfer occur through the double layer and latter due to the concentration gradient in the metal solution interface. When the polarization potential comes in the range of activation potential the important polarization measurement is Tafel extrapolation method.

Tafel extrapolation method

Polarization of the metal surface can be either anodic or cathodic; the anodic reaction being oxidation of the metal (anodic dissolution of metals) and cathodic being the reduction of H^+ ions to H_2 (cathodic hydrogen evolution). When the rate of anodic and cathodic reactions, both become equal, no charge accumulation will be there. The mixed potential observed at this instant is called the open circuit potential (OCP) and taken as corrosion potential or E_{corr}. To get the applied current density, (i_{app} as a function of the applied potential E), the potential between the reference electrode and working electrode is controlled and scanned at a constant rate. The potentiodynamic measurements were carried out for cathodic and anodic with a scan rate of 1mv/s. The Butler-Volmer equation[159] explains the polarization of reversible electrodes which are controlled by the activation polarization process.

$$i_{app} = i_{corr} \cdot \left[\exp\left(\frac{\alpha_A zF}{RT} \eta \right) - \exp\left(\frac{\alpha_C zF}{RT} \eta \right) \right] \tag{14}$$

where i_{app} is applied or measured current density and i_{corr} is corrosion current density; α_A and α_C are the charge transfer coefficients for anodic and cathodic reactions respectively. $\eta = E - E_{corr}$ gives the polarization (the difference between applied and corrosion potential);

z is valence of metal, F is Faraday constant; R is the universal gas constant and T is the absolute temperature. For anodic and cathodic polarizations, the Tafel slopes for the anodic and cathodic processes can be represented as,

$$b_a = \frac{2.303 \, RT}{\alpha_a zF} \tag{15}$$

$$b_c = \frac{2.303 \, RT}{\alpha_c zF} \tag{16}$$

The slope of a Tafel plot (b_a and b_c) gives information about the mechanism of the electrode reactions and the extrapolations of the cathodic and anodic curves gives the value of E_{corr}. The log i_{corr} values at the point of intersection of coordinates will give the value of corrosion current density from which the inhibition efficiency can be calculated using the following equation

$$\eta_{pol}\% = \frac{i_{corr} - i'_{corr}}{i_{corr}} \times 100 \tag{17}$$

where i_{corr} and i'_{corr} are uninhibited and inhibited corrosion current densities respectively[160,161].
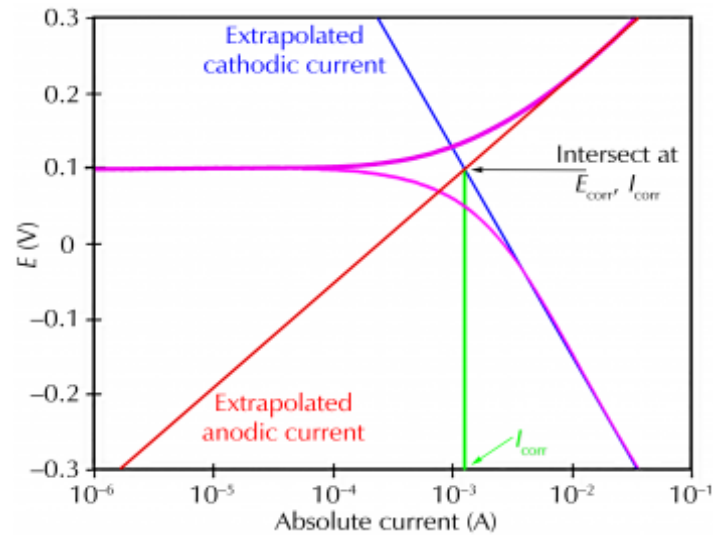
Fig.3.Tafel extrapolation method

Surface Morphological Studies

Surface studies of the MS specimens used for corrosion studies were done using SEM analysis, EDX spectral analysis and AFM analysis.

Scanning Electron Microscopic (SEM) Analysis was carried out on SEM Jeol JSM-4500 instrument. Micrographs of the MS surface before and after 24 hours immersion in acid solution with and without corrosion inhibitors were taken. The energy of the acceleration beam was 20kv and the given results are of 1000x magnitudes. Energy Dispersive X-ray (EDX) spectra were taken using BRUKER XFlash 6/10 instrument.The energy of the beam used was 30Mev. EDX spectra of the MS surface before and after 24 hours immersion in acid solution in the absence and presence of corrosion inhibitors were taken. Atomic Force Microscopic (AFM) Analysis was done using Bruker dimension edge model instrument in non-contact mode.

Biological studies of Curcuminoid analogues and their Transition metal chelates

The biological studies performed are Invitro cytotoxic study, Invivo antitumour study and effect of Schiff base compounds on solid tumour. Materials, cell lines, animals, chemicals etc. used in the studies are given in details.

Invitro cytotoxicity study

Materials

All reagents and chemicals used in the biological study were of analar grade.

Cell lines: Daltons Lymphoma Ascites cells and Ehrlich Ascites Carcinoma cells were obtained from the Adayar Cancer Research Institute, Chennai, India and maintained as transplantable tumours in Swiss albino mice by injecting a suspension of cells intraperitoneally (ip). The cells were aspired from the peritoneal cavity of the mouse after 15days of induction of tumour cells.

Preparation of Reagents:

Normal Saline: This was prepared by dissolving A.R.NaCl (0.85g) in 100 ml distilled water. Normal Saline is essential for preparing cell suspension, as the osmotic pressure due to it is isotonic with the fluids inside the cells and this will not cause death of the cell.

Phosphated Buffer Saline (PBS): It is used for maintaining the pH and isotonicity of the cells, failing which the cells may rupture during experiments. It is prepared by dissolving NaCl (8g), KCl(0.2g), $Na_2HPO_4.2H_2O$(1.44g) and KH_2PO_4(0.2g) in one litre distilled water.

Trypan Blue dye: Cell viability was determined using this dye which penetrates into dead cells and makes the identification of dead cells easier. It is prepared by dissolving 1 g Trypan blue in 100 ml distilled water.

Method

Invitro cytotoxicity studies were carried out using the Schiff bases and their metal complexes dissolved in minimum quantity of DMSO. The tumour cells aspirated from the peritoneal cavity of tumour bearing mice were washed with PBS (Phosphate Buffered Saline) and centrifuged for 15minutes at 1500 rpm. Cell viability was determined using Trypan blue exclusion method. Viable DLA cells (1×10^6 cells in 0.1 ml) were added to tubes containing various concentrations of the test compounds and the volume was made up to 1ml using PBS. Control tube contained only cell suspension. These mixtures were incubated for 3hrs at 37°C. Further, cell suspension was mixed with 0.1ml of 1% Trypan blue and kept for 2-3 minutes and loaded on a haemocytometer. The number of stained (dead) and unstained (live) cells were counted and percentage cytotoxicity was evaluated by Trypan blue exclusion method.

$$\% \; cytotoxicity = \left(\frac{No.of \; dead \; cells}{No.of \; dead \; cells + No.of \; live \; cells} \right) \times 100 \qquad (18)$$

Invivo antitumour studies

Cell lines: EAC and DLA cell lines were maintained as ascites tumours in the animal Swiss Albino mice. The tumour cells were aspirated and washed thrice with PBS. The cells were then suspended in saline solution so as to have a cell suspension of 1 million cells/ml. Then one ml of the cell suspension was injected into the peritoneal cavity of active Swiss albino mice. The test animals were fed with normal diet and within 10-14 days ascites fluid that contain cancer cells gets accumulated in the abdomen of the animal. The animals grow with this tumour in the body and die within 18-20 days. These cells are transmitted regularly by transferring it to other normal mice as mentioned above to maintain the cell lines.

Animals: Swiss albino mice (7-8 weeks old weighing 25-30g, male) were purchased from the Small Animal Breeding Station (SABS), Kerala Veterinary and Animal Sciences University, Mannuthy, Thrissur, Kerala. They were sheltered in well ventilated cages under standard conditions of temperature and humidity in the animal house of Amala Cancer Research Centre. The animals were fed with normal mouse chow (Lipton India) and water *ad libitum*.

All the animal experiments in the present study were carried out with the prior approval of the Institutional Animal Ethics Committee (IAEC) and were conducted strictly according to the rules of Committee for the Purpose of Control and Supervision of Experiments on Animals (No.149/PO/Rc/S/1999/CPCSEA) constituted by the Animal Welfare Division, Govt. of India.

Preparation of drug suspension

For animal studies, drug suspension was prepared by using CMC (carboxy methyl cellulose). Dissolved 0.05gm carboxy methyl cellulose in 10ml of distilled water.

For preparing the drug, 0.01gm Schiff bases and their metal complexes were dissolved in 5ml of ethanol. Both solutions were mixed in a 50ml beaker and kept the mixture in a water bath for the evaporation of ethanol to get the drug in the slurry form.

The standard drug cyclophosphamide was prepared by dissolving 25mg/kg body weight of the mice in phosphate buffered saline (PBS) solution. About 0.01 ml of this drug was given to each mouse for consecutive ten days.

Determination of tumour reducing activity

The animals (male mice, 6-8 weeks old) weighing 20-25g were divided into groups of 5 animals each. EAC cells (1×10^6 cells per animal) were injected into the peritoneal cavity of mice. One group of animals was kept as control, without injecting any test compound. The other groups were injected with different concentrations (20μg/ml, 10μg/ml and 5μg/ml) of the test compounds after the tumour formation and injections were continued for ten days. The mortality rate of animals due to tumour burden was noted and the percentage increase in life span (ILS) was calculated using the given formula.

$$\%ILS = \left(\frac{T-C}{C}\right) \times 100 \qquad (19)$$

Where, T and C are mean survival time of treated and control mice respectively in days[162].

Normal Swiss Albino mice

Tumour bearing mice

Determination of effects of compounds on solid tumour development

The Swiss albino mice were used to study the effect of the synthesized compounds on solid tumour volume reduction. Since the synthesized Schiff bases and their copper complexes are found to be more cytotoxic to DLA cell lines, they were used to study its potential to reduce solid tumour induced by DLA cell lines in mice. The animals were divided into groups of six. Viable DLA cells (1×10^6 cells per animal) were transplanted subcutaneously into the right hind limb of the mice. Drugs (50 and 100mg /kg of body weight) were injected to the animals on alternate days for two weeks. The group that received only DLA cells served as the control. The tumour development on animals was determined by measuring the diameter of the tumour growth in two perpendicular phases using vernier calipers, every third day for one month. The tumour volume was calculated using the formula given,

$$V = \frac{4}{3}\pi r_1 r_2^2 \qquad\qquad (2)$$

Where, r_1 and r_2 are the minor and major radii respectively[163].

PART IV

SYNTHESIS, CHARACTERIZATION, ELECTROCHEMICAL AND ANTITUMOUR STUDIES OF METAL CHELATES OF SCHIFF BASES DERIVED FROM CURCUMINOID ANALOGUES

CHAPTER I

SYNTHESIS AND CHARACTERIZATION OF SCHIFF BASES DERIVED FROM ARYL AZO DERIVATIVE OF 1,7-DIARYL HEPTA 1,6-DIENE-3,5-DIONES AND THEIR TRANSITIONMETAL CHELATES WITH Cu(II), Zn(II) & Ni(II)

SECTION-I

Synthesis and characterization of Schiff bases derived from aryl azo derivative of 1,7-bis(thiophen-2-yl)-hepta-1,6-diene-3,5-dione and 1,7-bis(3-methyl thiophen-2-yl)-hepta-1,6-diene-3,5-dione with ethylene diamine and their transition metal complexes

Synthesis and characterization of Schiff base ligands

This unit deals with the synthesis and characterization of two Schiff bases derived from aryl azo derivative of curcuminoid analogues with heterocyclic rings (thiophenyl ring). The compounds synthesized are bis(1,7-di(thiophen-2-yl)-4-(phenyl-hydrazono) - hepta-1, 6-diene-3,5-dione) ethylenediimine (1a) and bis (1,7-di(3-methyl thiophen-2-yl)-4-(phenyl-hydrazono)-hepta-1,6-diene-3,5-dione) ethylenediimine (1b) .

Synthesis of 1,7–dithiophenyl heptanoids

The 1,7–dithiophenyl heptanoids were prepared by the condensation of heterocyclic aldehydes (thiophen-2carboxaldehyde and 3–methyl thiophen–2-carboxaldehyde) with acetylacetone and boric oxide complex in ethyl acetate medium in the presence of tributyl borate and n – butyl amine. The reaction usually produce α,β- unsaturated 1,3-diketones with heterocyclic rings attached to it. The reaction products 1,7-di(thiophen-2-yl)hepta-1,6-diene-3,5dione and 1,7-bis(3-methyl thiophen-2-yl) hepta-1,6-diene-3,5-dione were purified by column chromatography over silica gel (60 – 120 mesh) using 4:1 (v/v) chloroform: acetone mixture as the eluent and recrystallized twice from the hot benzene to get pure crystalline material. The product formation can be represented in a schematic way (scheme 1.1)

scheme 1.1
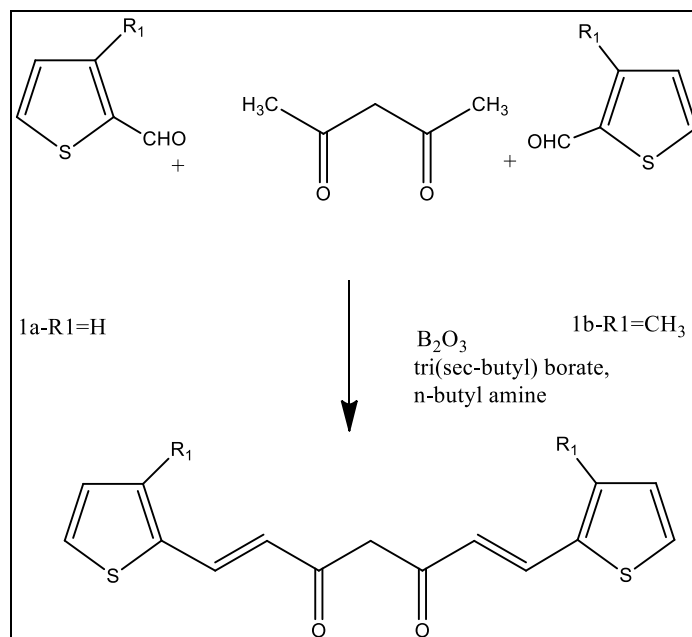
Synthesis of Schiff bases bis(1,7-di(thiophen-2-yl)-4-(phenyl-hydrazono)-hepta-1,6diene-3,5-dione)ethylenediimine and bis(1,7-di(3 methyl thiophen-2-yl)-4-(phenyl-hydrazono)-hepta-1,6diene-3,5-dione)ethylenediimine

The synthesized β-diketones were coupled with benzene diazonium salt. Benzene diazonium salt (0.01 mol) was prepared as reported earlier and it was added drop by drop to a solution of the β-diketones (0.01 mol in 15ml methanol) at below 0^0C with constant stirring. The precipitated compounds 1,7-bis(thiophen-2-yl)-4-(phenyl-hydrazono)-hepta-1,6-diene-3,5-dione and 1,7-bis(3-methyl thiophen-2-yl)-4-(phenyl-hydrazono)-hepta-1,6-diene-3,5-dione were filtered, washed with water and recrystallized from ethanol to get chromatographically pure (TLC) material. The Schiff bases were synthesized by the condensation of 1,7-bis(thiophen-2-yl)-4-(phenyl-hydrazono)-hepta-1,6-diene-3,5-dione and 1,7-bis(3-methyl thiophen-2-yl)-4-(phenyl-hydrazono)-hepta-1,6-diene-3,5-dione with 1,2-diaminoethane (en) as follows. An ethanolic solution of the 1,2-diaminoethane

(0.01mol, 20ml) was added to an ethanolic solution of the synthesized compound (0.02mol, 20ml). The solution was stirred using a magnetic stirrer for approximately 5 hours and evaporated at reduced pressure. The crystalline compound formed was filtered and recrystallized from hot methanol to get chromatographically (TLC) pure compound. The condensation product formation can be represented in a schematic way (scheme 1.2)
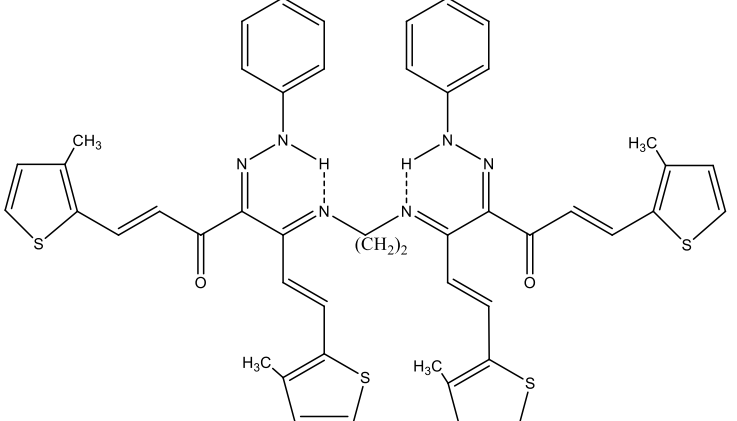
Scheme 1.2

1a,Ar= thiophen-2-yl; 1b, Ar= 3 methyl thiophen-2-yl
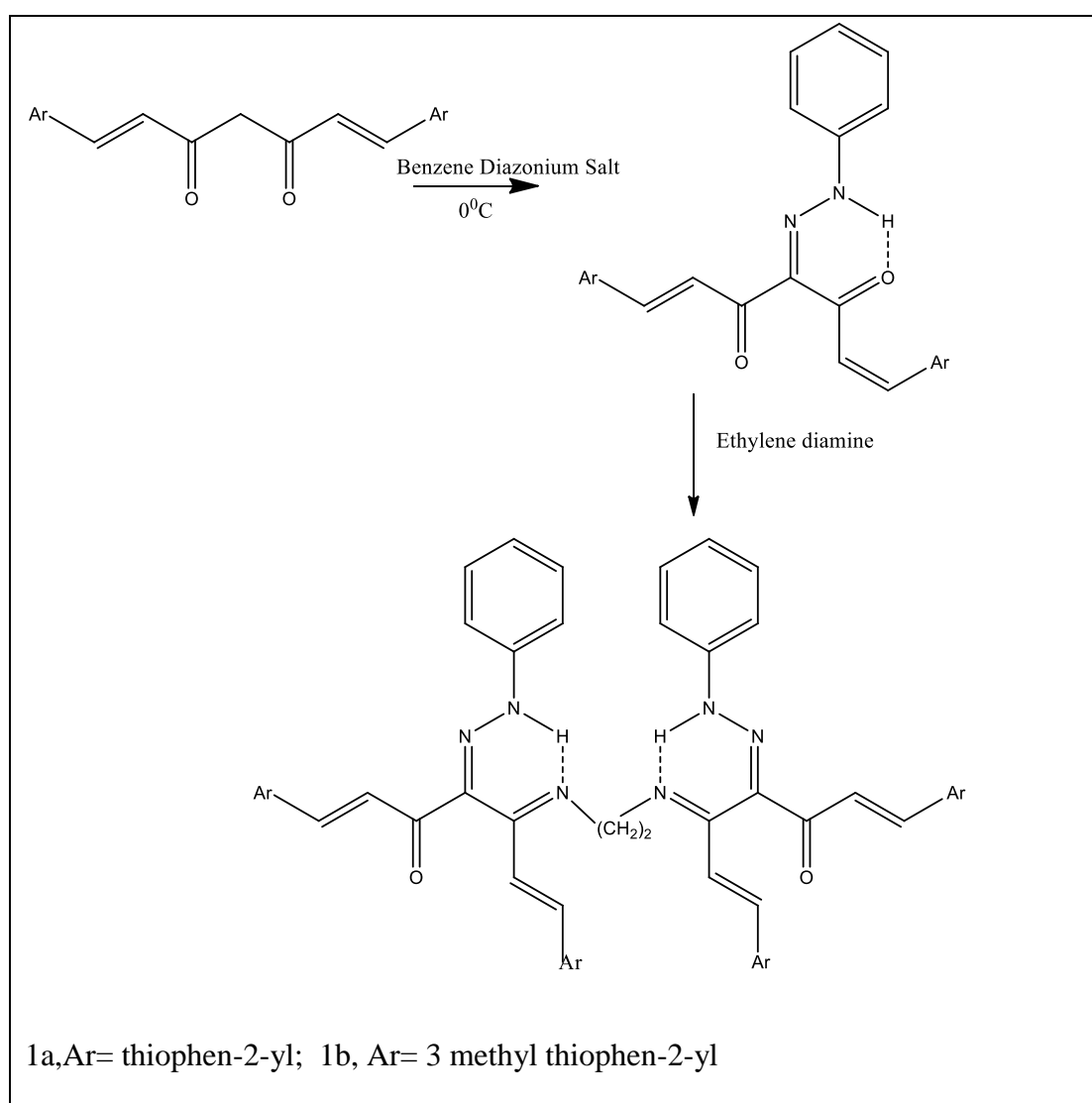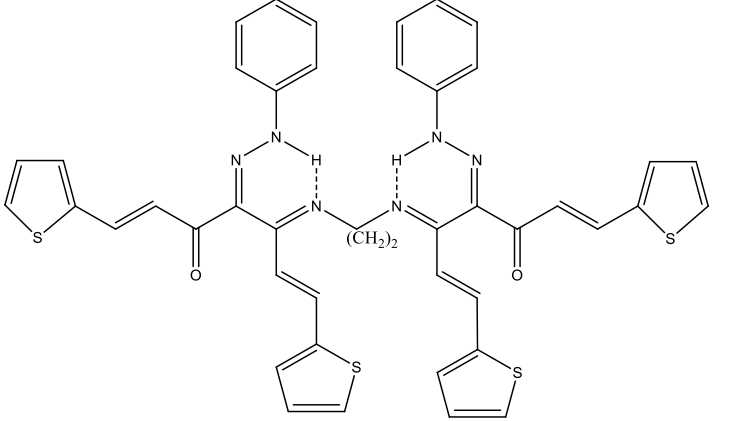
The Schiff base compounds are crystalline in nature and obtained in good yield nearly 75%. They show sharp melting point and are soluble in organic solvents like

ethylacetate, chloroform, acetone, ethanol, etc. The structures of the Schiff bases

prepared, its systematic name and yield are given in Table1.1

Table 1.1 Synthetic details of Schiff bases derived from aryl azo derivatives of thiophene substituted 1,7-diphenyl heptanoids

Compounds	Structure and systematic name of Schiff base ligands	Yield %
1a Systematic name Trivial name	 1,14-di(thiophen-2-yl) 5,10-di(ethylene- thiophen-2-yl)-6,9-diazotetradeca 1,5,9,13-tetraene -3,12-dione 4,11-diphenyl-hydrazone [TEDTDH] Bis(1,7-di(thiophen-2-yl)-4-(phenyl-hydrazono)-hepta-1,6-diene-3,5-dione)ethylenediimine	71
1b	 1,14-di(3 methyl-thiophen-2-yl) 5,10-di(ethylene- 3 methyl-thiophen-2-yl)-6,9-diazotetradeca 1,5,9,13-tetraene -3,12-dione 4,11-diphenyl-hydrazone [MTEDTDH] bis(1,7-di(3 methyl thiophen-2-yl)-4-(phenyl-hydrazono)-hepta-1,6-diene-3,5-dione)ethylenediimine	70

The observed C, H, N percentage and molecular weight determination together with the mass spectral data of the compounds clearly suggested the formation of bis-condensation product in which two equivalents of hydrazono compounds condensed with one equivalent of ethylene diamine as shown in Scheme 1.2

Characterization of Schiff bases derived from the aryl azo derivatives of thiophene substituted 1,7-diphenyl heptanoids

The Schiff bases 1a & 1b synthesized were characterized by various spectral techniques. UV, IR, 1H NMR, 13C NMR, 2D Cosy and Mass spectral techniques were used. The spectral techniques used are discussed below.

Table 1.2   Analytical & UV spectral data of 1a & 1b

Compounds	MP.(^{o}C)	Elemental analysis (%) Found/(Calculated)			Molecular weight	UV λ_{max} (nm)
		C	H	N		
1a	132	64.12 (64.51)	5.41 (5.66)	10.01 (10.25)	819.13	272, 356
1b	150	65.64 (65.86)	5.98 (6.21)	9.43 (9.60)	875.24	275, 352

IR spectra

Importance of IR spectra in establishing the hydrogen bonded imine hydrazone form has been well established. The spectra mainly gives idea about the nature of the carbonyl group, C=N groups present, whether NH is free or in the hydrogen bonded form. The presence of α,β − unsaturation in the   compounds can be

established using IR spectroscopy. The IR spectral data of compounds 1a&1b are presented in Table1.3.

Table 1.3   IR spectral data of Schiff bases derived from the aryl azo derivatives of thiophene substituted 1,7-diaryl heptanoids

Compounds		Probable IR assignments
1a	1b	
1658	1660	ν(C=O)
1628	1636	ν(C=N) hydrozono
1608	1600	ν(C=N) imine
1548	1552	ν (C-C) alkenyl
956	967	ν (CH=CH) trans
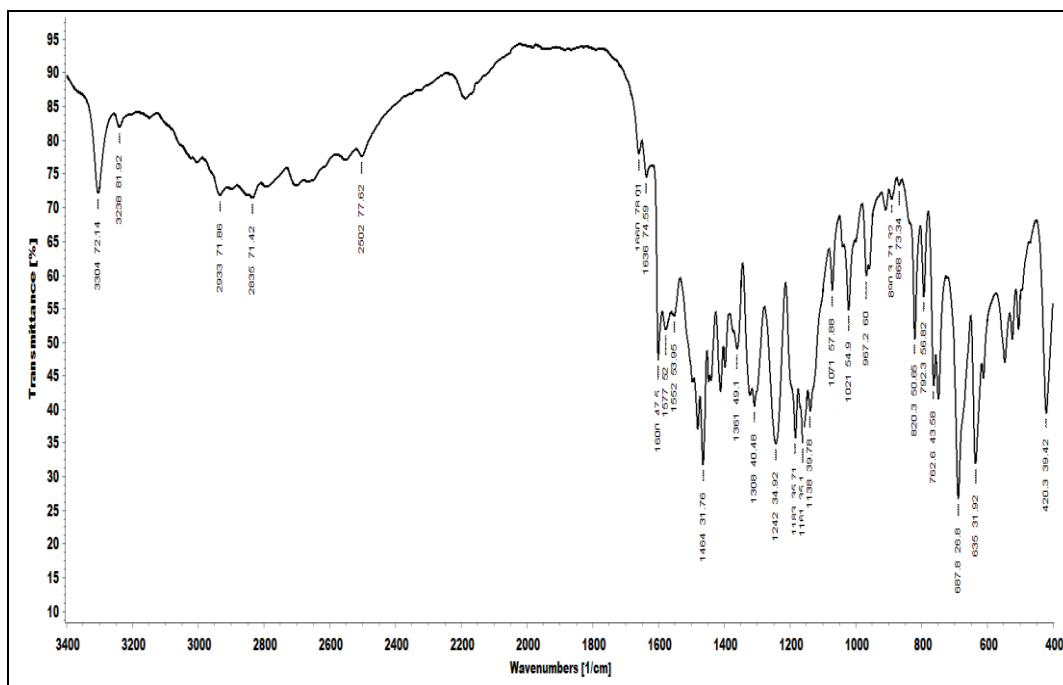
Fig.1.1   IR spectrum of Schiff base 1b

The values corresponding to free ν(C=O) are 1658 and 1660 cm^{-1} for 1a&1b respectively. Usually free carbonyl group with conjugation gives stretching frequency at ~ 1660 cm^{-1}. The hydrazono C=N showed its frequency band at 1628 and 1636 cm^{-1} for 1a and 1b respectively. The imine C=N showed its bands at 1608 and 1600 for 1a and 1b respectively. The peak at ~1577 can be assigned to the NH vibration. A weak, broad N-H stretch is observed for the N-H…N form at 3200-2400 cm^{-1}.Thus the observed position and intensity of these bands indicated that the compound exists in strong intra molecular hydrogen bonded form. Medium intensity vibrations were observed in the region 1530-1600 cm^{-1} due to various ν (C=C) vibrations of the thiophenyl ring system. Other IR peaks due to ν(C-C) alkenyl, ν $_{as}$(C-C-C) chelate ring, ν $_s$(C-C-C) chelate ring & β (C-H) chelate ring were present in the spectra. The IR spectra of these Schiff bases were also characterized by the trans ν(CH=CH) vibrations occurring at 956 & 967 cm^{-1} respectively for 1a & 1b. IR spectrum of 1b is given in Fig.1.1.

^{1}H NMR spectra

The different types of protons have their characteristic chemical shift values in ^{1}H NMR spectra. The numerical denomination in ppm of the chemical shift for a proton gives an indication regarding the type of proton originating that particular signal. The thiophenyl Schiff bases showed specific   peaks corresponding to NH, methylene, alkenyl and thiophenyl protons (Table.1.4). The NMR spectra of the aryl azo derivative of thiophene based diketones and its Schiff base (1a) are given in Fig 1.2 and Fig 1.3 respectively. Schiff base compounds 1a & 1b displayed a one proton singlet at ~ 8.5ppm assignable to strong intra molecularly hydrogen bonded NH proton. Another multiplet at ~ 2.7 ppm corresponds to the methylene protons

which was absent in the spectrum of aryl azo derivative. The spectral data suggested the structure given below.
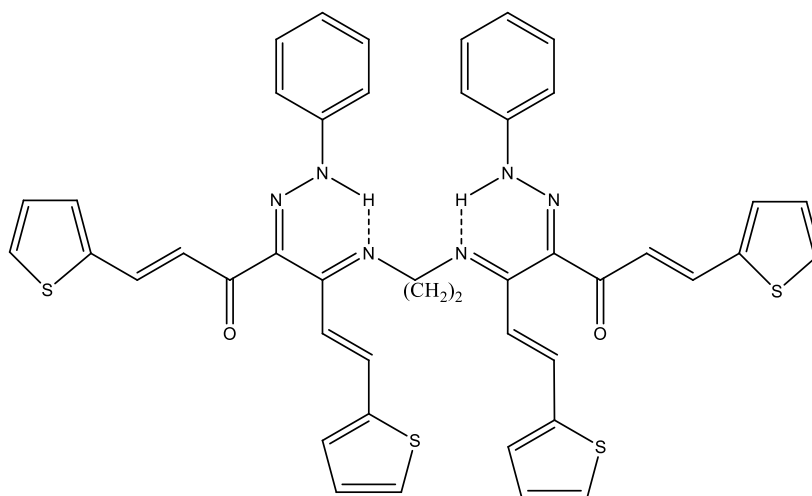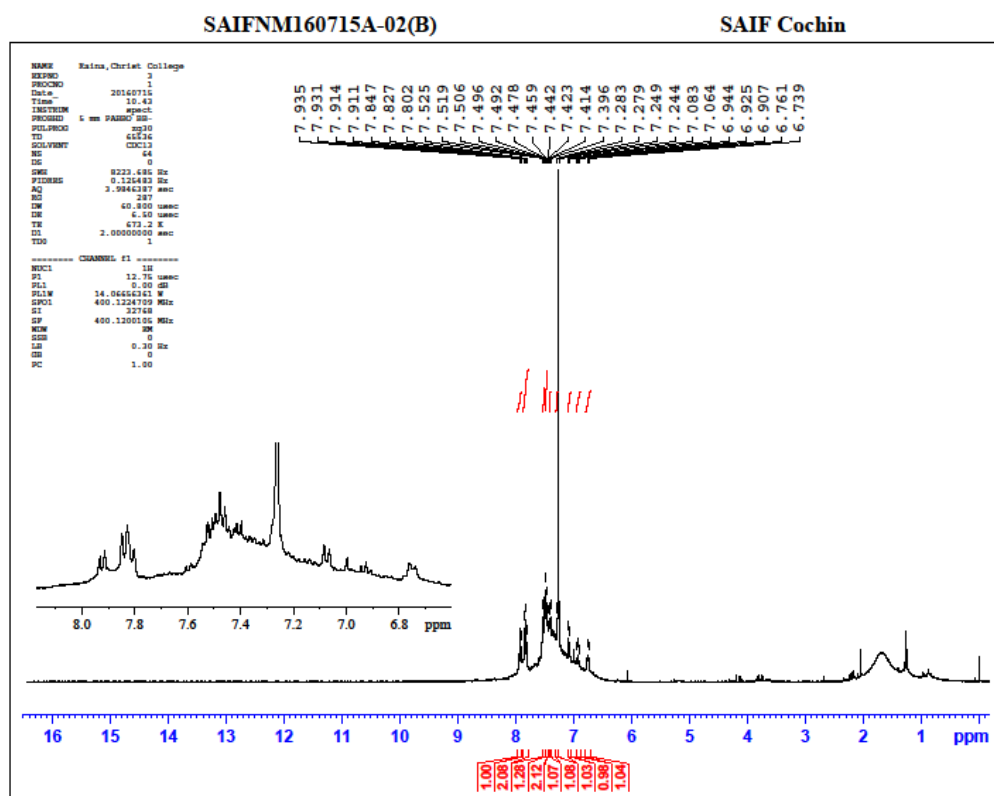

Hydrazono structure of Schiff base

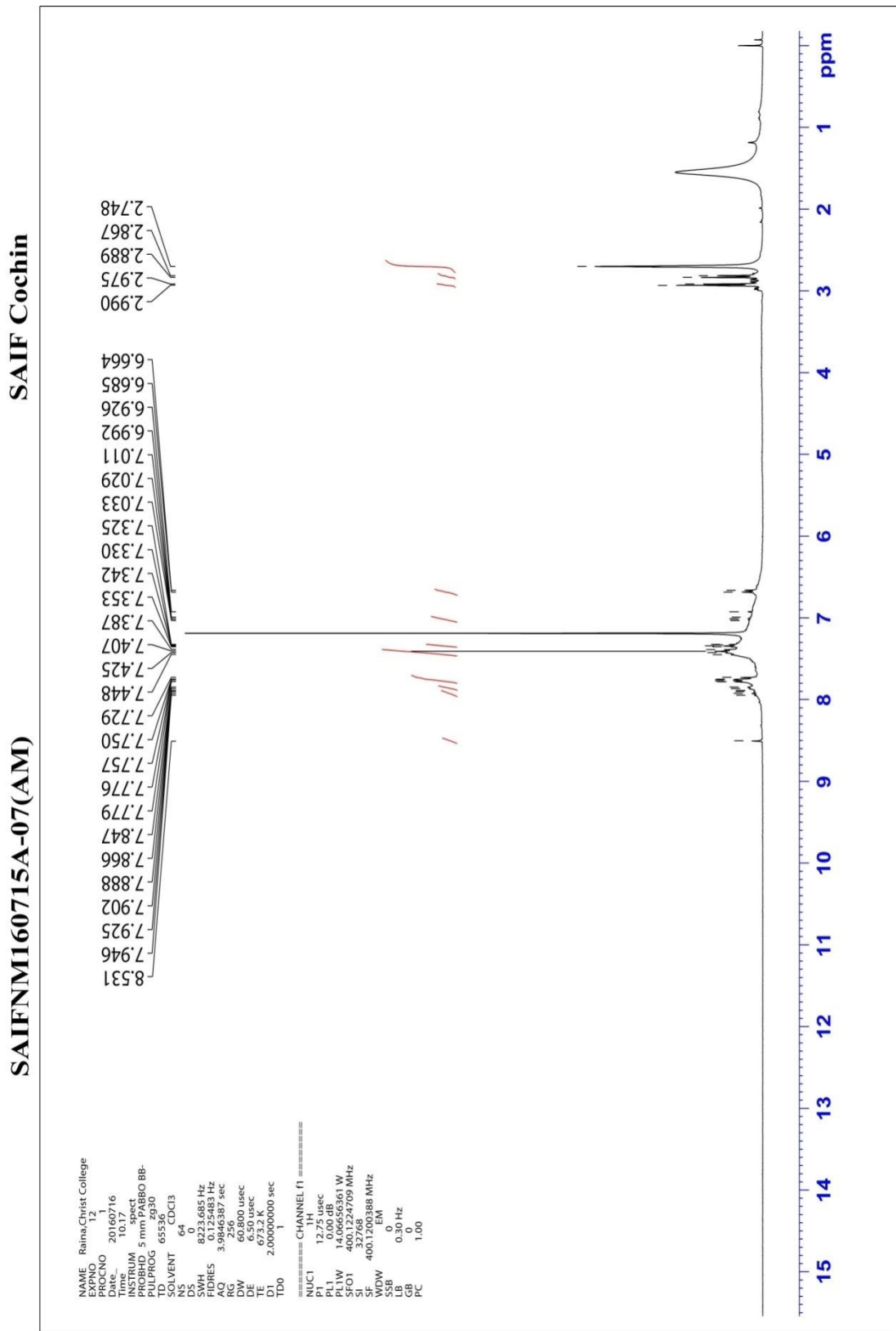**Fig.1.2   NMR spectrum of aryl azo derivative of thiophene substituted 1,7-diaryl heptanoids**

SAIF Cochin

8.531
7.946
7.925
7.902
7.888
7.866
7.847
7.779
7.776
7.757
7.750
7.729
7.448
7.425
7.407
7.387
7.353
7.342
7.330
7.325
7.033
7.029
7.011
6.992
6.926
6.685
6.664

2.990
2.975
2.889
2.867
2.748

SAIFNM160715A-07(AM)

ppm 15 14 13 12 11 10 9 8 7 6 5 4 3 2 1

Fig.1.3   NMR spectrum of Schiff base 1a

Table 1.4 **¹H** **NMR spectral data of Schiff bases derived from the aryl azo derivatives of thiophene substituted 1,7-diaryl heptanoids**

Compounds	Chemical shifts (δ ppm)				
	NH	Aryl	alkenyl	(CH$_2$)	CH$_3$
1a	8.531	7.011-7.88	6.664-7.946	2.74-2.990	-
1b	8.35	7.159-7.95	6.826-7.926	2.82-2.967	2.548

Further signals visible in the ¹H NMR spectra were that of the thiophenyl and phenyl ring protons which were present in the range δ 7 .01 − 7.84ppm and the alkenyl protons which were in the range 6.6 − 7.9ppm. The methyl substituent on the thiophenyl rings of Schiff base 1b showed a characteristic peak at 2.5ppm as assumed. The ¹H NMR spectra of 1a is given in Fig.1.3.

2D COSY NMR

Correlation spectroscopy (cosy) is a type of two dimensional nuclear magnetic resonance spectroscopy (2DNMR) and provides more information about a molecule than one dimensional NMR. 2D H' − H' COSY NMR spectrum of the aryl azo derivative of thiophene substituted 1,7-diaryl heptanoids was taken (Fig.1.4 & 1.5) as an additional information to the ¹H NMR spectrum. On comparing the spectrum with that of Fig.1.2, it was found that alkenyl and phenyl protons are exactly at the same position as mentioned earlier
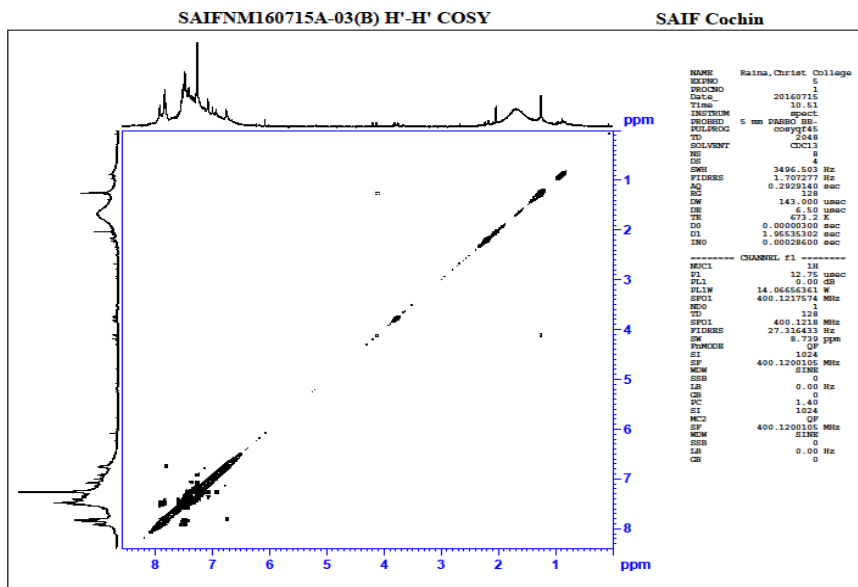
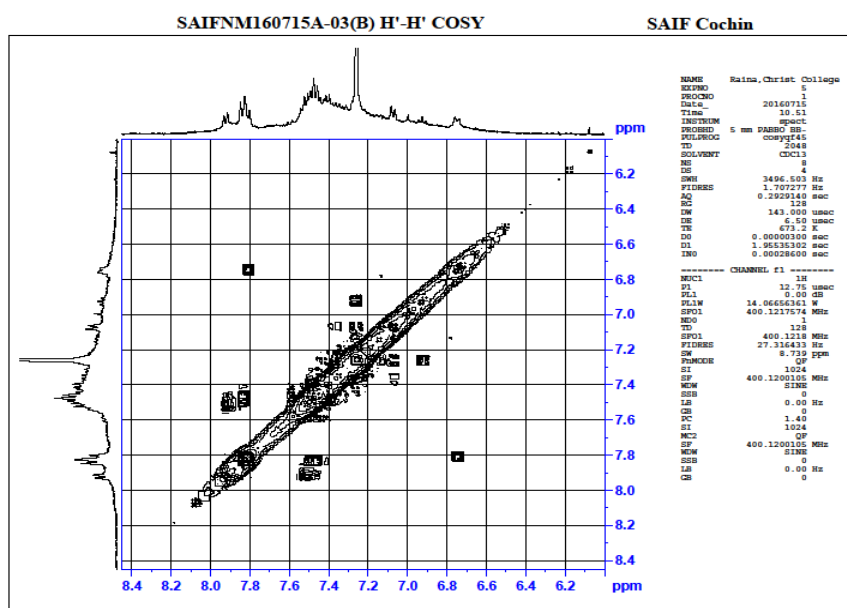**Fig.1.4 2D COSY NMR spectrum of aryl azo derivative of thiophene substituted 1,7-diaryl heptanoids**

Fig.1.5 2D COSY NMR spectrum of aryl azo derivative of thiophene substituted 1,7-diaryl heptanoids

^{13}C NMR spectra

The ^{13}C NMR spectral data of Schiff bases 1a and 1b are given in Table 1.5 & 1.6. In the ^{13}C NMR spectra, every non-equivalent carbon atom in an organic compound gives rise to specific peaks with a different chemical shift. The spectra help in the identification of chemically and magnetically dissimilar carbon atoms. The peak corresponding to C1 (methylene) was present at a position ~ at 44.2 ppm in 1a & ~46.484ppm in 1b. The C4 carbon of carbonyl appeared at a position at~ 192ppm in 1a & ~193ppm in 1b. In ^{13}C NMR, the carbonyl group carbons have the greater chemical shifts (down field). The alkenyl carbon atoms of both Schiff bases 1a & 1b were present at a position nearer to the thiophenyl ring system. They were seen at 134.21, 134.24ppm (C6) &123.40, 123.01ppm (C5) of Schiff bases 1a and 1b respectively. The ring carbon atoms showed peaks between 121 – 134ppm. The ^{13}C NMR spectra of Schiff base 1a and 1b are given in Fig.1.6 and Fig.1.7. In the ^{13}C NMR spectrum of 1b the carbon to which the methyl group is attached was shifted to 132.15ppm. Also in Schiff base 1b the methyl group was present at a position ~ 20ppm.
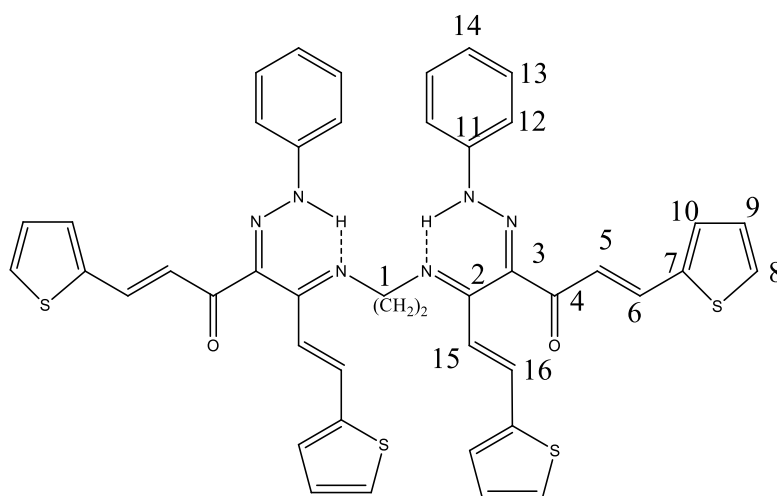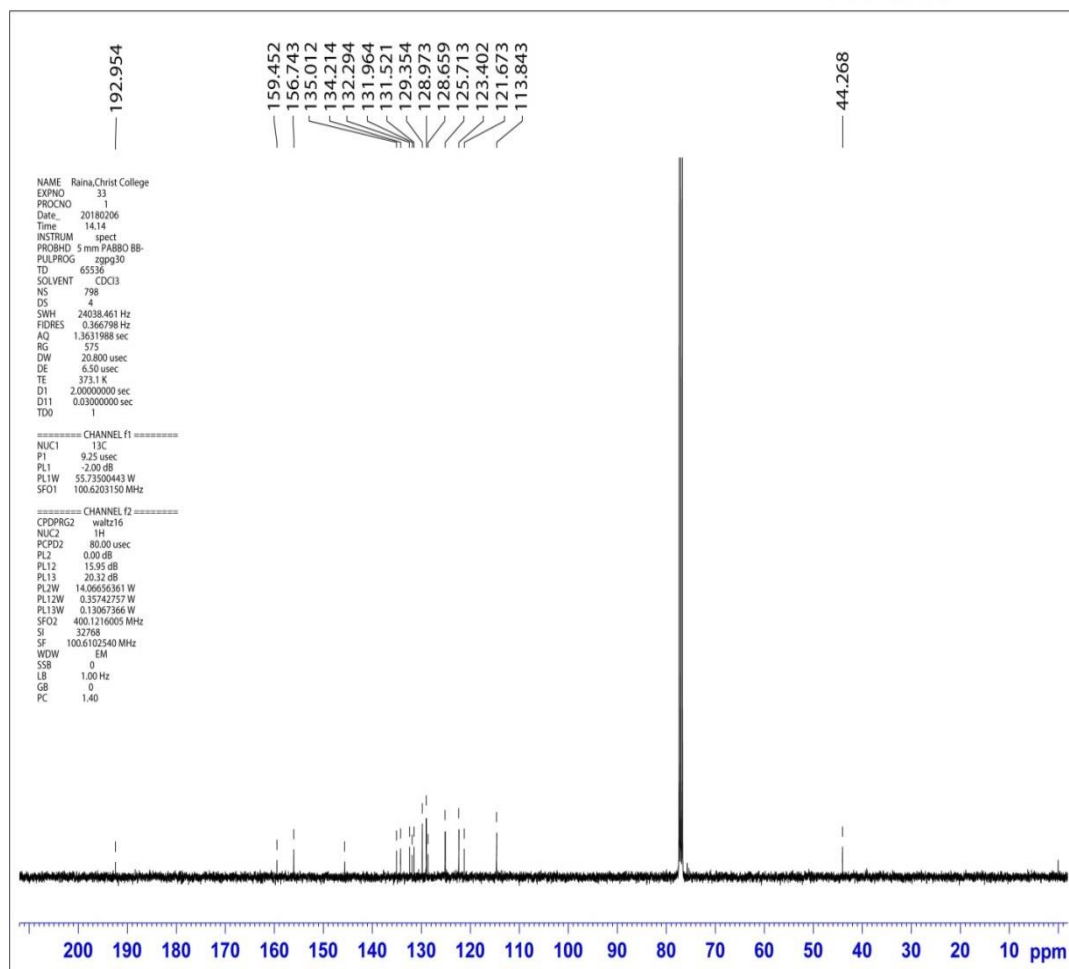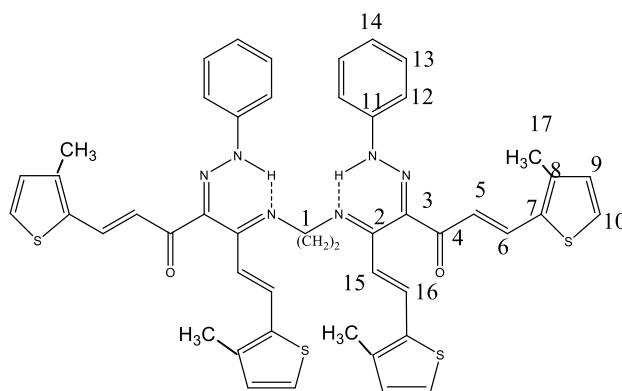

Structure representing different carbon atoms in 1a.

Fig.1.6 **^{13}C NMR spectrum of Schiff base 1a**

Table1.5 **^{13}C NMR spectral data of Schiff base 1a**

C1	C2	C3	C4	C5	C6	C7	C8
44.268	159.45	156.74	192.95	123.402	134.21	135.01	132.294
C9	C10	C11	C12	C13	C14	C15	C16
131.521	129.354	131.964	121.673	128.973	125.713	113.84	128.65

Structure representing different carbon atoms in 1b.

Table1.6 ^{13}C NMR spectral data of Schiff base 1b

C1	C2	C3	C4	C5	C6	C7	C8	C9
46.48	152.99	149.55	193.54	123.01	134.24	135.15	132.15	130.261

C10	C11	C12	C13	C14	C15	C16	C17	
129.798	131.75	121.24	128.96	15.117	114.63	128.96	20.36,19.42	
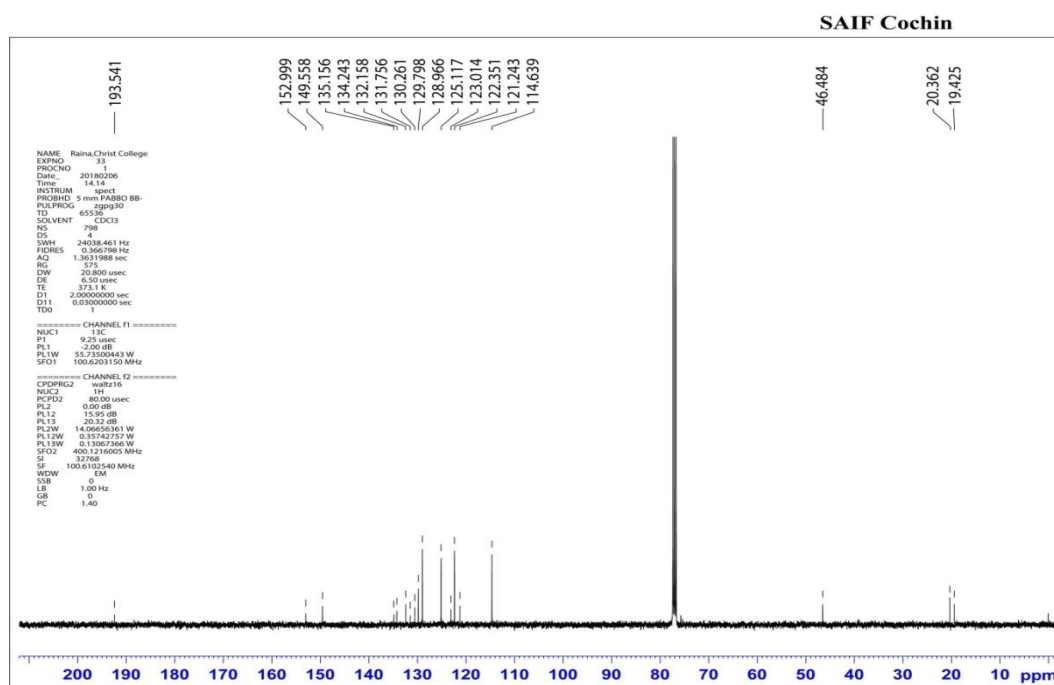
Fig1.7 ^{13}C NMR spectra of 1,7-di(3 methyl thiophen-2-yl)hepta-1,6-diene-3,5-dione

Mass Spectra

In the mass spectrum, ions were identified as a function of their m/z (mass to charge) ratio. The m/z value of the molecular ion peak seen in the mass spectrum gives the molecular weight of the compound. The fragmentation of the molecular ion produces a series of molecular fragments called the fragment ions. These ions appear at m/z values which corresponds to their individual masses. The mass spectra of the aryl azo derivative of thiophene substituted 1,7-diaryl heptanoids and corresponding Schiff base 1a are given in Fig.1.8 and Fig. 1.9 respectively. The mass spectrum of the aryl azo derivatives showed an intense molecular ion peak at 392 and a base peak at 105 which was due to the $[C_6H_5N_2]^+$ ion. The mass spectrum of Schiff Base 1a showed a molecular ion (M+1) peak at 810 and a base peak (the most intense peak) at 143 which was due to fragment G in Scheme 1.3. On comparing the mass spectra of aryl azo derivative and its Schiff base it is evident that the mass is doubled in case of Schiff base. The removal of various groups from the molecular ion, according to the pattern, led to the formation of smaller fragments which can be easily identified in the mass spectrum and are given in Table 1.7. Mass peaks due to the elimination of small groups like O, OH, CO, SC_3H_3, C_2H_2, CH_2, $CH_2=C=O$, $CH=C=O$, C_2H_2O etc. were present in the spectra of 1a and 1b. In the mass spectrum of 1a and 1b some small fragments were observed other than the fragmental pattern shown in Scheme 1.3. A strong peak was observed at 738 due to the removal of a sulphur and 3CH groups.
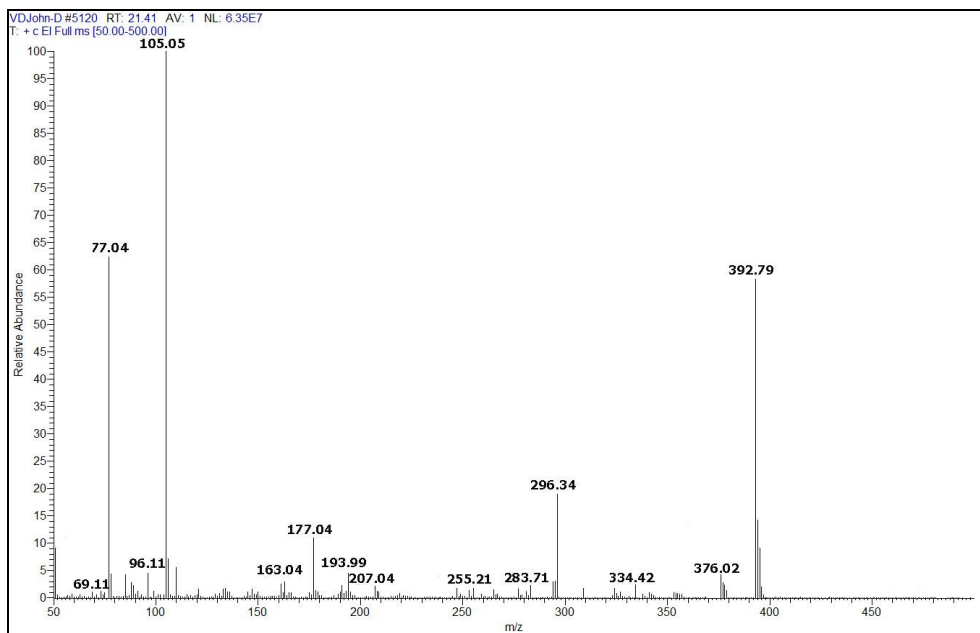
Fig1.8   Mass spectrum of aryl azo derivative of 1,7-di(thiophen-2-yl)hepta-1,6-diene-3,5-dione
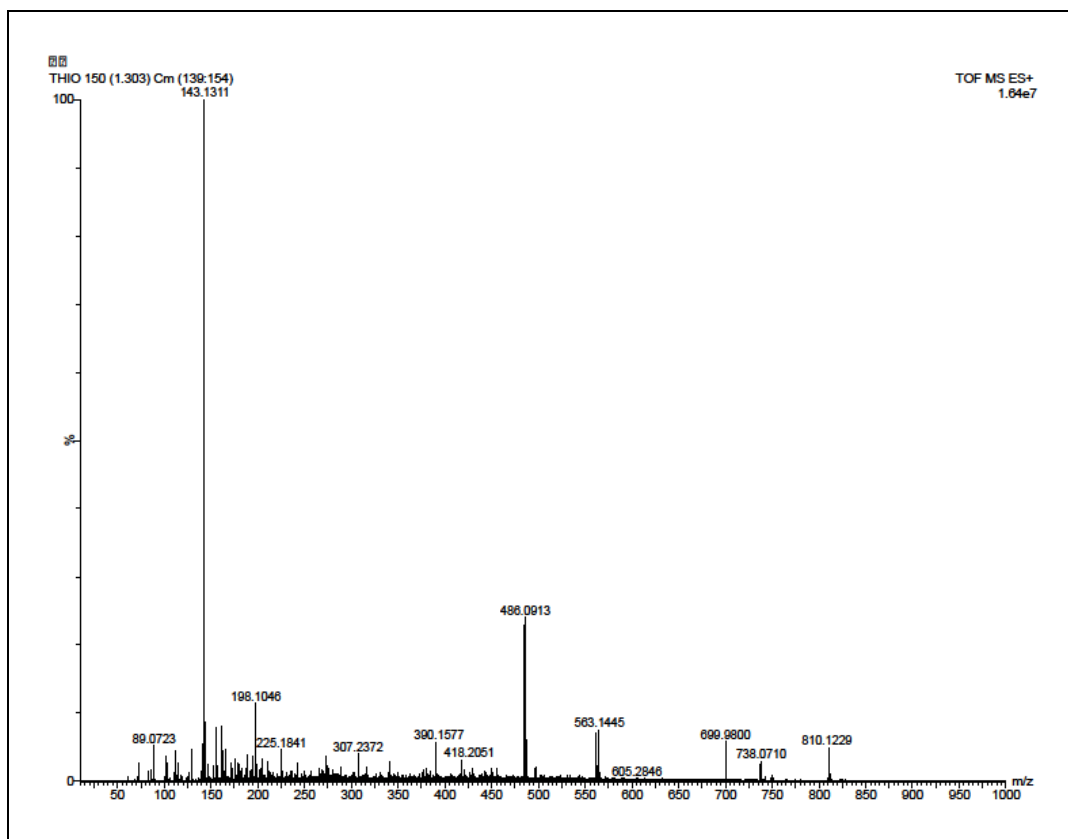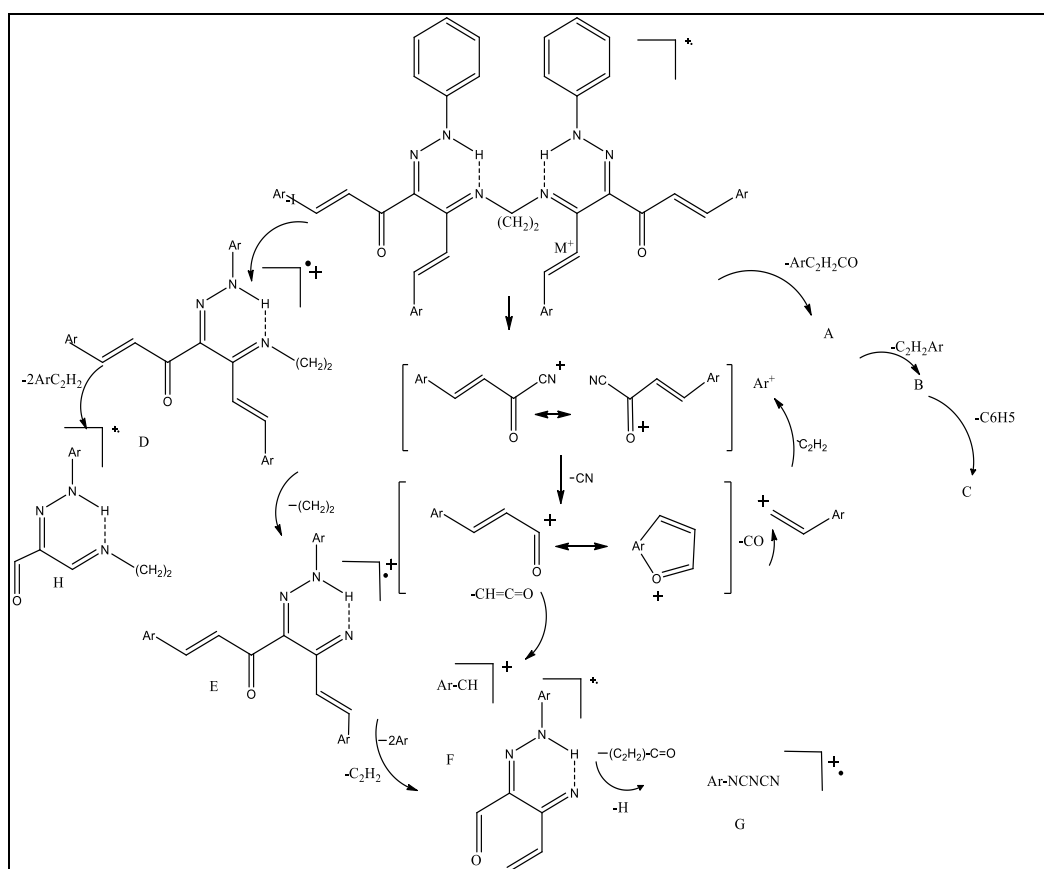

Fig.1.9   Mass spectrum of Schiff base 1a

Table1.7   Mass spectral fragmental pattern of 1a and 1b

Fragments	Ligands	M+1,M ions	A	B	C	D	E	F	G
Mass	1a	810	699	563	486	418	390	198	143
Patterns	1b	875	752	601	524	457	428	198	143

*The alphabets correspond to the fragments given in **Scheme 1.3.**

Scheme 1.3 Mass fragmentation pattern of Schiff bases

1a, Ar=thiophen-2yl,   1b, Ar= 3 methyl thiophen-2yl

Optimized molecular structure

Optimized molecular structure was obtained by DFT method using B3LYP/6-31G (d,p)basis set. The structure of the inhibitor molecule for the optimization process was drawn using Gauss view 5.0. The optimized molecular structure of Schiff base 1a is given in Fig.1.10
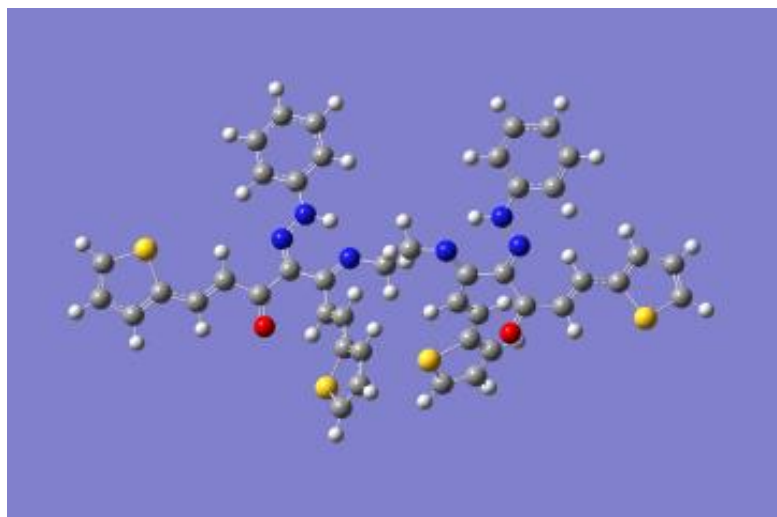

Fig.1.10   The optimized molecular structure of the TEDTDH (1a) using DFT at the B3LYP/6-31G (d,p)basis set.

Synthesis and characterization of metal chelates of Schiff bases 1a and 1b

Synthesis of metal complexes of Schiff base (1a) and Schiff base (1b)

Copper(II),Zinc(II) and Nickel(II) complexes of Schiff base (1a) and Schiff base (1b) were synthesized by the following general method.

To a refluxing solution of the Schiff base (0.01 mol) in methanol (20ml), a methanolic solution of metal salt (0.01mol) was added. After three hours of refluxion of the reaction mixture was cooled to the room temperature. The precipitated complex was filtered, washed with 1:1 methanol:water mixture and recrystallized from the hot methanol.

Preparation of Cu(II) complex of the ligands

The Cu(II) complexes were prepared by adding a methanolic solution of copper(II)acetate (20 ml, 0.01mol) to a solution of 1a&1b (20 ml, 0.01 mol) in methanol and refluxed gently for three hours. After reducing the volume to half, the solution was then cooled to room temperature. The precipitated complex was filtered, washed with 1:1 methanol:water mixture and recrystallized from hot methanol.

**Preparation of Zn(II) complex of the ligands**

The Zn(II) complexes of the Schiff bases were prepared by adding a methanolic solution of zinc acetate (20 ml, 0.01mol) to a solution of 1a & 1b (20 ml, 0.01 mol) in methanol and refluxed gently for three hours. After reducing the volume to half, the solution was cooled to room temperature. The precipitated complex was filtered, washed with 1:1 methanol:water mixture and recrystallized from hot methanol.

Preparation of Ni(II) complex of the ligands

The Ni(II) complexes of the Schiff bases 1a and 1b were prepared by adding a methanolic solution of nickel(II) acetate (20 ml, 0.01mol) to a solution of 1a & 1b (20 ml, 0.01 mol) in methanol and repeating the above procedure.

The reaction involved in the formation of complexes is represented below in Scheme 1.4

Scheme 1.4
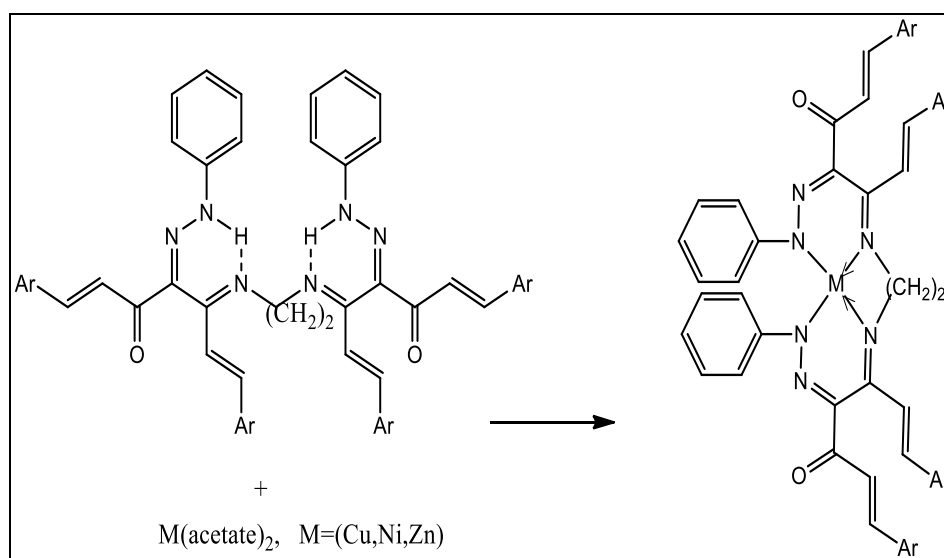
1a, Ar= thiophen-2-yl   1b,   Ar= 3 methyl thiophen-2-yl

Characterization of metal complexes of Schiff bases 1a and 1b

Transition metal chelates (Cu, Zn and Ni) of ligands 1a & 1b were characterized using physical, analytical and spectral data. The spectral techniques used in characterization comprise UV, IR, NMR and Mass spectral analysis. Elemental analysis (C, H, N and metal percentages), physical data and UV, IR spectral data of metal complexes of Schiff base 1a are given in Table 1.8 and metal complexes of

Schiff base 1b are given in Table1.9 respectively. The data given below suggest a

ML stoichiometry for all complexes prepared.

Table 1.8   Analytical and spectral data of metal complexes of Schiff base 1a

Metal chelates	M.P. (^{o}C)	Elemental analysis (%) Found/(calculated)				IR stretching bands (cm^{-1})		
		C	H	N	Metal	Free C=O	CN	M-N
Cu(II)	286	59.83 (60.00)	4.02 (5.03)	8.42 (9.54)	6.18 (7.21)	1656	1629 1587	507 503
Ni(II)	259	59.27 (60.34)	4.98 (5.06)	8.45 (9.59)	5.64 (6.70)	1660	16191591	501 504
Zn(II)	226	58.78 (59.88)	4.99 (5.02)	8.46 (9.52)	6.25 (7.40)	1674	1625 1589	506 503

Table 1.9   Analytical and spectral data of metal complexes of Schiff base 1b

Metal chelates	M.P. (^{o}C)	Elemental analysis (%) Found/(calculated)				IR stretching bands (cm^{-1})		
		C	H	N	Metal	Free C=O	CN	M-N
Cu(II)	286	60.53 (61.54)	4.53 (5.59)	7.64 (8.97)	6.83 (7.04)	1663	1624 1593	505 502
Ni(II)	259	60.75 (61.86)	4.52 (5.62)	8.93 (9.01)	5.49 (6.53)	1659	16351590	506 504
Zn(II)	226	60.39 (61.42)	4.47 (5.58)	7.92 (8.95)	6.18 (7.22)	1668	1628 1592	506 503

IR spectra

The intramolecularly hydrogen bonded NH band at ~1565 cm^{-1} for ligand 1a and the band at 1577 cm^{-1} for ligand 1b, disappeared and two bands of medium intensity at ~500 – 550 cm^{-1} appeared for complex. The strong band assignable to the free carbonyl moiety appeared in the region ~1670 cm^{-1} in the spectra of all metal complexes. Non-involvement of the carbonyl group in coordination was supported by the above observation. The replacement of NH proton by a metal ion was also evident from the absence of the broad band in the region of 2300 -3000 cm^{-1} present in the ligand. All these supported the formation of metal complexes. There was no change in the nature of alkenyl groups due to the metal complexation. The IR spectra of Ni(II) complex of Schiff base 1b is depicted in Fig.1.11 .
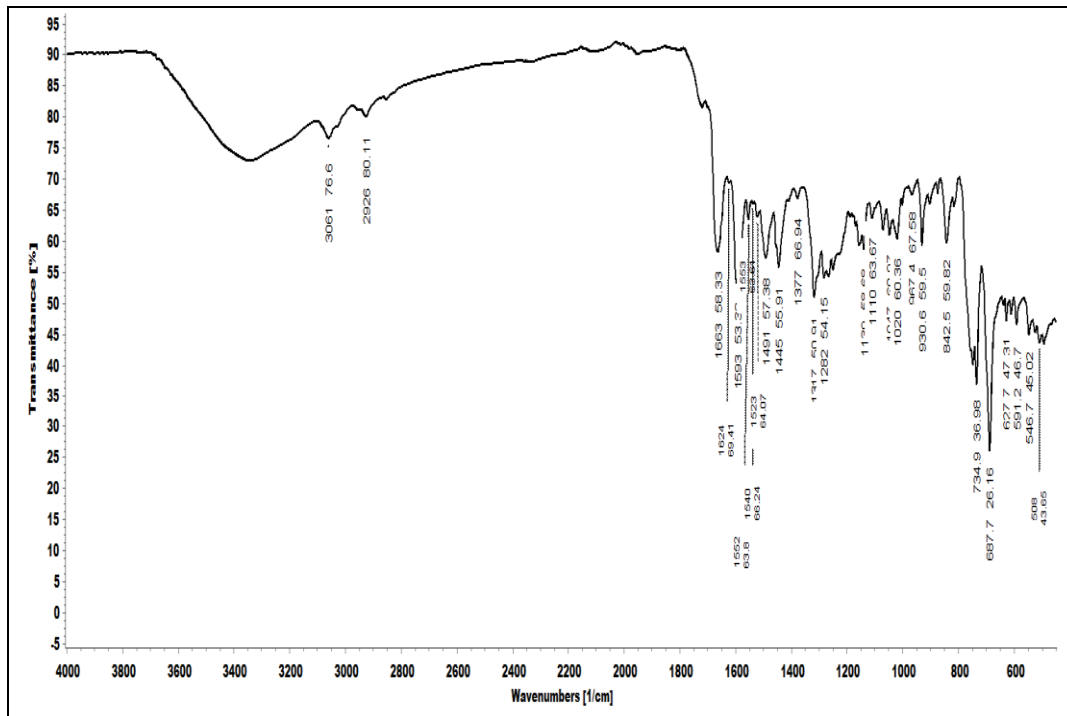
Fig.1.11 The IR spectra of Ni(II) complex of Schiff base 1b

^{1}H NMR spectra

A specific feature of ^{1}H NMR spectra of metal complexes was the absence of singlet signal at δ ~ 8.5ppm which suggested the replacement of NH proton in the Schiff base ligands by metal atom in metal complexes. The thiophenyl and alkenyl protons were not altered much since they were not involved in metal complexation. The methylene proton signals were consistent. Thus the spectra of ligand and complexes were much similar except those of NH proton. The ^{1}H NMR spectra of Cu(II) complex of ligand 1a is presented in Fig 1.12.
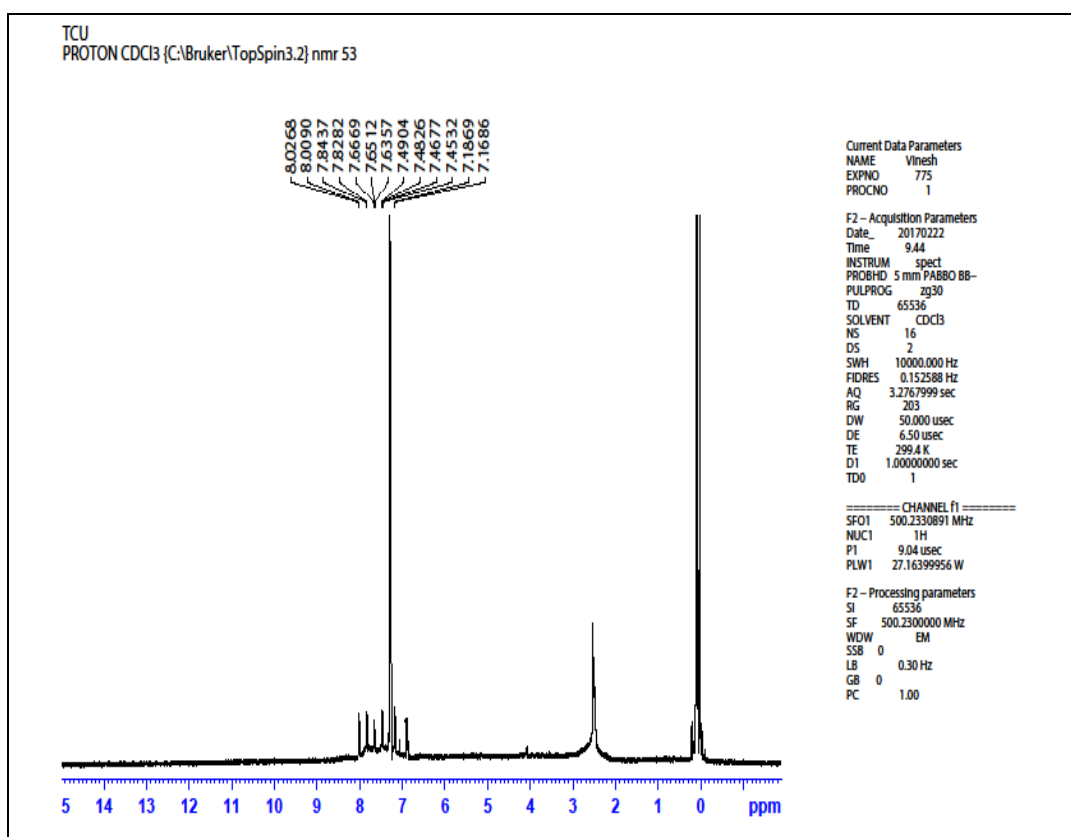
Fig 1.12 ^{1}H NMR spectra of Cu(II) complex of ligand 1a

Mass spectra

In mass spectra, all the complexes showed relatively intense peaks at m/z corresponding to the ML stoichiometry, where M is metal and L is Schiff   base ligand. Mass spectral fragments are very important in elucidating the structure of

metal complexes.   In all the cases [ML]$^+$ ion peak (the molecular ion peak) obtained was less intense than the base peak formed. The mass spectral analysis showed that stepwise removal of aryl groups was a characteristic feature of all the complexes. Smaller fragments like O, OH, CH etc. were also eliminated. Peaks due to [L]+ and its fragments were also identified in the spectrum. Mass spectrum of Ni(II) complex of 1a is given in Fig.1.13. The Ni(II) complexes of 1a and 1b showed a molecular ion peak at 875 and 931 respectively. The Cu(II) complexes of 1a and 1b showed molecular ion peaks at 878 and 937 respectively. The Zn(II) complexes of 1a and 1b had their molecular ion peaks at 881 and 938 respectively.
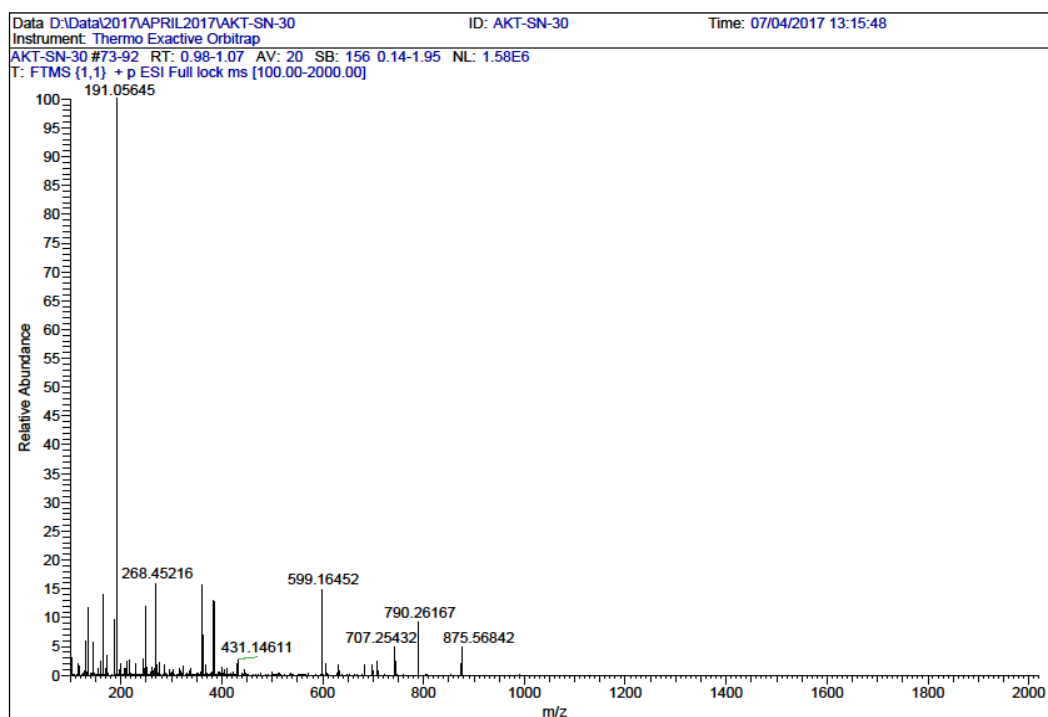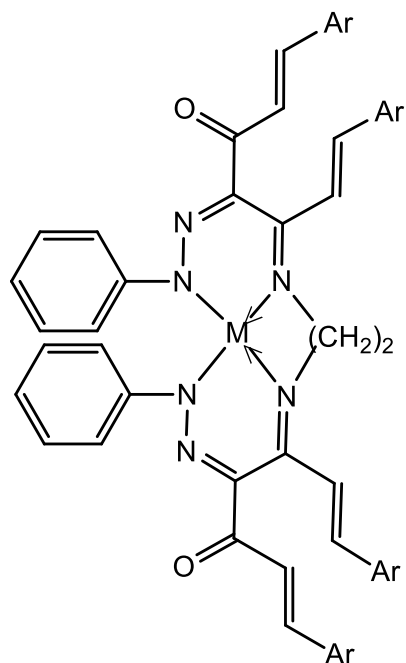

Fig.1.13 Mass spectrum of Ni(II) complex of 1a .

The observed UV, IR, ^{1}H NMR and Mass spectral data clearly reveals that metal chelates of Cu, Zn and Ni are having ML stoichiometry(metal ligand ratio is 1:1).The confirmed structure of metal chelates is given below

1a, Ar=thiophen-2yl, 1b, Ar= 3 methyl thiophen-2yl

SECTION II

Synthesis and characterization of Schiff base ligands derived from aryl azo derivatives of 1,7-bis(2 methyl phenyl)-hepta-1,6diene-3,5-dione and 1,7-bis(2 hydroxy phenyl)-hepta-1,6diene-3,5-dione with ethylene diamine and their transition metal chelates

Synthesis and characterization of Schiff base ligands

This unit describes the synthesis and characterization of Schiff bases derived from aryl azo derivatives of curcuminoid analogues with mono substituted phenyl rings in them.

Synthesis of mono substituted 1,7–diaryl heptanoids

The 1,7- diaryl heptanoids with methyl and hydroxy substituted phenyl rings were synthesized by the condensation of the aldehydes (2-methyl benzaldehyde and 2-hydroxy benzaldehyde) with acetylacetone-boric oxide complex (prepared by stirring the acetyl acetone and B_2O_3 for 1 hour) in ethyl acetate medium in presence of tri(sec-butyl) borate and n-butyl amine as condensing agent. This method led to the formation of the 1,7diarylheptanoids. The 1,7diarylheptanoid was formed by the condensation of two molecules of aldehyde with one molecule of acetyl acetone. Its representation in a schematic way is shown in Scheme 1.5.

Scheme 1.5
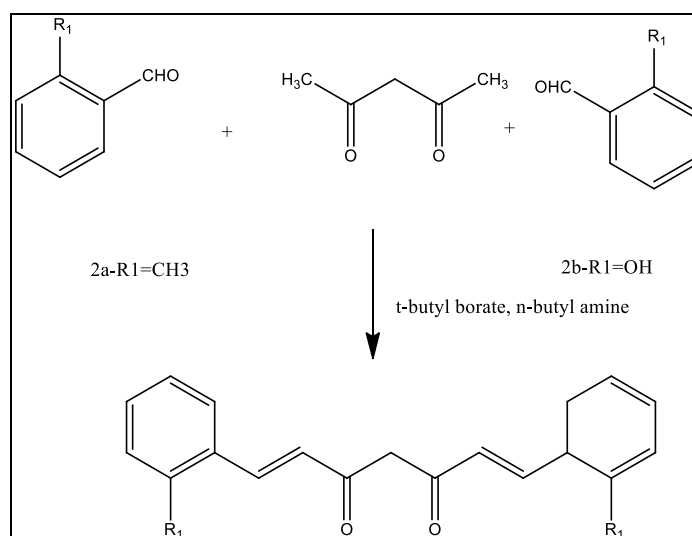
The products 1,7-di(2- methyl phenyl)hepta-1,6-diene-3,5-dione(2a) and 1,7di(2-hydroxy phenyl) hepta-1,6-diene-3,5-dione(2b)were purified by column chromatography using 4:1 (v/v) chloroform:acetone mixture as the eluent, over silica gel (60 – 120 mesh) and recrystallized the compounds twice from hot benzene to get pure crystalline material.

Synthesis of Schiff bases bis(1,7-di(2 methyl phenyl)-4-(phenyl-hydrazono)-hepta-1,6diene-3,5-dione)ethylenediimine and bis(1,7-di(2 hydroxy phenyl)-4-(phenyl-hydrazono)-hepta-1,6diene-3,5-dione) ethylenediimine

The synthesized β-diketones were coupled with benzene diazonium salt. Benzene diazonium salt (0.01 mol) was prepared as reported earlier and was kept below 0^0C and it was added drop by drop to a solution of the β-diketones (0.01 mol in methanol) at below 0^0C with constant stirring. Sodium acetate (2mg) was added to the mixture to keep the pH of the mixture in the range 6-7.The precipitated compounds 1,7-bis(2-methyl phenyl)-4-(phenyl-hydrazono)-hepta-1,6-diene-3,5-dione and 1,7-bis(2-hydroxy phenyl)-4-(phenyl-hydrazono)-hepta-1,6-diene-3,5-dione were filtered, washed with water and recrystallized from methanol to get chromatographically pure (TLC) material. The Schiff bases were synthesized by the condensation of 1,7-bis(2 methyl phenyl)-4-(phenyl-hydrazono)-hepta-1,6diene-3,5-dione and 1,7-bis(2 hydroxy phenyl)-4-(phenyl-hydrazono)-hepta-1,6diene-3,5-dione with 1,2-diaminoethane (en) as follows. A methanolic solution of the 1,2-diaminoethane (0.01mol, 20ml) was added to an methanolic solution of the synthesized hydrazono compounds (0.02mol, 20ml). The solution was stirred with a magnetic stirrer for approximately 5 hours and allowed to evaporate at reduced pressure. The crystalline compound formed, was filtered and recrystallized

from hot methanol to get chromatographically (TLC) pure compound. The compound was formed by the condensation of two aryl azo derivatives and one ethylene diamine molecule. The schematic diagram is shown below.
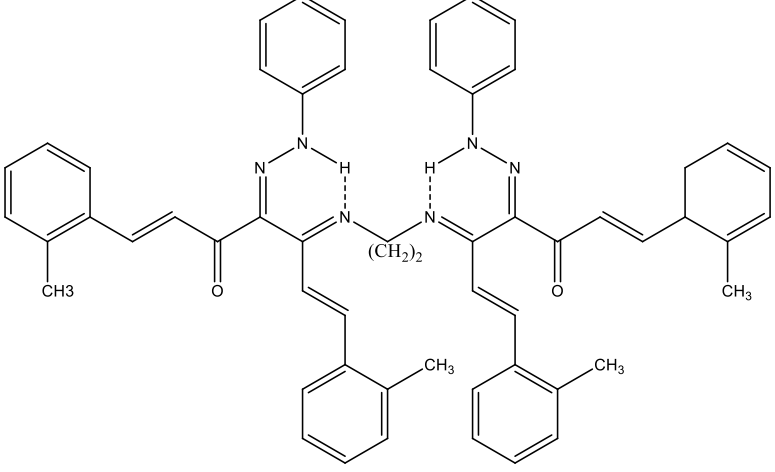
Scheme 1.6.

2a, Ar= 2methyl phenyl   2b, Ar= 2 hydroxy phenyl
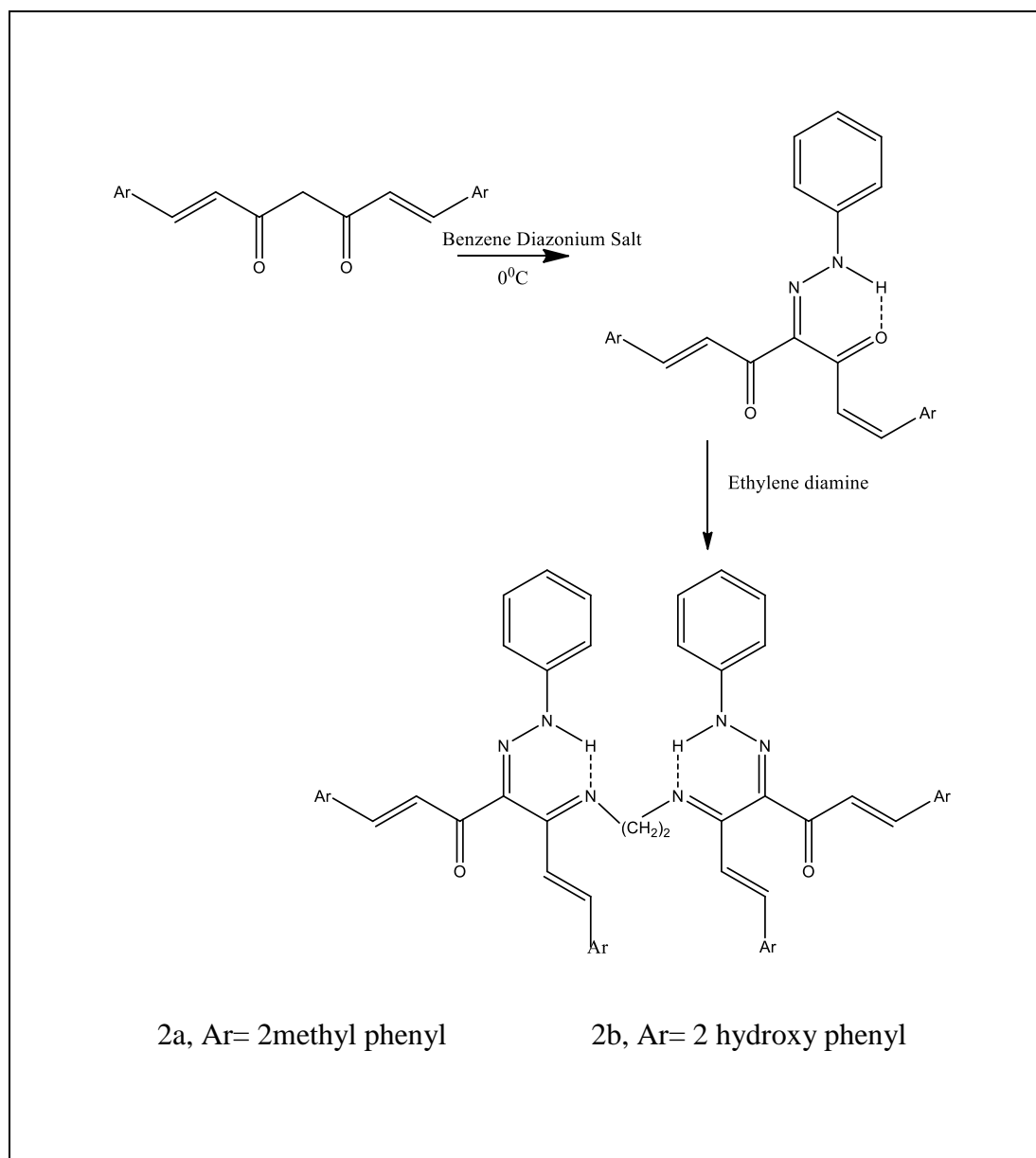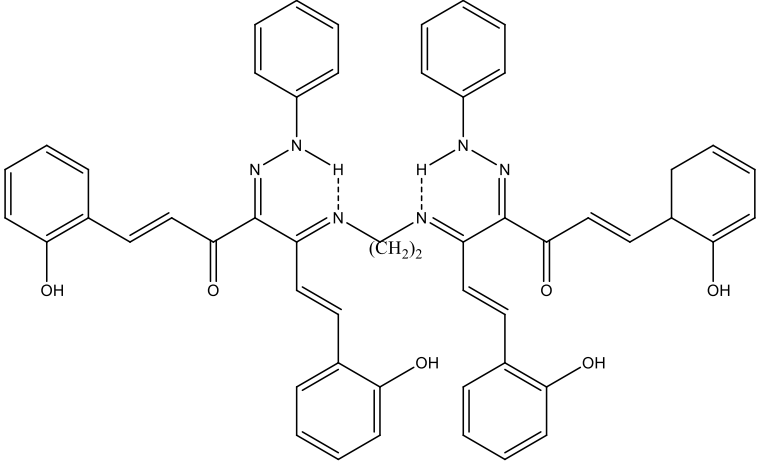
Characterization of Schiff Bases

The condensation reaction yielded crystalline solids soluble in common organic solvents like acetone, ethanol, methanol, chloroform. Elemental data suggested the condensation of one diamine with two equivalents of substituted aryl azo compounds. So only one carbonyl group of aryl azo compound and both the amino groups of the primary amine is involved in the Schiff base condensation reaction and would have reacted to form the compounds. The C, H,N analysis, molecular weight determination (Table1.11) together with mass spectral data of the compounds was in conformity with the suggested structure. The structures of the compounds prepared, its systematic name and yield are given in Table1.10.

Table 1.10   Synthetic details of Schiff bases derived from aryl azo derivatives of mono substituted 1,7-diphenyl heptanoids

Compounds	Structure and systematic name of Schiff base ligands	Yield %
2a		63
Systematic name	1,14-di(2-methyl phenyl) 5,10-di(ethylene- 2- methyl phenyl)- 6,9-diazotetradeca 1,5,9,13-tetraene -3,12-dione 4,11-diphenyl-hydrazone [MEDTDH]	

2b		76
Systematic name	1,14-di(2 hydroxy phenyl) 5,10-di(ethylene- 2- hydroxy phenyl)-6,9-diazotetradeca 1,5,9,13-tetraene -3,12-dione 4,11-diphenyl-hydrazone [HEDTDH]	

Both the Schiff base ligands 2a & 2b are crystalline in nature and show sharp melting points. They were obtained in good yields nearly 63 and 76% respectively. They are readily soluble in organic solvents like ethanol, methanol, acetone, chloroform. The observed C, H, N percentage and molecular weight determination (Table1.11) along with mass spectral data of the compounds clearly suggested the formation of intramolecularly hydrogen bonded imine-hydrazone form.

Table 1.11   Analytical & UV spectral data of 2a & 2b

Compounds	MP.(^{o}C)	Elemental analysis (%) Found/(Calculated)			Molecular weight	UV λ_{max} (nm)
		C	H	N		
2a	124	79.52 (79.97)	6.01 (6.23)	9.76 (9.99)	841.05	278,354
2b	160	73.42 (73.56)	5.14 (5.22)	9.81 (9.89)	848.94	272,349

IR Spectra

The IR spectra of the compound 2a showed three strong bands at 1660 cm^{-1},1636 cm^{-1} and 1600 cm^{-1} .The band at 1660 cm^{-1} showed the presence of free carbonyl group not involved in hydrogen bonding. The comparison of the spectra of the aryl azo compound and Schiff base 2a, revealed that the bands at 1636 and 1600 were due to the stretching of the C=N groups. The band at 1600 (low frequency band) was due to the imine C=N. The band at 1636 was due to the hydrazono C=N. The medium intensity bands appeared at 1550 to 1600cm^{-1} range were due to the C=C vibrations. In case of all the compounds a prominent peak appeared at~1575cm^{-1} can be assigned to NH deformation vibration.
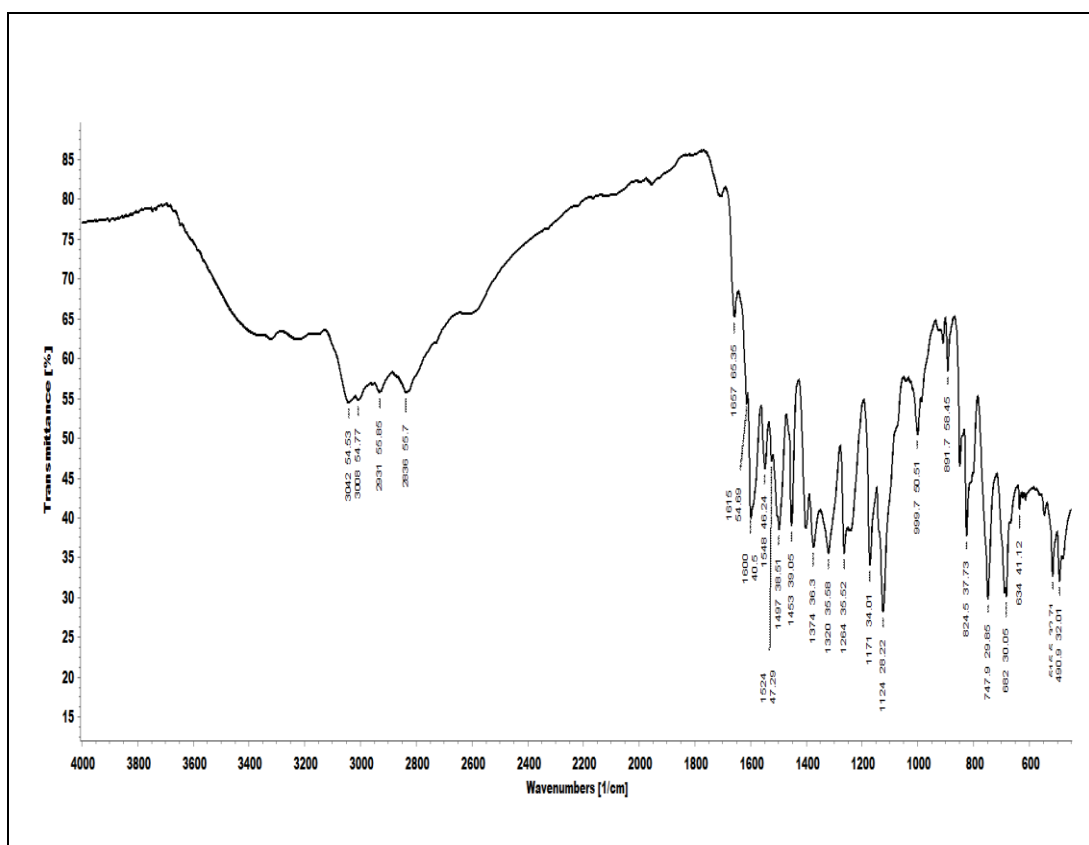

Fig.1.14 IR Spectrum of Schiff base HEDTDH (2b)

The broad band present in the region 2500cm^{-1} to 3500cm^{-1} showed the presence of strong intramolecular N-H…N hydrogen bonding. Thus the IR spectra strongly supported the suggested structure for the Schiff bases. Important IR bands and their probable assignments are given in Table 1.12

Table 1.12 IR spectral data of Schiff bases derived from aryl azo derivatives of mono substituted 1,7-diaryl heptanoids

Compounds		Probable IR assignments
2a	2b	
1660	1657	v(C=O)
1636	1615	Hydrazono v(C=N)
1600	1600	Imine v(C=N)
1552	1548	v (C-C) alkenyl
967	972	v (CH=CH) trans

^{1}H NMR Spectra

The ^{1}H NMR spectra of Schiff bases derived from mono substituted 1,7-diaryl heptanoids also supported the presence of intramolecularly hydrogen bonded N-H...N protons in the compounds. The peaks corresponding to N-H protons were observed at approximately δ 8.7ppm.The methyl substituted derivative showed the corresponding peak at ~ 1.748 ppm. The hydroxyl group substituted Schiff base derivative showed the peak corresponding to OH group at ~ 9.964ppm. (Table 1.13). The various proton signals observed in the spectra are given in Table 1.13

Table 1.13   ^{1}H NMR spectral data of Schiff bases 2a and 2b

Compounds	Chemical shifts (δ ppm)				
	NH	Aryl	alkenyl	CH_2	CH_3/OH
2a	8.327	7.01-7.742	6.85-7.926	2.79-2.883	1.748
2b	8.651	7.35-7.857	6.78-8.044	2.54-2.898	9.964

The aryl protons showed nmr signals in the region δ 7.359-7.857ppm and the alkenyl protons showed signals in the region of δ 6.788-8.044ppm. The methyl group on aryl ring in 1a showed a signal at 1.748 where the hydroxyl group on aryl ring of 2b was present at ~ 9.964ppm. The ^{1}H nmr spectral data of 2b are brought out in Fig.1.14.
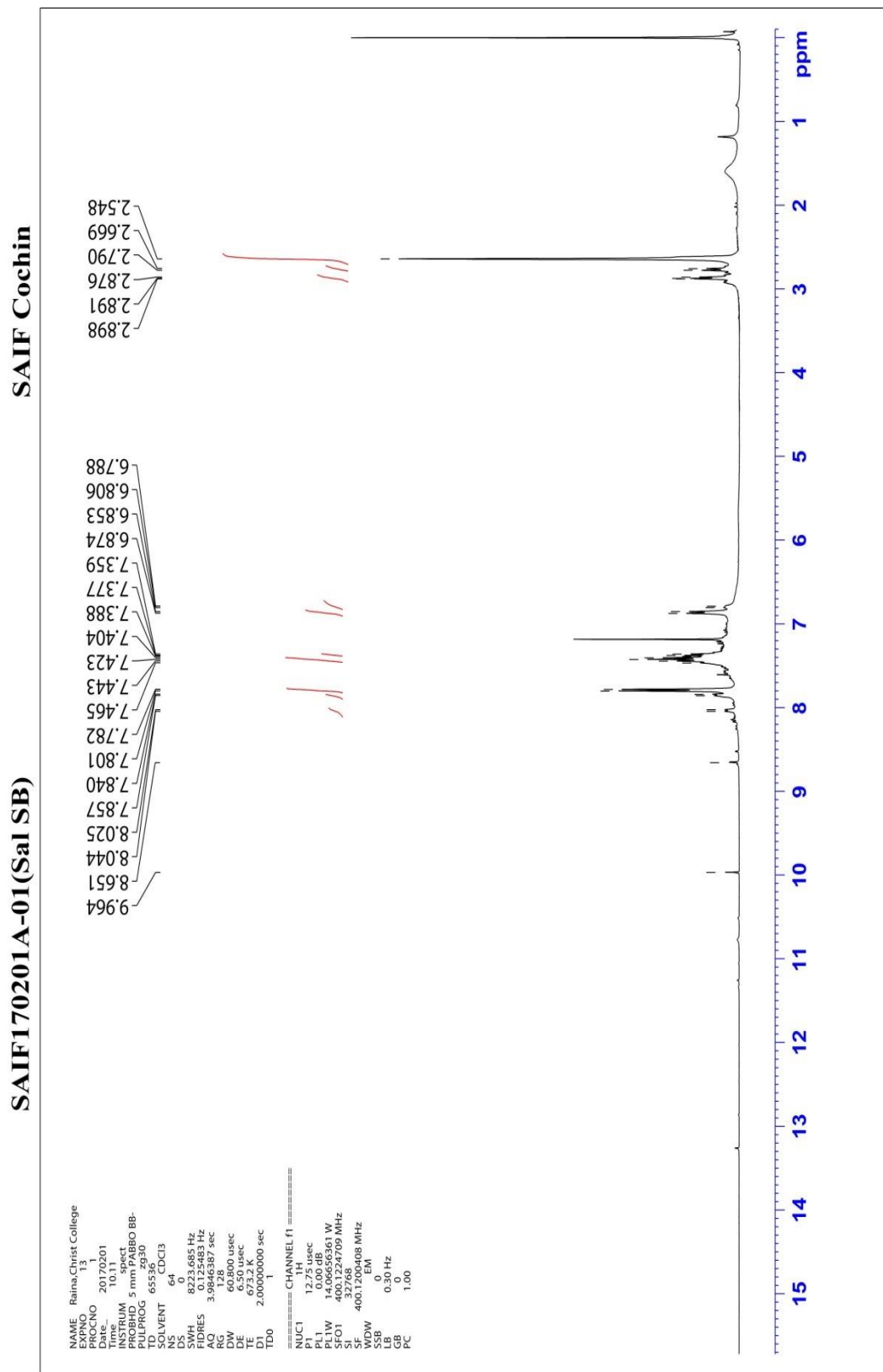
Fig.1.14 NMR Spectrum of HEDTDH (2b)

¹³C NMR spectra

The ¹³C NMR spectral details of 2a & 2b are presented in Table 1.14 & 1.15 respectively. The peak corresponding to methylene (C1) carbon is present at position ~42ppm for 2a and 41ppm for 2b. C4 the carbonyl carbon appeared at a position at~ 192ppm for 2a and 191ppm for 2b. Only one signal for keto carbon atom showed that both keto groups are in the same environment. The C6 the alkenyl carbons at position nearer to the phenyl ring system show a down shielded peak at ~134ppm.The aromatic carbon atoms were present between 121– 131ppm. ¹³CNMR spectra of 2b is reproduced in Fig.1.15

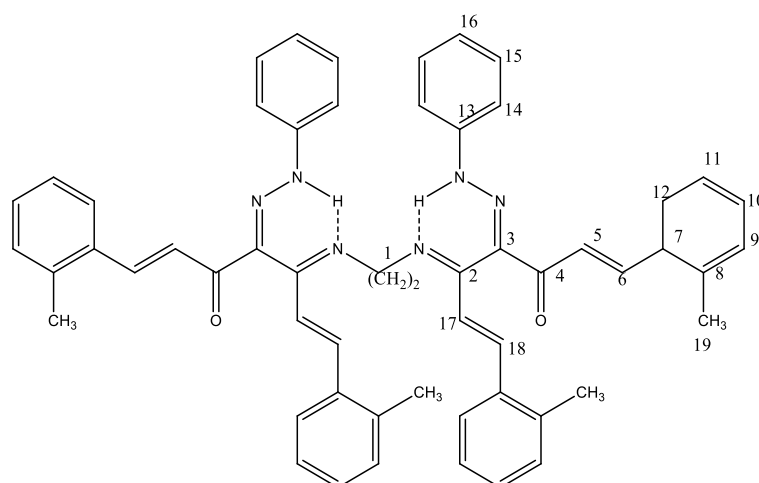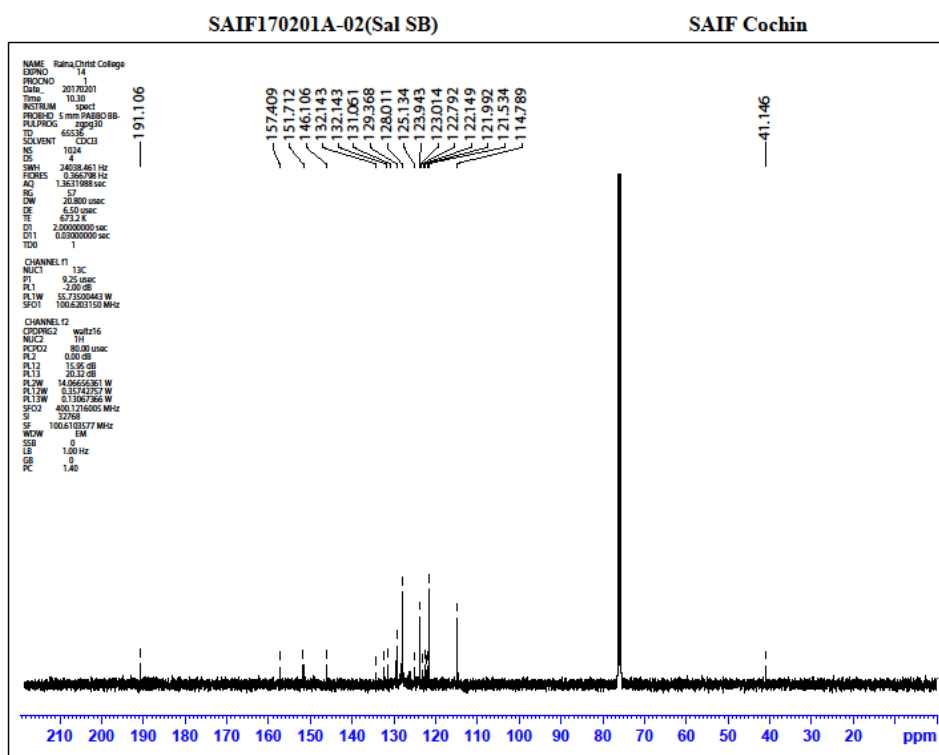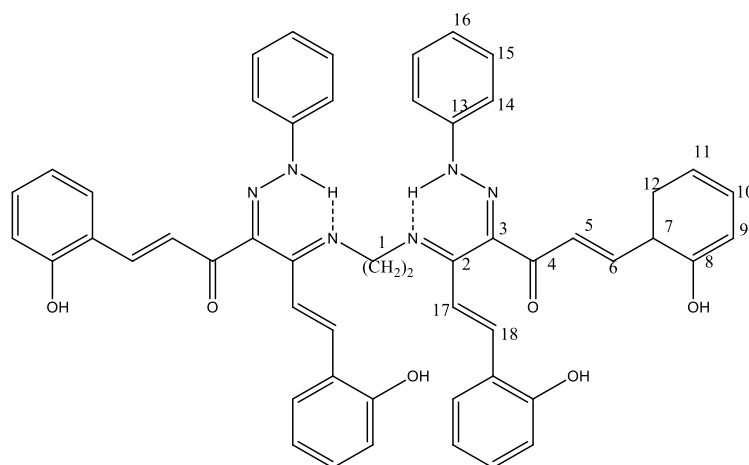**Structure representing different carbon atoms in 2a**

Table 1.14   ¹³C spectral details of 2a.

C1	C2	C3	C4	C5	C6	C7	C8	C9	
42.25	159.16	151.73	192.53	121.73	133.32	132.84	130.67	124.653	
C10	C11	C12	C13	C14	C15	C16	C17	C18	C19
122.75	122.21	123.94	131.47	121.15	129.56	124.73	112.11	126.32	29.12

Structure representing different carbon atoms in 2b.

Fig.1.15. ^{13}C NMR spectra of Schiff base 2b

Table.1.15 ^{13}C spectral details of Schiff base 2b

C1	C2	C3	C4	C5	C6	C7	C8	C9
41.14	157.40	151.71	191.10	121.53	134.25	132.143	146.10	128.01
C10	C11	C12	C13	C14	C15	C16	C17	C18
122.79	122.14	123.01	131.02	121.99	129.36	125.13	114.78	123.94

Mass spectra

The most vital application of mass spectra is the determination of molecular weight of organic compounds. Both the molecular ion peaks as well as fragment ion peaks can be observed in the Mass spectra. The mass spectra also give indication about the various fragmentation modes of the compounds. Mass spectra of aryl azo derivative of 2 hydroxy phenyl substituted diketones are given in Fig.1.16 which gives a M+1 peak at m/z 413 and a base peak at 69 which corresponds to [NH-CN-CO]+ ion. The mass spectra of both Schiff bases 2a and 2b showed M^+ and $[M+1]^+$ peaks as molecular ion peaks respectively. Elimination of important groups like CH_2, C_2H_2, Ar- C_2H_2-C=O$^+$, ArNH$^+$ from the molecule gave different fragment ion peaks. The important peaks appeared in the mass spectra of Schiff bases can be appropriately accounted by the fragmentation pattern as given in (Scheme 1.7) and the values obtained are shown in Table 1.16.
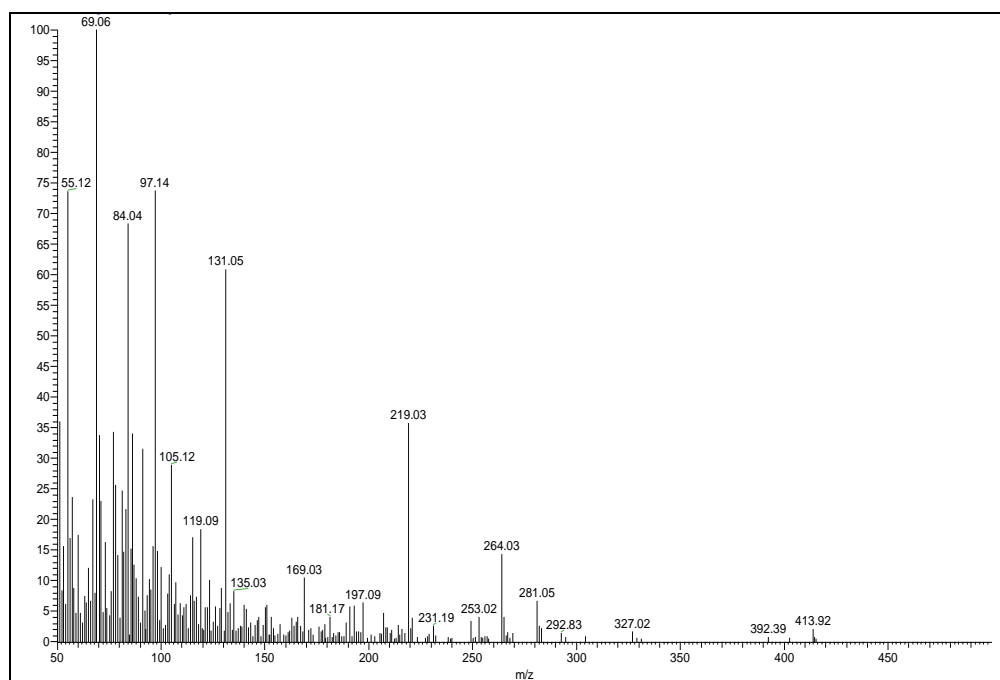

Fig. 1.16 Mass spectra of aryl azo derivative of 2 hydroxy phenyl substituted diketones

The M$^+$ ion of 2a is observed at 841 and the (M+1)$^+$ ion of 2b is observed at 849. Other important peaks of 2a &2b are due to fragment ion peaks which can be explained from their fragmentation patterns. In the mass spectrum of 2a, the molecular ion peak is observed at 841.The base peak is observed at 143 and can be assigned to the peak of   [Ar-NH-CN-CN]$^+$.

 Mass spectrum of 2b is given in Fig.1.17 and in the mass spectrum of 2b, there is an intense molecular ion peak at 849.The base peak is observed at 505 which is due to the fragment C in the mass fragmentation pattern. The peak at 198 is due to [Ph-NH-CN-CN-CO-CH]$^+$ ion and at   143 is due to removal of [CO-CH] group from base peak ion.
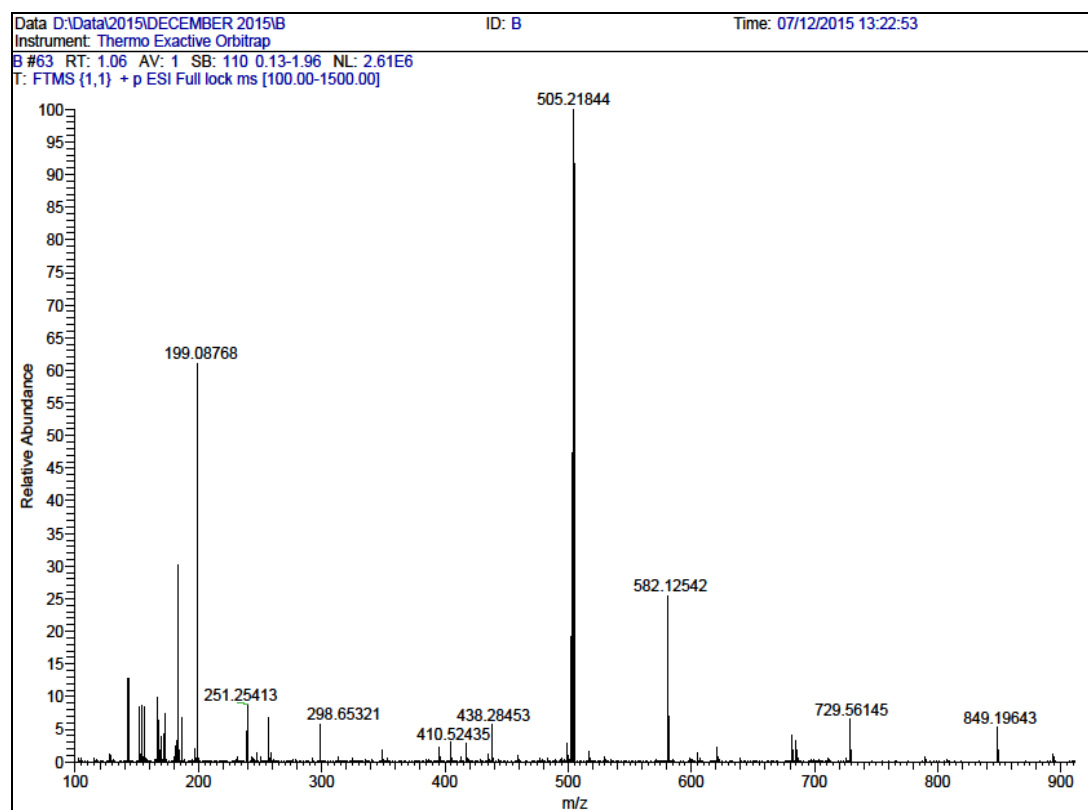

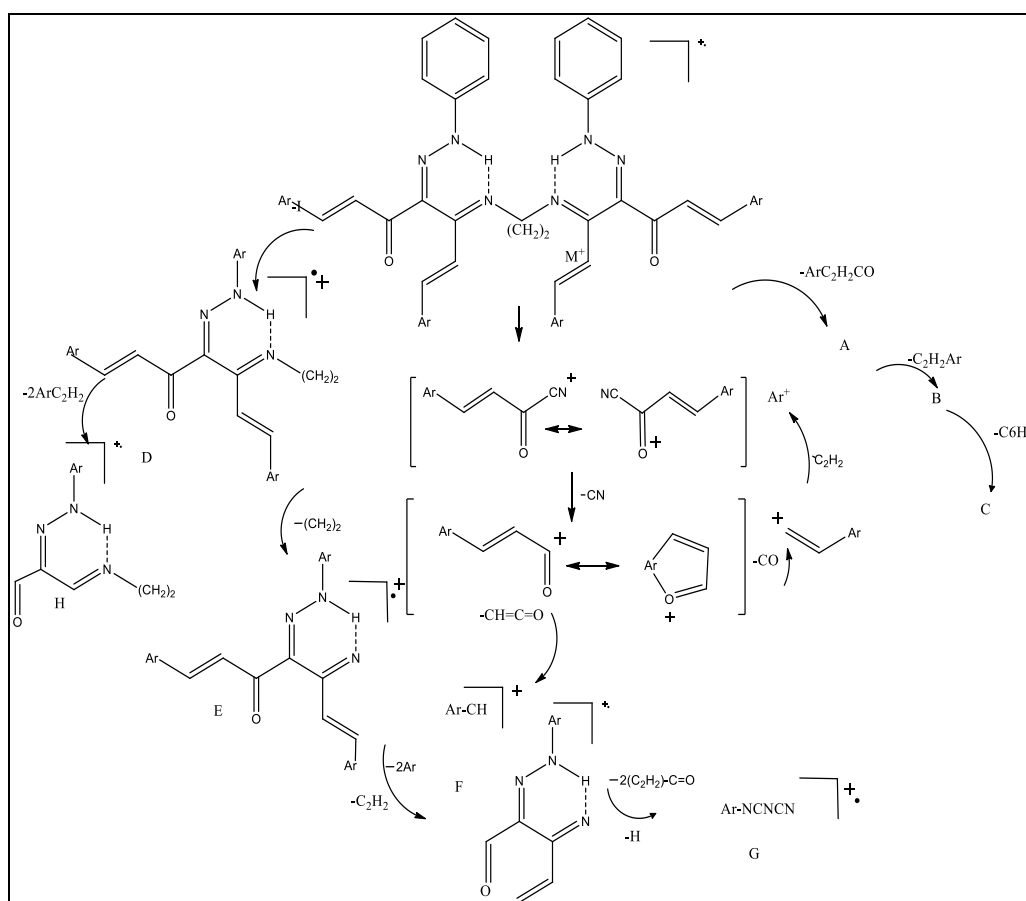**Fig. 1.17   Mass spectra of Schiff base 2b**

Table 1.16   Mass spectral data of 2a & 2b

Fragments	Ligands	M,M+1 ions	A	B	C	D	E	F	G
Mass Patterns	2a	841	724	579	502	435	407	198	143
	2b	849	729	582	505	438	410	199	143

*The alphabets correspond to the fragments given in **Scheme 1.7.**

Scheme 1.7 Mass fragmentation pattern of Schiff bases

Ar = 2 methyl phenyl for 2a, 2 hydroxy phenyl for 2b

Synthesis and characterization of metal complexes of Schiff bases 2a and 2b

Synthesis of metal complexes

Copper(II), Zinc(II) and Nickel(II) complexes of Schiff bases 2a and 2b   were synthesized by the following general method.

A methanolic solution of metal salts of Cu(II), Zn(II) and Ni(II) (0.01mol, 25ml) was added to a methanolic solution of the ligand (0.01mol, 25ml). The reaction mixture was refluxed for approximately 3 hours and reduced to half of the original volume. The precipitated complex was filtered, washed with 1:1, methanol: water mixture and recrystallized from hot methanol.

Preparation of Cu(II) complex of the ligands

 The Cu(II) complexes were prepared by adding a methanolic solution of copper(II)acetate (25 ml, 0.01mol) to a solution of 2a &2b (25 ml, 0.01 mol) in methanol and refluxed gently for three hours. After reducing the volume to half of the original volume, the solution was cooled to the room temperature. The precipitated Schiff base complex was filtered and washed with 1:1, methanol:water mixture and recrystallized from hot methanol.

**Preparation of Zn(II) complex of the ligands**

The Zn(II) complexes of the Schiff bases were prepared by adding a methanolic solution of zinc acetate (25 ml, 0.01mol) to a solution of 2a & 2b (25 ml, 0.01 mol) in methanol and refluxed gently for three hours. After reducing the original volume to half, the solution was cooled to room temperature. The precipitated Zn(II) complex was filtered, washed with 1:1, methanol:water mixture and recrystallized from hot methanol.

Preparation of Ni(II) complex of the ligands

The Ni(II) complexes of the Schiff bases were prepared by addition of methanolic solution of nickel(II) acetate (25 ml, 0.01mol) to a solution of 2a&2b (25 ml, 0.01 mol) in methanol and thereby repeating the procedure above.

The reaction path in the formation of Schiff base complexes is represented below in Scheme 1.8

Scheme 1. 8
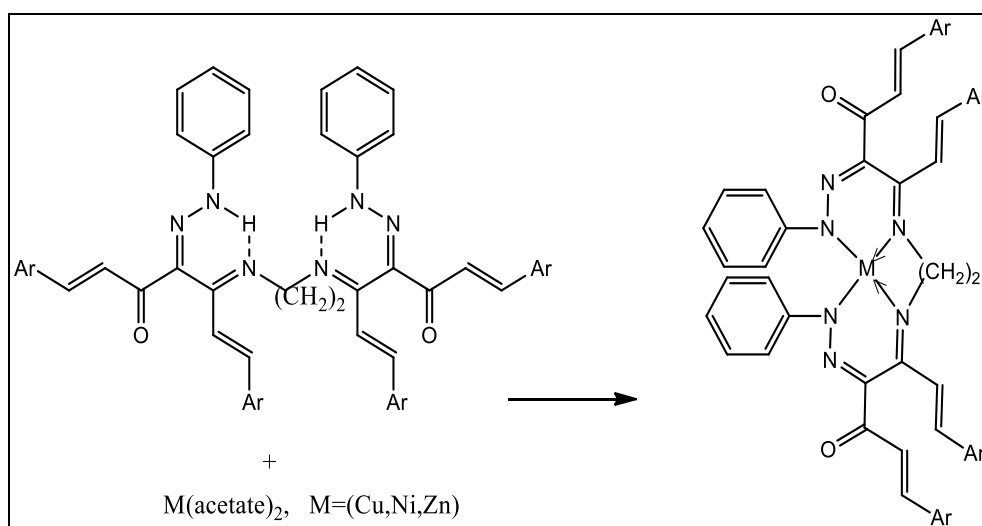
Ar = 2 methyl phenyl for 2a, 2 hydroxy phenyl for 2b

Characterization of metal complexes of Schiff bases 2a and 2b

Transition metal chelates (of metals Cu, Zn and Ni) of Schiff base ligands 2a & 2b were characterized using the physical, analytical and spectral data. Elemental analysis data (C, H, N and metal percentages), physical data & spectral data of metal complexes of Schiff bases 2a &2b are presented in Table 1.17 and Table 1.18 respectively. The data presented below suggest a ML stoichiometry for all

complexes synthesized. Magnetic moment measurements showed that Ni(II) and Zn(II) complexes are diamagnetic and Cu(II) chelates are paramagnetic in nature.

Table 1.17   Analytical and spectral data of metal complexes of Schiff base 2a

Metal chelates	M.P. (^{o}C)	Elemental analysis (%) Found/(calculated)				IR stretching bands (cm^{-1})		
		C	H	N	Metal	Free C=O	CN	M-N
Cu(II)	292	74.42 (74.51)	5.49 (5.58)	9.25 (9.31)	6.91 (7.04)	1667	1619 1591	504 501
Ni(II)	264	74.53 (74.92)	5.38 (5.61)	9.18 (9.36)	6.42 (6.53)	1657	1625 1590	506 503
Zn(II)	235	74.21 (74.36)	5.16 (5.57)	8.92 (9.29)	6.91 (7.22)	1659	1631 1593	505 504

Table 1.18   Analytical and spectral data of metal complexes of Schiff base 2b

Metal chelates	M.P. (^{o}C)	Elemental analysis (%) Found/(calculated)				IR stretching bands (cm^{-1})		
		C	H	N	Metal	Free C=O	CN	M-N
Cu(II)	284	68.12 (68.59)	4.09 (4.64)	8.94 (9.23)	6.58 (6.97)	1661	1623 1588	505 502
Ni(II)	268	68.53 (68.96)	4.47 (4.67)	8.99 (9.27)	6.32 (6.48)	1658	1629 1592	507 503
Zn(II)	228	68.11 (68.45)	4.23 (4.64)	9.02 (9.21)	6.92 (7.16)	1670	1631 1589	508 504

IR spectra

The presence of a strong band in the region ~1660 cm^{-1} was one salient feature of the metal complex which was due to presence of free carbonyl group. This made it clear that the free carbonyl group present in the Schiff base is not involved in the

metal complexation. But the peak due to free C=N (imine) which was present at ~ 1600 cm^{-1} disappeared and a new band appeared at ~ 1550-1600 cm^{-1}. The hydrazone C=N only affected marginally and appeared at ~1630.The substitution of NH proton in the ligand, by a metal ion in the complex was evident from the absence of the NH deformation band ~ 1575 cm^{-1} and the absence of a broad band in the region of 2300 -3500 cm^{-1} which was present in the ligand. Moreover two new medium intensity bands appeared in the complex at ~500-550 cm^{-1} .The new bands can be assigned to the metal coordinated N, νM-N. This also gave evidence for Schiff base metal complex formation. The IR spectrum of the Ni(II) complex of 2a is given in Fig.1.18. The unchanged nature of trans CH=CH vibrations was evidenced by the peak in the region 969 cm^{-1}.
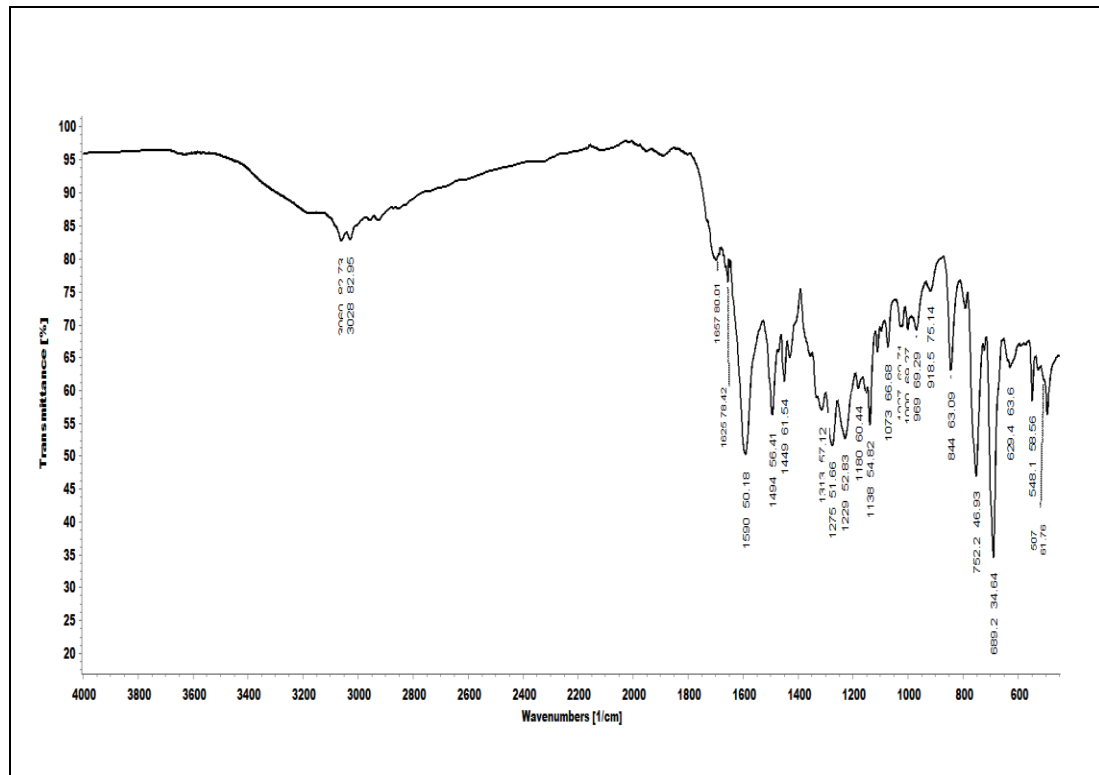

Fig.1.18 The IR spectrum of the Ni(II) complex of Schiff base 2a

¹H NMR spectra

The main feature of NMR spectra of metal complex is the absence of singlet signal at δ ~ 8.65ppm which was due to the NH protons present in the ligands. This indicated the replacement of NH proton by metal atom in metal complexes. The phenyl and alkenyl protons were not altered much since they are not involved in metal complexation. Thus the spectra of ligand and complexes agree well with 1:1 metal ligand stoichiometry and are similar except those of NH proton. The ¹H NMR spectra of Ni(II) complex of ligand 2b is given in Fig 1.19
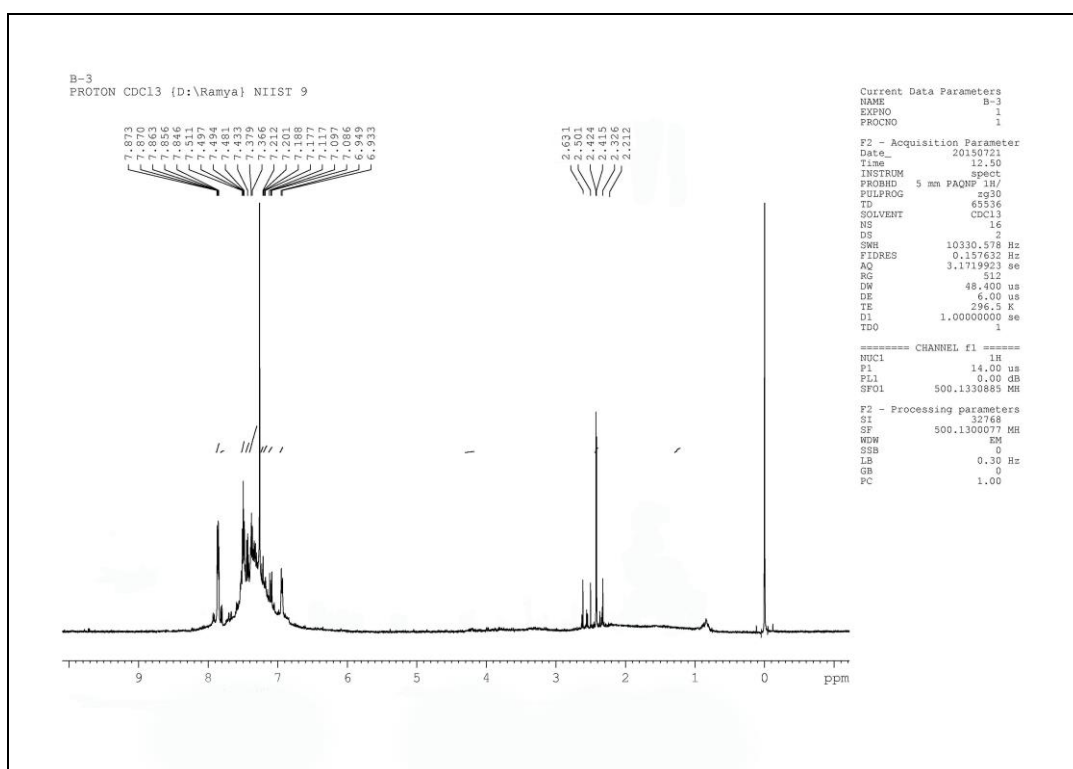

Fig 1.19 ¹H NMR spectra of Ni(II) complex of ligand 2b

Mass spectra

In the mass spectra, all the complexes showed relatively intense peaks at m/z corresponding to ML stoichiometry, corresponding to the molecular ion [ML]$^+$ where M is metal and L is Schiff base ligand. Mass spectral fragments are the helping tools in elucidating the structure of metal complexes. Smaller molecules like CH, O, OH, etc. were also eliminated. The mass spectral data indicated that stepwise removal of aryl groups was the characteristic feature of all the complexes. Peaks due to fragments of ML+ were also spotted in the spectrum . Mass spectrum of Cu(II) complex of 2b is given in Fig 1.20
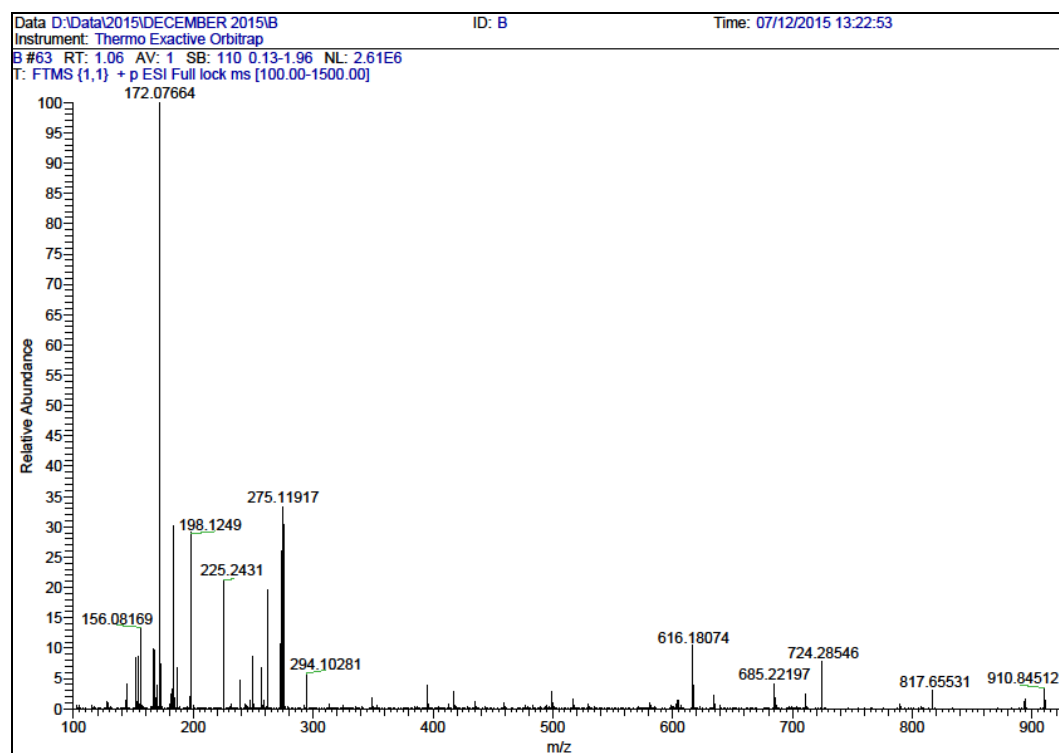

Data D:\Data\2015\DECEMBER 2015\B   ID: B   Time: 07/12/2015 13:22:53
Instrument: Thermo Exactive Orbitrap
B #63 RT: 1.06 AV: 1 SB: 110 0.13-1.96 NL: 2.61E6
T: FTMS {1,1} + p ESI Full lock ms [100.00-1500.00]

Fig 1.20 Mass spectrum of copper chelate of Schiff base 2b

In the mass spectrum of Cu(II) complex of Schiff base 2b , observed a molecular ion peak at 910. Another intense peak is seen at 616 which was due to the removal

of two aryl groups and CO groups from the molecular ion. The peak at 172 was due to the fragment ion formed by the $[Cu-N_3OC_4H_3]$ ion. All the metal complexes Cu(II), Ni(II) and Zn(II) of Schiff bases of 2a and 2b showed molecular ion peaks and intense base peaks as assumed.

The observed UV, IR, 1H NMR and Mass spectral data clearly revealed that metal chelates of Cu, Zn& Ni are having ML stoichiometry(metal ligand ratio is 1:1).The confirmed structure of metal chelates is shown below
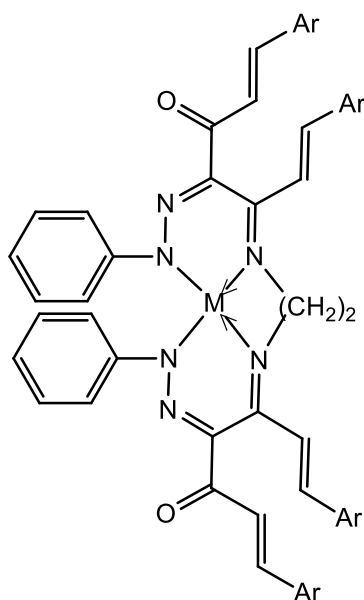
Ar = 2 methyl phenyl for 2a, 2 hydroxy phenyl for 2b

SECTION III

Synthesis and characterization of Schiff bases derived from aryl azo derivatives of 1,7-bis(aryl)hepta 1,6-diene-3,5-diones with di & trisubstituted phenyl ring and ethylene diamine and their transition metal complexes

Synthesis and characterization Schiff bases

This unit describes the synthesis and characterization of Schiff bases derived from aryl azo derivatives of curcuminoid analogues with a di-substituted and tri-substituted phenyl rings in them. The curcuminoid analogues are compounds quite similar to natural curcumin in structure which is 1,7-bis(3-methoxy-4-hydroxy phenyl)-hepta-1,6-diene-3,5-dione and it is a symmetrical di-substituted compound. Three Schiff bases 3a, 3b and 3c derived from aryl azo derivatives of 1,7-bis(3-ethoxy-4hydroxyphenyl)hepta-1,6-diene-3,5-dione, 1,7-bis(2,4-dihydroxy phenyl) hepta-1,6-diene3,5-dione and 1,7-bis(3,4,5-trimethoxy phenyl) hepta-1,6-diene-3,5-dione were synthesized. The Schiff base 3a contains an ethoxy and hydroxyl group on the phenyl ring. The Schiff base ligand 3b contains di-substituted phenyl rings with hydroxyl group in 2,4 positions. The Schiff base ligand 3c had been prepared with a tri-substituted phenyl ring with three methoxy groups in 3,4,5 positions.

Synthesis of di and tri substituted 1,7–diphenyl heptanoids

The curcuminoid analogues with di and trisubstituted phenyl rings at positions 1,7 were prepared by the condensation of di-substituted benzaldehydes, (3-ethoxy-4-hydroxy benzaldehyde, 2,4dihydroxy benzaldehyde) and tri-substituted benzaldehyde(3,4,5-trimethoxy benzaldehyde) with the acetyl acetone-boric oxide

complex in the ethyl acetate medium in presence of tri(sec-butyl) borate and n-butyl amine. The reaction can be represented in a schematic way in Scheme 1.9

Scheme 1.9

3a-$R_1=R_4=H$, $R_2=OCH_2CH_3$, $R_3=OH$
3b-$R_1,R_3=OH$, $R_2,R_4=H$

3c-$R_1=H$, $R_2,R_3,R_4=OCH_3$
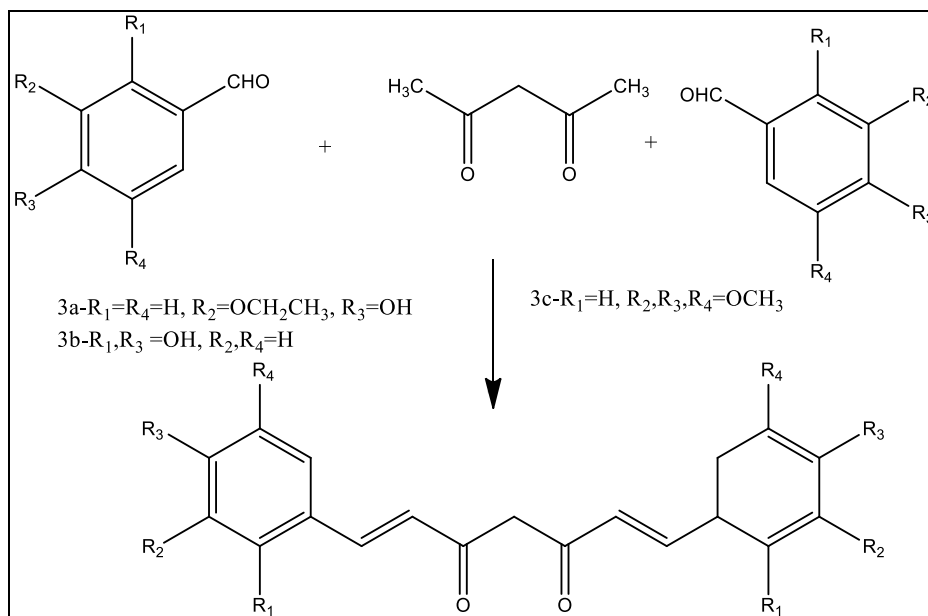
Here 2 moles of di and tri substituted benzaldehyde reacted with 1 mole of 1,3-diketone to form the 1,7-diphenyl heptanoids. The above reaction produced two products namely 1,7-diaryl heptanoids as the major product and 6-aryl hexanoids as the minor product. The major product was purified by column chromatography over silica gel (60 – 120 mesh) using 4:1 (v/v) chloroform:acetone mixture as the eluent and recrystallized twice from hot benzene to get pure crystalline compounds.

Synthesis of Schiff bases

Schiff bases derived from aryl azo derivative of 1,7-di aryl heptanoids was synthesized as follows. Aniline was diazotised (0.01 mol) as already reported. Excess nitrous acid present in the solution (diazonium salt solution) was destroyed by addition of urea to it. It was then added to the 15 ml methanolic solution of 1,7

di aryl heptanoids(0.01 mol) which was kept at 0^oC.The pH of the mixture had kept in the range 6-7. The precipitated aryl azo compound was filtered, washed with water and recrystallized twice from hot methanol to get chromatographically pure product.

The condensation of the aryl azo compound synthesized above with ethylene diamine gave the Schiff base. Methanolic solution of the diamine (0.01 mol, 20ml) was added to methanolic solution of aryl azo compound (0.02mol, 20ml). The solution was stirred for five hours and evaporated at reduced pressure. The crystalline product formed was filtered and recrystallized from hot methanol to get chromatographically pure compound. The product formation is represented schematically below.

Scheme 1.10

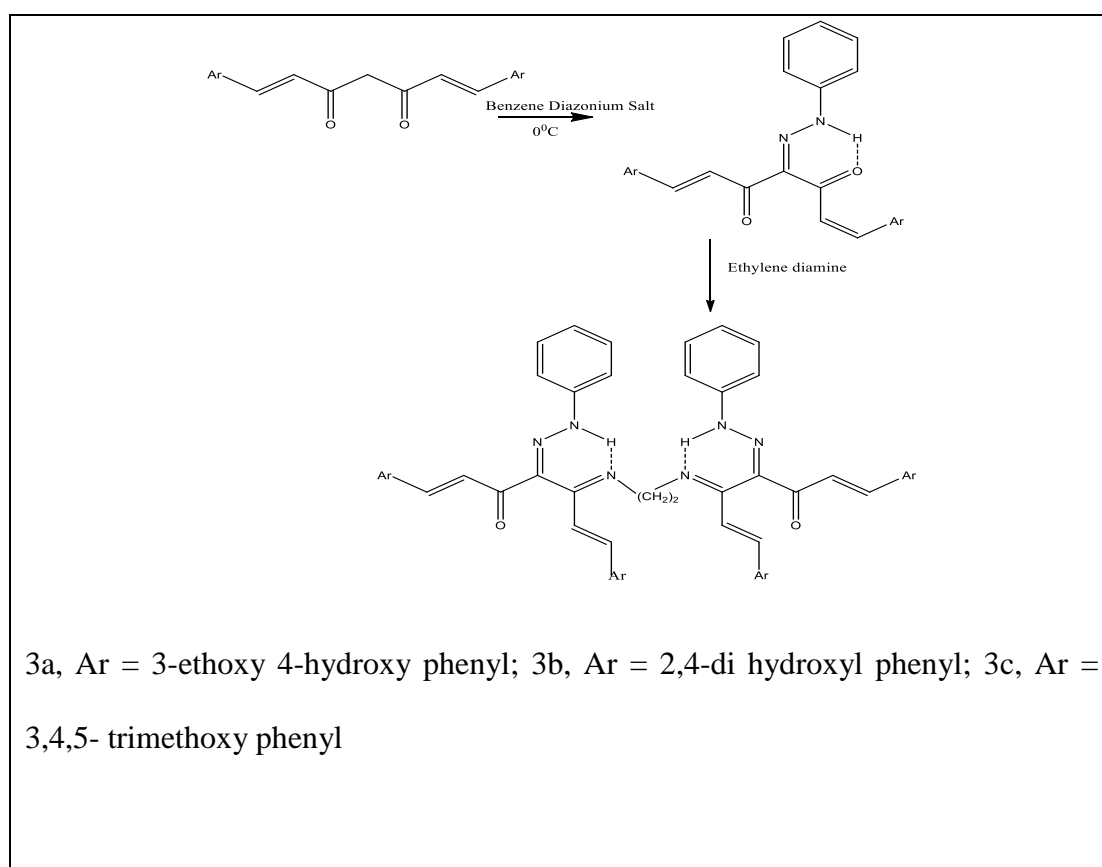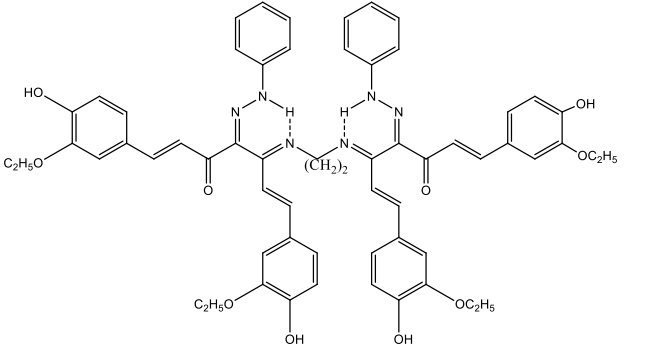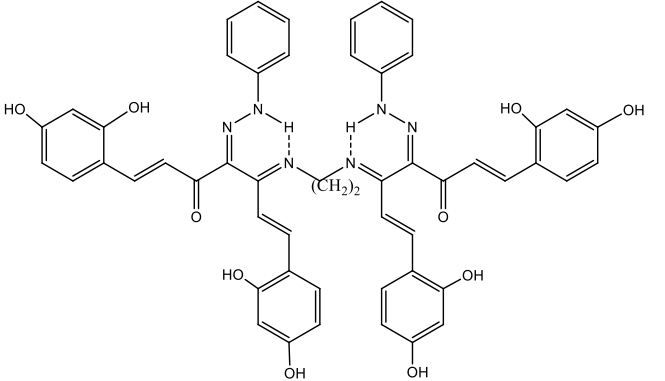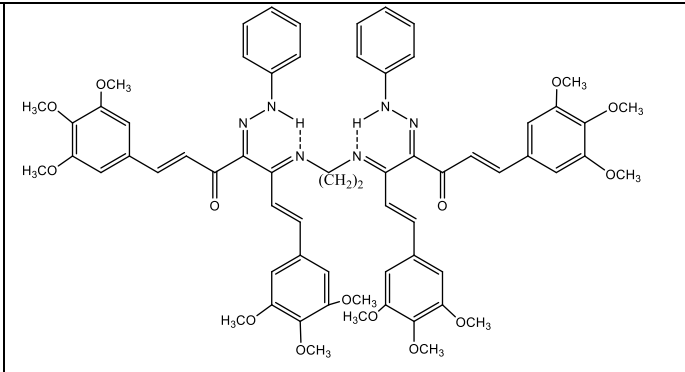3a, Ar = 3-ethoxy 4-hydroxy phenyl; 3b, Ar = 2,4-di hydroxyl phenyl; 3c, Ar = 3,4,5- trimethoxy phenyl

Table 1.19   Synthetic details of Schiff bases derived from aryl azo derivatives of di and tri substituted 1,7-diphenyl heptanoids

Compounds	Structure and systematic name of Schiff base ligands	Yield %
3a	 1,14-di(3-ethoxy 4-hydroxy phenyl) 5,10-di(ethylene- 3-ethoxy 4-hydroxy phenyl)-6,9diazotetradeca 1,5,9,13-tetraene -3,12-dione 4,11-diphenyl-hydrazone [EHEDTDH]	78
3b	 1,14-bis(2,4-dihydroxy phenyl) 5,10-bis(ethylene- 2,4 dihydroxy phenyl)-6,9diazotetradeca 1,5,9,13-tetraene -3,12-dione 4,11-diphenyl-hydrazone [DHEDTDH]	72

3c

1,14-di(3,4,5-trimethoxy phenyl) 5,10-di(ethylene- 3,4,5 -trimethoxy phenyl)-6,9diazotetradeca 1,5,9,13-tetraene -3,12-dione 4,11-diphenyl-hydrazone [TMEDTDH] | 79 |

The Schiff base compounds 3a, 3b & 3c are crystalline in nature, brownish black in colour and showed sharp melting points. They are soluble in organic solvents like acetone, ethyl acetate, chloroform, methanol etc. The observed C, H, N percentage and molecular weight determined are given in Table 1.20. This along with the mass spectral data of the compounds suggested the structure of the compound is as given in Scheme 1.10.

Table 1.20   Analytical & UV spectral data of 3a, 3b & 3c

Compounds	MP.(^{o}C)	Elemental analysis (%) Found/(Calculated)			Molecular weight	UV λ_{max} (nm)
		C	H	N		
3a	146	69.63 (70.29)	5.59 (5.89)	7.92 (8.19)	1025.14	275, 349
3b	158	68.39 (68.41)	4.58 (4.85)	8.94 (9.20)	912.93	271, 354
3c	175	66.93 (67.11)	5.31 (5.98)	7.15 (7.33)	1145.25	276, 372

Characterisation of the Schiff base compounds 3a, 3b and 3c.

The Schiff bases 3a, 3b and 3c were synthesized and characterized by UV, IR, 1H NMR, 13C NMR and Mass spectral techniques.

UV spectra

The electronic spectra of the Schiff bases were recorded in methanol and the data analysed are given in Table1.20.All the Schiff base compounds in methanolic solution showed a broad characteristic UV –visible absorption at around 300-500nm and showed a maximum absorption band at wavelength in-between 260-340 nm and a weak absorption band in the range 420-445 nm. The maximum absorption observed was due to the electronic dipole allowed $\pi \rightarrow \pi^*$ excitations of the extended conjugation system of the molecule and the weak absorption band due to dipole forbidden n$\rightarrow \pi^*$ transitions.

IR spectra

The IR spectrum of all the Schiff base compounds 3a, 3b & 3c showed a broad band in the range from 2800-3600 cm^{-1} which was due to ν NH group in hydrogen bonded form. The medium intensity bands observed in the region 2500-3000 cm^{-1} are assigned to the ν N-H vibrations and methyl group motions. The important absorption band at nearly 1670 cm^{-1} was due to the free C=O group in the compounds. This is the most important functional group available for IR elucidation. The value of free carbonyl absorption is higher than the value of the conjugated C=O group. This is a proof for free C=O existence in the compounds. The probable IR values assigned due to ν(CH=CH) trans, ν (C-C) alkenyl etc. are given in Table 1.21. The IR band at 868 cm^{-1} is due to out of plane C-H vibrations

of Schiff base compounds 3a, 3b and 3c. The IR spectrum of 3a is presented in Fig.1.21.

Table 1.21   IR spectral data of Schiff bases derived from aryl azo derivatives of di and tri substituted 1,7-diaryl heptanoids

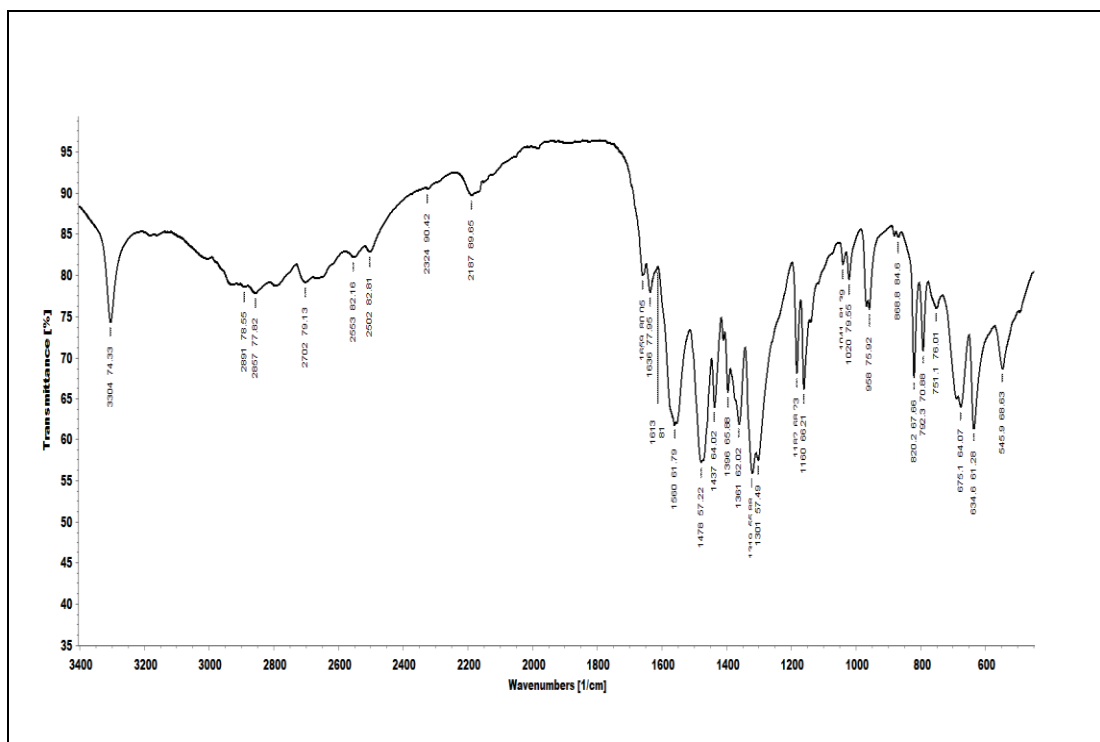| Compounds			
3a	3b	3c	Probable IR assignments
1659	1652	1657	ν(C=O)
1638	1628	1630	Hydrazono ν(C=N)
1613	1610	1608	Imine ν(C=N)
1542	1532	1541	ν (C-C) alkenyl
967	972	982	ν (CH=CH) trans

Fig. 1.21   IR spectral data of Schiff base 3a

^{1}H NMR spectra

The ^{1}H NMR spectra of di & tri substituted Schiff bases showed specific peaks corresponding to NH, methylene, alkenyl, methyl, phenyl and phenolic groups (Table 1.22). Schiff bases displayed a one proton singlet at ~ 8.5 ppm assignable to intra molecularly hydrogen bonded NH proton. Another multiplet at ~ 2.8ppm corresponds to the methylene protons. The NH proton and methylene proton can be identified from the structure given below. Phenyl protons were present at a very specific region of 7.0 – 7.9 ppm whereas alkenyl protons peaks were distributed over a region of 6.7 – 8.044ppm. The ^{1}H NMR spectra of 3c is shown in Fig.1.22.

Table1.22 ^{1}H NMR spectral data of Schiff bases derived from aryl azo derivatives of di and tri substituted 1,7-diphenyl heptanoids

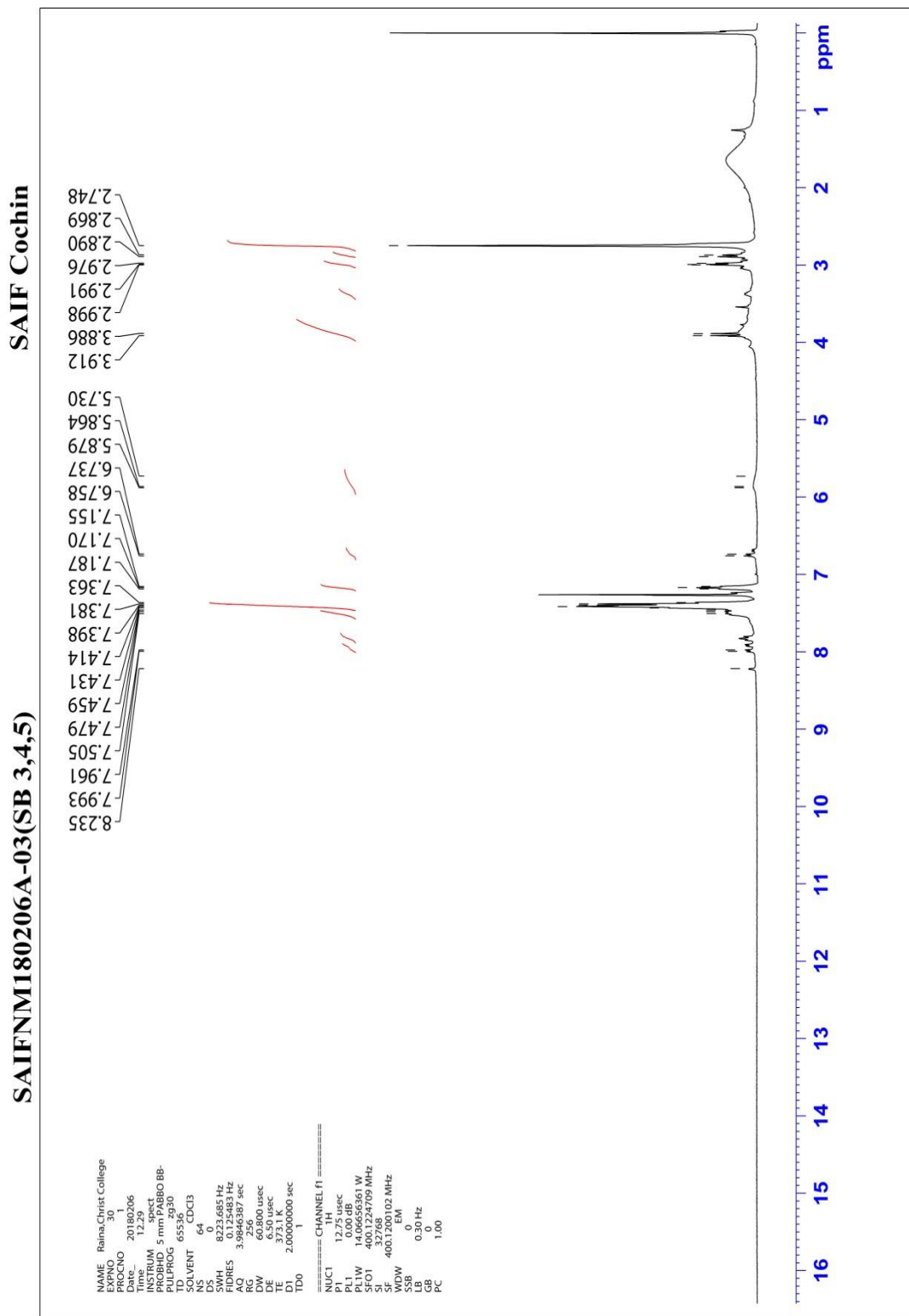| Compounds	Chemical shifts (δ ppm)				
	NH	Aryl	alkenyl	(CH_2)	$OCH_2CH_3/OH/$ OCH_3
3a	8.45	7.15-7.951	6.78-8.04	2.761-2.902	4.17,1.480
3b	8.63	7.026-7.81	6.86-7.854	2.79-3.163	9.748
3c	8.235	7.155-7.96	6.73-7.993	2.748-2.998	3.886-3.912

Fig.1.22 ¹H NMR spectrum of Schiff base 3c

The methyl protons of 3a were observed at a region of 1.480-1.514 whereas that of –OCH$_2$- protons were present at a region of 4.17-4.22 ppm. Methoxy protons of 3c are observed at 3.912ppm. The phenolic proton of 3a is seen at 9.832 ppm whereas that of 3b is observed at 10.04ppm

^{13}C NMR spectra

The ^{13}C NMR spectral data of 3a, 3b & 3c are given in Table 1.23, 1.24 & 1.25. ^{13}C NMR spectrum of 3a is depicted in Fig.1.23. The peak corresponding to methylene (C1) carbon is present ~ at 42.847ppm. C4 carbon of carbonyl appears at a position at~ 192 ppm. The alkenyl carbon C6 present at a position nearer to the phenyl ring system showed peaks at ~134ppm. The aromatic carbon atoms are present between 115 – 145 ppm. In 3a C9 carbon which is attached to the ethoxy group is seen at 145.427ppm whereas that of C10attached to hydroxyl group is seen at 146.23 ppm. The ethoxy carbon atoms of 3a are observed at 64.23 & 20.22 ppm.

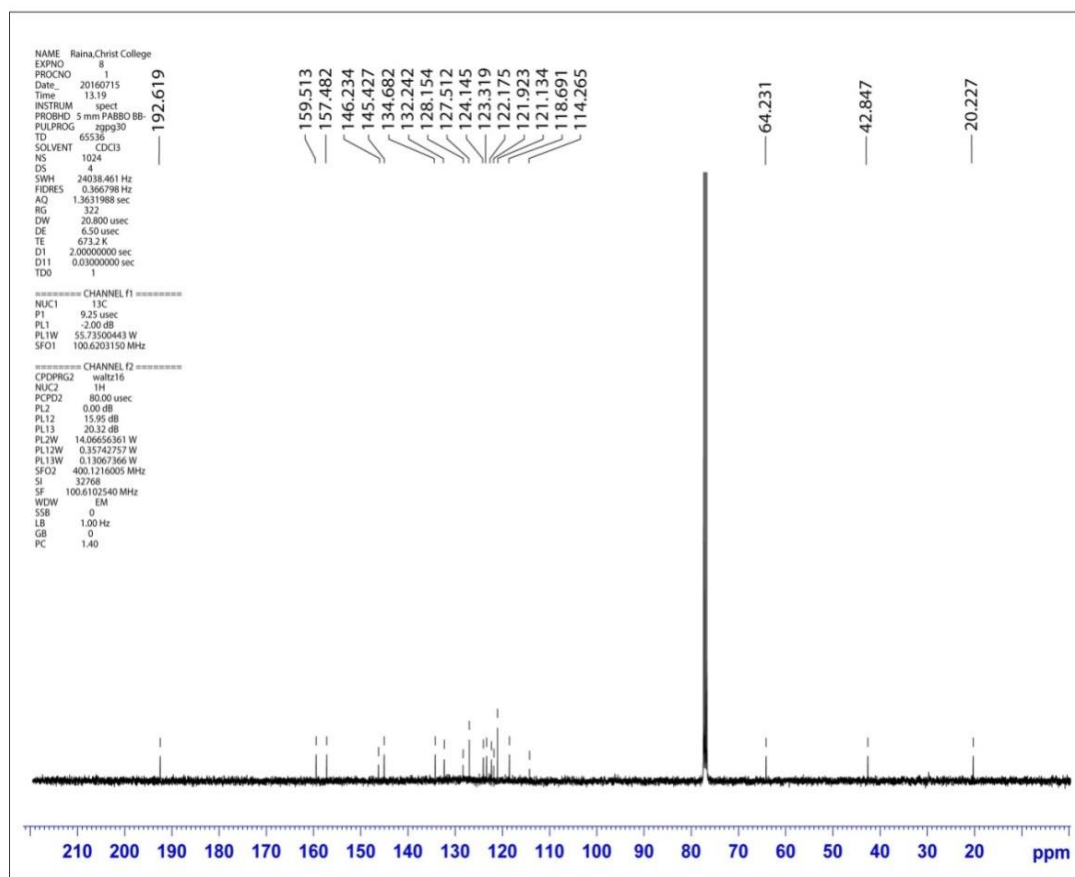**Structure representing different carbon atoms in 3a**
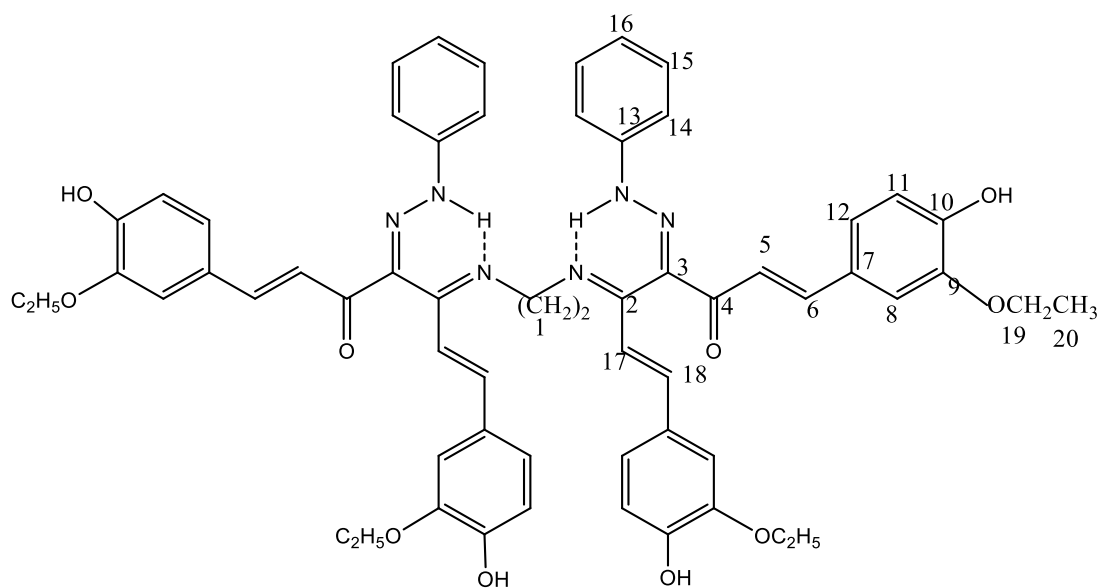
Fig.1.23 ¹³C NMR spectra of Schiff base 3a

Table 1.23 ¹³C NMR spectral data of Schiff base 3a (chemical shift in ppm)

C1	C2	C3	C4	C5	C6	C7	C8	C9	C10
42.84	159.51	157.48	192.61	123.31	134.68	127.51	118.69	145.42	146.23
C11	C12	C13	C14	C15	C16	C17	C18	C19	C20
118.69	121.13	132.24	121.28	124.14	122.17	114.26	128.15	64.23	20.22

Structure representing different carbon atoms in 3b
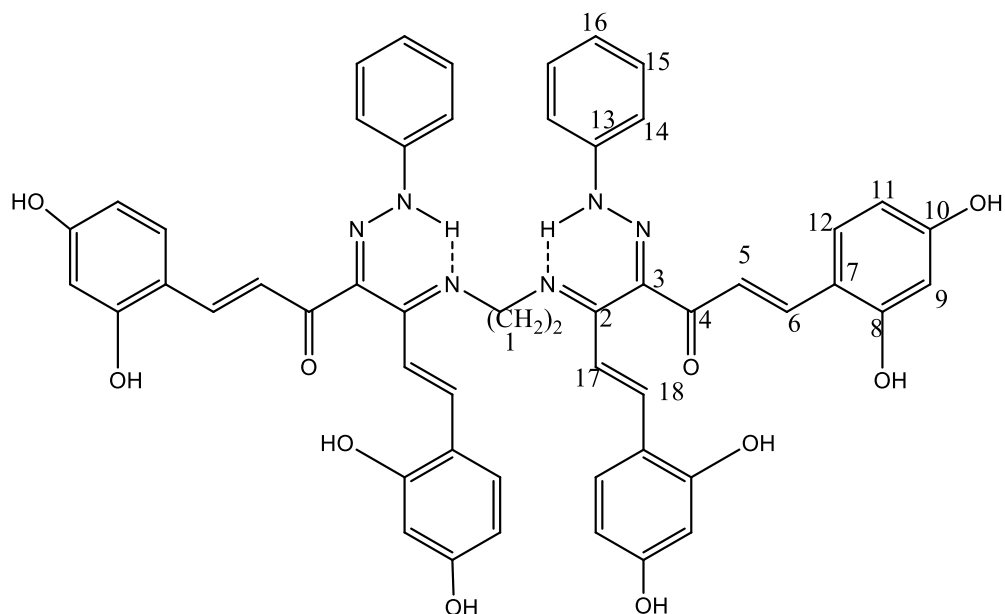
Table 1.24 ^{13}**C NMR spectral data of Schiff base 3b (chemical shift in ppm)**

C1	C2	C3	C4	C5	C6	C7	C8	C9
43.12	160.38	158.15	191.27	123.52	135.73	127.62	149.68	106.21
C10	**C11**	**C12**	**C13**	**C14**	**C15**	**C16**	**C17**	**C18**
147.92	119.38	121.45	130.21	121.85	124.82	122.76	114.58	129.69

SAIFNM160715A-05(A)

NAME   Raina,Christ College
EXPNO   8
PROCNO   1
Date_   20160715
Time   13.19
INSTRUM   spect
PROBHD   5 mm PABBO BB-
PULPROG   zgpg30
TD   65536
SOLVENT   CDCl3
NS   1024
DS   4
SWH   24038.461 Hz
FIDRES   0.366798 Hz
AQ   1.3631988 sec
RG   322
DW   20.800 usec
DE   6.50 usec
TE   673.2 K
D1   2.00000000 sec
D11   0.03000000 sec
TD0   1

======== CHANNEL f1 ========
NUC1   13C
P1   9.25 usec
PL1   -2.00 dB
PL1W   55.73500443 W
SFO1   100.6203150 MHz

======== CHANNEL f2 ========
CPDPRG2   waltz16
NUC2   1H
PCPD2   80.00 usec
PL2   0.00 dB
PL12   15.95 dB
PL13   20.32 dB
PL2W   14.06656361 W
PL12W   0.35742757 W
PL13W   0.13067366 W
SFO2   400.1216005 MHz
SI   32768
SF   100.6102540 MHz
WDW   EM
SSB   0
LB   1.00 Hz
GB   0
PC   1.40

183.368
160.169
158.513
153.563
153.498
150.631
134.682
132.242
128.999
128.686
125.775
124.506
123.713
122.408
121.518
114.265
59.234
56.234
56.193
46.479
44.927

Fig. 1.24 ^{13}**C NMR spectra of 3c**

Table 1.25 ^{13}**C NMR spectral data of Schiff base 3c (chemical shift in ppm)**

C1	C2	C3	C4	C5	C6	C7	C8	C9	C10	C11
46, 44	160.16	158.51	183.3	123.71	134.6	128.6	119.1	153.56	150.63	153.4

C12	C13	C14	C15	C16	C17	C18	C19	C20	C21	
121.5	132.24	122.4	124.5	122.4	114.2	128.9	56.23	59.23	56.19	

Structure representing different carbon atoms in 3c
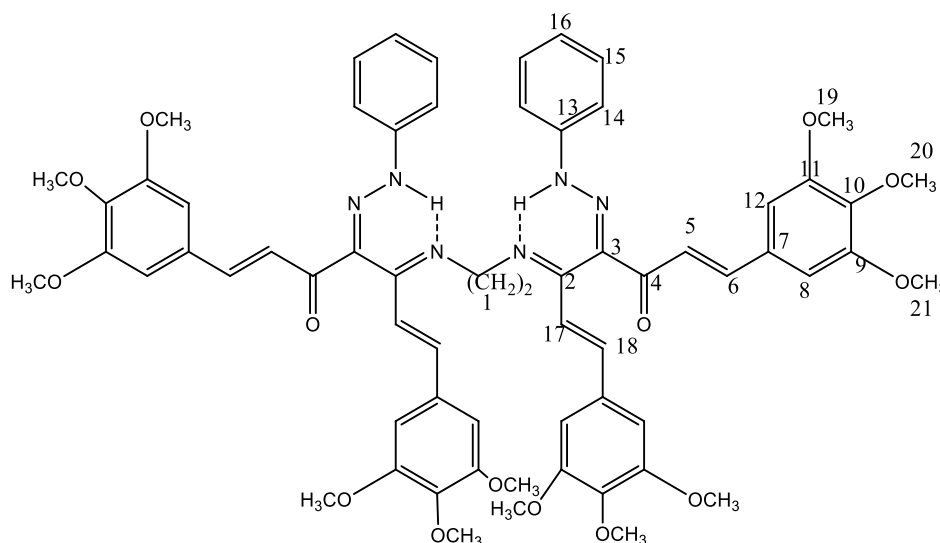
In 3b, the C1 carbon gave a peak at 43.12 ppm. The C4 carbon of the carbonyl group produced a peak at 191.27 ppm. The hydroxyl groups are attached to carbons C8 & C10 and the peaks are observed at positions 149.68 & 147.92 respectively. The carbons in the aromatic ring are observed in the range 119-135 ppm.

In 3c, methoxy groups are attached to carbon atoms C9, C10 & C11. The peaks are down shielded and are observed at position 150 ppm for C10 and 153.5& 153.4 for C9 and C11 respectively. Methoxy carbon atoms are present at positions 56.23, 59.23 & 56.19ppm

Mass spectra

The mass spectra of Schiff base 3c showed distinct M+ ion peak at 1145. The elimination of important groups from the Schiff base molecule gave rise to different fragments (Scheme 1.11) and the values obtained are depicted in Table 1.26. The mass spectrum of Schiff base 3c is displayed in Fig.1.25. Smaller fragments like OH, O, CH_2 etc. were removed from the molecular ion and gave their respective peaks in the Spectrum. Fig.1.26 gives the SIM mode for the Schiff

base 3c taken using LCMS (Liquid chromatography/Mass spectrometry). This clearly showed the formation of molecular ion peak at 1145.

Table1.26 Mass spectral details of Schiff base 3a, 3b and 3c

Fragments	Ligands	M,M+1,M ions	A	B	C	D	E	F	G
Mass	3a	1025	862	671	594	527	499	198	142
Patterns	3b	914	778	614	537	470	442	199	143
	3c	1145	952	731	654	587	559	198	143

*The alphabets correspond to the fragments given in **Scheme 1.11**
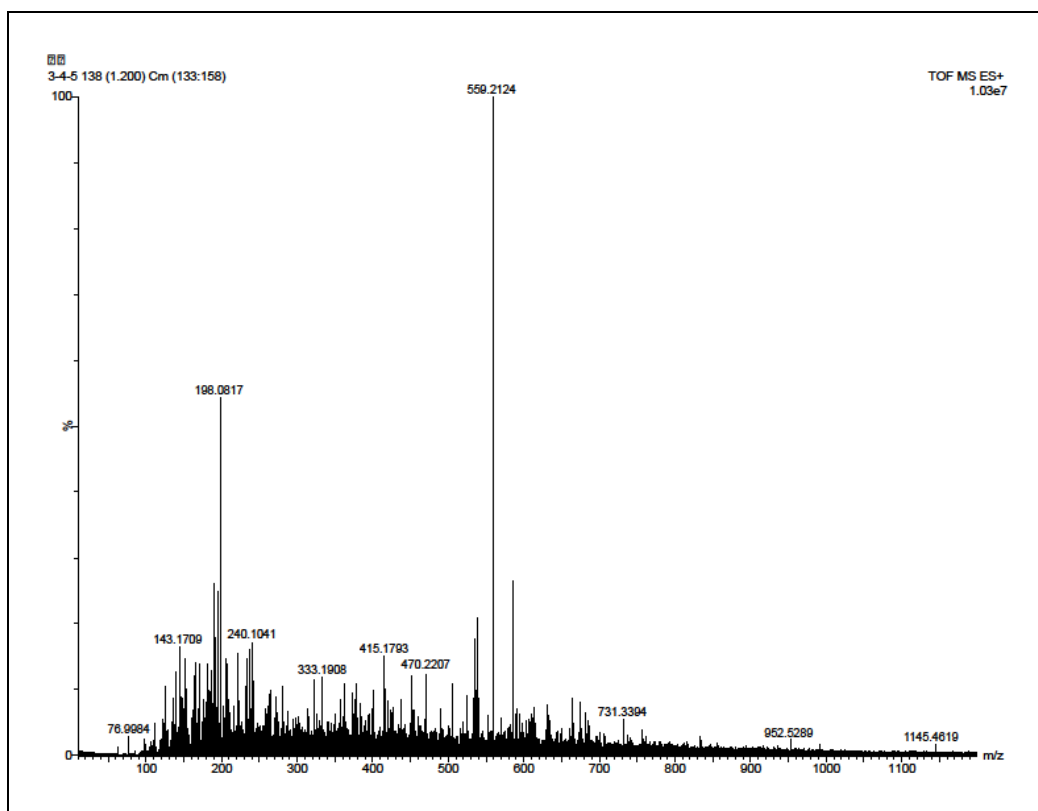
Fig.1.25 Mass spectrum of Schiff base 3c
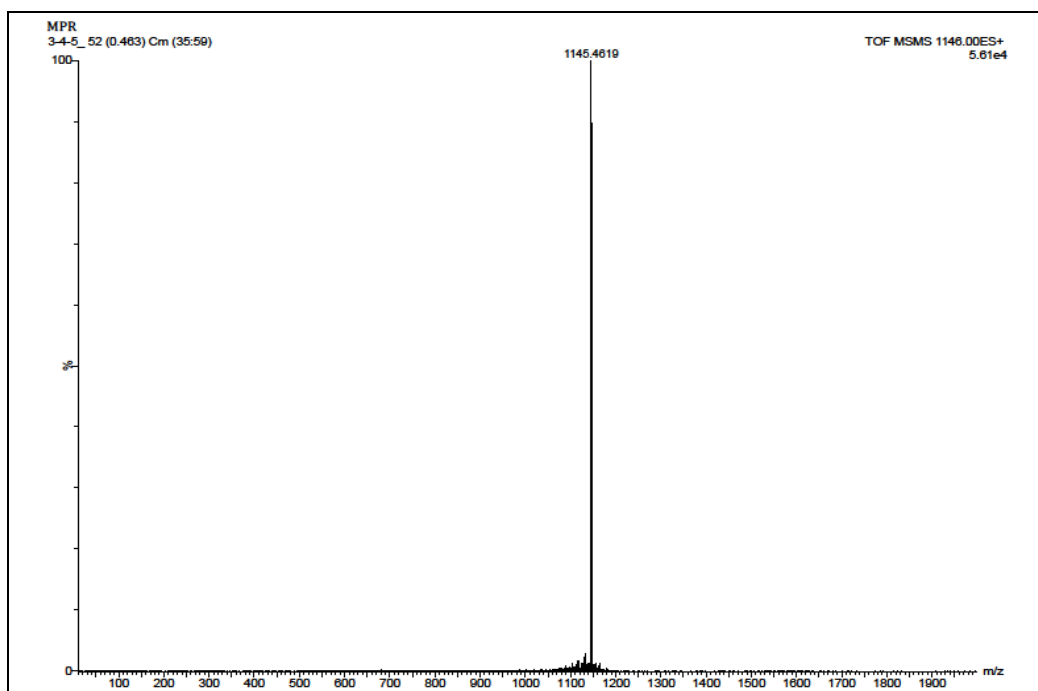
Fig.1.26 Selected ion monitoring (SIM) mode of mass spectrum of Schiff base 3c

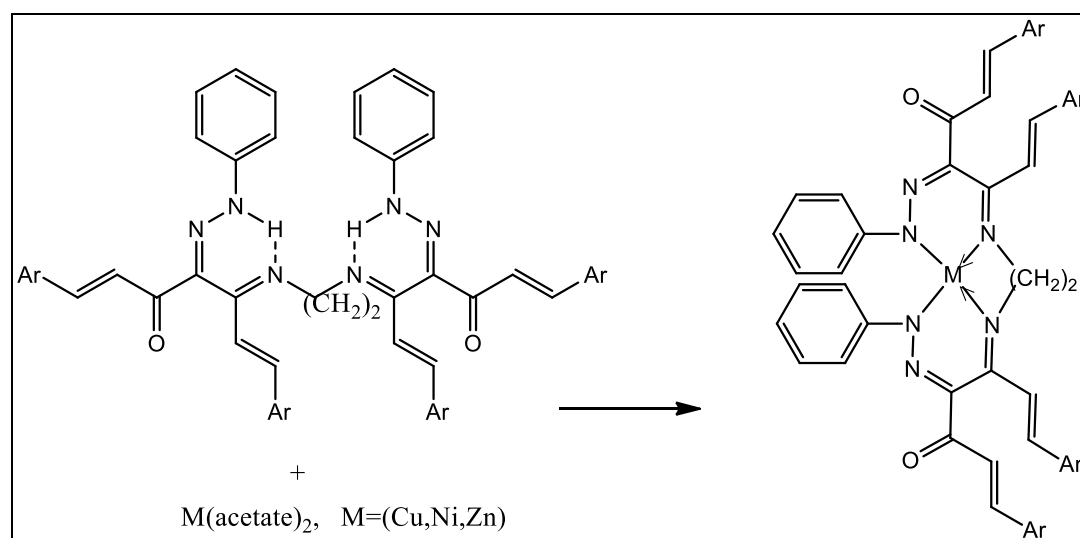**Scheme 1.11 Mass fragmentation pattern of Schiff bases**
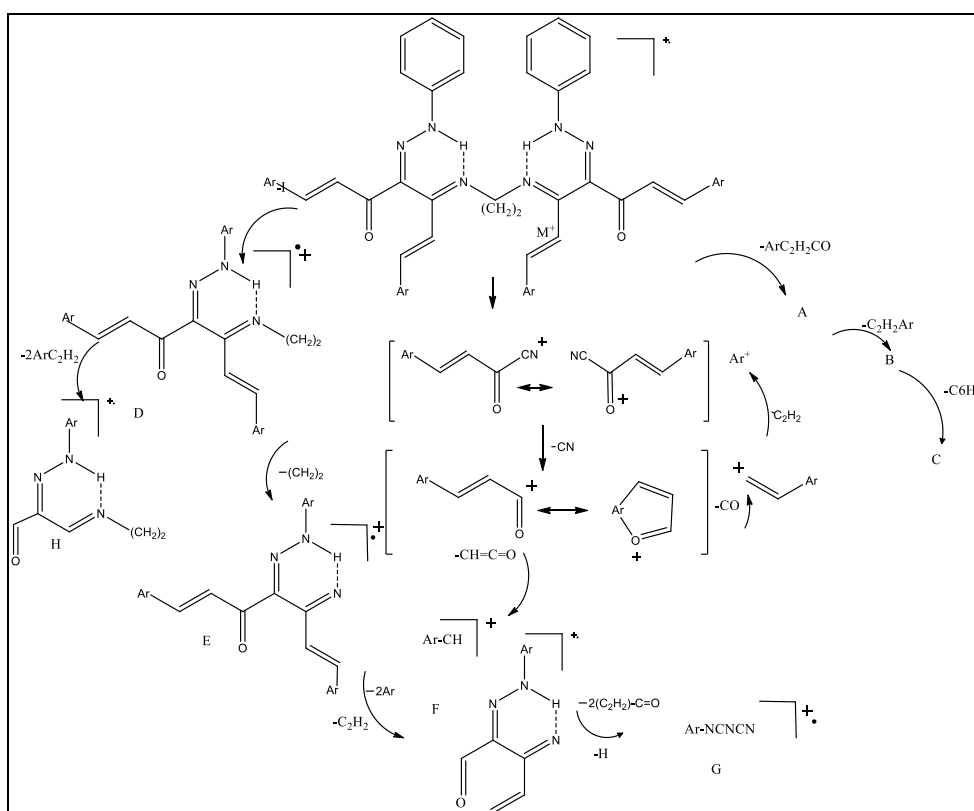
3a, Ar= 2 ethoxy 4hydroxy phenyl,   3b, Ar= 2,4 di hydroxy phenyl,   3c, Ar= 3,4,5 trimethoxy phenyl

Synthesis and characterization of metal chelates of Schiff bases 3a, 3b and 3c

Synthesis of metal complexes of Schiff bases 3a, 3b and 3c

Copper(II), Zinc(II) and Nickel(II) complexes of Schiff bases derived from aryl azo derivatives of curcuminoid analogues with ethoxy hydroxy, dihydroxy and trimethoxy substituted phenyl rings were synthesized by the following typical method. To the refluxing solution of the Schiff base ligand (0.01 mol) in methanol (20ml), a methanolic solution of metal salt (0.01mol, 20ml)was added and the reaction mixture was refluxed for nearly three hours and allowed to cool to room temperature. The metal salts used for the preparation of Cu(II), Zn(II) and Ni(II) complexes are Copper acetate, Zinc acetate and Nickel acetate respectively. The precipitated complex was then filtered, washed with 1:1, methanol:water mixture and recrystallized from hot methanol. The general reaction involved in the formation of complexes is given below in Scheme1.12.

Scheme1.12

3a, Ar = 2-ethoxy 4-hydroxy phenyl, 3b, Ar = 2,4-di hydroxy phenyl, 3c, Ar = 3,4,5- trimethoxy phenyl

Characterization of transition metal complexes of Schiff bases derived from aryl azo derivative of curcuminoid analogues with di & tri substituted phenyl rings

Metal chelates (Cu, Zn and Ni) of Schiff base ligands 3a, 3b & 3c were characterized using analytical and several spectral techniques like UV, IR, NMR and mass data. Elemental analysis data (C, H, N and metal percentages), physical data, UV and IR spectral data are given in Table 1.27, 1.28 & 1.29. The analytical data together with mass spectral data suggest a ML stoichiometry for all the synthesized Schiff base complexes.

Table 1.27   Analytical and spectral data of metal complexes of Schiff base 3a

Metal chelates	M.P. (^{o}C)	Elemental analysis (%) Found/(calculated)				IR stretching bands (cm^{-1})		
		C	H	N	Metal	Free C=O	CN	M-N
Cu(II)	286	66.08 (66.31)	4.84 (5.37)	7.52 (7.73)	5.39 (5.84)	1625	1625 1590	508 503
Ni(II)	259	66.43 (66.61)	4.97 (5.40)	7.55 (7.76)	5.13 (5.42)	1659	1631 1594	506 502
Zn(II)	226	65.87 (66.20)	5.01 (5.37)	7.58 (7.72)	5.82 (6.00)	1674	1623 1592	507 504

Table 1.28   Analytical and spectral data of metal complexes of Schiff base 3b

Metal chelates	M.P. (°C)	Elemental analysis (%) Found/(calculated)				IR stretching bands (cm⁻¹)		
		C	H	N	Metal	Free C=O	CN	M-N
Cu(II)	286	63.92 (64.09)	4.01 (4.34)	8.59 (8.64)	6.28 (6.52)	1665	1618 1594	507 501
Ni(II)	259	64.02 (64.41)	4.13 (4.36)	8.22 (8.66)	5.99 (6.05)	1668	1626 1591	504 502
Zn(II)	226	63.69 (63.97)	4.17 (4.33)	8.37 (8.60)	6.62 (6.69)	1658	1622 1589	506 504

Table 1.29   Analytical and spectral data of metal complexes of Schiff base 3c

Metal chelates	M.P. (°C)	Elemental analysis (%) Found/(calculated)				IR stretching bands (cm⁻¹)		
		C	H	N	Metal	Free C=O	CN	M-N
Cu(II)	286	63.14 (63.69)	5.01 (5.51)	6.31 (6.96)	5.11 (5.26)	1671	1621 1593	506 504
Ni(II)	259	63.85 (63.95)	5.18 (5.53)	6.70 (6.99)	4.63 (4.88)	1663	162415 91	508 505
Zn(II)	226	63.29 (63.60)	5.23 (5.50)	6.32 6.95)	5.25 (5.40)	1662	1631 1590	507 502

IR spectra

The IR spectra of all metal complexes followed similar pattern but different from that of the Schiff base ligands. A representative IR spectrum of the Schiff base metal complex has been depicted in Fig.1.27. In complexes the bands due to free C=N was shifted to lower frequencies ~ 1550-1600 during complexation. This suggested that the Schiff base ligand coordinated with the central metal ions through the imine C=N group. The peak of carbonyl moiety which was present at ~ 1670 cm^{-1} remained the same. The NH deformation band in the region ~ 1570 cm^{-1} and broad band in the region of 2600 -3500 cm-1 present in the ligand reduced in the spectra of Schiff metal complexes. This indicated replacement of the chelated proton by the metal ion during complex formation. The new bands occurred in the range 500 and 550 cm $^{-1}$ further supported the formation of M-N bond (metal-nitrogen). The IR spectrum of Zn(II) complex of 3a is shown in Fig.1.27.
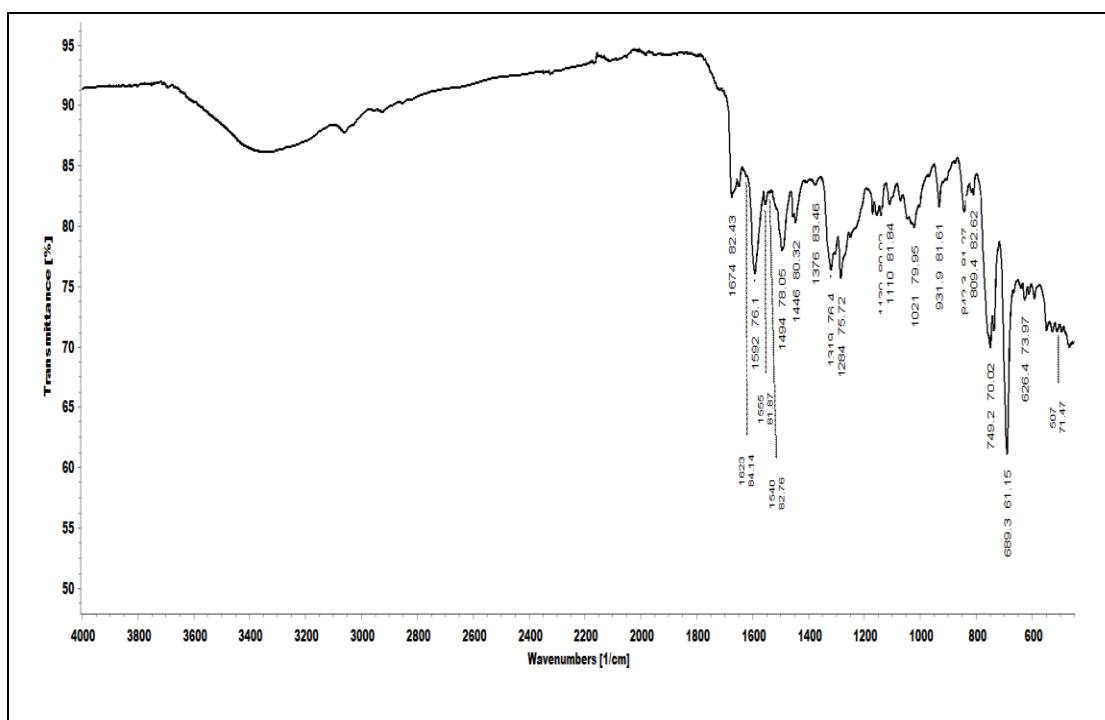
Fig.1.27   IR spectrum of Zn(II) complex of 3a.

¹H NMR spectra

The NH proton present in the Schiff base ligands was replaced by metal atom in metal complexes. This is evident by the disappearance of the nmr signal at δ ~ 8.23 ppm in metal complexes. The phenyl and alkenyl protons signals were not altered much since they are not involved in metal complex formation. Thus the spectra of Schiff base ligands and complexes are much similar except those of NH proton. The NMR spectrum of Ni(II) complex of 3c is shown in Fig.1.28.
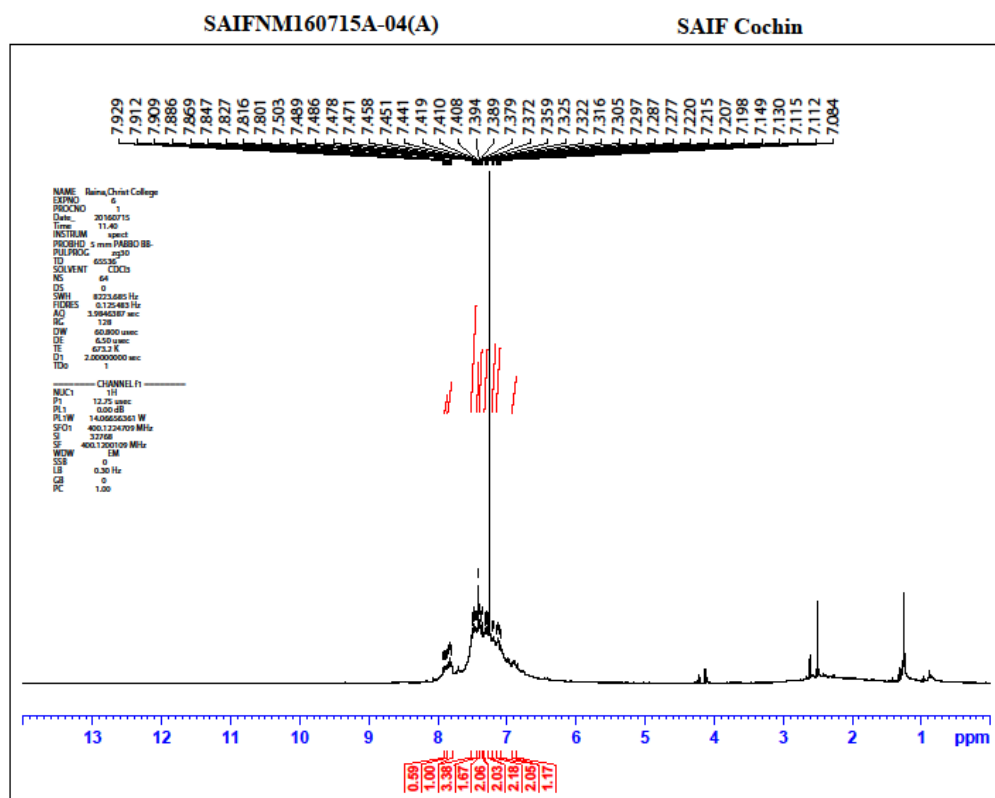

Fig.1.28   NMR spectrum of Ni(II) complex of Schiff base 3c.

Mass spectra

Mass spectral fragments are a significant tool in elucidating the structure of metal complexes. The mass spectrum of Zn(II) complex of Schiff base 3a is given

below(Fig1.29). Peaks due to stepwise removal of aryl groups were present in the mass spectra of metal complexes. In all the cases, the molecular ion peak and the intense base peak were also observed.
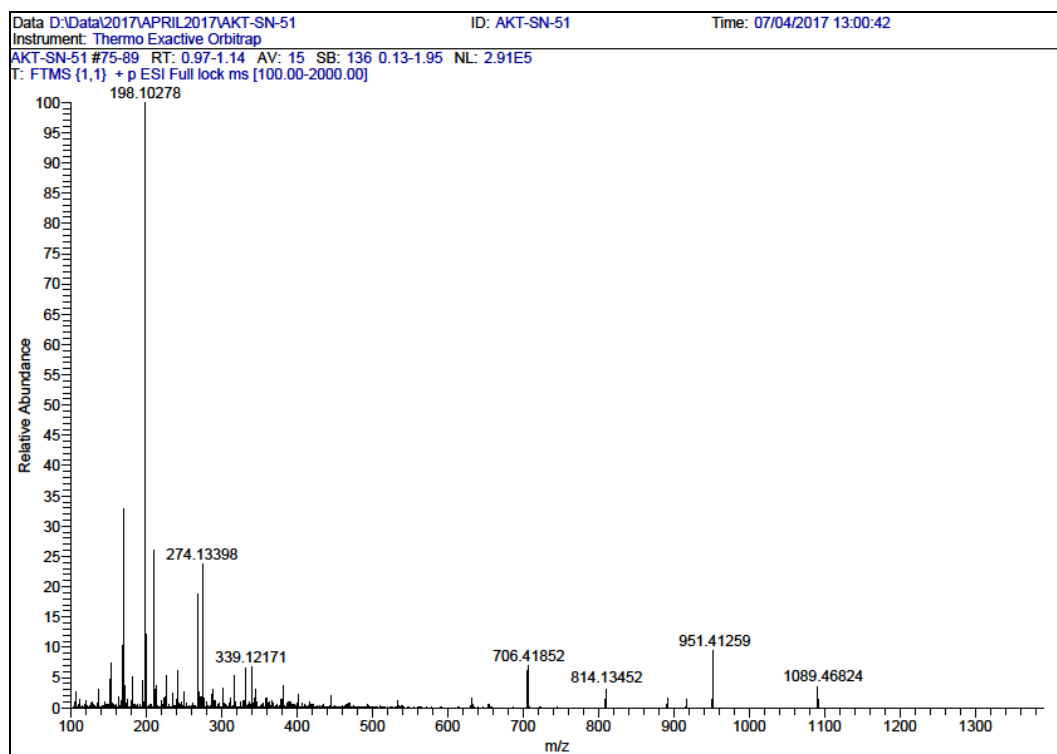

Fig.1.29 Mass spectrum of Zn(II) complex of Schiff base 3a.

In the mass spectrum of Zn(II) complex of 3a, a less intense M+ 1 peak is observed at 1089. The peak at 951 is due to the removal of one aryl group from the molecular ion. The intense peak at 814 is due to the removal of two aryl groups from molecular ion. The peak at 706 is due to the fragment ion formed by the removal of 2 ArC_2H_2CO groups from molecular ion (Ar =3-ethoxy 4-hydroxy phenyl).The base peak is observed at 198 due to the $[Zn-N_3C_3O]^+$. The peaks at 274 and 172 are due to fragments of ligand.

From the observed UV, IR, 1H NMR and Mass spectral data, the metal complexes of the Schiff compounds have a ML stoichiometry as given below.
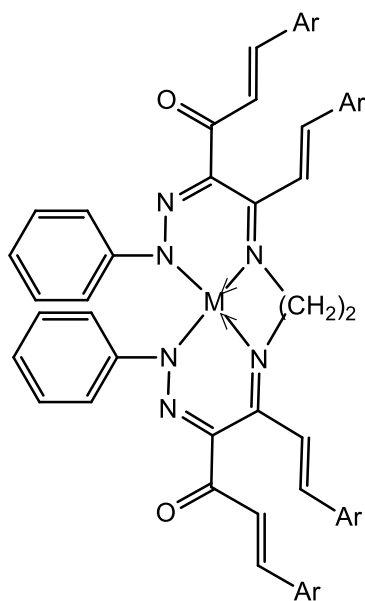
3a, Ar = 3-ethoxy 4-hydroxy phenyl,   3b, Ar = 2,4-di hydroxy phenyl,   3c, Ar = 3,4,5- trimethoxy phenyl

SECTION IV

Synthesis and characterization of Schiff bases derived from aryl azo derivative of curcuminoid analogues with naphthyl and substituted naphthyl rings and ethylene diamine and their transition metal chelates

Synthesis and characterization of Schiff bases

This unit explains the synthesis and characterization of Schiff bases derived from curcuminoid analogues with naphthyl and substituted naphthyl rings in place of phenyl rings in natural curcuminoids. The Schiff base ligands synthesized here include bis (1,7- di (naphthyl) – 4 - (phenyl - hydrazono) - hepta-1, 6 - diene-3,5-dione)diimine (4a) and bis(1,7-di(2-methoxynaphthyl)-4-(phenyl-hydrazono)-hepta-1,6-diene-3,5dione)ethylenediimine (4b) and bis(1,7-di(2-hydroxynaphthyl)-4-(phenyl-hydrazono)-hepta-1,6-diene-3,5-dione)ethylenediimine(4c)

Unit II of this chapter describes the synthesis and characterization of metal complexes of the above mentioned Schiff base ligands with the transition metal ions Cu(II),Zn(II) and Ni(II). The introduction of the naphthyl ring systems in the α,β unsaturated diketone moiety modifies the chemical and biochemical properties of the Schiff base compounds.

 Synthesis of substituted derivatives of 1,7-dinaphthyl-1,6-heptadiene-3,5-diones

The curcuminoid analogues discussed in this section are 1,7-dinaphthyl-1,6-heptadiene-3,5-dione, 1,7-bis(2-methoxynaphthyl)1,6-heptadiene-3,5-dione and 1,7-bis(2-hydroxynaphthyl)1,6-heptadiene3,5-dione.They were prepared by the condensation of poly cyclic aromatic aldehydes (1-naphthaldehyde,

2methoxynaphthaldehyde and 2-hydroxynaphthalehyde) with acetyl acetone-boric oxide complex in ethyl acetate medium in the presence of tri-sec-butyl borate and n-butyl amine. The product obtained was purified by the column chromatography over silica gel (60–120 mesh) by using 4:1 (v/v) chloroform : acetone mixture as the eluent and recrystallized twice from the hot benzene to get pure crystalline material.

Scheme1.13

4a-Ar=1-Naphthyl
4b-Ar=2-Methoxy naphthyl
4c-Ar=2-hydroxy naphthyl
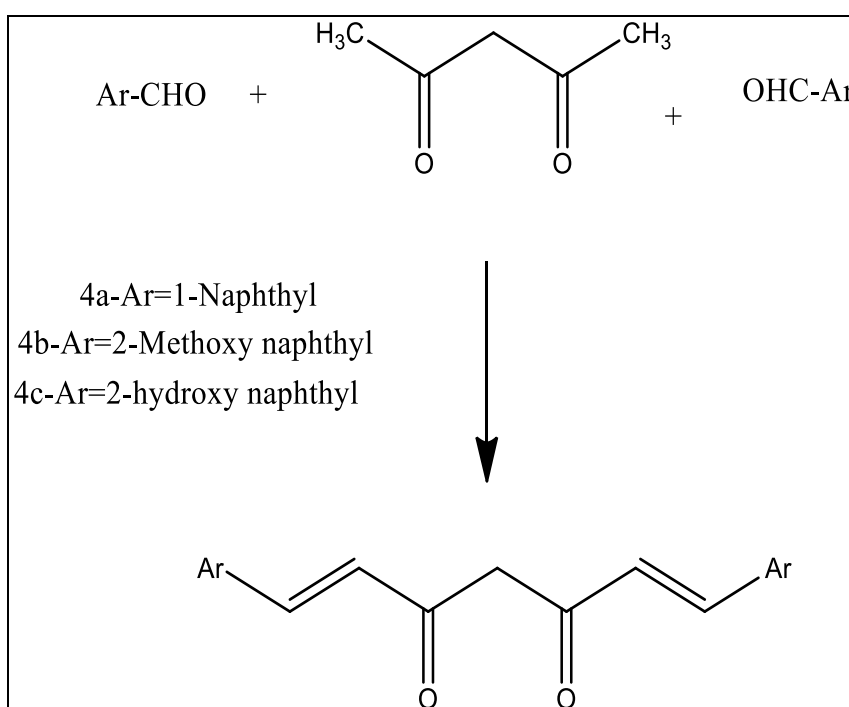
Synthesis of Schiff bases

The β-diketones synthesized above were coupled with benzene diazonium salt(0.01 mol) which was prepared as reported earlier and was kept below 0^0C .The benzene diazonium salt was added drop by drop to a solution of the β-diketones(0.01mol) in 15 ml methanol at below 0^0C with constant stirring. Sodium acetate (2mg) was then added to the mixture to keep the pH of the mixture in the range 6-7. The precipitated compounds were filtered, washed with water and recrystallized from

methanol to get chromatographically pure (TLC) material. The Schiff bases were then synthesized by the condensation of above precipitated hydrazono compounds with 1,2-diaminoethane (en) as follows. A methanolic solution of the 1,2-diaminoethane (0.01mol, 20ml) was added to a methanolic solution of the synthesized hydrazono compounds (0.02mol, 20ml). The solution was stirred for approximately 5 hours and evaporated at reduced pressure. The crystalline compound formed, was filtered and recrystallized from hot methanol to get chromatographically (TLC) pure compound. The schematic diagram for the product formation is given below.

Scheme1.14

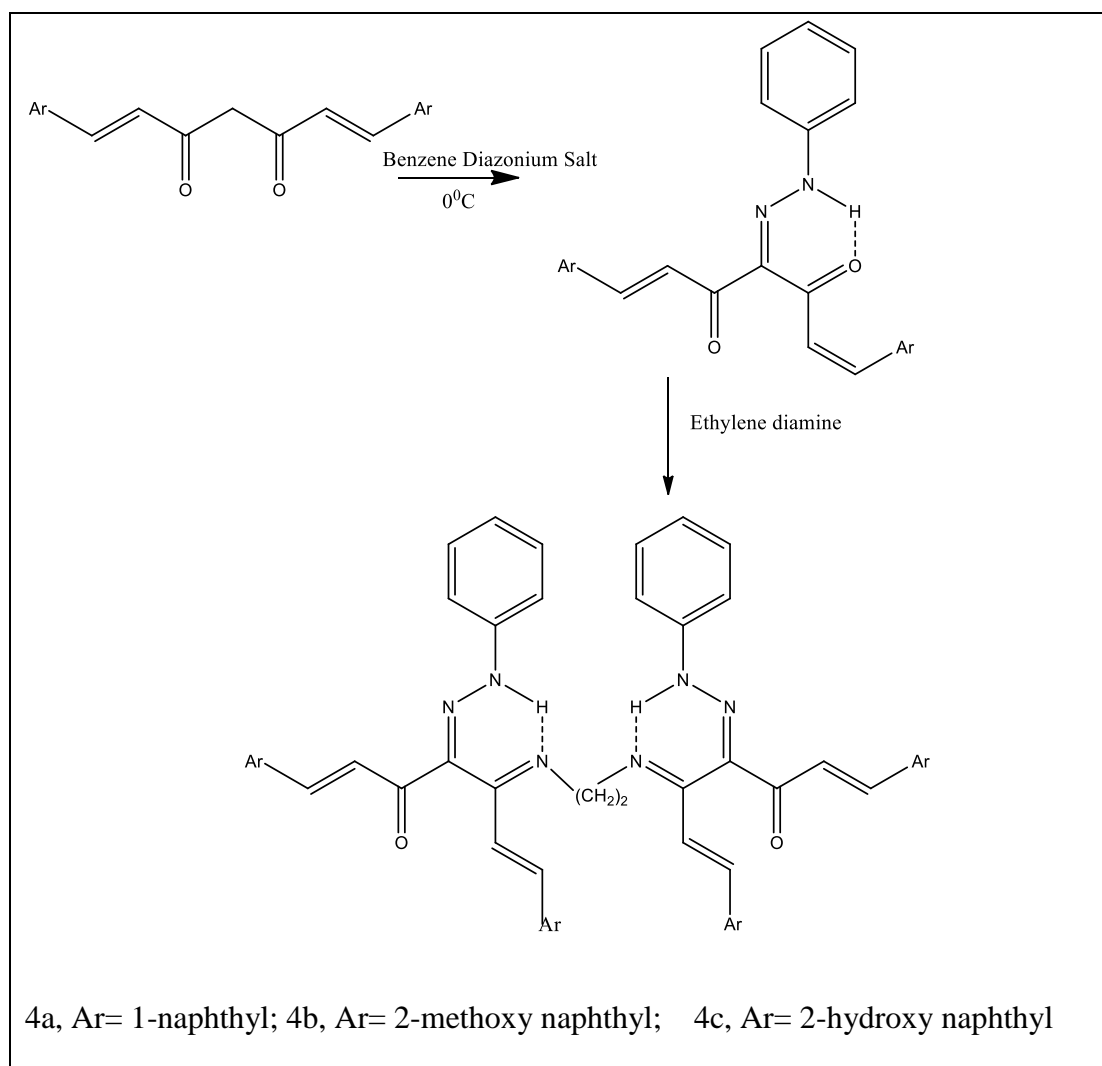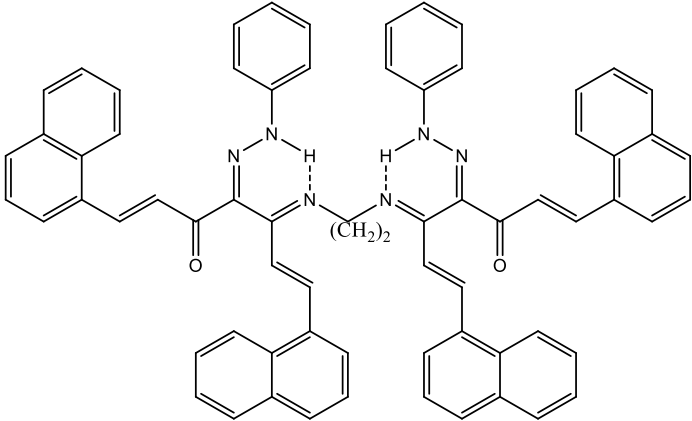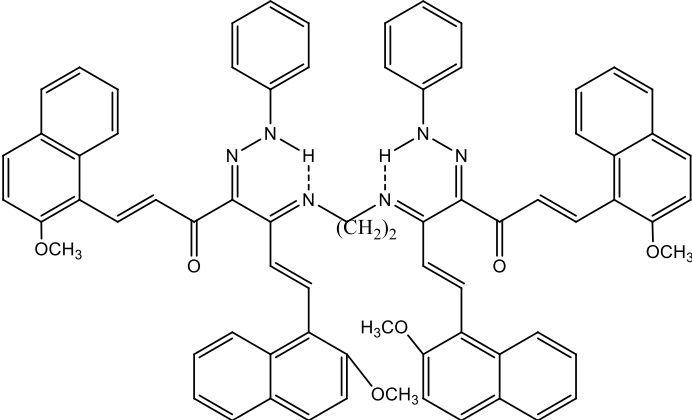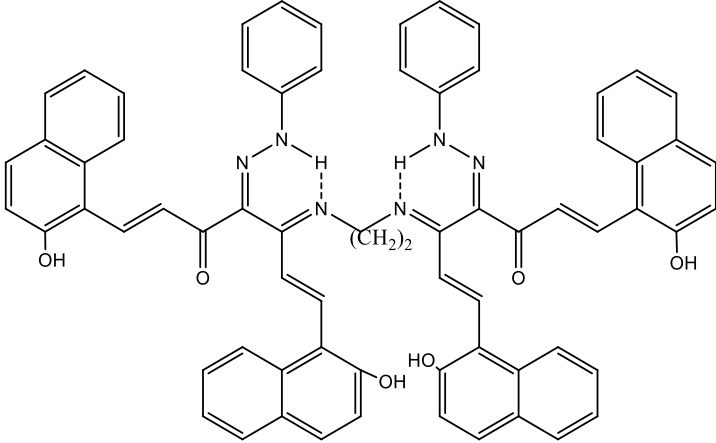4a, Ar= 1-naphthyl; 4b, Ar= 2-methoxy naphthyl;   4c, Ar= 2-hydroxy naphthyl

Table 1.30 Synthetic details of Schiff bases derived from aryl azo derivatives of di and tri substituted 1,7-diphenyl heptanoids

Compounds	Structure and systematic name of Schiff base ligands	Yield %
4a	 1,14-di(naphthyl) 5,10-di(ethylene- naphthyl)-6,9diazotetradeca 1,5,9,13-tetraene -3,12-dione 4,11-diphenyl-hydrazone [NEDTDH]	71
4b	 1,14-bis(2-methoxy naphthyl) 5,10-bis(ethylene-2-methoxy naphthyl)-6,9diazotetradeca 1,5,9,13-tetraene -3,12-dione 4,11-diphenyl-hydrazone[MNEDTDH]	70

1,14-di(2-hydroxynaphthyl) 5,10-di(ethylene- 2-hydroxy naphthyl)-6,9diazotetradeca 1,5,9,13-tetraene -3,12-dione 4,11-diphenyl-hydrazone [HNEDTDH]

| 4c | | 69 |

All the Schiff base compounds prepared (4a, 4b, 4c) are crystalline solids and showed sharp melting point. They are insoluble in water and were soluble in organic solvents like acetone, chloroform, ethyl acetate, methanol etc. The elemental analysis data, determined molecular weight and the melting point of the Schiff base compounds are shown in Table 1.31. The UV spectral data of the Schiff base compounds is also included in the table below.

Table 1.31   Analytical & UV spectral data of 4a, 4b & 4c

Compounds	MP.(^{o}C)	Elemental analysis (%) Found/(Calculated)			Molecular weight	UV λ_{max} (nm)
		C	H	N		
3a	124	82.63 (82.90)	5.03 (5.32)	8.26 (8.53)	985.17	276, 362
3b	160	78.01 (78.23)	5.19 (5.47)	7.38 (7.60)	1105.28	273, 358
3c		77.14 (77.84)	4.78 (4.99)	7.81 (8.01)	1049.17	278,367

Spectral Characterization of Schiff bases

Schiff base Compounds 4a, 4b and 4c were synthesized and were characterized by various spectral techniques like UV, IR, 1H NMR, 13C NMR and Mass spectral techniques.

IR spectra

In these Schiff base compounds the position and intensity of the carbonyl stretching frequency and CN stretching frequency depends on the molecular structure in its immediate vicinity and is useful in characterizing the type of carbonyl and C=N functions. Presence of NH group in these Schiff base molecules can be very well established using IR spectroscopy. All the Schiff base compounds were quite symmetrical with the carbonyl groups attached to aliphatic carbons, the olefinic groups were intervened between the naphthyl and carbonyl group. IR spectra of 4a, 4b and 4c were characterized by the presence of strong bands at 1608 cm^{-1}, 1618 cm^{-1} and 1602 cm^{-1} respectively due to the imine group. The decrease in NH frequency from the normal value can be explained due to hydrogen bonding. There was a band in the region ~1660 cm^{-1} which was assignable due to free C=O group. This showed that the Schiff base compounds are in the intramolecularly hydrogen bonded form. All the compounds showed bands in the region ~1630 cm^{-1} which are assigned to hydrazono C=N bonds and in the range ~819 cm^{-1} which are assigned to C=C bonds of olefinic groups. In the spectra, the intramolecular hydrogen bonded NH group showed a broad band in the region 2250-3600 cm^{-1}. There are a number of medium intensity vibrations in the region 1070-1530 cm^{-1} due to various stretching vibrations of the phenyl group, alkenyl group & chelate ring. The bands observed in the region 969, 970 and 972 cm^{-1} were assigned to the

trans CH=CH vibrations. The important IR absorptions and their probable values are given in Table 1.32. IR spectrum of Schiff base compound 4b is represented in Fig.1.30.

Table1.32   IR spectral data of Schiff base compounds 4a,4b and 4c

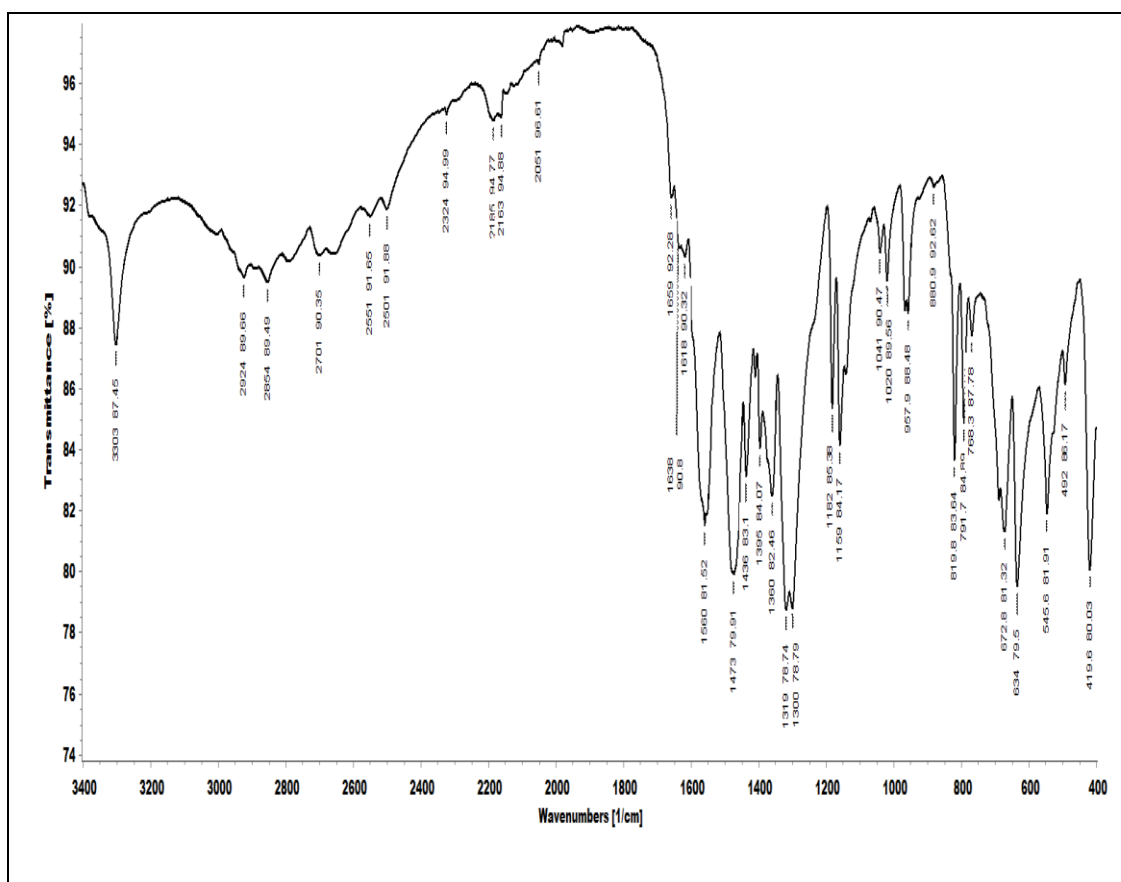| Compounds			
4a	4b	4c	Probable IR assignments
1664	1659	1657	ν(C=O)
1626	1638	1628	Hydrazono ν(C=N)
1608	1618	1602	Imine ν(C=N)
1531	1532	1542	ν (C-C) alkenyl
969	970	972	ν (CH=CH) trans

Fig.1.30 IR spectrum of Schiff base compound 4b.

^{1}H NMR spectra

The ^{1}H NMR spectra of all compounds 4a, 4b & 4c displayed a one proton singlet downfield at ~ 8.24ppm and another singlet peak at δ ~ 2.8ppm due to intra molecularly hydrogen bonded NH proton and methylene protons respectively. The position of these signals were varied slightly in all Schiff base compounds because they are influenced by the electronic effects of groups attached to the C=N function. The ^{1}H NMR spectra of all Schiff base compounds showed specific peaks corresponding to NH, methylene, alkenyl, methoxy, phenyl and hydroxyl groups. The methoxy substituent on the naphthyl rings in Schiff base compound 4b displayed a signal at 4.044 ppm. The hydroxyl protons substituent on the naphthyl rings in Schiff base 4c displayed a signal at 9.637 ppm. The assignments of various proton signals seen in the spectra of the compounds are given in Table 1.33. The hydrogen bonded structure of the Schiff base compound representing NH and methylene proton is given below. The ^{1}H NMR spectra of Schiff base compound 4c is brought out in figure 1.31.
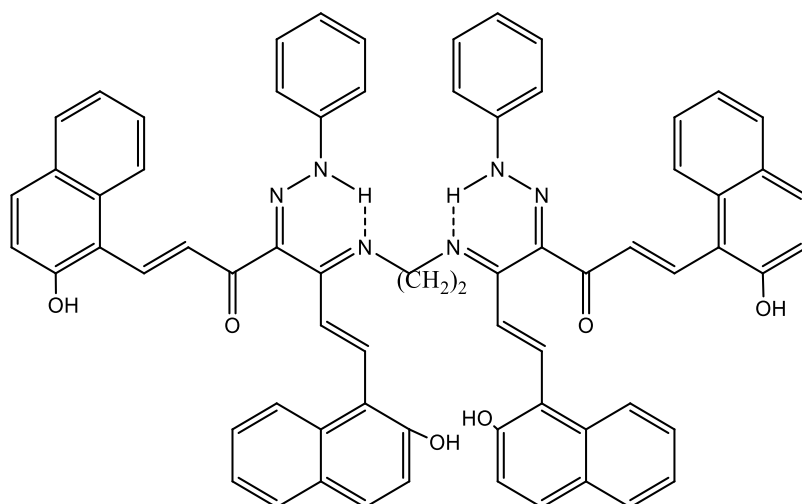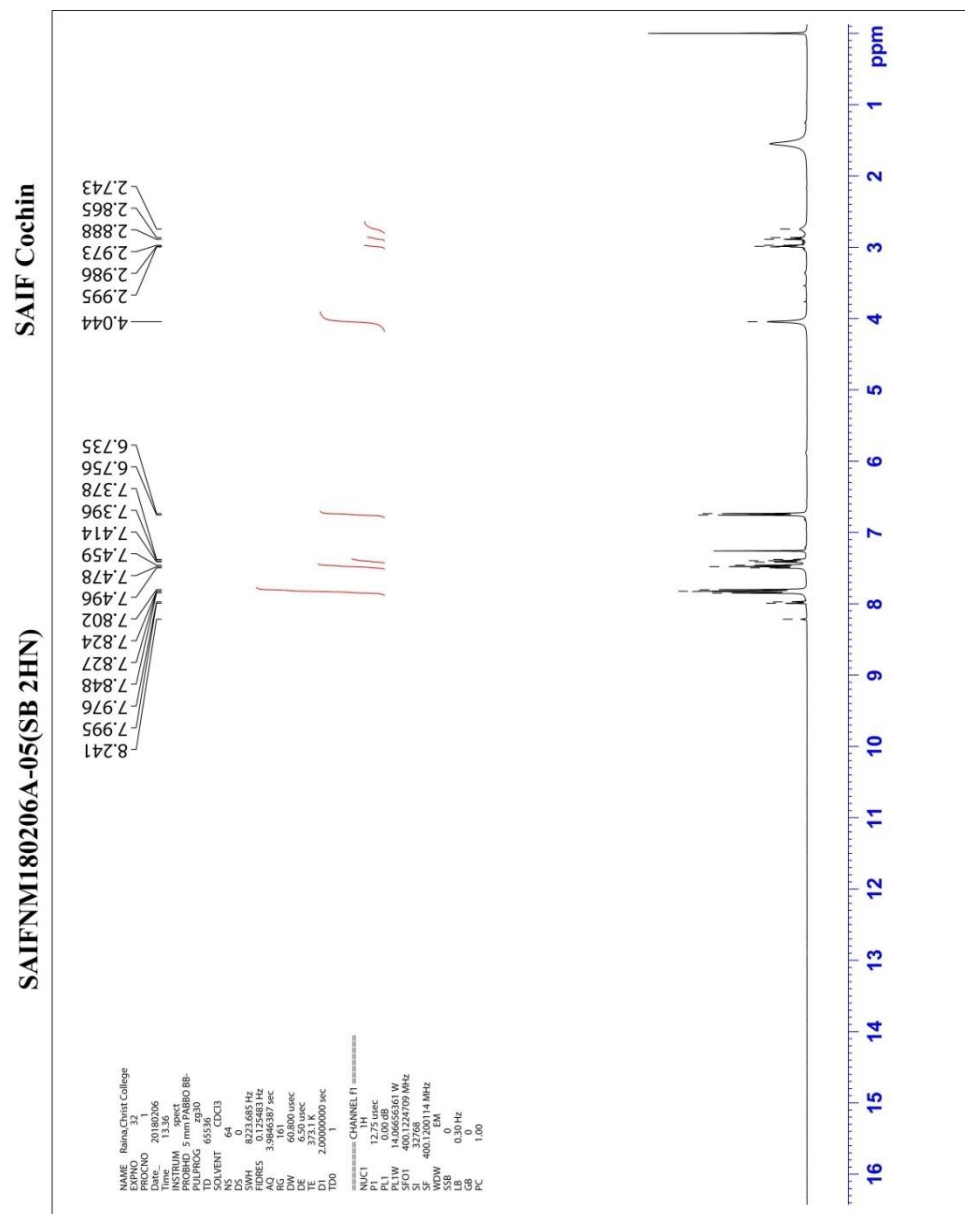
Table1.33 **^{1}H NMR spectral data of Schiff bases 4a, 4b and 4c**

Compounds	Chemical shifts (δ ppm)				
	NH	Aryl	alkenyl	(CH$_2$)	OCH$_3$/OH
4a	8.45	7.15-7.951	6.78-8.044	2.81-3.265	-
4b	8.241	7.37-7.848	6.73-7.995	2.74-2.995	4.044
4c	8.35	7.04-8.132	6.81-7.985	2.89-2.913	9.637

Fig. 1.31 **^{1}H NMR spectra of Schiff base compound 4b.**

^{13}C NMR SPECTRA

The ^{13}C NMR spectra of all the compounds 4a, 4b & 4c give idea about the non-equivalent carbon atoms in the molecule. Each non-equivalent carbon atom gives rise to a peak with a different chemical shift. The ^{13}C NMR spectral data of all the compounds are given in Table 1.34, 1.35 & 1.36.In the compound 4a, the peak corresponding to methylene (C1) carbon is present ~ at 42ppm. C4 carbon of carbonyl appears at the lowest field value, the position of the peak is at~ 193 ppm. The alkenyl carbon atoms (C5 &C6) are present at a position nearer to121 & 133ppm respectively. The C7 is part of the naphthyl ring and is also attached to olefinic carbon and gave a peak at ~131 ppm. The aromatic carbon atoms are present between 122 – 136 ppm.

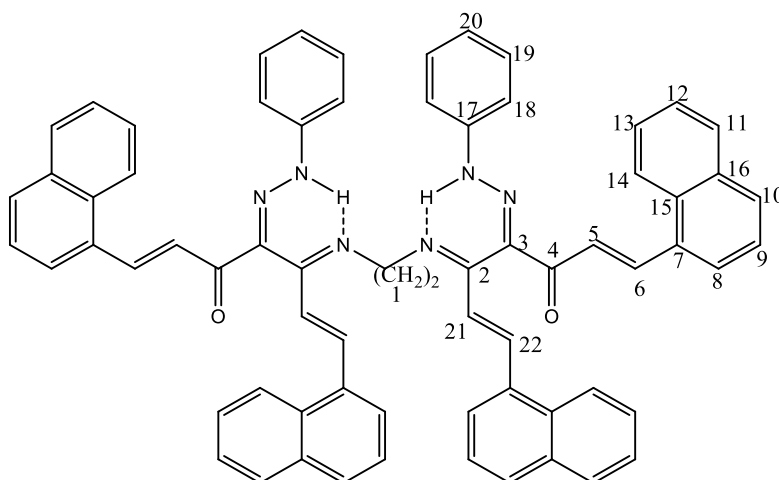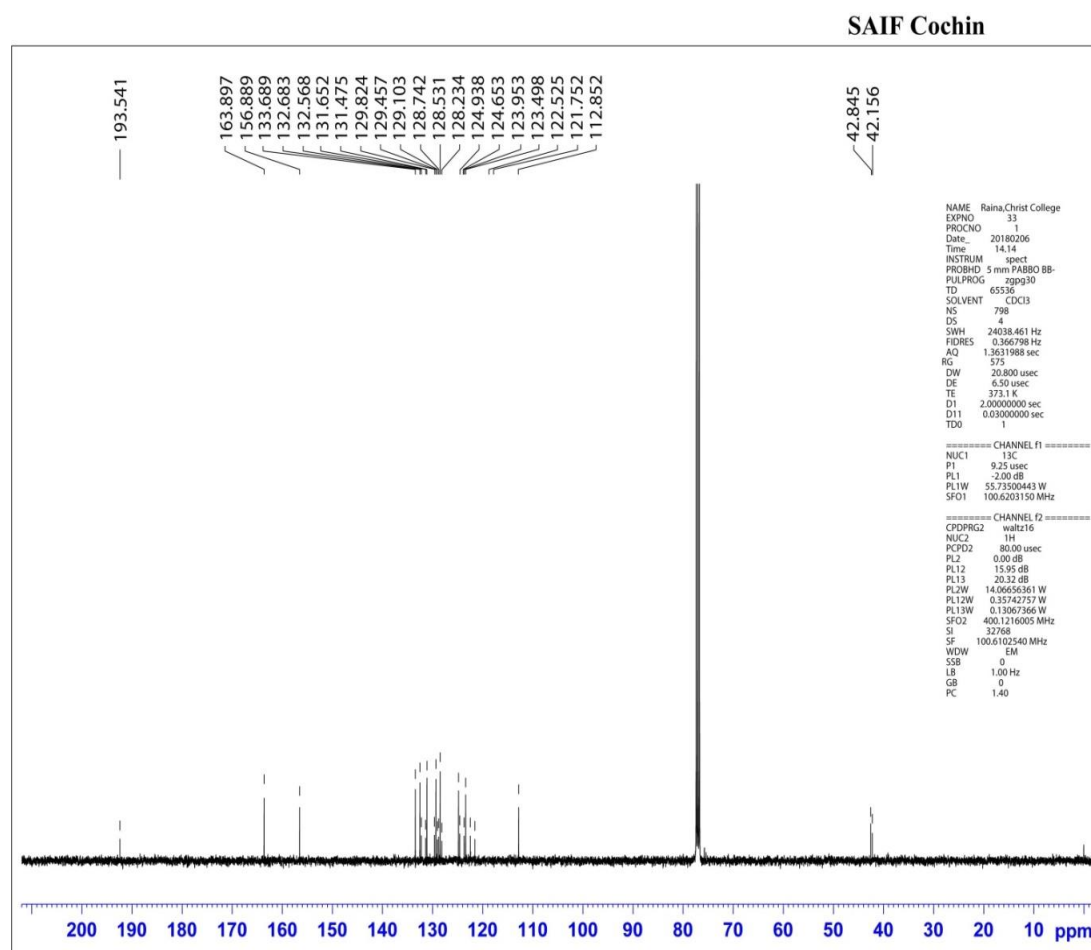**Structure representing different carbon atoms in 4a**

Table 1.34 ^{13}C NMR spectral data of Schiff base 4a

C1	C2	C3	C4	C5	C6	C7	C8	C9	C10	C11
42.1,42.8	163.8	156.8	193.541	121.7	133.6	131.6	124.9	123.9	129.4	129.10
C12	C13	C14	C15	C16	C17	C18	C19	C20	C21	C22
123.4	124.6	128.2	132.6	128.5	132.5	122.5	129.8	128.7	112.8	131.4

Fig. 1.32 ^{13}C NMR spectra of Schiff base compound 4a.
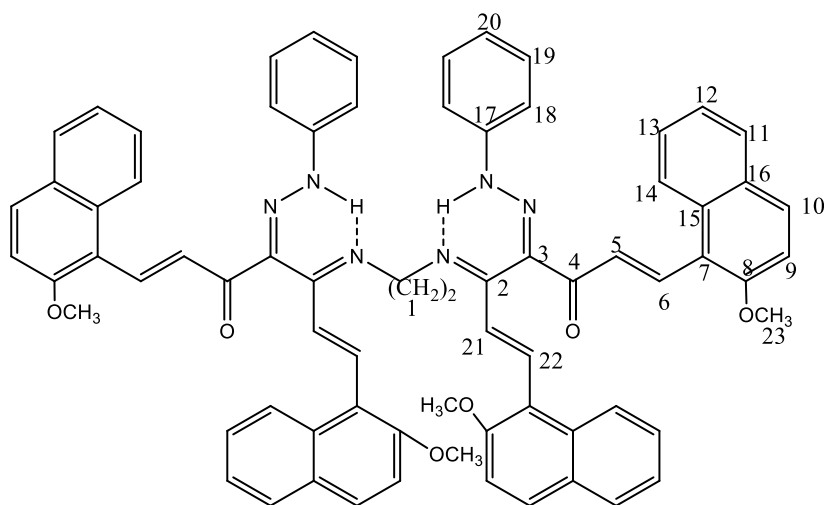
Structure representing different carbon atoms in 4b

Table 1.35 ^{13}C NMR spectral data of Schiff base 4b

C1	C2	C3	C4	C5	C6	C7	C8	C9	C10	C11	
42.3	159.3	157.2	190.7	121.5	134.6	132.8	142.4	123.2	130.7	129.1	
C12	C13	C14	C15	C16	C17	C18	C19	C20	C21	C22	C23
123.8	124.2	128.7	132.9	128.7	130.3	122.4	129.2	128.6	113.7	131.8	58.2

Structure representing different carbon atoms in 4c
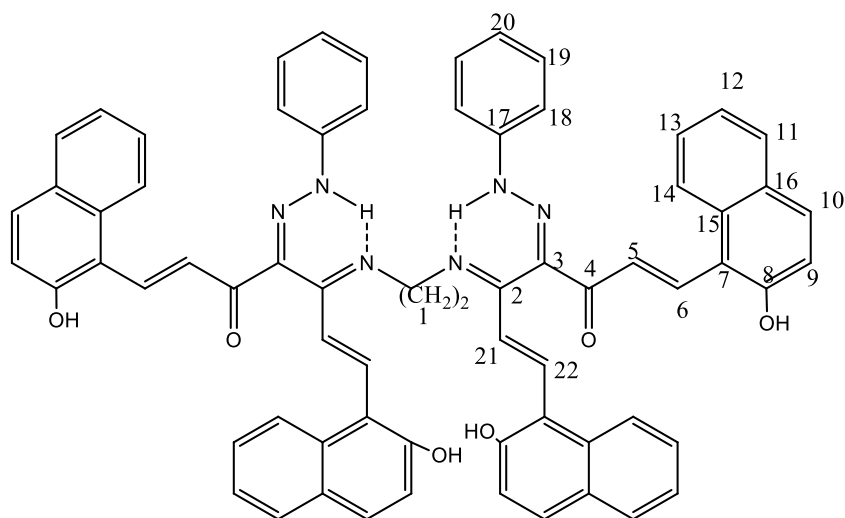
Table 1.36 ^{13} **C NMR spectral data of Schiff base 4c**

C1	C2	C3	C4	C5	C6	C7	C8	C9	C10	C11
43.1	159.4	158.3	192.27	121.4	134.8	132.6	147.9	122.3	129.2	129.7
C12	C13	C14	C15	C16	C17	C18	C19	C20	C21	C22
123.9	124.4	128.5	133.6	128.3	132.8	122.1	129.2	128.5	113.1	132.4

Mass spectra

The $(M+1)^+$ ion peak of Schiff base 4a was observed at 987. Other important peaks of ligand 4a were due to fragment ions which are represented in Table 1.37.

The mass spectrum of Schiff base 4b showed an intense molecular ion peak at 1105. An intense base peak was observed at m/z=199 which was due to fragment ion F. The peaks observed at 922, 711, 634, 143 were due to fragment ions. The formation of the fragment ions can be explained from the fragmentation form represented in Scheme 1.15 below. The important fragment ions are represented in Table 1.37.

The mass spectra of Schiff base 4c showed molecular ion (M+1) peak at 1050.The base peak in the spectrum of Schiff base 4c was seen at m/z=198 which was due to $[Ph-N-CN-CN-C=O-CH]^+$ion. Another intense peak was observed at m/z=880 which was due to removal of Ar = 1-naphthyl ring. The elimination of important small groups like C_2H_2,$-CH_2=C=O$,$-CH_2$,$-CH=C=O$ from the molecule gave different fragment ion peaks. The schematic diagram for the formation of fragment ions is shown in Scheme 1.13 and the m/z values of the fragment ions are given in Table 1.37. Smaller fragments like CH_2, O, OH etc. were removed from the

molecular ion and are shown in the spectrum. The mass spectrum of 4c and the SIM mode of molecular ion peak of 4c are presented in Fig.1.33 and Fig.1.34. respectively.

Table 1.37 Mass spectral data of 4a, 4b and 4c

Fragments	Ligands	M+1,M, M+1 ions	A	B	C	D	E	F	G
Mass Patterns	4a	987	832	651	574	507	479	198	142
	4b	1105	922	711	634	567	539	199	143
	4c	1050	880	683	606	539	511	198	143

*The alphabets correspond to the fragments given in Scheme 1.13
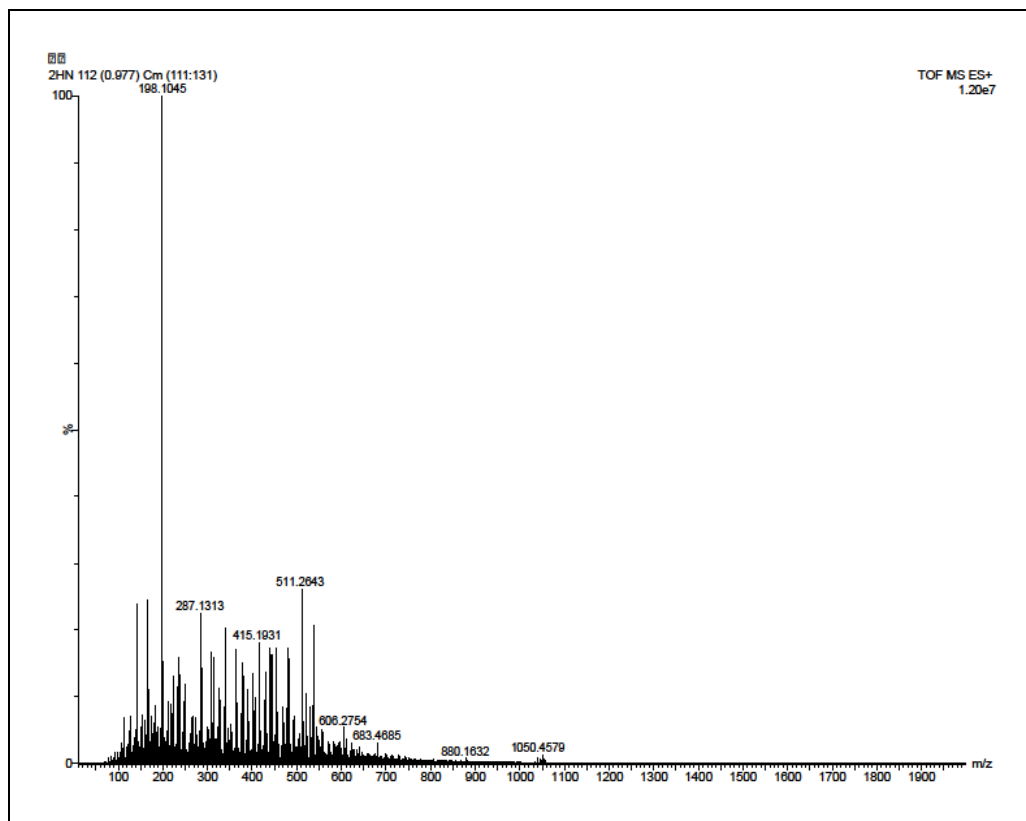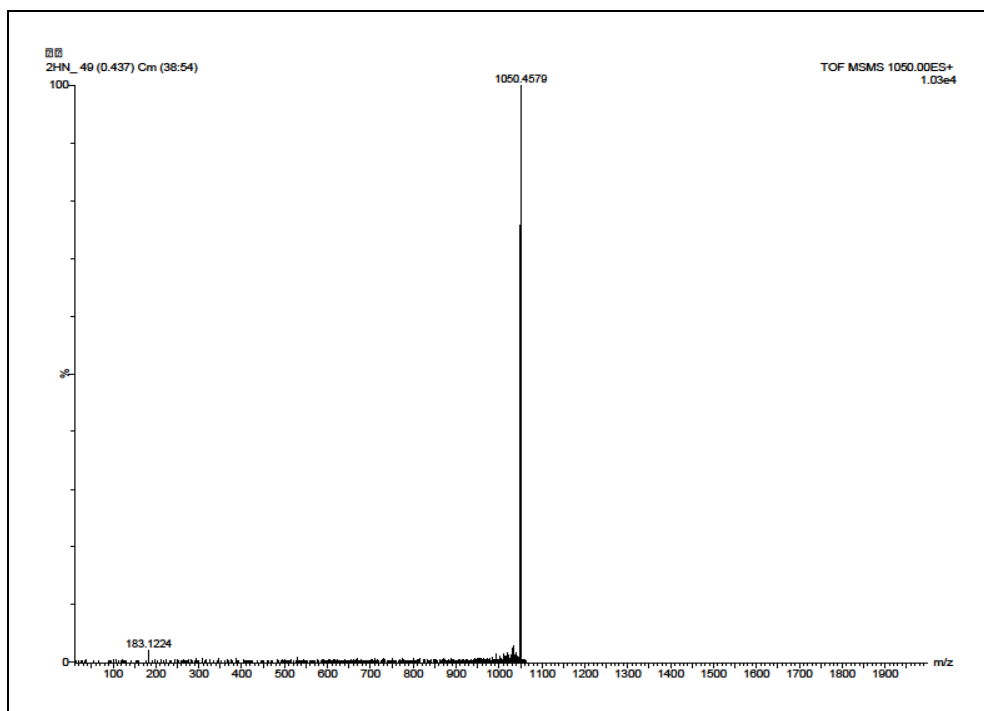
Fig.1.33 Mass spectrum of Schiff base 4c

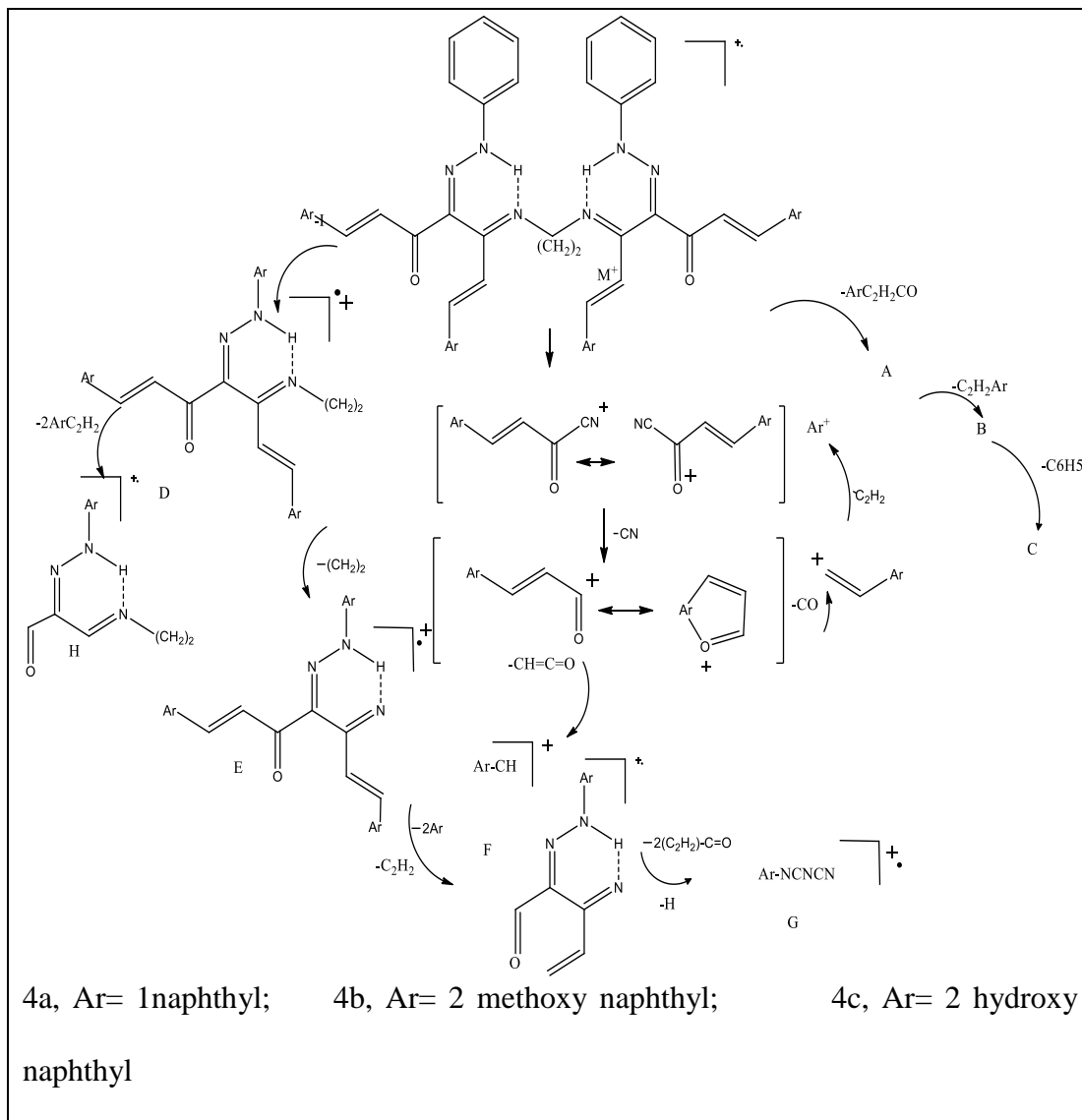**Fig.1.34 Selected ion monitoring (SIM) mode of mass spectrum of 4c.**

Scheme 1.15 Mass Fragmentation pattern of Schiff bases

4a, Ar= 1naphthyl;   4b, Ar= 2 methoxy naphthyl;   4c, Ar= 2 hydroxy
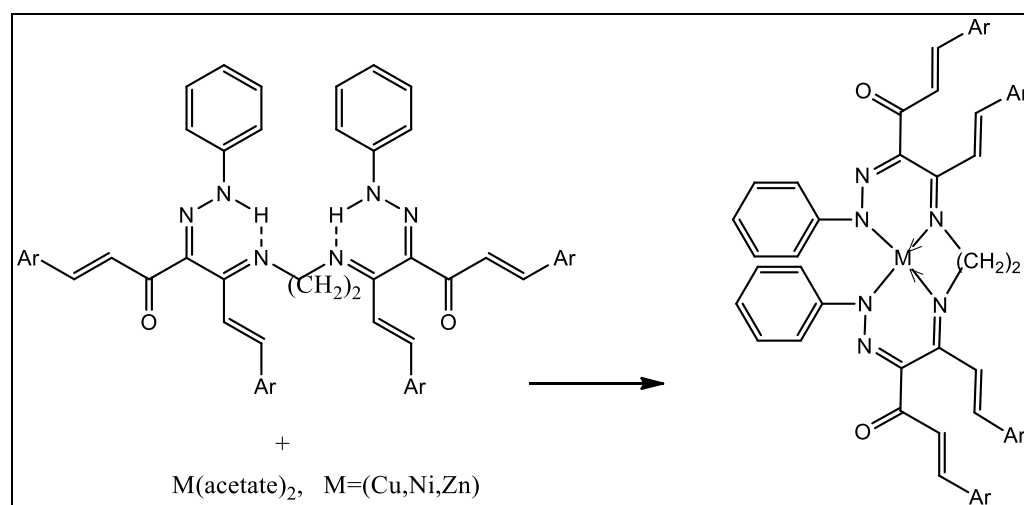
naphthyl

Synthesis and characterization of transition metal chelates of Schiff bases derived from aryl azo derivatives of 1,7-dinaphthyl heptanoids with methoxy &hydroxy substituted naphthyl ring

Synthesis of metal complexes of Schiff bases 4a, 4b and 4c

Copper(II), Zinc(II) and Nickel(II) complexes of Schiff bases derived from aryl azo derivatives of curcuminoid analogues with naphthyl rings and substituted naphthyl rings (hydroxyl, methoxy groups)were synthesized by the following general method.

To a refluxing solution of the Schiff base ligand (0.01 mol) in methanol (20ml), a methanolic solution of metal salt (0.01mol) was added and the reaction mixture was refluxed for three hours and cooled to room temperature. The metal salts used for synthesis were Copper acetate, Zinc acetate and Nickel acetate for the preparation of Cu(II),Zn(II) & Ni(II) complexes respectively. The precipitated complex was then filtered, washed with 1:1, methanol:water mixture and recrystallized from hot methanol. The reaction involved in the formation of complexes is given below in Scheme1.16.

Scheme1.16

4a, Ar= 1naphthyl; 4b, Ar= 2 methoxy naphthyl;   4c, Ar= 2 hydroxy naphthyl

Characterization of transition metal complexes of Schiff bases 4a, 4b and 4c

Metal chelates (Cu, Zn, and Ni) of Schiff base ligands 4a, 4b and 4c were characterized using analytical and various spectral techniques like UV, IR, NMR and mass spectral data. The elemental analysis data (C, H, N and metal percentages), physical data, UV and IR spectral data are given in Table 1.38, 1.39 & 1.40. The analytical data along with mass spectral data suggested a ML stoichiometry for all the synthesized complexes.

Table 1.38   Analytical and spectral data of metal complexes of Schiff base 4a

Metal chelates	M.P. (^{o}C)	Elemental analysis (%) Found/(calculated)				IR stretching bands (cm^{-1})		
		C	H	N	Metal	Free C=O	CN	M-N
Cu(II)	286	77.87 (78.02)	4.43 (4.81)	7.85 (8.02)	5.12 (5.84)	1668	1625 1590	507 504
Ni(II)	259	78.03 (78.39)	4.04 (4.83)	7.90 (8.06)	4.96 (5.42)	1659	1627 1591	506 502
Zn(II)	226	77.21 (77.89)	4.69 (4.80)	7.74 (8.01)	5.93 (6.00)	1662	1620 1593	505 502

Table 1.39   Analytical and spectral data of metal complexes of Schiff base 4b

Metal chelates	M.P. (^{o}C)	Elemental analysis (%) Found/(calculated)				IR stretching bands (cm^{-1})		
		C	H	N	Metal	Free C=O	CN	M-N
Cu(II)	286	73.85 (74.11)	4.92 (5.01)	6.93 (7.20)	5.57 (5.84)	1654	1629 1593	503 501
Ni(II)	259	74.01 (74.42)	4.85 (5.03)	7.07 (7.23)	4.90 (5.42)	1663	1621 1590	507 504
Zn(II)	226	73.58 (73.99)	4.84 (5.00)	6.89 (7.19)	5.91 (6.00)	1668	1625 1589	505 503

Table 1.40   Analytical and spectral data of metal complexes of Schiff base 4c

Metal chelates	M.P. (^{o}C)	Elemental analysis (%)				IR stretching bands (cm^{-1})		
		Found/(calculated)						
		C	H	N	Metal	Free C=O	CN	M-N
Cu(II)	286	73.37 (73.53)	4.34 (4.53)	7.11 (7.56)	5.21 (5.72)	1661	1618 1591	508 503
Ni(II)	259	73.02 (73.85)	4.18 (4.55)	6.92 (7.59)	5.17 (5.30)	1665	1626 1593	506 502
Zn(II)	226	73.15 (73.41)	4.10 (4.52)	7.32 (7.55)	5.62 (5.87)	1672	1627 1590	507 504

IR spectra

In the IR spectra of metal chelates of Schiff base ligands, the band due to free imine C=N of the ligand at ~1618 cm^{-1} disappeared and instead a band assignable to stretching of the coordinated C=N appeared at ~1550-1600cm^{-1}. Additional bands appear at ~500-550 cm^{-1} assignable to ν (M–N) vibration. The broad band in the region of 2600 -3500 cm^{-1} present in the Schiff base ligand was also reduced in the spectra of metal complexes. The NH deformation band at ~1560cm^{-1} also disappeared in the spectra of metal complexes. This gave an indication of the replacement of the chelated proton by the metal ion during complex formation. The IR spectrum of Cu(II) complex of 4b is depicted in Fig.1.35.
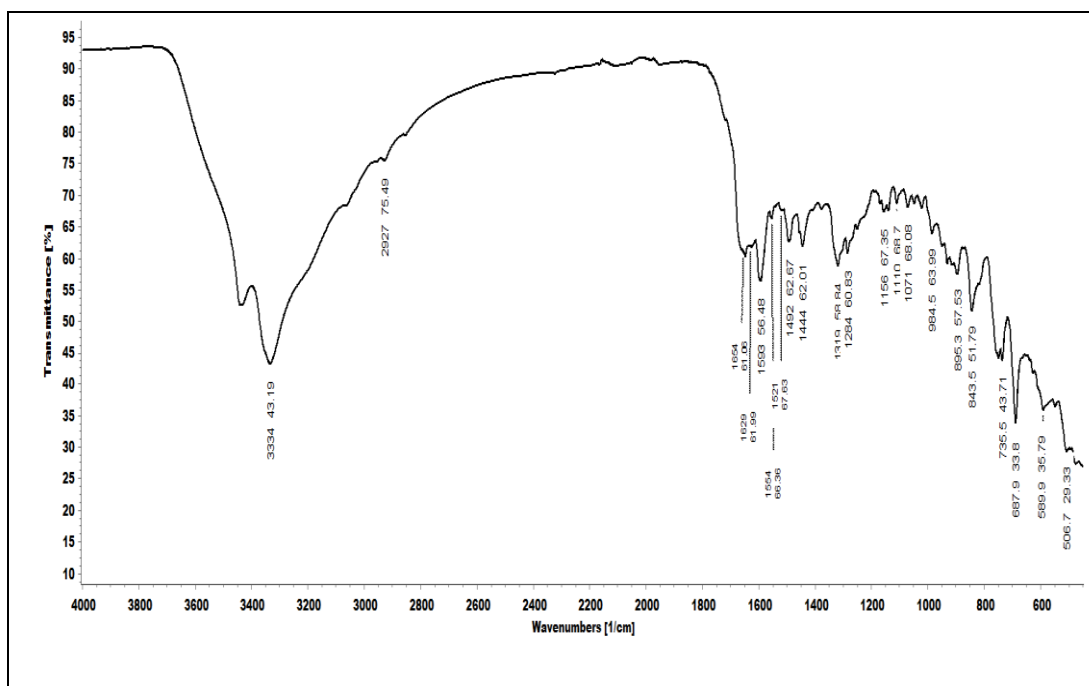
Fig.1.35 The IR spectrum of Cu(II) complex of Schiff base 4b

^{1}H NMR spectra

The NH proton present in the Schiff base ligands was replaced by metal atom in metal complexes. This was clear by the disappearance of the signal at δ ~ 8.24ppm in metal complexes. The phenyl and alkenyl protons of the ligands were not altered in complexes much since they were not involved in complexation. There was a slight shift of methylene signals to the downfield of the spectra. Thus the spectra of ligand and complexes were much similar except those of NH proton.

Mass spectra

The use of mass spectroscopy for the establishment of the stoichiometry and structure of metal Schiff base complexes has been well rooted. It has been shown from the mass spectral analysis that stepwise removal of aryl group is a characteristic feature of all the complexes. Electronic and steric effect of the groups attached to the C=N function strongly influences the stability of various fragments formed under mass spectral condition. The suggested formulation and structure of

complexes are clearly in agreement with the observed spectra of complexes. The mass spectrum of Cu(II) complex of 4a has an intense molecular ion peak at 1046.The peaks due to the removal of 2 Ar and 4 Ar groups from the molecular ion where Ar=1-naphthyl were also found.

The mass spectrum of Zn(II) complex of 4b is given below. The molecular ion peak is less intense and observed at 1168.The intense peak in the spectrum at 196 is due to the $[Zn-C_6H_3N_3]^+$The base peak is observed at 273 which is assigned to [Ph-$Zn-C_6H_3N_3]^+$The peaks at 1011 and 853 are due to the removal of Ar and 2 Ar groups respectively from the molecular ion where Ar=2-hydroxy naphthyl.

The mass spectrum of Ni(II) complex of 4c has an intense M+1 peak at 1106.The peaks due to the removal aryl groups from the molecular ion where Ar=1-naphthyl were also observed. All the complexes showed characteristic molecular ion peaks and the fragment ion peaks in their corresponding mass spectra.
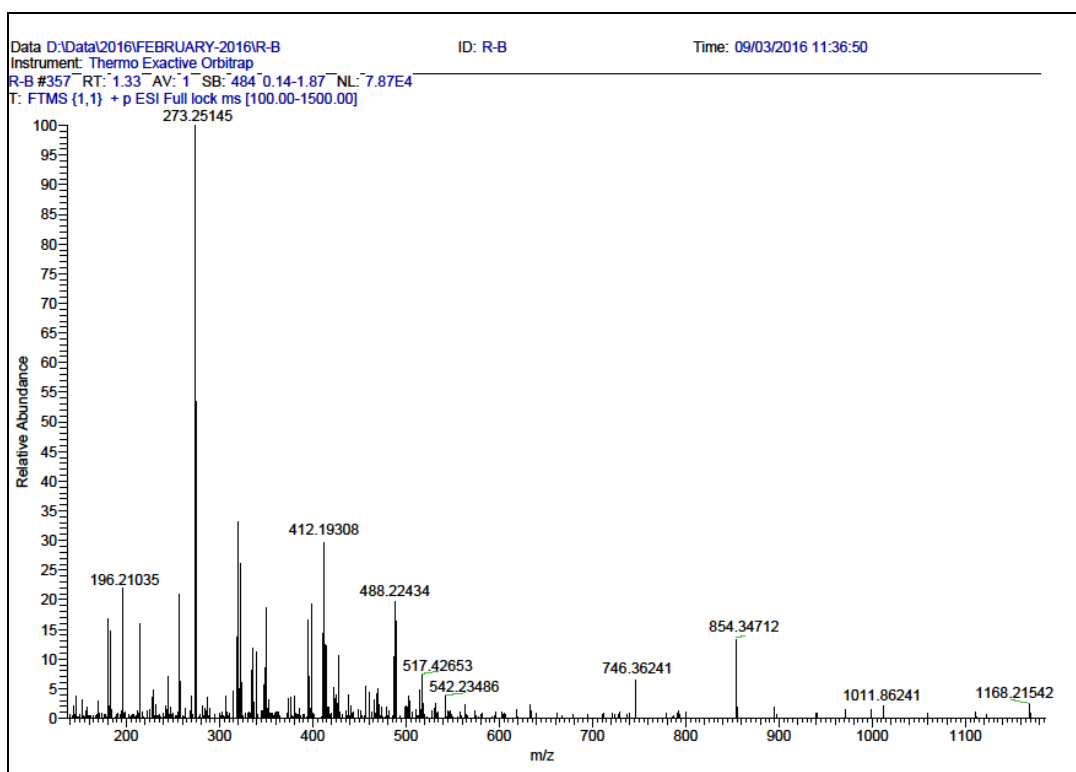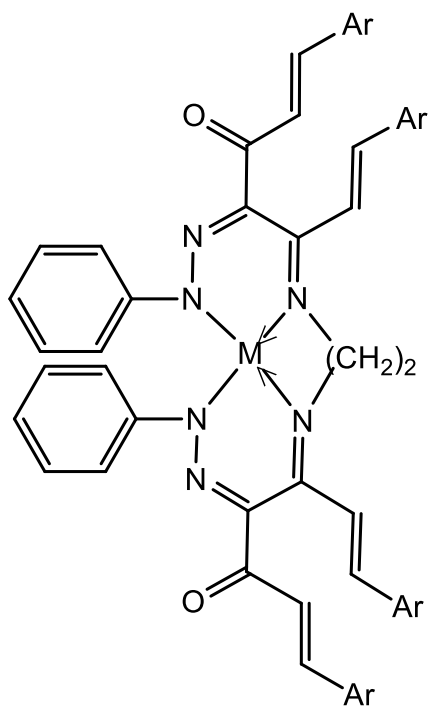

Fig.1.36 Mass spectrum of Zn (II) complex of Schiff base 4b.

The observed UV, IR, 1H NMR and Mass spectral data clearly revealed that metal chelates of Cu, Zn and Ni having ML stoichiometry(metal Schiff base ligand ratio is 1:1).The confirmed structure of metal chelates of Schiff bases is given below.


4a, Ar=naphthyl,   4b, Ar= 2 methoxy naphthyl,   4c, Ar= 2 hydroxy naphthyl

CONCLUSION

Ten Schiff bases derived from aryl azo derivatives of 1,7-diaryl heptanoids (curcuminoid analogues) have been synthesized and were characterized. They were categorized into three structural types (type1, type2 & type3) based on the nature of aryl groups as follows. Type 1 Schiff bases with thiophenyl ring, Type 2 Schiff bases with monosubstituted, disubstituted & trisubstituted phenyl ring and Type 3 with polynuclear naphthyl ring.
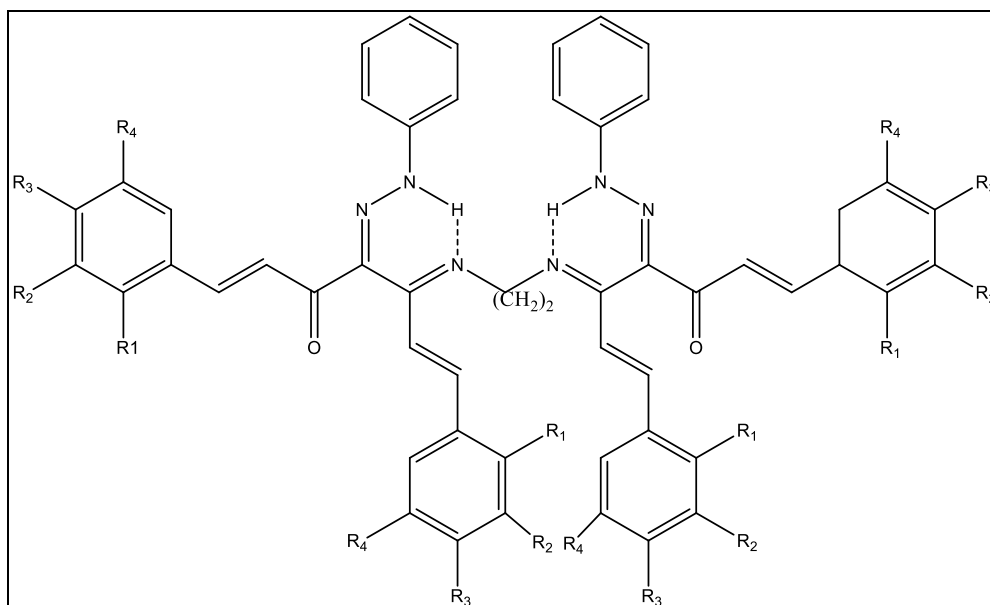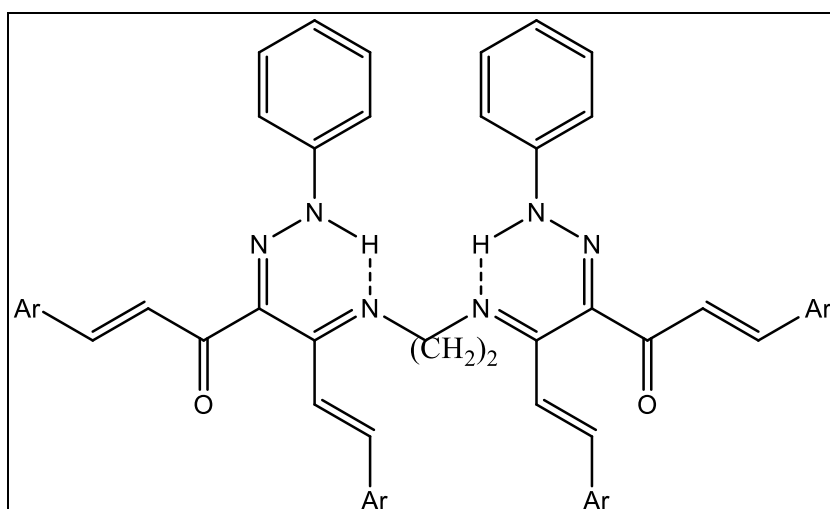
TYPE 1
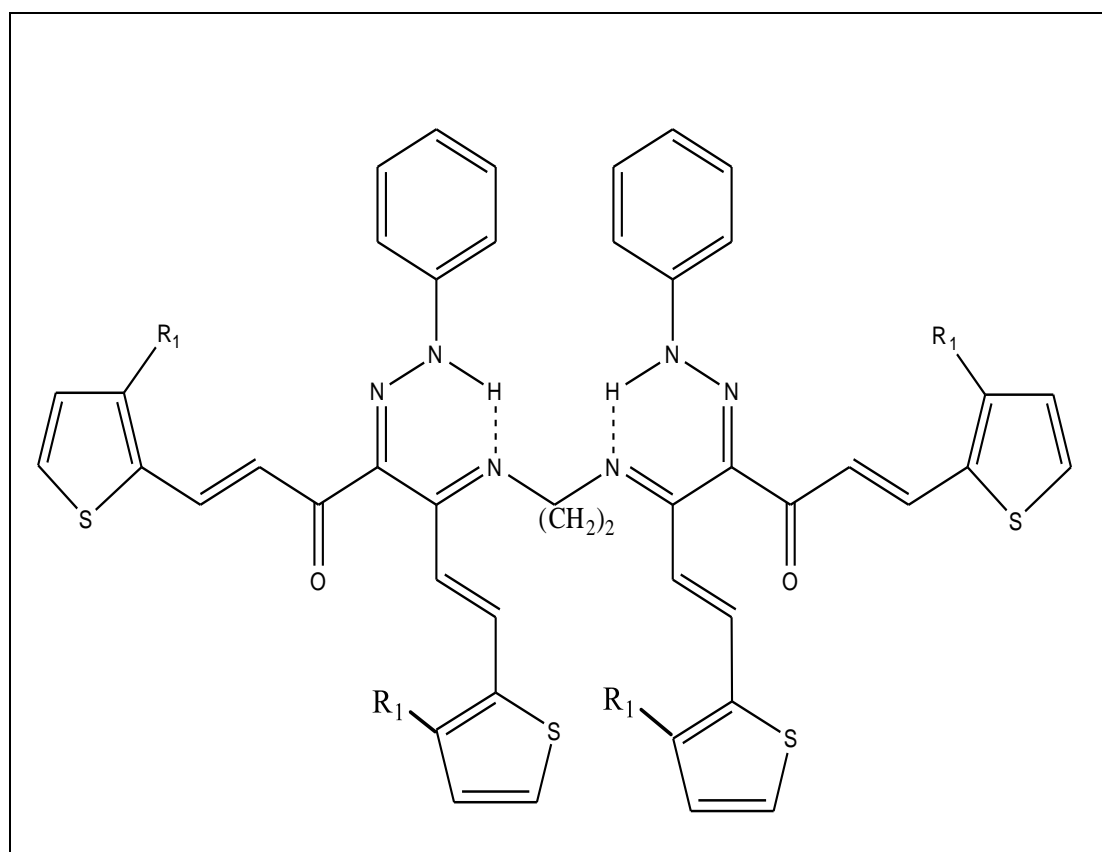
1a, R$_1$=H   **1b, R$_1$=CH$_3$**

TYPE 2

Compounds	R_1	R_2	R_3	R_4
2a	CH_3	H	H	H
2b	OH	H	H	H
3a	H	OCH_2CH_3	OH	H
3b	OH	H	OH	H
3c	H	OCH_3	OCH_3	OCH_3

TYPE 3

4a, Ar=naphthayl   4b, Ar= 2methoxy naphthyl   4c, Ar= 2 hydroxy naphthyl

Analytical and spectral data of all the compounds clearly supported the existence of intramolecularly hydrogen bonded imine hydrazono form. All these compounds form stable metal complexes with Cu(II), Zn(II) and Ni(II) having ML stoichiometry. In all the metal complexes, only the nitrogen atoms of the imine group and hydrazono group are involved in bonding with the formation of a stable metal ion. The analytical and spectral data clearly suggested that metal binding groups such as –OH, sulphur of thiophenyl ring etc. present in the Schiff base ligands are not involved in bonding with metal ions.

CHAPTER II

ANTICORROSIVE ACTIVITY OF SCHIF BASES TEDTDH, DHEDTDH, NEDTDH, HEDTDH AND TMEDTDH ON MILD STEEL IN ACIDIC MEDIA

ANTICORROSIVE ACTIVITY OF SCHIF BASES TEDTDH, DHEDTDH, NEDTDH, HEDTDH AND TMEDTDH ON MILD STEEL IN ACIDIC MEDIA

Five different green Schiff bases 1,14-di(thiophen-2-yl) 5,10-di(ethylene thiophen-2-yl)-6,9diazotetradeca 1,5,9,13-tetraene -3,12-dione 4,11-diphenyl-hydrazone [TEDTDH], 1,14-di(2-hydroxy phenyl) 5,10-di(ethylene- 2- hydroxy phenyl)-6,9diazotetradeca 1,5,9,13-tetraene -3,12-dione 4,11-diphenyl-hydrazone [HEDTDH], 1,14-di(2,4-dihydroxy phenyl) 5,10-di(ethylene- 2,4-dihydroxy phenyl)-6,9diazotetradeca 1,5,9,13-tetraene -3,12-dione 4,11-diphenyl-hydrazone [DHEDTDH], 1,14-di(naphthyl) 5,10-di(ethylene- naphthyl)-6,9diazotetradeca 1,5,9,13-tetraene -3,12-dione 4,11-diphenyl-hydrazone [NEDTDH] and 1,14-di(3,4,5-trimethoxy phenyl) 5,10-di(ethylene- 3,4,5-trimethoxy phenyl)-6,9diazotetradeca 1,5,9,13-tetraene -3,12-dione 4,11-diphenyl-hydrazone [TMEDTDH] were synthesized and characterised as explained in chapter 1.The corrosion inhibition behaviour of the five synthesized Schiff bases on mild steel (MS) in acidic medium (hydrochloric acid and sulphuric acid) were investigated using conventional gravimetric method, Electro chemical impedance spectroscopy and Potentiodynamic measurements. Adsorption studies were conducted to get information about the mechanism of adsorption and surface behavior of adsorbed species. To analyze the thermodynamic parameters of corrosion, corrosion rates of mild steel in aggressive acid medium at different temperatures were also estimated the surface analysis was done using Scanning electron microscopy, Atomic force microscopic analysis and Energy Dispersive X-ray (EDX) spectroscopy.

This chapter comprises two sections. Section I explains the anti-corrosive activity of the five synthesized Schiff bases in 1.0M hydrochloric acid

solution and section II describes the anti-corrosive activity of the above Schiff bases in 0.5M sulphuric acid solution. The gravimetric studies, electro chemical impedance spectroscopic studies and polarisation studies are included in each section.

SECTION I

Corrosion inhibition studies of schif bases TEDTDH, DHEDTDH, NEDTDH, HEDTDH, and TMEDTDH on mild steel in 1.0M hydrochloric acid medium

Five Schiff bases TEDTDH, DHEDTDH, NEDTDH, HEDTDH, and TMEDTDH were investigated for their anticorrosive activity using the test solutions of different concentrations of inhibitors 50ppm, 75ppm, 100ppm and 150ppm in 1.0M HCl. Mild steel pieces of standard composition were used for the studies. The weight loss method and different electrochemical methods were used to study the anti-corrosive nature of the Schiff bases.

Weight Loss Measurements

Well-polished, washed, dried mild steel coupons were immersed in aggressive hydrochloric acid solution in the presence and the absence of the Schiff base inhibitors. The weight loss developed for the MS specimens was measured after twenty four hours. The corrosion inhibition values obtained for each Schiff base shows the characteristics of that particular inhibitor.

The corrosion rate obtained for the different inhibitors are shown in Table 2.1.The results show that the corrosion rate (k) depends on the concentration of the inhibitor. The corrosion rate decreases as the concentration of the inhibitor increases. The mild steel specimen immersed in hydrochloric acid solution showed a corrosion rate of 4.401 $mgcm^{-2}h^{-1}$. The different values of corrosion rate obtained in the presence and absence of inhibitor molecules showed that the Schiff base inhibitors lowered the corrosion rate of the MS to a greater extent. The decrease in the corrosion rate with the increase in the concentration of the inhibitor is due to

the increased adsorption of the inhibitor molecules on the metal surface. Fig. 2.1 exhibits the comparison of corrosion rate of different inhibitors.

Table 2.1 Corrosion rates of MS in mgcm^{-2}h^{-1} in the presence and absence of Schiff base inhibitors TEDTDH, DHEDTDH, NEDTDH, HEDTDH, and TMEDTDH in 1.0M HCl

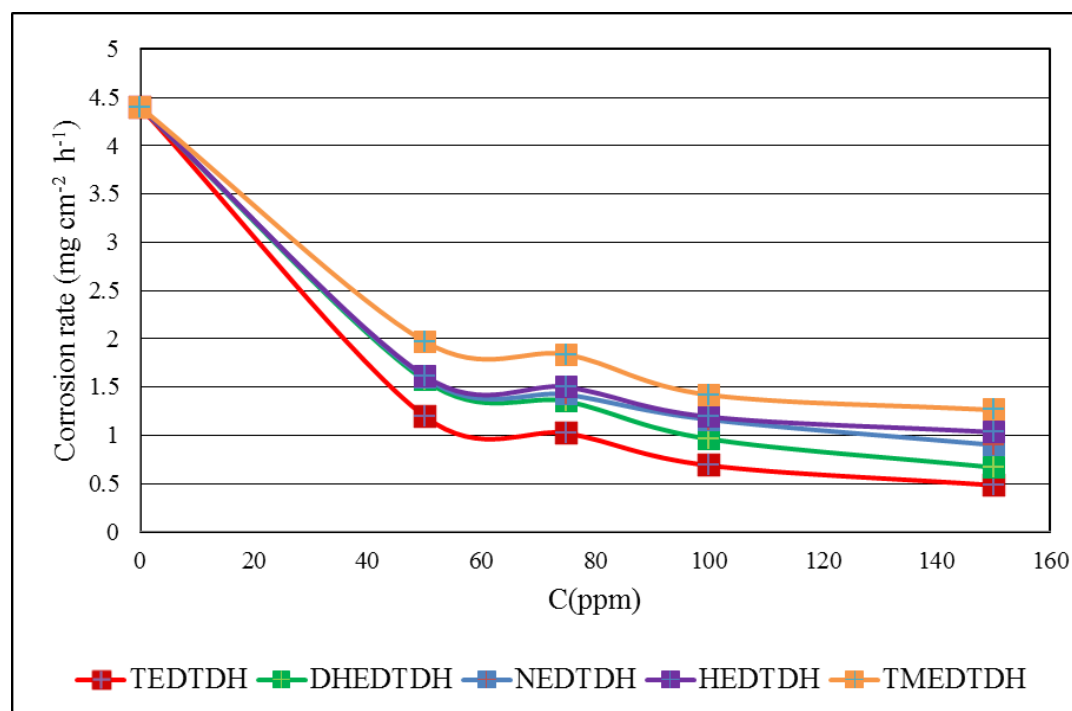| C(ppm)	TEDTDH	DHEDTDH	NEDTDH	HEDTDH	TMEDTDH
0	4.401	4.401	4.401	4.401	4.401
50	1.197	1.571	1.599	1.617	1.972
75	1.021	1.352	1.422	1.499	1.837
100	0.687	0.962	1.163	1.191	1.419
150	0.483	0.667	0.899	1.032	1.262

Fig. 2.1 Variation of corrosion rates of MS with the concentration of Schiff base inhibitors TEDTDH, DHEDTDH, NEDTDH, HEDTDH, and TMEDTDH in 1.0M HCl

The corrosion inhibition efficiencies obtained are given in Table 2.2. The analysis of the values revealed that inhibition efficiency increases with increase in the

concentration of the inhibitor. The TEDTDH showed maximum efficiency of 89% because of the presence of aromatic rings, four sulphur atoms from four thiophenyl rings, nitrogen atoms and oxygen atoms in the molecule. In addition to this, the TEDTDH molecule possesses somewhat planar structure which was confirmed by the optimized geometry determination using DFT and this is beneficial to the strong binding of the inhibitor molecule on the metal surface. It was very difficult to increase the concentration of imines in acid medium due to their poor solubility in acid media and therefore the corrosion investigations were limited in the concentration range 50ppm-150ppm. All Schiff bases behaved as comparatively good inhibitors which may be attributed to the presence of aromatic rings, nitrogen and oxygen atoms. The good inhibition efficiencies indicate that the Schiff base inhibitors adsorbed effectively on M.S. surface and led to formation of a strong metal – inhibitor interaction and also it decreases the chloride ion attack on MS surface. The figure 2.2 shows the comparison of corrosion inhibition efficiencies of the Schiff base inhibitors.

Table 2.2 Inhibition efficiencies of Schiff base inhibitors TEDTDH, DHEDTDH, NEDTDH, HEDTDH, and TMEDTDH on MS in 1.0M HCl

	Inhibitors η				
C(ppm)	TEDTDH	DHEDTDH	NEDTDH	HEDTDH	TMEDTDH
50	72.8	64.3	63.67	63.26	55.19
75	76.8	69.28	67.69	65.94	58.26
100	84.39	78.14	73.57	72.94	67.76
150	89.03	84.84	79.57	76.55	71.32

The Schiff base DHEDTDH also showed considerable inhibition efficiency against MS corrosion. A maximum of 84% inhibition efficiency was attained by this

inhibitor molecule at a concentration of 150ppm. This molecule possesses aromatic ring systems; oxygen atoms and nitrogen atoms. The presence of electron density of the aromatic ring systems, azomethine linkage and electron donor atoms are the core causes in which the molecule showed better inhibition efficiency. Even though the molecule is less planar as per the optimized geometry, two benzene rings, the oxygen atoms and nitrogen atoms remain in the same plane, which is a reasonable condition to adsorb the inhibitor molecule on the metal surface.
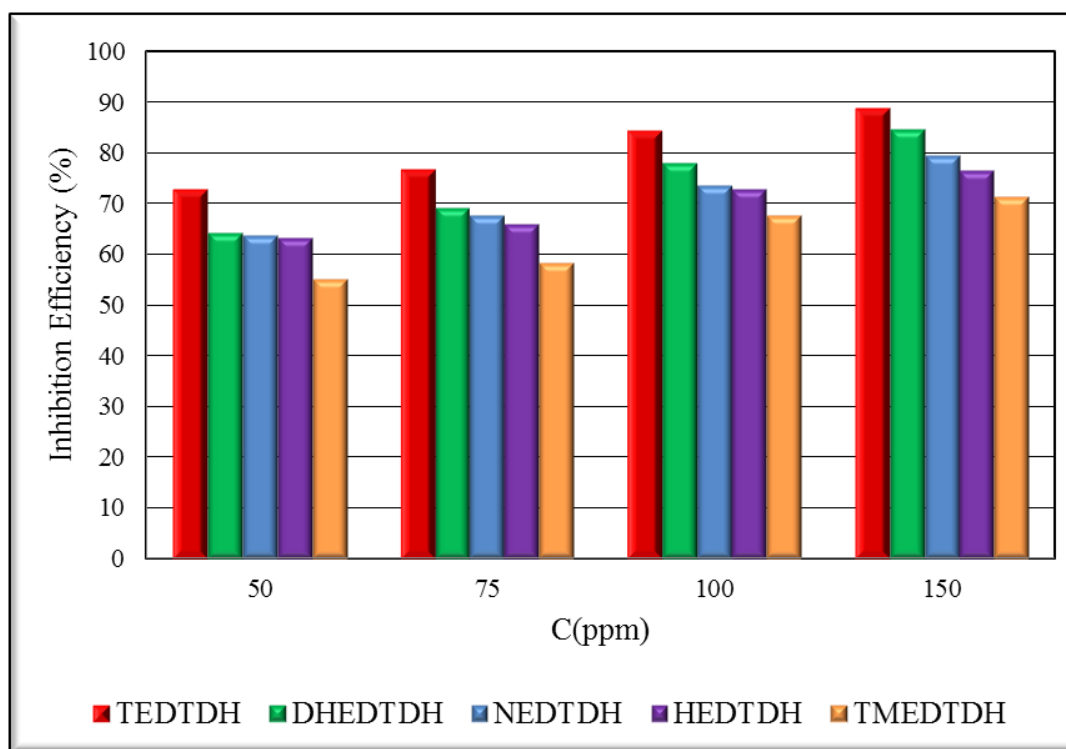

Fig.2.2 Comparison of corrosion inhibition efficiencies ($\eta w\%$) of Schiff base inhibitors TEDTDH, DHEDTDH, NEDTDH, HEDTDH, and TMEDTDH on MS in 1.0M HCl

The low corrosion inhibition of the molecule TMEDTDH, compared to the previously described molecules, may be attributed to steric hindrance caused by the methyl groups of methoxy groups. Even though the molecule is equipped with atoms with active corrosion inhibition property, the steric factor of the molecule

prevents the appreciable interaction with the metal surface. The molecules NEDTDH and HEDTDH exhibited comparatively low inhibition efficiency. A maximum of 79% and 76% efficiency was noticed with these molecules at 150ppm concentration. On comparing the structures of two molecules, one can understand that the only difference between the two molecules is presence of one more aromatic ring in former instead of an oxygen atom in the second one. Even though the second molecule is equipped with more electron rich oxygen atom, the electron cloud present in the aromatic ring of the former molecule made it more effective. These two molecules displayed almost same corrosion inhibition efficiencies on the MS surface.

Comparison of corrosion inhibition efficiencies of Schiff base inhibitors with their parent diketo compounds

The corrosion inhibition behaviour of Schiff base inhibitors were compared with their parent diketo compounds at three different concentrations. The parent aryl azo derivatives such as 1,7-bis(thiophen-2-yl)-hepta-1,6-diene-3,5-dione (TPHD), 1,7-bis(2,4-dihydroxy phenyl)-hepta-1,6-diene-3,5-dione(DHPHD), 1,7-bis(naphthyl)-hepta-1,6-diene-3,5-dione (NPHD), 1,7-bis(2-hydroxy phenyl)-hepta-1,6-diene-3,5-dione(HPHD) and 1,7-bis(3,4,5-trimethoxy phenyl)-hepta-1,6-diene-3,5-dione(TMPHD) exhibited lower corrosion inhibition on metal surface when compared to that of the Schiff bases. The superior inhibitory power of the Schiff base inhibitor molecules was clearly established, which can be attributed to the presence of more number of aromatic rings and electron donor atoms. The results are pictured in Fig. 2.3.

Table 2.3 Comparison of corrosion inhibition efficiencies with their parent diketo compounds

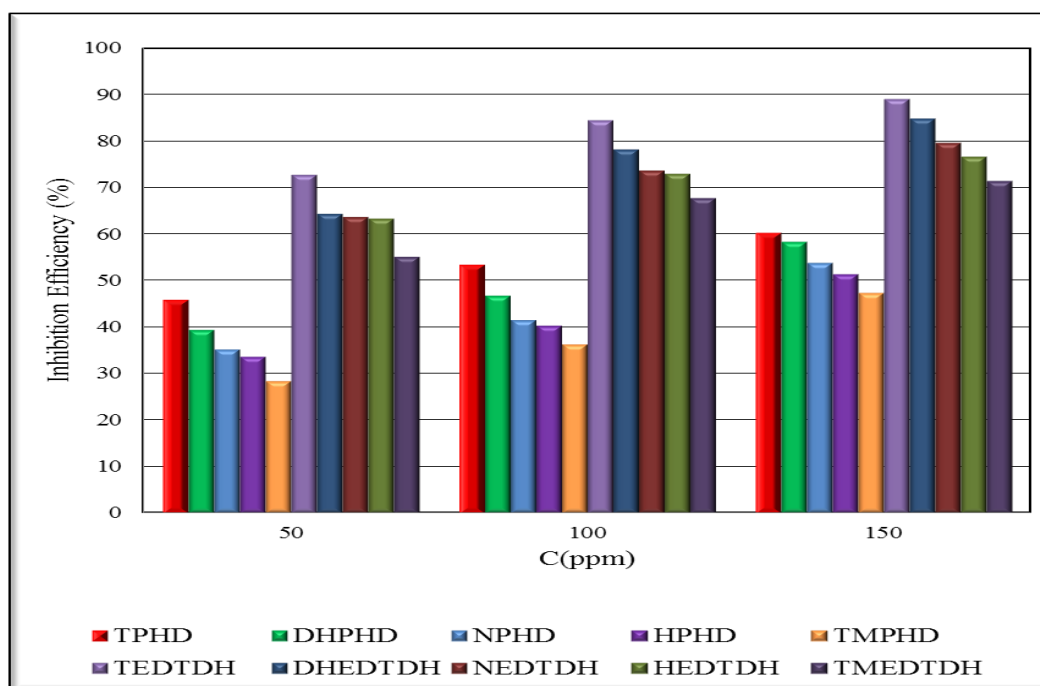| Compounds	Concentration(ppm)		
	50	100	150
TPHD	45.8	53.42	60.15
DHPHD	39.48	46.71	58.32
NPHD	35.21	41.58	53.67
HPHD	33.74	40.29	51.24
TMPHD	28.36	36.21	47.27
TEDTDH	72.8	84.39	89.03
DHEDTDH	64.3	78.14	84.84
NEDTDH	63.67	73.57	79.57
HEDTDH	63.26	72.94	76.55
TMEDTDH	55.19	67.76	71.32

Fig.2.3 Comparison of corrosion inhibition efficiencies of Schiff base inhibitors with their parent compounds

Adsorption Isotherms

Adsorption isotherms provide information about the mechanism of adsorption and surface behavior of adsorbed species. Attempts were made to fit the data from weight loss method to most common adsorption isotherms and the most suitable isotherm with the highest correlation coefficient (R^2) was selected. Different types of adsorption isotherms considered here are Langmiur, Temkin, Freundlich and Frumkin isotherms. Schiff bases TEDTDH and DHEDTDH followed Freundlich adsorption isotherm. The Langmuir isotherm was found to fit best for NEDTDH, HEDTDH and TMEDTDH during the inhibition process on metal surface which confirms the adsorption of inhibitor molecules on the metal surface. The adsorption isotherms obtained are represented in the Figures 2.4 to 2.8 and the parameters from the analysis of isotherms are listed in Table 2.4.
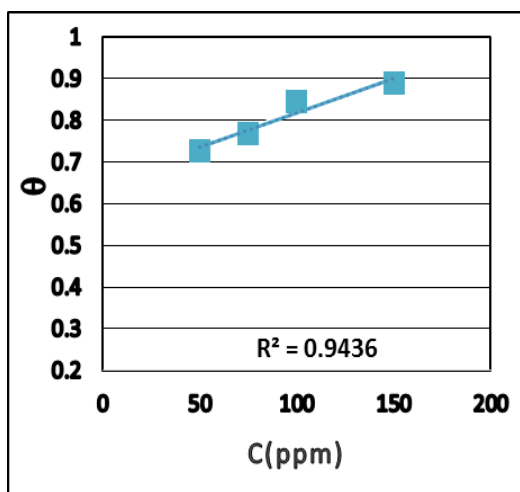

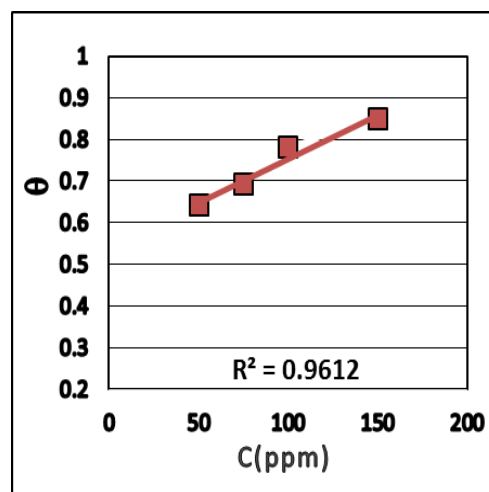**Fig.2.4 Freundlich Adsorption isotherm for TEDTDH on MS in 1.0M HCl**

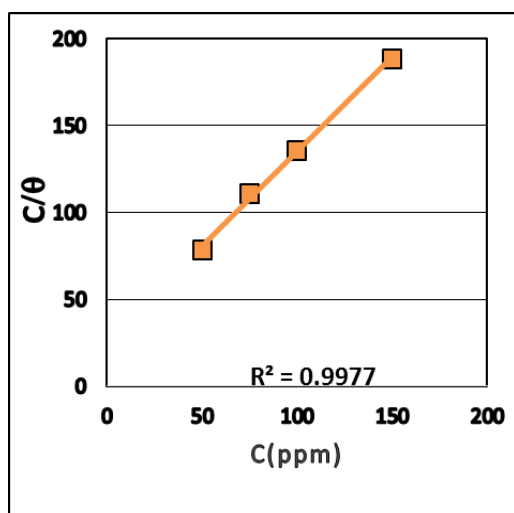**Fig.2.5 Freundlich Adsorption isotherm for DHEDTDH on MS in 1.0M HCl**

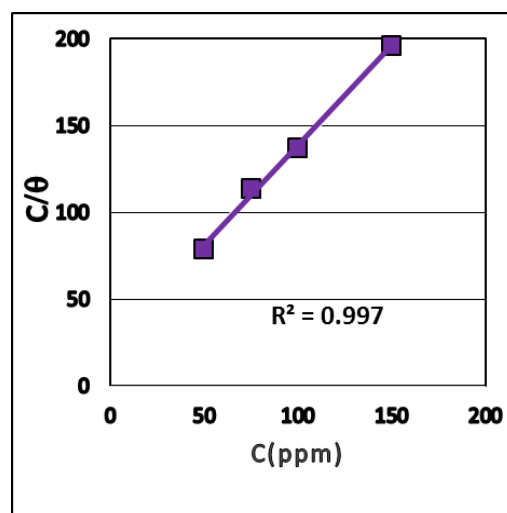**Fig.2.6 Langmuir Adsorption isotherm for NEDTDH on MS in 1.0M HCl**

Fig.2.7 Langmuir Adsorption isotherm for HEDTDH on MS in 1.0M HCl
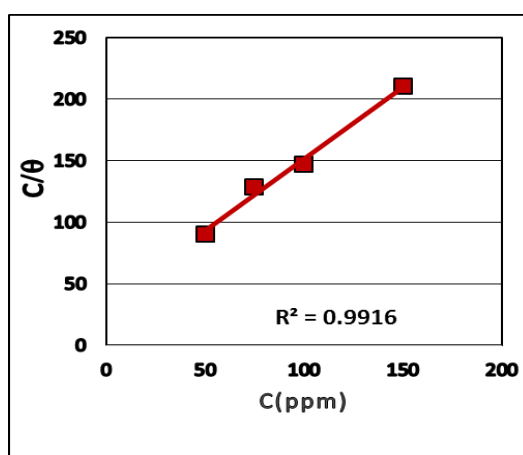

Fig.2.8 Langmuir Adsorption isotherm for TMEDTDH on MS in 1.0M HCl

Table 2.4 Thermodynamic parameters for the adsorption of TEDTDH, DHEDTDH, NEDTDH, HEDTDH, and TMEDTDH on MS in 1.0M HCl

Parameters	TEDTDH	DHEDTDH	NEDTDH	HEDTDH	TMEDTDH
K_{ads}	4482	3503	24579	22309	30032
ΔG^{o}_{ads} KJmol^{-1}	-28.19	-27.64	-32.06	-31.842	-37.832

The negative values of ΔG^0_{ads} for all the inhibitor molecule indicate that the adsorption of inhibitor molecules on the metal surface is a spontaneous process. The studies reveal that the value of ΔG^0_{ads} up to -20 KJ/mol or lower is consistent with electrostatic interactions between the charged inhibitor molecule and charged metal which indicates a process of physisorption. The ΔG^0_{ads} value around -40KJ/mol or higher is considered as evidence for coordinate covalent bonding of molecules on metal surface(Chemisorption)[13,164,113].The obtained ΔG^0_{ads} value lies between -27 and -37.83KJ/mol suggesting that the inhibitor adsorption on MS is not merely physisorption or chemisorption but includes a comprehensive adsorption of both. For the Schiff base inhibitor molecules NEDTDH and TMEDTDH the free energy of adsorptions ΔG^0_{ads} were comparatively higher than that of the other inhibitor molecules suggesting that these inhibitors are more firmly adsorbed by forming a monolayer on the surface of the metal through chemical interaction

Effect of temperature

The effect of temperature on corrosion rate of the MS specimens were also studied using weight loss studies of the Schiff base inhibitors in the temperature range 30-60^{0}C. The activation energy E_a and Frequency factor A of corrosion with and without the inhibitor was calculated using Arrhenius equation,

$$K = A \; exp\left(-\frac{E_a}{RT}\right)$$

where K is the rate of corrosion, Ea is the activation energy, A is the frequency factor, T is the temperature in Kelvin scale and R is the gas constant. The linear

plots drawn between log K Vs 1000/T with regression coefficients close to unity reveal that the corrosion of MS in HCl can be explained using the simple kinetic model for all the inhibitor Schiff base molecules. Plots of log K Vs 1000/T and log (K/T) Vs 1000/T in the presence and absence of the inhibitor are given in Figures 2.9 to 2.18. Enthalpy and entropy of activation (ΔH^*, ΔS^*) were determined from the transition state theory using the equation

$$K = (\frac{RT}{Nh})\exp(\frac{\Delta S^*}{R})\exp(\frac{-\Delta H^*}{RT})$$

where N is the Avogadro number and h is the Planck's constant. Table 2.5 gives the activation energy, frequency factor and thermodynamic parameters of corrosion. The high value of activation energy E_a of dissolution of the metal with the maximum concentration of the inhibitor implies the increase in the reluctance of dissolution of metal. Positive enthalpies with a systematic rise expose the endothermic nature of dissolution of metal and the increasing difficulty of undergoing corrosion. The entropy of activation ΔS also increases with the increase in inhibitor concentration. At the lower concentrations of the inhibitor molecules, the entropy of activation gives a high negative value indicating that the molecules are in highly ordered state than that at the initial state. But as the concentration of inhibitor increases, the disordering of activated complex takes place and the entropy of activation goes to less negative side.
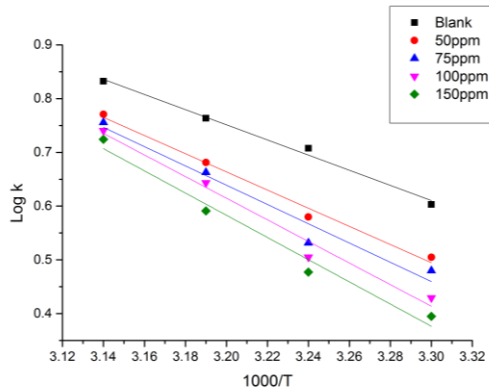
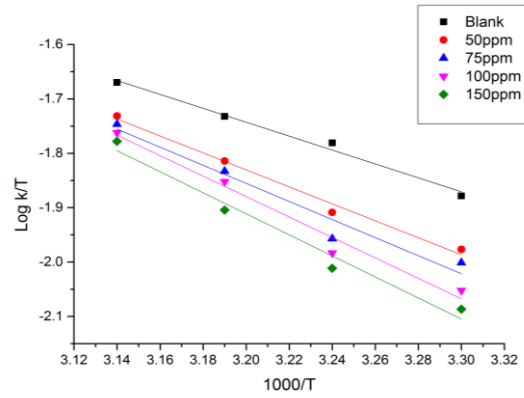**Fig.2.9 Arrhenius plots for the corrosion of MS in the absence and presence of TEDTDH in 1.0M HCl.**

Fig.2.10 Plots of log (k/T) vs 1000/T for the corrosion of MS in the absence and presence of TEDTDH in 1.0M HCl.

Fig.2.11 Arrhenius plots for the corrosion of MS in the absence and presence of DHEDTDH in 1.0M HCl.

Fig.2.12 Plots of log (k/T) vs 1000/T for the corrosion of MS in the absence and presence of DHEDTDH in 1.0M HCl

.

Fig.2.14 Arrhenius plots for the corrosion of MS In the absence and presence of NEDTDH in 1.0M HCl.

Fig.2.13 Plots of log (k/T) vs 1000/T for the corrosion of MS in the absence and presence of NEDTDH in 1.0M HCl.
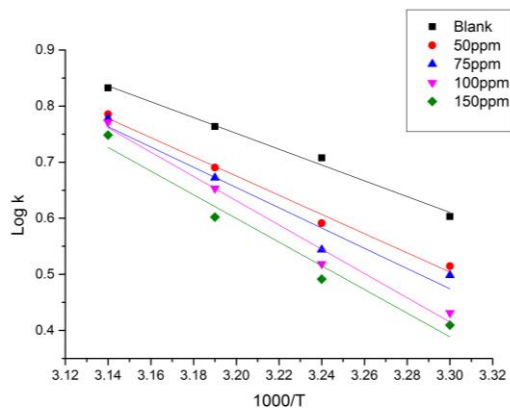
Fig.2.15 Arrhenius plots for the corrosion of MS In the absence and presence of HEDTDH in 1.0M HCl.

Fig.2.16 Plots of log (k/T) vs 1000/T for the corrosion of MS in the absence and presence of HEDTDH in 1.0M HCl.

Fig.2.17 Arrhenius plots for the corrosion of MS In the absence and presence of TMEDTDH in 1.0M HCl.
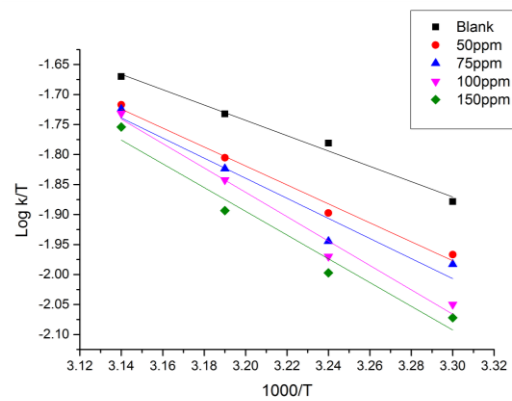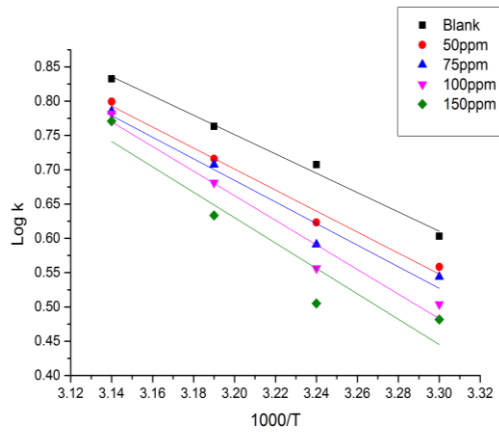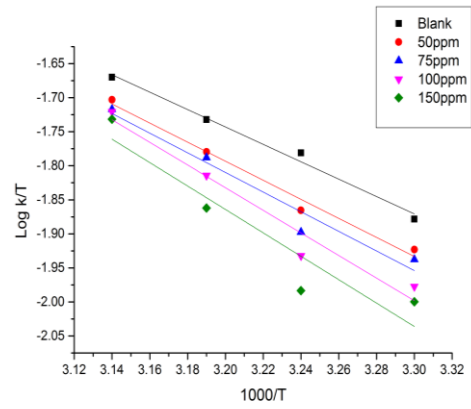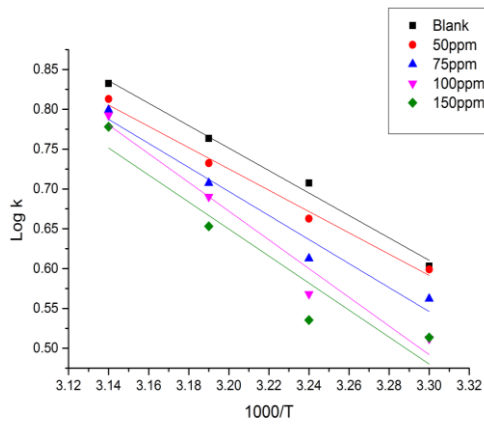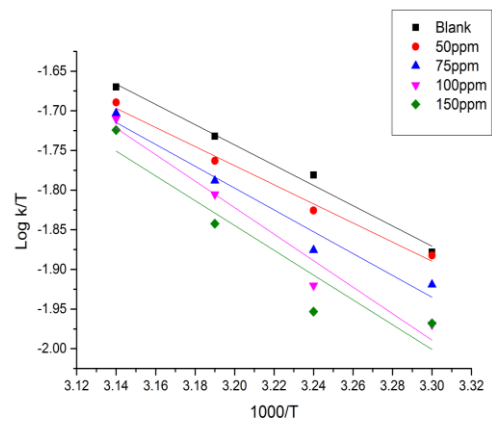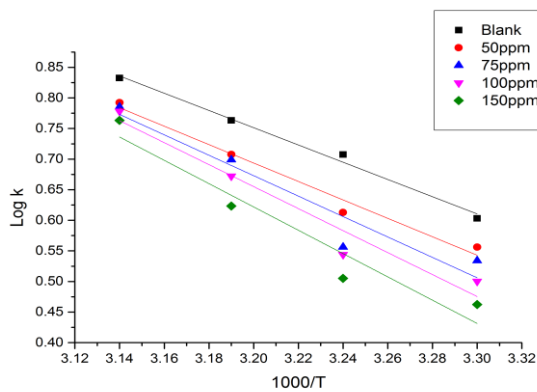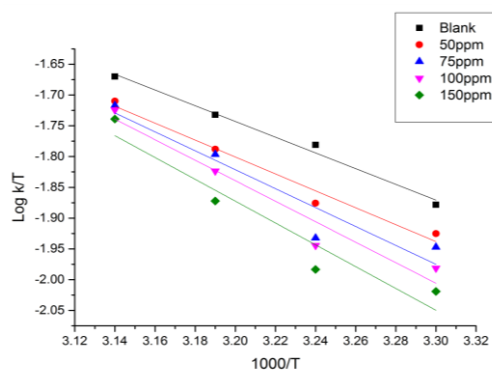
Fig.2.18 Plots of log (k/T) vs 1000/T for the corrosion of MS in the absence and presence of TMEDTDH in 1.0M HCl.

Table 2.5 Thermodynamic parameters of corrosion of MS in the presence and absence of Schiff base inhibitors TEDTDH, DHEDTDH, NEDTDH, HEDTDH, and TMEDTDH in 1.0M HCl

Inhibitor	C (ppm)	A	E_a KJmol^{-1}	ΔH^* (kJ mol^{-1})	$-\Delta S^*$ (J mol^{-1} K^{-1})
	Blank	1.8×10^5	26.98	24.46	152.68
	50	1.2×10^6	32.36	29.84	137.14
TEDTDH	75	2.4×10^6	34.33	31.81	131.31
	100	1.1×10^7	38.49	35.97	118.47
	150	1.6×10^7	39.54	37.02	115.71
	50	1.4×10^6	32.76	30.24	135.63
DHEDTDH	75	2.7×10^6	34.57	32.05	130.23
	100	3.6×10^7	41.42	38.9	108.76
	150	2.3×10^7	40.41	37.89	102.6
	50	3.3×10^5	28.83	26.31	147.85
NEDTDH	75	1.0×10^6	31.95	29.43	138.26
	100	2.5×10^6	34.4	31.88	130.77
	150	5.2×10^6	36.46	33.94	124.81
	50	4.0×10^5	29.32	26.8	146.16
HEDTDH	75	5.2×10^5	30.13	27.61	143.89
	100	2.5×10^6	34.32	31.8	130.9
	150	3.6×10^6	35.44	32.92	127.92
	50	2.0×10^5	27.59	23.07	157.63
TMEDTDH	75	3.3×10^5	28.88	26.36	147.64
	100	2.8×10^6	34.52	32	137.07
	150	3.2×10^6	32.46	39.94	130.08

Surface morphological studies

SEM images recorded were used to study the surface morphology of MS specimen in acidic solution. Fig. 2.19 (a, b, c) shows the 1000 times magnified images of polished MS, the corroded MS in HCl solution and the surface of MS immersed in 1.0M HCl solution containing inhibitor after 24hours respectively. A number of pits and cracks are seen in the SEM image of MS immersed in HCl solution (Fig. b). These are the results of aggressive action of HCl on MS Surface. In the presence of inhibitor (Fig. c) the surface is free from the pits and cracks except polishing line. This is due to the formation of a barrier film by the inhibitor. The inhibitor prevents the metal dissolution and protects the MS from corrosion.
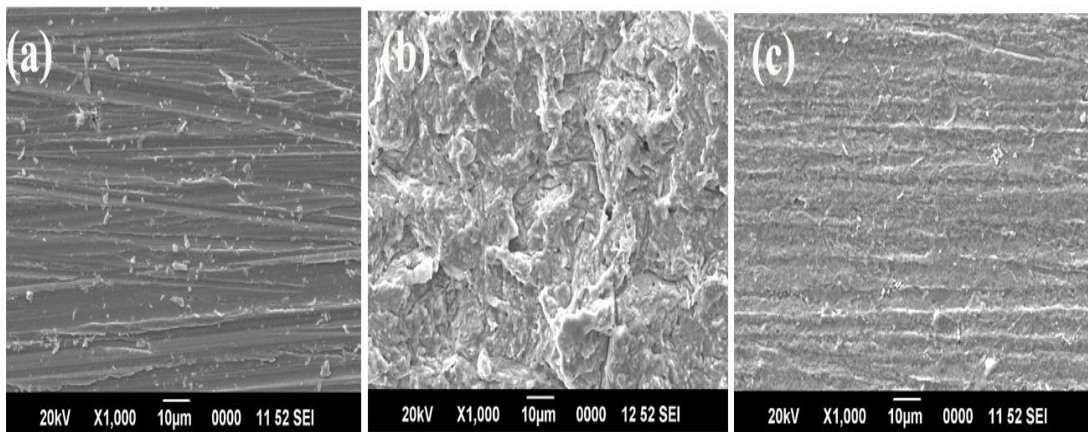
Fig.2.19 SEM images of polished MS (a), MS in the absence (b) and presence of 150ppm of the inhibitor TEDTDH (c) after 24 hours of immersion time.
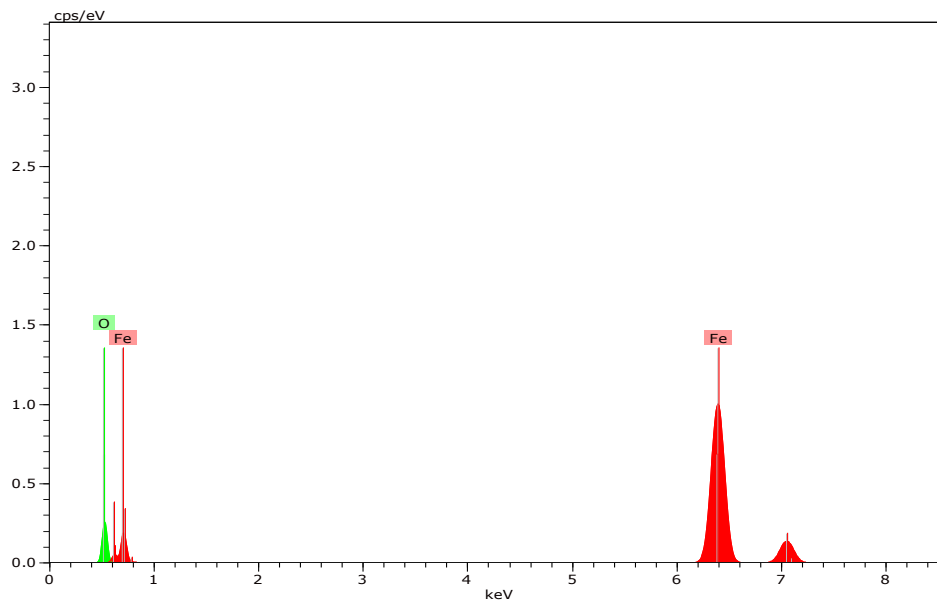
Fig.2.20 EDX spectra of MS in the absence of the inhibitor
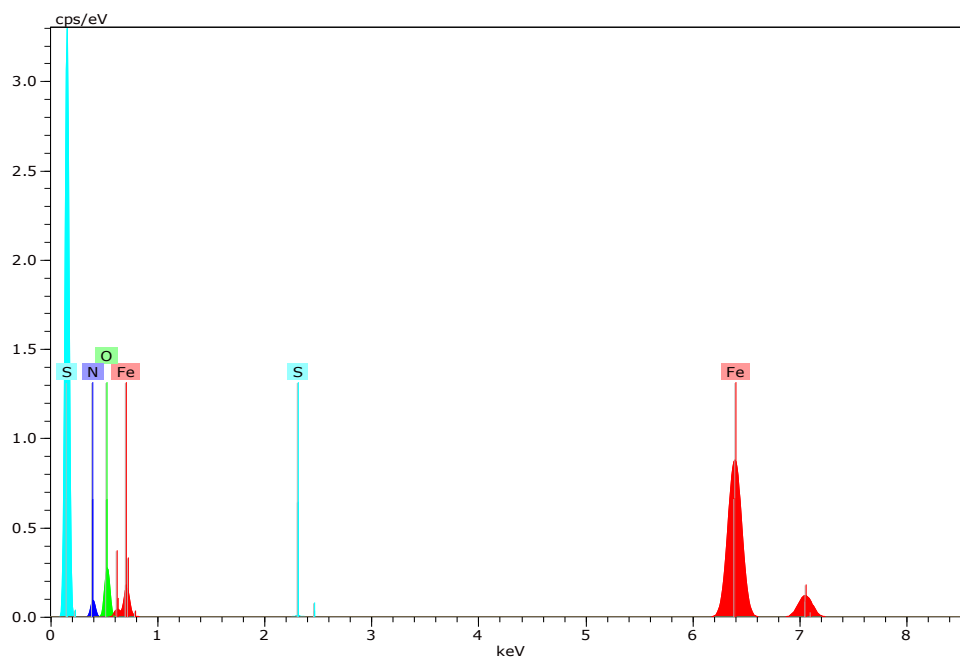
Fig.2.21 EDX spectra of MS in presence of 150ppm of the TEDTDH inhibitor

Energy Dispersive X-ray (EDX) spectra were used to determine the elements present on the MS surface before and after exposure to the inhibitor solution. Fig.2.20 and Fig 2.21 shows the EDX spectra of the MS surface in the absence and presence of inhibitor solution. In uninhibited solution only the peaks for iron and oxygen are present on the sample. In the spectra of the inhibited solution, there are

peaks for nitrogen, sulphur and a more enhanced peak for oxygen. The data reveals
the presence of an organic compound containing Sulphur, Oxygen and Nitrogen on
sample surface. The higher electron density on the functional groups leads to the
formation of a surface film through greater adsorption and consequently higher
inhibition. The protective film formed decreases the surface area available for the
reduction of H^+ ions and acts as a strong barrier to further anodic metal dissolution.

Fig.2.22 AFM images of MS in the absence (a, b) and presence of 150ppm of the inhibitor TEDTDH(c,d).

Atomic Force Microscopy (AFM) is the most versatile and powerful microscopy technology for studying the surface morphology of samples at nano to micro scale. The two dimensional and three dimensional AFM images of the MS surface exposed to 1.0M HCl solution and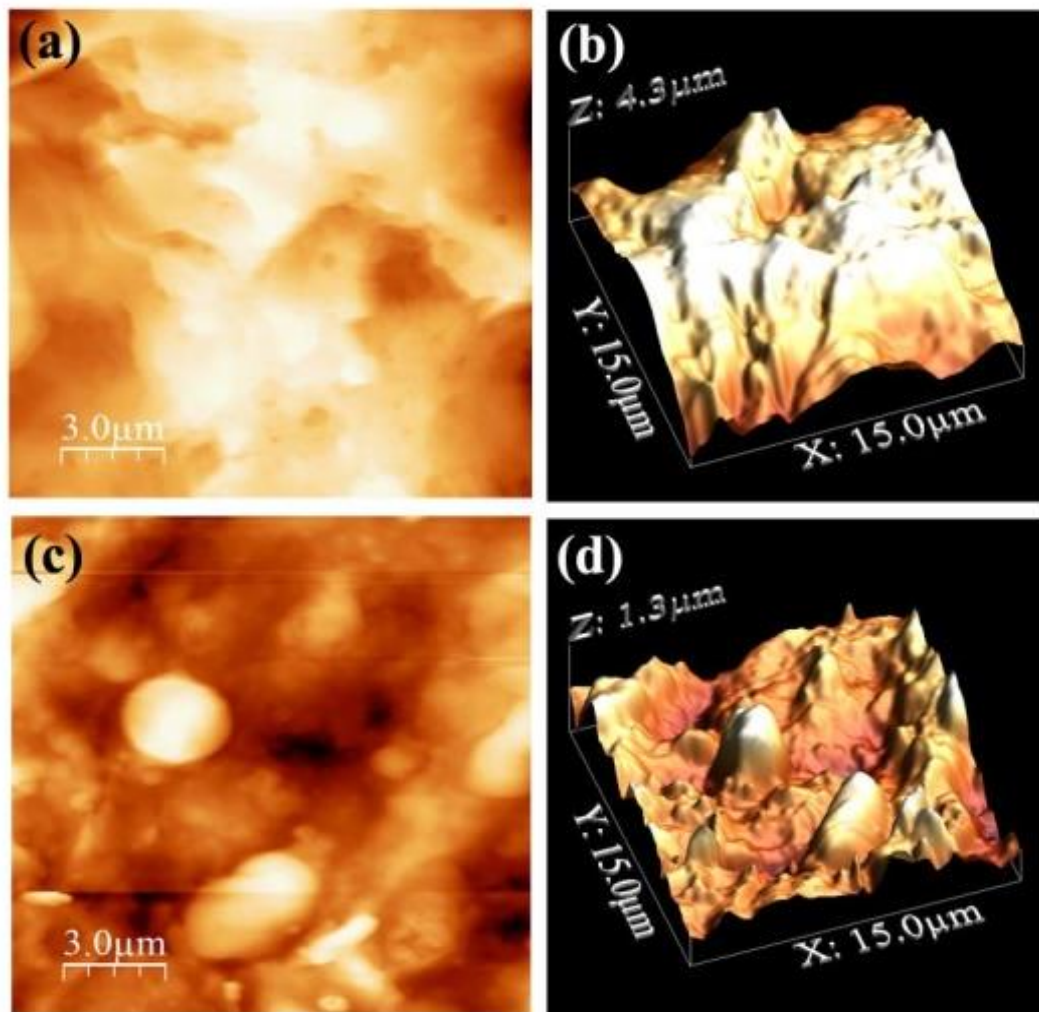 with 100ppm of TEDTDH for 24 hrs. are given in Fig.2.22. The AFM images of MS in 1.0M HCl Fig.2.22. (a, b) shows the presence of many narrow pits of few micro meter ranges. The Fig.2.22 (c, d) is that of the MS surface exposed to 150ppm of the inhibitor for 24hrs which shows the presence of a uniform inhibitor layer over the MS surface due to the adsorption of the inhibitor on the MS surface. The protective barrier film formed prevents the corrosion thereby increasing the inhibition efficiency.

Electrochemical studies on corrosion

Electrochemical corrosion techniques involved in corrosion studies are EIS measurements and potentiodynamic polarization studies. Electrochemical studies can produce fast and reproducible results. The experiments were carried out using three electrode cell, in which a platinum electrode acted as the counter electrode and SCE as the reference electrode. The exposed area of the metal specimen acted as the working electrode. Tafel polarization data helps to predict the nature of site of adsorption, whether cathodic, anodic or both sites. The mild steel specimens were immersed in the acid solution for one hour prior to the analysis with and without inhibitor and the results obtained provide a mechanistic approach to explain the inhibitive action of the various Schiff base compounds in acidic media.

Electrochemical impedance spectroscopic studies.

The Nyquist plots and combined bode and impedance plots of MS in 1.0M HCl solution in the absence and presence of different concentrations of inhibitors   are

shown in Fig.2.23 to 2.27. The parameters associated with impedance analysis such as the charge transfer resistance (R_{ct}) , double layer capacitance (C_{dl}) and the percentage efficiency calculated are given in Table 2.6. The value of R_{ct} is a measure of electron transfer across the metal solution interface and it will be inversely proportional to rate of corrosion. It is evident that the R_{ct} values are increasing with increase in the concentration of the inhibitor. In case of uninhibited solution, the reduction of H^+ ions is completely charge transfer controlled and the R_{ct} obtained was only $34.9 \Omega cm^2$. In the case of inhibitor solution, the R_{ct} of the MS was relatively larger when compared to the blank solution. This shows that the inhibitor molecule adsorbed on the MS surface decreases the area available for H^+ ion reduction. At the same time the value of CPE decreases with the concentration of inhibitor as the inhibitor displaces the other ions originally adsorbed on the surface. The results show that the protective adsorption layer formed by the inhibitor molecules on steel provides an effective barrier to the corrosion media. This barrier film by the inhibitor molecule on the MS either decreases the local dielectric constant and/or increases the thickness of electrical double layer. The η% value is maximum (92%) for 150ppm of the inhibitor. The results of EIS studies are in accordance with the results obtained from weight loss method. The absolute value of impedance and phase shifts are plotted as a function of frequency in two different plots giving a Bode plot.

Fig. 2.23a Nyquist plots of MS in the presence and absence of TEDTDH in 1.0M HCl

Fig. 2.23b Bode plots of MS in the presence and absence of TEDTDH in 1.0M HCl
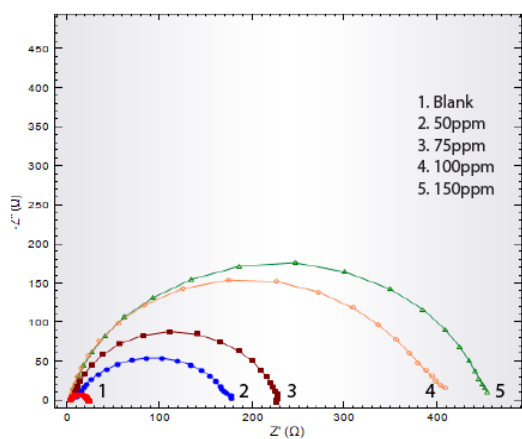
Fig. 2.24a Nyquist plots of MS in the presence and absence of DHEDTDH in 1.0M HCl
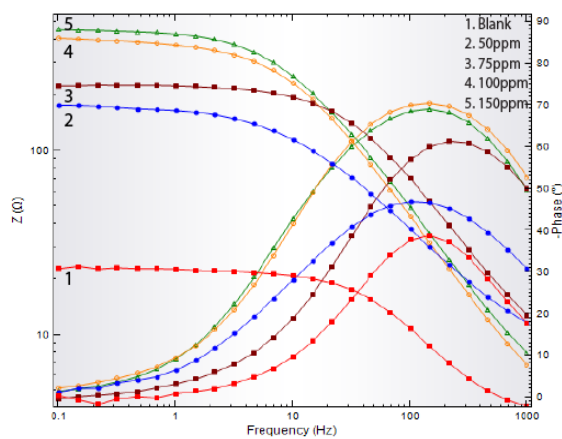
Fig. 2.24b Bode plots of MS in the presence and absence of DHEDTDH in 1.0M HCl
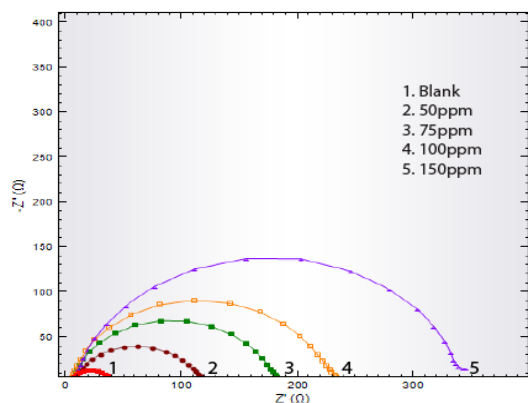
Fig. 2.25a Nyquist plots of MS in the presence and absence of NEDTDH in in1.0M HCl
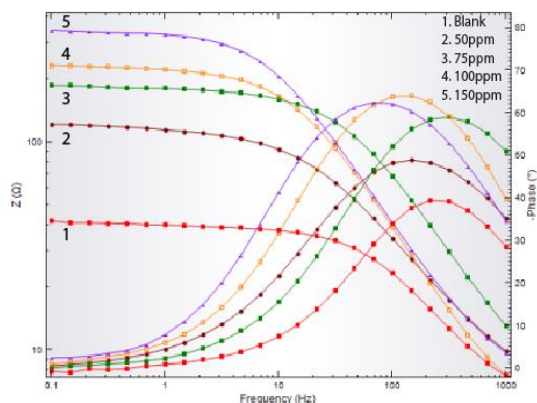
Fig. 2.25b Bode plots of MS in the presence and absence of NEDTDH in 1.0M HCl
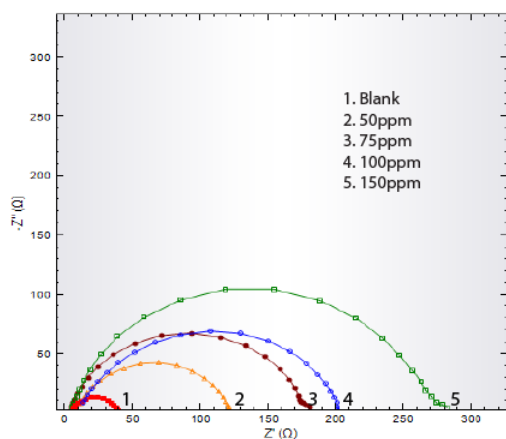
Fig. 2.26a Nyquist plots of MS in the presence and absence of HDDTDH in 1.0M HCl

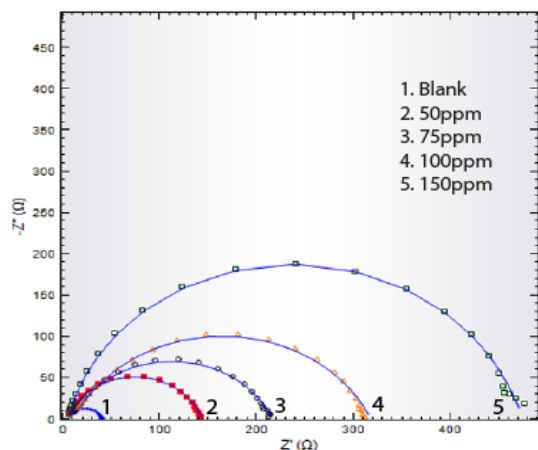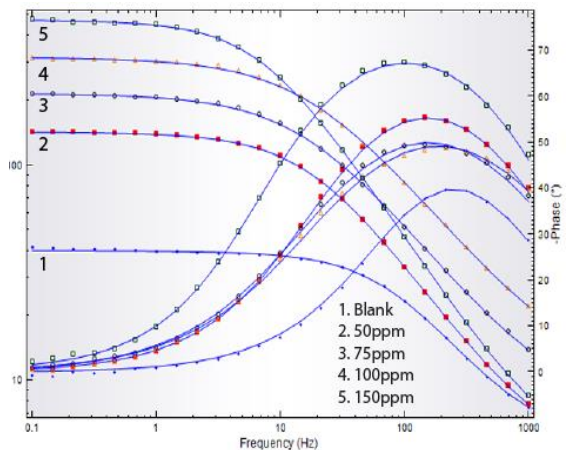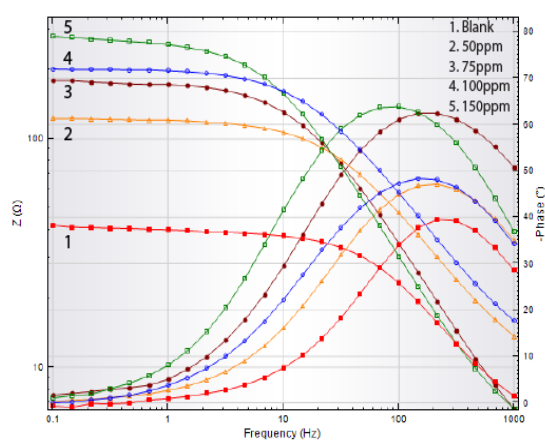**Fig. 2.26b** Bode plots of MS in the presence and absence of HDDTDH in 1.0M HCl
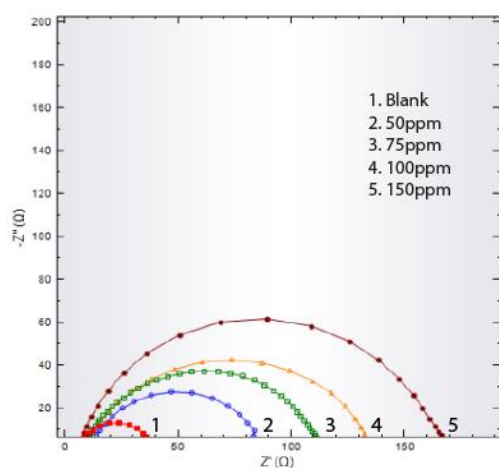
Fig. 2.27a Nyquist plots of MS in the presence and absence of TMEDTDH in 1.0M HCl
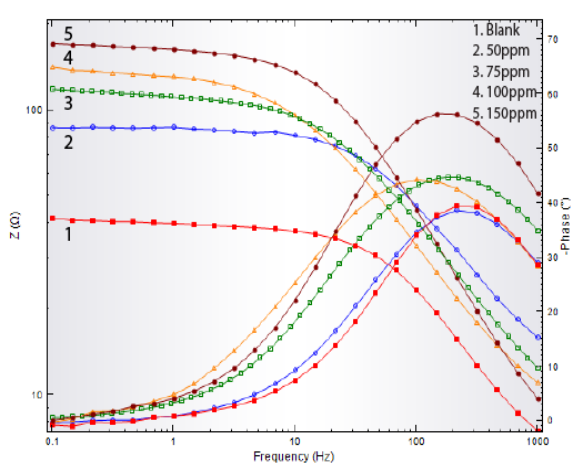
Fig. 2.27b Bode plots of MS in the presence and absence of TMEDTDH in 1.0M HCl

Table 2.6Electrochemical impedance parameters of MS in the presence and absence of TEDTDH, DHEDTDH, NEDTDH, HEDTDH, and TMEDTDH on MS in 1.0M HCl

Inhibitor	Conc.	$R_{ct}(\Omega cm^2)$	$CPE(\mu Scm^{-2})$	$\eta_{EIS}\%$
	blank	34.9	164	
	50ppm	139	150	74.89
TEDTDH	75ppm	209	143	83.30
	100ppm	308	96.3	88.66
	150ppm	438	32.6	92.031
	50ppm	170	237	79.47
	75ppm	220	49	84.13
DHEDTDH	100ppm	328	37.5	89.35
	150ppm	372.9	34.5	90.64
	50ppm	115	203	69.65
	75ppm	178	54	80.39
NEDTDH	100ppm	197	42	82.28
	150ppm	290	43	87.96
	50ppm	116	117	69.91
	75ppm	148	110	76.41
HEDTDH	100ppm	195	119	82.10
	150ppm	227	57	84.62
	50ppm	76	188	54.07
	75ppm	110	106	68.27
TMEDTDH	100ppm	131	100	73.35
	150ppm	163	74	78.58

It is quite clear from the impedance results that the inhibitor molecule TEDTDH displayed marked inhibition efficiency compared to other Schiff base molecules. A maximum efficiency of 92%was obtained with 150ppm concentration of the Schiff base inhibitor. Even at the smallest concentration, the molecule TEDTDH exhibited 74.89% efficiency. The presence of aromatic rings in the molecule and polarizing sulphur atoms in the thiophene ring system and the azomethine linkage are responsible for its excellent activity.

The results were in right agreement with the data obtained from weight loss method for TEDTDH. Other inhibitors DHEDTDH, NEDTDH, HEDTDH, and TMEDTDH were also able to exhibit better inhibition efficiencies even though slightly less than that of TEDTDH. The second and third Schiff base inhibitors were having almost similar inhibition efficiency at their highest concentration, i.e. around 90%. Besides the presence of aromatic rings, azomethine linkage also helps the inhibitor molecules to bind strongly on the metal surface and to exhibit very high inhibition efficiency. The inhibition capacities of different Schiff base inhibitors are compared in Figure2.28.
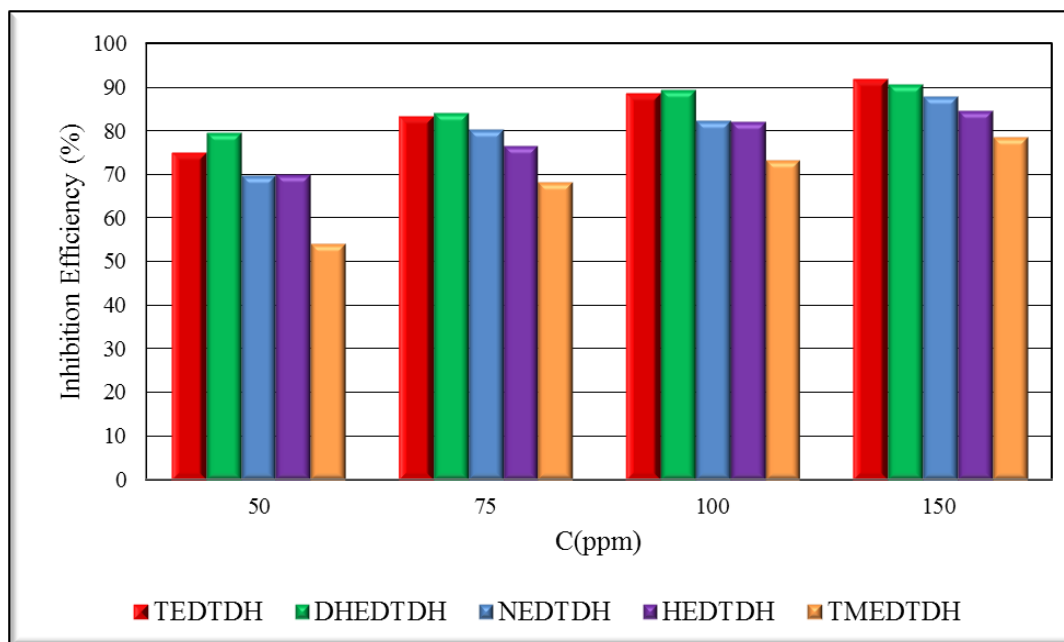
Fig. 2.28 Comparison of corrosion inhibition efficiencies (η_{EIS}%) of Schiff bases TEDTDH, DHEDTDH, NEDTDH, HEDTDH, and TMEDTDH on MS in 1.0M HCl

Potentiodynamic polarization studies

The polarization studies helps to analyze the corrosion inhibition efficiencies of Schiff bases by using Tafel extrapolation analysis. From the Tafel extrapolation method, different corrosion parameters such as corrosion potential (E_{corr}), corrosion current density (i_{corr}), cathodic and anodic slope values were obtained. Using these parameters inhibition efficiencies of the Schiff base inhibitor molecules were calculated. The potentiodynamic polarization curves of the MS in 1M HCl in the presence and absence of five Schiff base inhibitors are shown in Fig.2.29 to Fig.2.33. The literature suggests that if the corrosion potential displacement on addition of inhibitor is greater than 85 mv the inhibitor can be classified as cathodic or anodic type and if it is less than 85 mv, then the inhibitor can be considered as a mixed type of inhibitor[165]. It has been also reported that the adsorption of the inhibitors containing aromatic rings occurs mostly normal to the surface and the

inhibiting action is mainly due to the simple geometric blocking of the available cathodic and anodic sites on the metal surface.

Using the Nova Software the cathodic and anodic slopes of Tafel plots were determined. The corresponding corrosion potential (E_{corr}) and current density (I_{corr}) obtained are given in Table 2.7. The Tafel plots show that the addition of inhibitors has a pronounced inhibitive effect on the anodic and cathodic part of the curves, while the corrosion potential (E_{corr}) is only slightly shifted. In the inhibited solution the E_{corr} has shifted from the E_{corr} value of the uninhibited solution. This shift of E_{corr} indicates that this Schiff base has the ability to inhibit the acid corrosion of M.S. It can be seen that the E_{corr} values shifts in the range of 2-45 mv cathodically and in case of NEDTDH anodically however, a definite trend cannot be seen in the shift of E_{corr} values.
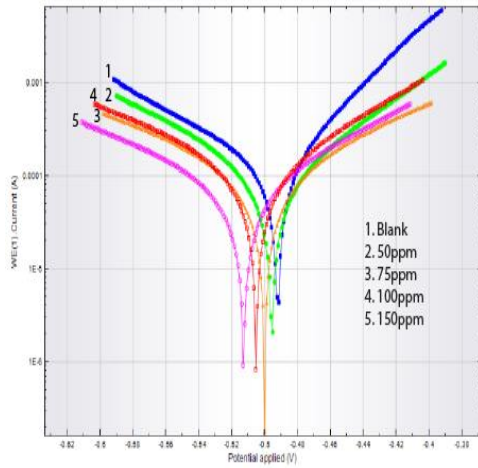
Fig.2.29 Tafel plots of MS in 1.0M HCl solution in the presence and absence of TEDTDH
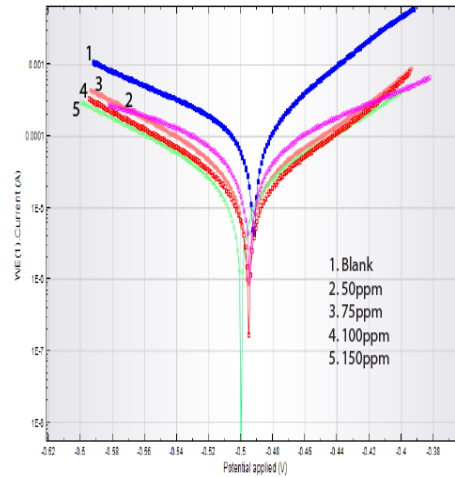
Fig.2.30 Tafel plots of MS in 1.0M HCl solution in the presence and absence of DHEDTDH
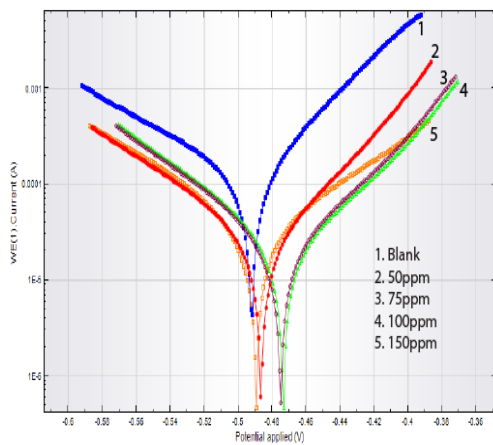
Fig.2.31 Tafel plots of MS in 1.0M HCl solution in the presence and absence of NEDTDH
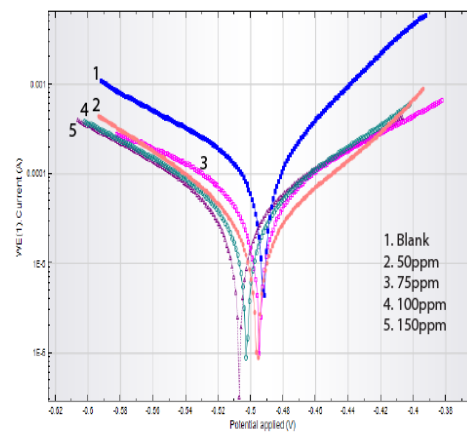
Fig.2.32 Tafel plots of MS in 1.0M HCl solution in the presence and absence of HEDTDH
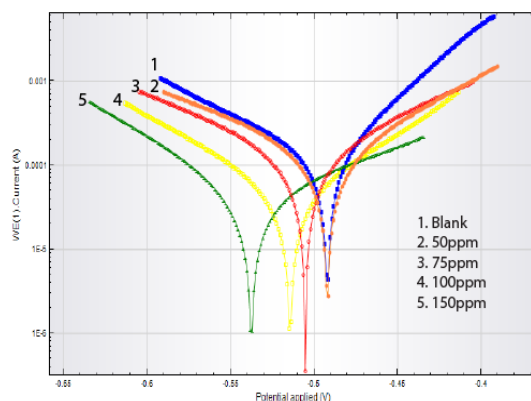
Fig.2.33 Tafel plots of MS in 1.0M HCl solution in the presence and absence of TMEDTDH

The polarization curves show that the cathodic and anodic current densities are decreasing gradually with increasing concentrations of the inhibitor. A more pronounced decrease in cathodic part in case of TEDTDH indicates that the inhibitor affects the cathodic branch of corrosion process in a significant manner. This is due to a greater suppression of the cathodic hydrogen evolution than the anodic metal dissolution. On analyzing the data presented in Table 2.7, it can be noted that the anodic and cathodic slope variations are different for each inhibitor. The values of the slopes β_a and β_b of the Tafel plots are varying which confirms that the inhibitors are influencing the corrosion reactions; inhibitors are forming a barrier film on metal surface creating a substantial resistance against the charge transfer at the interface[166]. NEDTDH is slightly anodic type. For the inhibitors TEDTDH, DHEDTDH, HEDTDH, and TMEDTDH, the cathodic and anodic slopes are slightly varied .Hence these inhibitors can be considered as a mixed type inhibitor with a predominant cathodic action.

Table 2.7 Potentiodynamic polarization parameters of MS in the presence and absence of Schiff base inhibitors TEDTDH, DHEDTDH, NEDTDH, HEDTDH, and TMEDTDH in 1.0M HCl

Inhibitor	Concentration (ppm)	b_a (mV/dec)	b_c (mV/dec)	E_{corr} (V)	j_{corr} ($\mu A/cm^2$)	θ	η_{pol} %
	blank	75	112	-0.493	209.95		
	50	72	87	-0.495	39.98	0.8096	80.96
TEDTDH	75	78	82	-0.5	23.25	0.8893	88.93
	100	63	86	-0.505	18.843	0.9103	91.03
	150	73	94	-0.513	10.815	0.9818	94.84
	50	76	92	-0.499	38.947	0.8145	81.45
	75	74	88	-0.494	34.236	0.8369	83.69
DHEDTDH	100	82	102	-0.496	20.318	0.9032	90.32
	150	72	87	-0.495	12.629	0.9398	93.98
	50	87	86	-0.489	57.924	0.7241	72.41
	75	103	81	-0.485	38.868	0.8149	81.49
NEDTDH	100	98	82	-0.475	24.83	0.8817	88.17
	150	97	78	-0.474	17.045	0.9188	91.88
	50	73	82	-0.495	39.809	0.8104	81.04
	75	84	99	-0.496	29.09	0.8614	86.14
HEDTDH	100	95	87	-0.502	21.015	0.8999	89.99
	150	76	85	-0.506	18.445	0.9121	91.21
	50	73	95	-0.492	60.84	0.7102	71.02
	75	68	97	-0.505	50.573	0.7591	75.91
TMEDTDH	100	64	92	-0.514	42.745	0.7964	79.64
	150	102	93	-0.537	21.22	0.8989	89.89

According to polarization analyses, the general trend of inhibition efficiency follows the pattern TEDTDH> DHEDTDH>NEDTDH>HEDTDH>TMEDTDH. This order is same as that obtained from weight loss measurements. The results showed that the inhibition efficiency of the Schiff base inhibitor molecules increased considerably with increase in the concentration of inhibitor, reaching a maximum of 94.84% for 150ppm of inhibitor. The potentiodynamic measurements revealed that the synthesized Schiff bases acted as good corrosion inhibitor for MS against 1.0M HCl solution
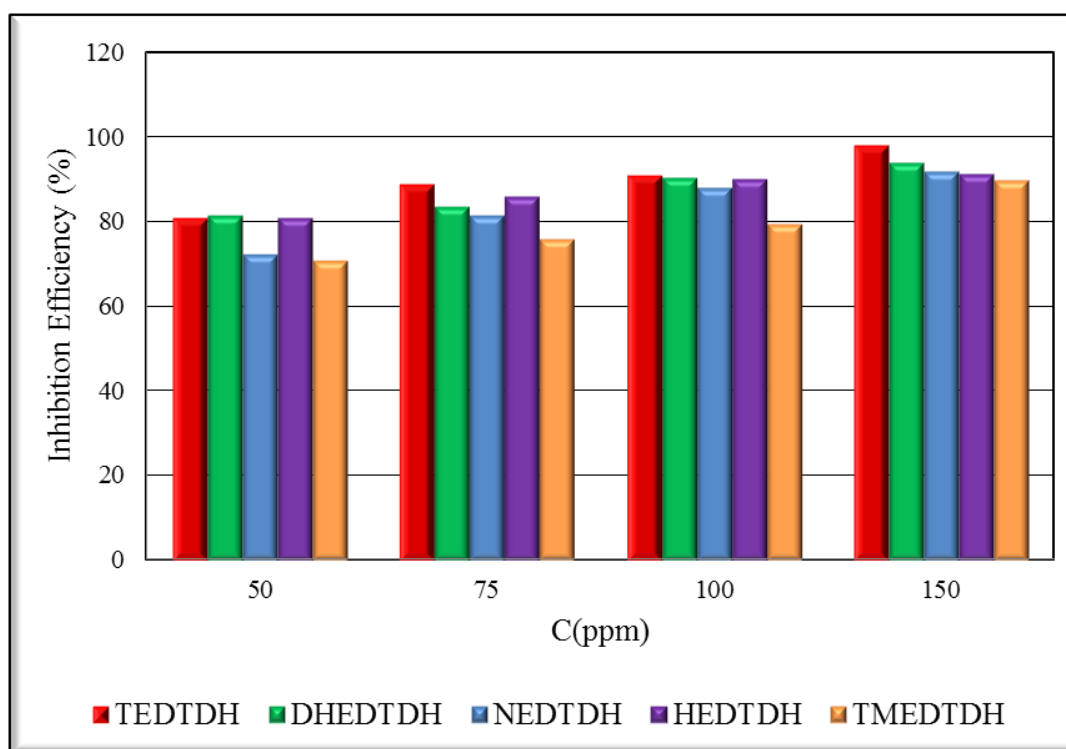
Fig. 2.34 Comparison of corrosion inhibition efficiencies (η_{pol}%) of Schiff base TEDTDH, DHEDTDH, NEDTDH, HEDTDH, and TMEDTDH on MS in 1.0M HCl

Mechanism of inhibition

Corrosion inhibitors are made from different types of substances such as amino acid derivatives, organic molecules, ionic liquids etc. To understand the mechanism of corrosion a number of factors must take into consideration such as nature of metal, nature of inhibitor, the environment and the electrochemical potential at the metal solution interface. In hydrochloric acid solution without inhibitor, the anodic dissolution occurs in an extreme way. It is well known that the chloride ions have a small degree of hydration and due to specific adsorption; they bring an excess positive charge towards the solution side of metal attracting most of the cations. The Schiff base molecule exist as protonated through nitrogen atoms in HCl solutions and the protonated inhibitor molecule could be assorted on the metal surface via, chloride ions. This will cause an electrostatic attraction between the protonated Schiff base inhibitor molecules and the metal surface reduces the anodic oxidation of Fe to Fe^{2+}. After the first electrostatic adsorption of the inhibitor molecules via, formerly adsorbed chloride ions the Schiff base molecule would directly be adsorbed on to the metal surface. The anodic sites on metal surface have vacant d orbitals of Fe^{2+} ions, which interact with the electrons of the inhibitor and adsorb the inhibitor leading to the formation of a strong barrier film on metal surface. The presence of π electrons and the non-bonded electrons of S, N and O, all contributes to the strong metal inhibitor interaction. Besides, the double bonds present in the inhibitor molecule allows the back donation of metal d electrons to the π^* orbital. Figure 2.35 illustrates the schematic representation of adsorption of inhibitor molecules on the metal surfaces
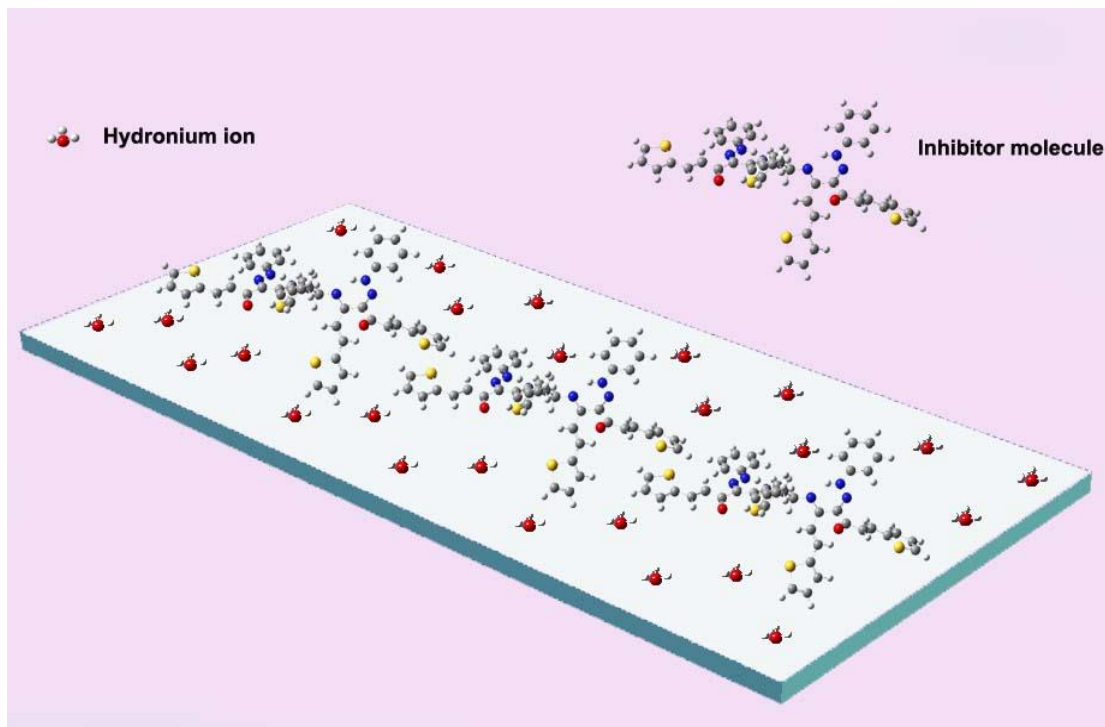
Fig.2.35 Schematic representation of corrosion inhibition by Schiff base inhibitor molecules on MS surface

SECTION II

Corrosion inhibition studies of schiff base inhibitors TEDTDH, NEDTDH, DHEDTDH, HEDTDH and TMEDTDH on mild steel in 0.5M H_2SO_4

The corrosion inhibition capacity of the Schiff base inhibitors were investigated in 0.5M sulphuric acid solution. Different electrochemical and non-electrochemical methods were used for the studies like weight loss measurements, electrochemical impedance studies and potentiodynamic polarization studies. It is known that the inhibition efficiency of Schiff bases are not that much prominent in sulphuric acid as that in hydrochloric acid medium. The rate of corrosion is high in sulphuric acid medium as it is more aggressive than hydrochloric acid medium. Hydrochloric acid medium and sulphuric acid medium are the two industrial conditions where the need for efficient inhibitors is a must.

Weight loss studies

The gravimetric measurements were carried out using MS specimens after immersed in 0.5M H_2SO_4 solution with and without inhibitor for 24 hours. The corrosion rate (K) and the inhibition efficiency (η) obtained are shown in the tables 2.8 and 2.9.

The maximum efficiency (76.89%) was shown by the Schiff base inhibitor TEDTDH. The analysis of the obtained data collected in the Table 2.8 showed a decrease of corrosion rate with increase in the concentration of the inhibitor molecule in all cases. The least corrosion rate for TEDTDH was obtained at a concentration of 150ppm of the inhibitor molecule. The aromatic rings in addition to the azomethine linkage, highly polarizable 'S' atom and the oxygen atoms make the molecule gets adsorbed on the surface metal atoms strongly which results in the greater inhibition capacity.

Table 2.8 Corrosion rates of MS in mgcm^{-2}h^{-1} in the presence and absence of Schiff base inhibitors TEDTDH, NEDTDH, DHEDTDH, HEDTDH, and TMEDTDH in 0.5M H$_2$SO$_4$

C(ppm)	TEDTDH	NEDTDH	DHETDH	HEDTDH	TMEDTDH
0	20.94	20.94	20.94	20.94	20.94
50	12.76	13.99	17.45	18.98	19.02
75	10.21	12.81	16.01	16.29	17.1
100	7.32	8.35	12.27	13.46	15.47
150	4.84	7.16	10.43	10.89	13.64
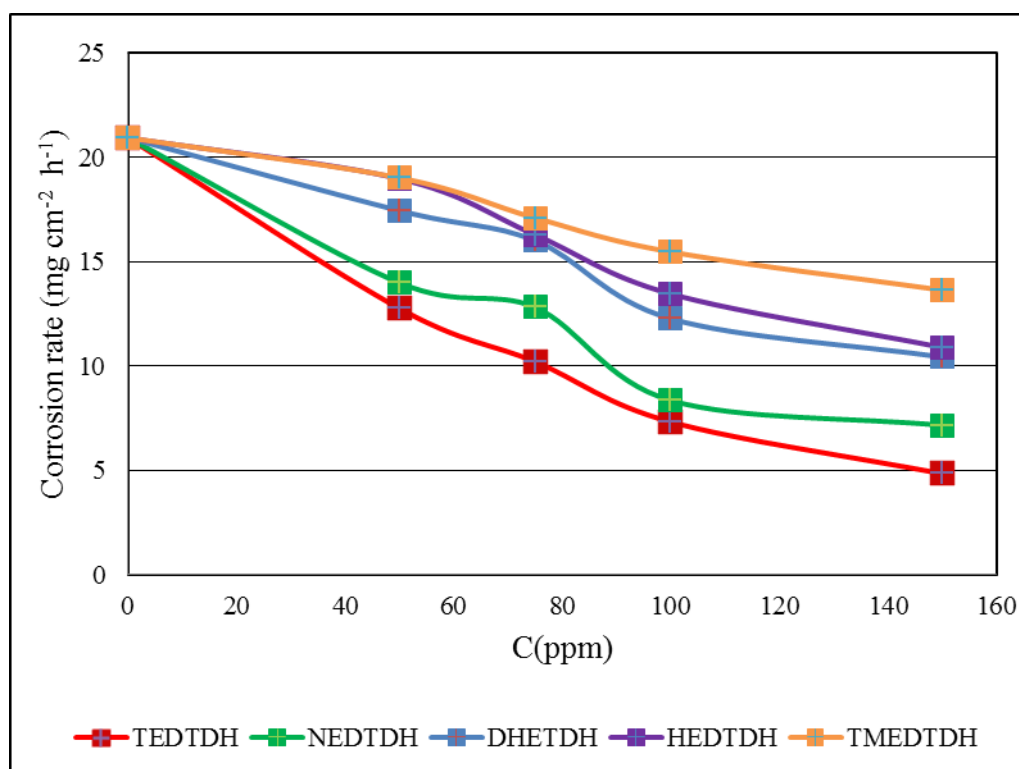
Fig.2.36 Variation of corrosion rates of MS with the concentration of Schiff base inhibitors TEDTDH, NEDTDH, DHEDTDH, HEDTDH, and TMEDTDH in 0.5M H$_2$SO$_4$

The last three Schiff base inhibitors DHETDH, HEDTDH and TMEDTDH exhibited lower inhibition efficiency than the TEDTDH and NEDTDH on MS

corrosion against sulphuric acid medium. The lower corrosion inhibition efficiency compared to the other two may be attributed to the highly aggressive nature of sulphuric acid medium and the intensive hydrolysis of the Schiff base molecules in the sulphuric acid solution.

Table 2.9 Inhibition efficiencies of Schiff base inhibitors TEDTDH, NEDTDH, DHEDTDH, HEDTDH, and TMEDTDH in 0.5M H$_2$SO$_4$

	Inhibitors				
C(ppm)	TEDTDH	NEDTDH	DHEDTDH	HEDTDH	TMEDTDH
50	39.06	33.19	16.67	9.36	9.17
75	51.24	38.83	23.54	22.21	18.34
100	65.04	60.12	41.4	35.72	26.12
150	76.89	65.81	50.19	47.99	34.86
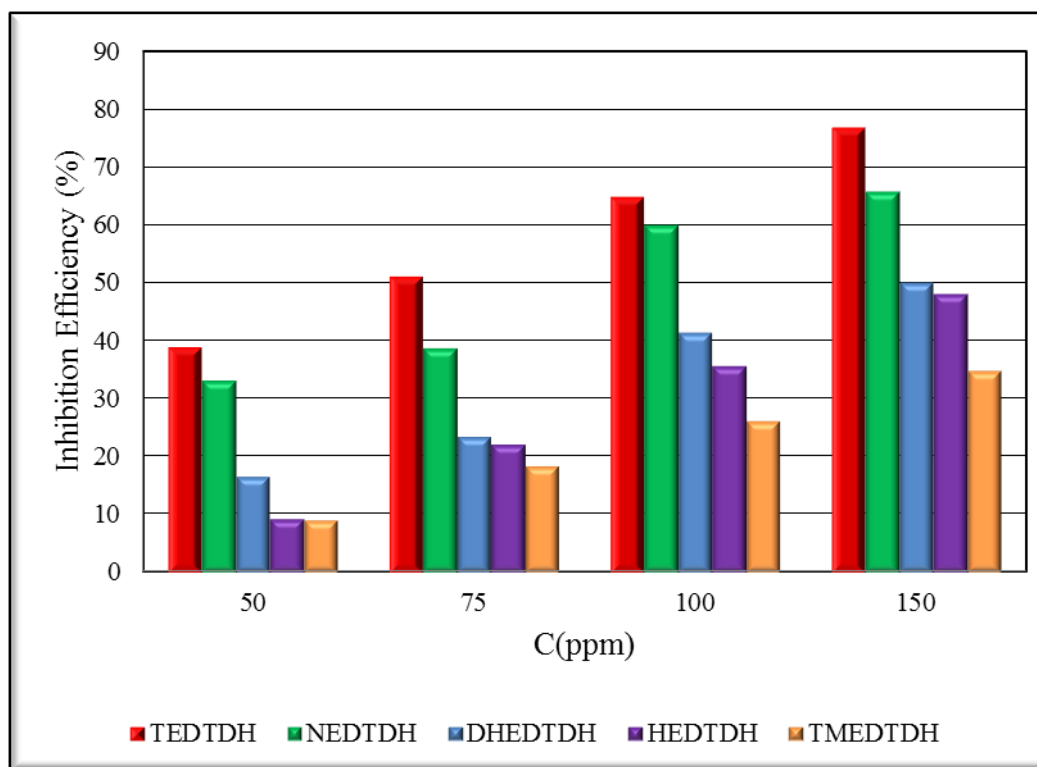
Fig.2.37 Comparison of corrosion inhibition efficiencies (η$_w$%) of Schiff base inhibitors TEDTDH, NEDTDH, DHEDTDH, HEDTDH, and TMEDTDH in 0.5M H$_2$SO$_4$ on MS

Adsorption isotherms

The adsorption isotherm helps to identify the mechanism of interaction of the inhibitor and the surface of metal specimens. Different adsorption isotherms were studied and the best fit isotherm for the adsorption was selected with highest correlation coefficient. The adsorption isotherms are shown in Figures 2.38 to 2.42
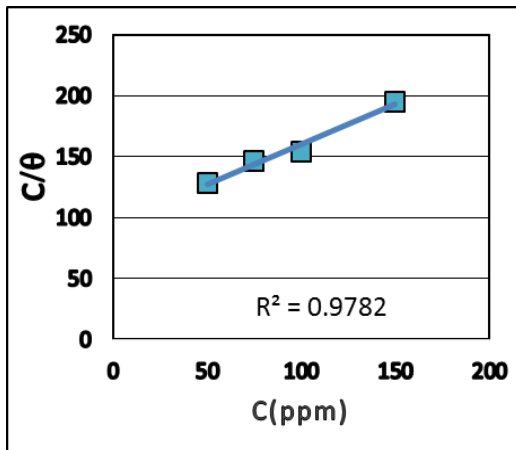
Fig.2.38 Langmuir adsorption isotherm for TEDTDH on MS in 0.5M H$_2$SO$_4$
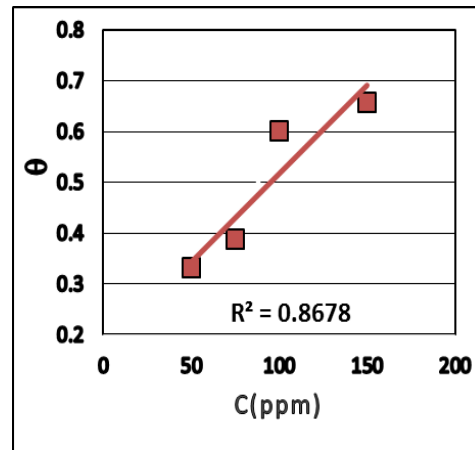
Fig.2.39 Freundlich adsorption isotherm for NEDTDH on MS in 0.5M H$_2$SO$_4$
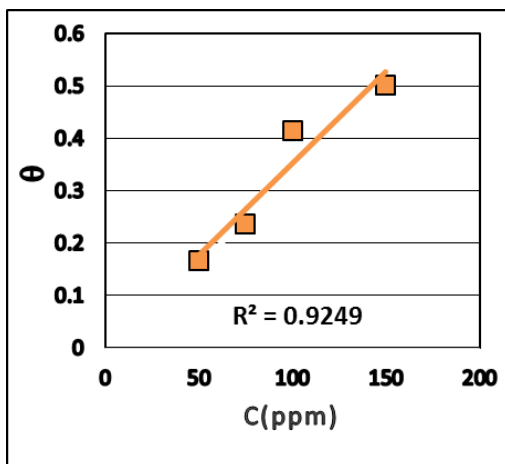
Fig.2.40 Freundlich adsorption isotherm for DHEDTDH on MS in 0.5M H2SO4
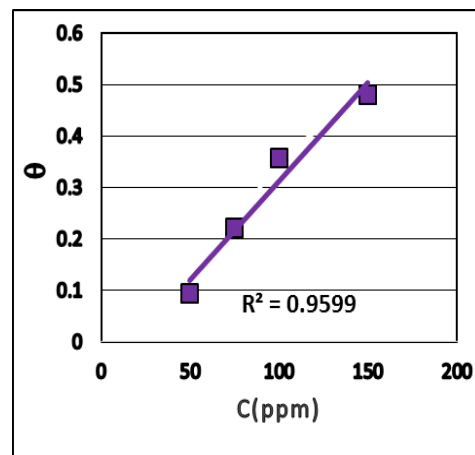
Fig.2.41 Freundlich adsorption isotherm for HEDTDH on MS in 0.5M H$_2$SO$_4$
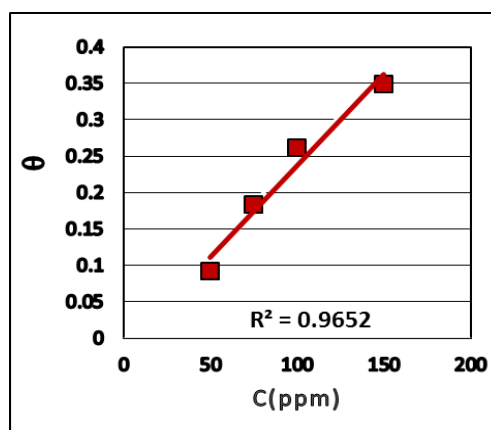
Fig.2.42 Freundlich adsorption isotherm for TMEDTDH on MS in 0.5M H$_2$SO$_4$

The best fit adsorption isotherm for NEDTDH, DHEDTDH, HEDTDH and TMEDTDH was Freundlich isotherm, which can be represented as

$$\theta = K_{ads}C$$

where C is the concentration of the inhibitor molecule, θ is the fractional surface coverage and K$_{ads}$ is the adsorption equilibrium constant. At the same time for TEDTDH inhibitor molecule, follows Langmuir isotherm and exhibit single layer adsorption characteristics. The Langmuir adsorption isotherm can be represented as follows

$$\frac{C}{\theta} = \frac{1}{K_{ads}} + C$$

The calculated K$_{ads}$ and ΔG^0_{ads} values are given in the Table 2.10. According to the obtained ΔG^0_{ads} values it can be suggested that the adsorption of Schiff Base molecules on the MS surface involves 2 types of interaction, physisorption and chemisorption. The highest negative value for TEDTDH indicated the strong absorption of inhibitor on the MS surface and also the spontaneity of the process. The low values of ΔG^0_{ads} for last three indicated the multilayer adsorption of these Schiff base molecules on the metal surface. From the results it was clear that in

aggressive sulphuric acid medium also these Schiff bases were able to make a protective film over the MS surface.

Table 2.10 Thermodynamic parameters for the adsorption of Schiff base inhibitors HEDTDH, TEDTDH, DHEDTDH, TMEDTDH, and NEDTDH on MS in 0.5M H$_2$SO$_4$

Parameters	TEDTDH	NEDTDH	DHEDTDH	HEDTDH	TMEDTDH
K$_{ads}$	26472	1248	1004	1178	1035
ΔG^o_{ads} KJmol^{-1}	-33.42	-30.52	-24.8	-25.166	-24.873

SURFACE MORPHOLOGICAL STUDIES

The effect of inhibitor molecules on MS surface was studied with SEM analyses, AFM analysis and EDX spectral analysis. The analysis of the metal surfaces exposed to 0.5M H$_2$SO$_4$ with and without inhibitor was taken. On comparing Figures 2.43 and 2.44, it can be seen that the surface of MS was seriously scratched and damaged in the acidic solution. Figure 2.45 represents the image of the metal in the presence of the NEDTDH molecules (150ppm, 24 h) it can be seen that the damage occurred on the surface was fairly reduced in presence of the Schiff base inhibitor.It is evident from the EDX spectral analysis that MS specimen in the presence of inhibitor have peaks for nitrogen and and an enhanced peak for oxygen.
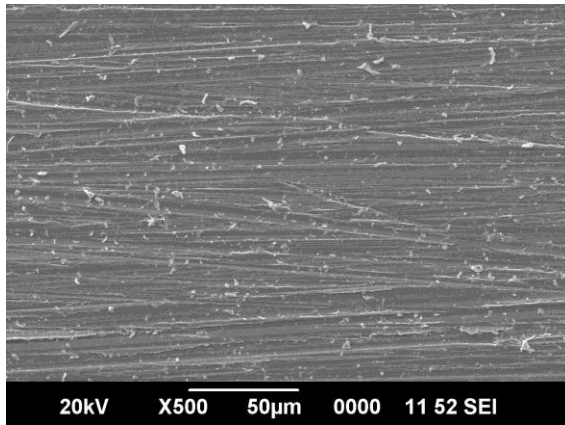
Fig.2.43 SEM image of the bare MS   **Fig.2.44 SEM image of MS surface in 0.5M H₂SO₄ after 24 h**
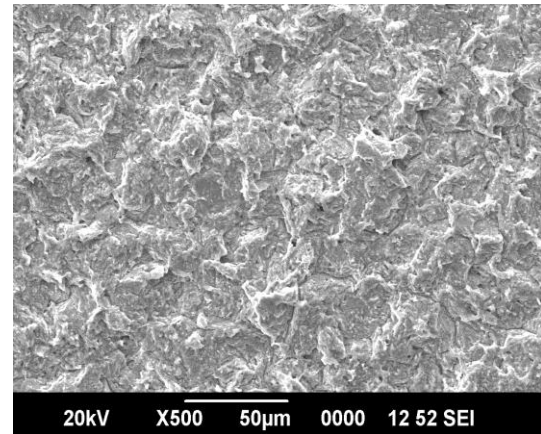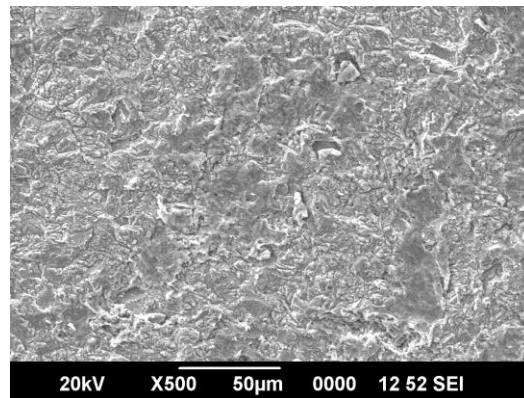
Fig.2.45 SEM image of MS surface in 0.5M H₂SO₄ and NEDTDH after 24 h
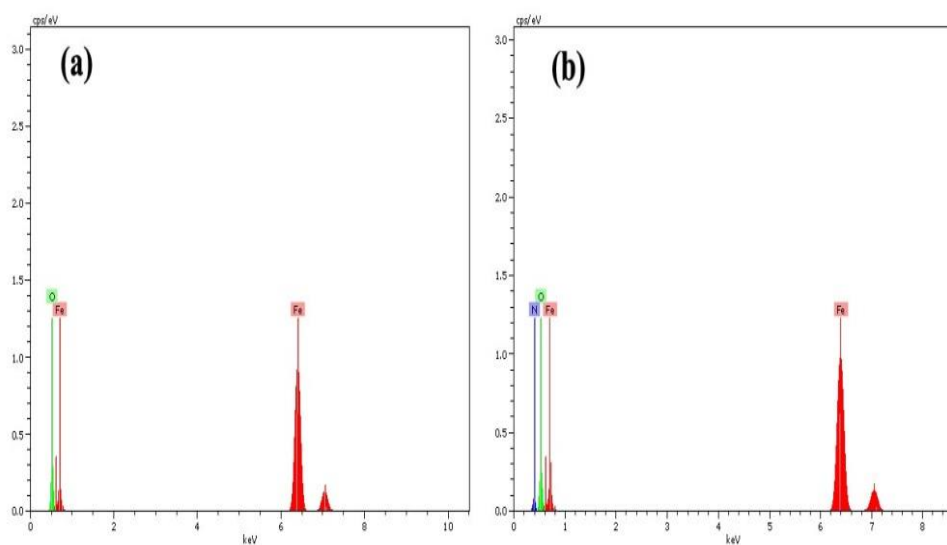
Fig. 2.46 EDX spectra of MS surface in 0.5M H₂SO₄ and NEDTDH after 24 h

Corrosion inhibition studies on parent diketo compounds

Corrosion inhibition characteristics of the parent diketo compounds of each Schiff base inhibitor were studied and compared. The results are shown in table 2.11. The parent compounds consists of 1,7-bis(thiophen-2-yl)-hepta-1,6-diene-3,5-dione (TPHD), 1,7-bis(2,4-dihydroxy phenyl)-hepta-1,6-diene-3,5-dione(DHPHD), 1,7-bis(naphthyl)-hepta-1,6-diene-3,5-dione (NPHD), 1,7-bis(2-hydroxy phenyl)-hepta-1,6-diene-3,5-dione(HPHD) and 1,7-bis(3,4,5-trimethoxy phenyl)-hepta-1,6-diene-3,5-dione(TMPHD). These compounds were taken in 75ppm, 100ppm and 150ppm concentrations in 0.5M H_2SO_4 and their inhibition efficiencies against MS corrosion for a period of 24 hours were investigated using gravimetric method.

Table 2.11 Corrosion inhibition efficiencies (η_w%) of parent compounds on MS surface in 0.5M H_2SO_4

Compounds	Concentration(ppm)		
	50	100	150
TPHD	18.25	31.41	36.78
NPHD	15.27	25.19	31.28
DHPHD	8.68	21.35	29.42
HPHD	5.27	15.94	22.18
TMPHD	5.93	13.48	19.72
TEDTDH	39.06	65.04	76.89
NEDTDH	33.19	60.12	65.81
DHEDTDH	16.67	41.4	50.19
HEDTDH	9.36	35.12	47.99
TMEDTDH	9.317	26.12	34.86
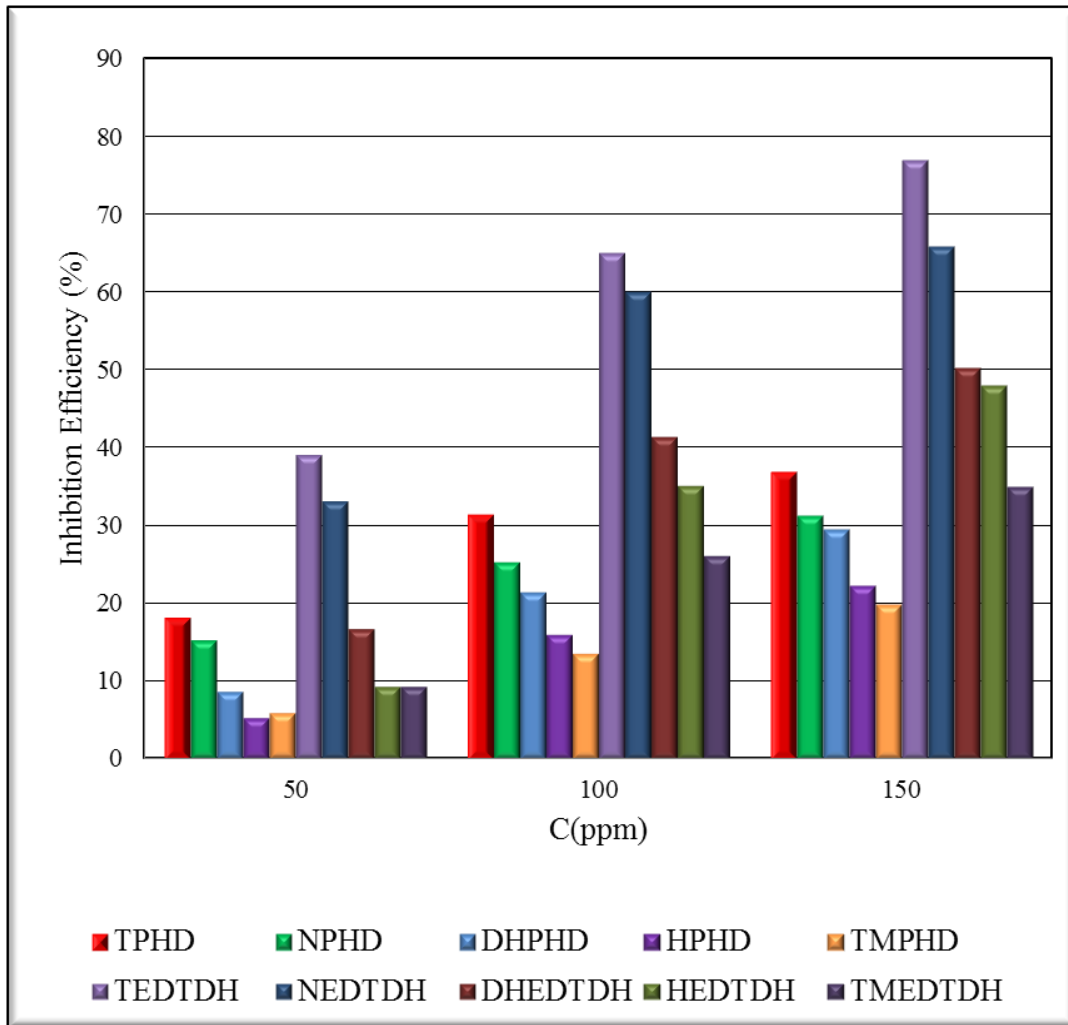
Fig. 2.47 Comparison with corrosion inhibition efficiencies (η_w%) of parent compounds on MS surface in 0.5M H_2SO_4

Electrochemical studies on corrosion

Electrochemical methods comprise impedance and potentiodynamic techniques in sulphuric acid medium. Electrochemical impedance measurements give rapid results when compared to the weight loss studies. The five newly synthesized Schiff base inhibitor molecules were subjected to electrochemical studies on MS in highly aggressive 0.5M H_2SO_4 medium. EIS and Tafel polarization studies were carried out to get a quick and reliable outcome on the inhibition capabilities of the inhibitors on MS.

Electrochemical impedance spectroscopic (EIS) studies

The impedance studies were performed using metrohm autolab PGSTAT 50519 and a three electrode system. The OCP was stabilized and the measurements were taken using NOVA software. The frequency range for EIS measurements were 1 KHz to 100MHz with amplitude of 10mv at OCP by applying AC signal. The MS specimens acted as working electrode of three electrode system and the EIS measurements were carried out with and without inhibitor in 0.5M sulphuric acid medium. The platinum electrode and saturated calomel electrode acted as counter and reference electrodes respectively. Nyquist plots and Bode plots were obtained in sulphuric acid medium. Figures 2.48 to 2.52 gives the representative Nyquist plot and Bode plots.

The parameters obtained (R_{ct}) charge transfer resistance, constant phase element CPE and the percentage inhibition efficiency at different concentration of the inhibitor are given in the Table 2.12 . The inhibition efficiencies were calculated using the following expression

$$\eta\% = \frac{R'_{ct} - R_{ct}}{R'_{ct}} \times 100$$

where R_{ct} and R'_{ct} are the charge transfer at metal solution interface in the presence

and absence of inhibitor respectively.
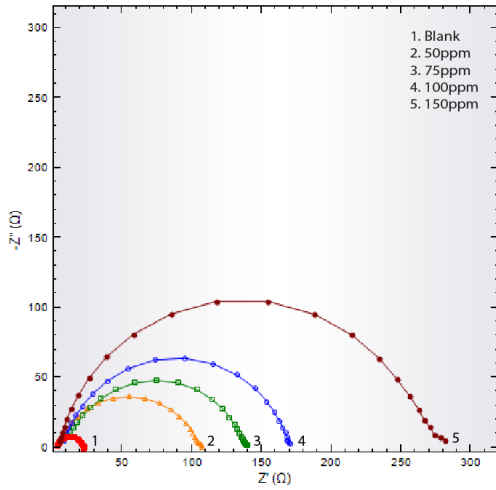
Fig. 2.48a Nyquist plots of MS in the presence and absence of TEDTDH in 0.5M H$_2$SO$_4$
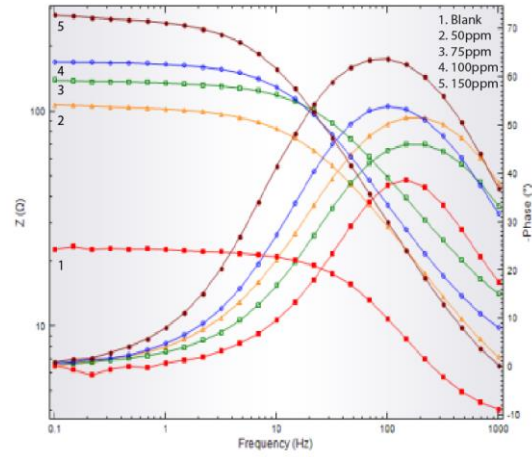
Fig. 2.48b Bode plots of MS in the presence and absence of TEDTDH in 0.5M H$_2$SO$_4$

Fig. 2.49a Nyquist plots of MS in the presence and absence of NEDTDH in 0.5M H$_2$SO$_4$

Fig.2.49b Bode plots of MS in the presence and absence of NEDTDH in 0.5M H$_2$SO$_4$

Fig. 2.50a Nyquist plots of MS in the presence and absence of DHEDTDH in 0.5M H$_2$SO$_4$

Fig. 2.50b Bode plots of MS in the presence and absence of DHEDTDH in 0.5M H$_2$SO$_4$

Fig. 2.51a Nyquist plots of MS in the presence and absence of HEDTDH in 0.5M H$_2$SO$_4$

Fig. 2.51b Bode plots of MS in the presence and absence of HEDTDH in 0.5M H$_2$SO$_4$

Fig. 2.52a Nyquist plots of MS in the presence and absence of TMEDTDH in 0.5M H$_2$SO$_4$

Fig. 2.52b Bode plots of MS in the presence and absence of TMEDTDH 0.5M H$_2$SO$_4$

It is clear from Nyquist plots and representative Bode diagrams that in uninhibited solution, a slightly deprived semicircular shape is obtained which indicated the charge transfer controlled corrosion process. The difference between real impedance at lower and higher frequencies is considered as R_{ct} charge transfer resistance which is the resistance between metal and outer Helmholtz plane. The highest R_{ct} value of Schiff base molecule TEDTDH indicated the strong inhibition behavior of TEDTDH. The inhibition efficiency of TEDTDH is 91% at 150ppm concentration.

Inhibitors NEDTDH and DHEDTDH also exhibited better inhibition efficiency against sulphuric acid corrosion. NEDTDH showed an inhibition effect of 90.86% of highest concentration. The R_{ct} values are directly proportional to the concentration, as the concentration increases R_{ct} values also increases. But the CPE decreases with the increase in inhibitor concentration may be attributed to the increase in thickness of electrical double layer or decrease in dielectric constant

Table 2.12 Electrochemical impedance parameters of MS in the presence and absence of HEDTDH, TEDTDH, DHEDTDH, TMEDTDH, and NEDTDH on MS in 0.5 M H$_2$SO$_4$

Inhibitor	Conc.(ppm)	$R_{ct}(\Omega cm^2)$	CPE(μScm^{-2})	$\eta\%$
	blank	19	336	
	50	102	200	81.37
TEDTDH	75	130	128	85.38
	100	164	112	88.41
	150	215	52	91.16
	50	70	460	72.86
	75	98.2	298	80.65
NEDTDH	100	110	221	82.73
	150	208	117	90.87
	50	58	196	67.24
	75	72	188	73.61
DHEDTDH	100	88.5	126	78.53
	150	115	77	83.48
	50	48.8	170	61.07
	75	56.4	168	66.31
HEDTDH	100	77.3	160	75.42
	150	95	70	80
	50	40.3	274	52.85
	75	44.9	189	57.68
TMEDTDH	100	52	140	63.46
	150	63	57	69.84

.

Fig. 2.53 Comparison of corrosion inhibition efficiencies (η_{EIS}%) of Schiff base TEDTDH, NEDTDH, DHEDTDH, HEDTDH, and TMEDTDH on MS in 0.5 M H$_2$SO$_4$

The inhibition efficiencies from EIS data were higher than that obtained from gravimetric analysis and these analyses results were not comparable. Since electrochemical measurements give a rapid result for corrosion analysis it will only give the corrosion inhibition capacities of inhibitor molecules on metal surface at the first stage of treatment. The molecules will gradually hydrolyze into their parent aryl azo compounds and thus show low inhibition efficiency in H$_2$SO$_4$ medium than the Schiff base molecules if kept for a long span of 24 hours. This makes it clear why gravimetric corrosion inhibition efficiencies are lower than the efficiencies obtained from electrochemical results. Comparatively least efficiency was reported in the case of inhibitor TMEDTDH. Even at the highest concentration 150ppm it has showed 69.84% inhibition efficiency. The order of performances of the studied Schiff base inhibitor molecules on MS can be given as TEDTDH > NEDTDH > DHEDTDH > HEDTDH > TMEDTDH.

Potentiodynamic polarization studies

The behaviour of the Schiff base inhibitors towards polarization of metal specimens were investigated by Tafel extrapolation analysis. Polarization studies recorded the anodic and cathodic polarization curves. Polarization plots were obtained in the electrode potential range from -1 to +1 mV from OCP at a scan rate of 1mV/sec. Tafel polarization analysis were performed by extrapolating anodic and cathodic curves to obtain the corrosion current densities(I_{corr}). The percentage of inhibition efficiency ($\eta_{pol}\%$) was evaluated from the measured I_{corr} values using the following relation.

$$\eta_{pol}\% = \frac{i_{corr} - i'_{corr}}{i_{corr}} \times 100$$

where i_{corr} and i'_{corr} are uninhibited and inhibited corrosion current densities respectively

From the polarization analyses, parameters like corrosion current density (I_{corr}), corrosion potential (E_{corr}), cathodic slope (b_c) and anodic slope (b_a) were obtained and are presented in Table 2.13 Using these parameters the percentage inhibition efficiency ($\eta_{pol}\%$) was also determined. It is evident, from the Tafel parameters for the corrosion inhibition studies of various Schiff base inhibitors on the MS surface that the corrosion current density (I_{corr}) decreased to a great extent with increasing the inhibitor concentration. This decrease in corrosion current density can be attributed to the increase in the adsorption of the inhibitor molecules with concentration. The TEDTDH molecules showed a highest of 93.97% inhibition efficiency at 150ppm concentration in the Tafel plot analysis. This was followed by the inhibitor compound NEDTDH, which has got 91.8% efficiency at its highest concentration. Other Schiff base inhibitors also exhibited good inhibition

performances; all of them were showing >50 % inhibition capacity even at the lowest concentration 50ppm. The Tafel curves are given in Fig.2.54 to 2.58
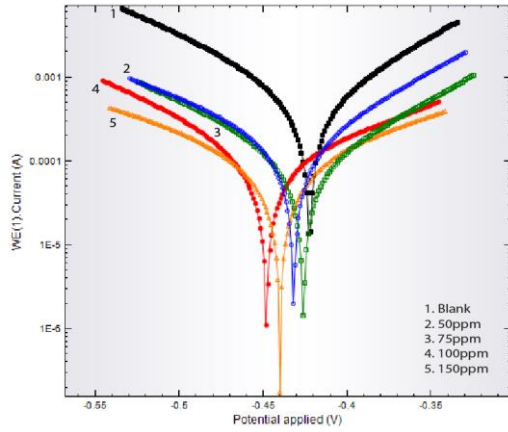
Fig.2.54 Tafel plots of MS in the presence and absence of TEDTDH in 0.5M H₂SO₄
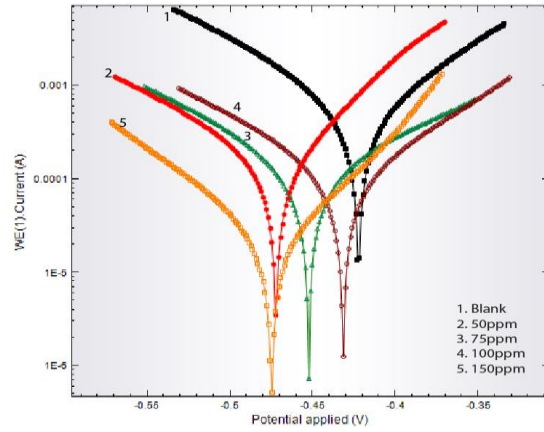
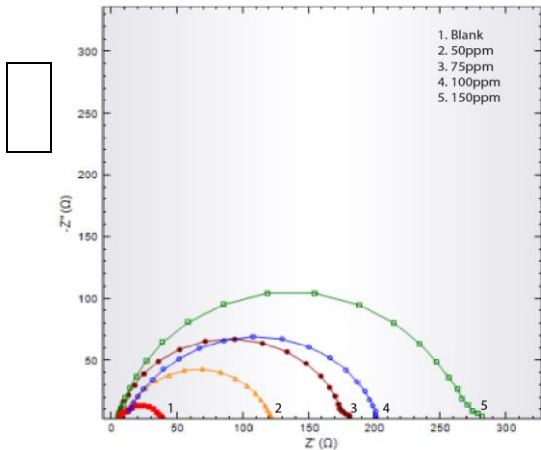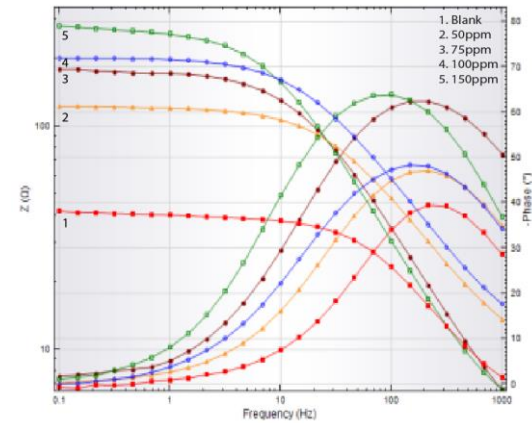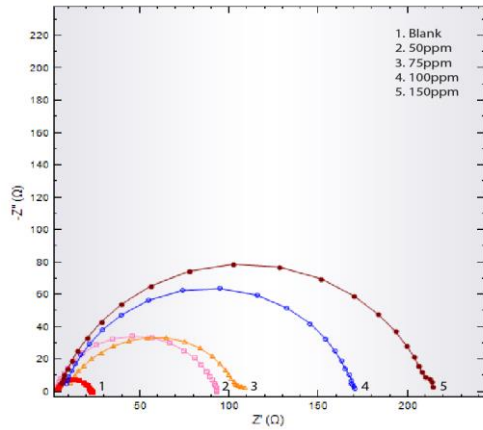**Fig.2.55 Tafel plots of MS in the presence and absence of NEDTDH in 0.5M H₂SO₄**
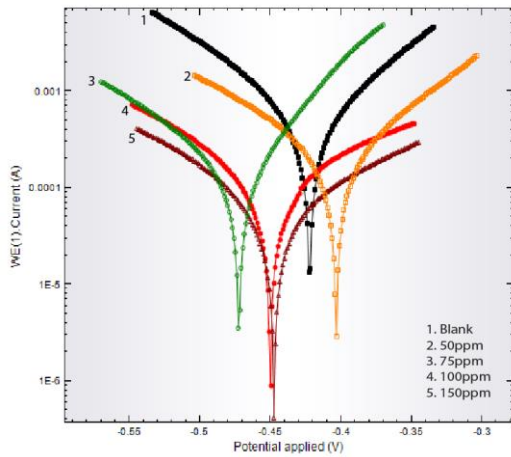
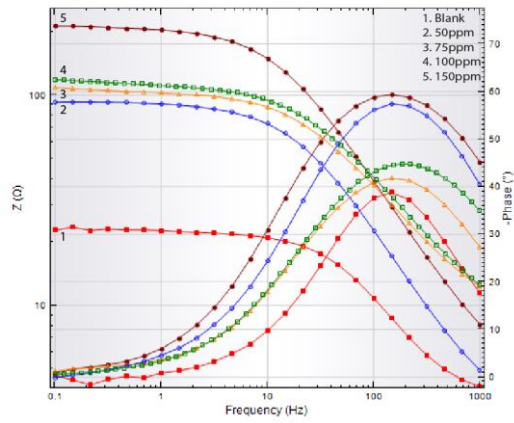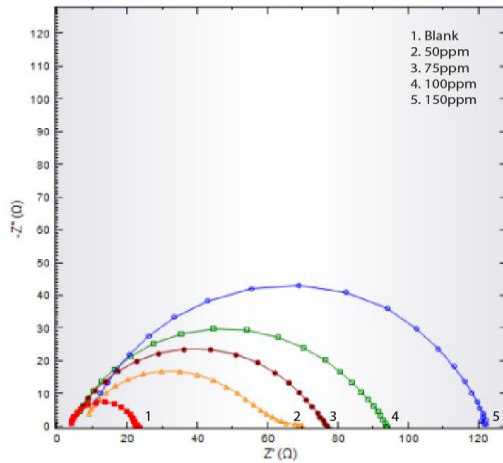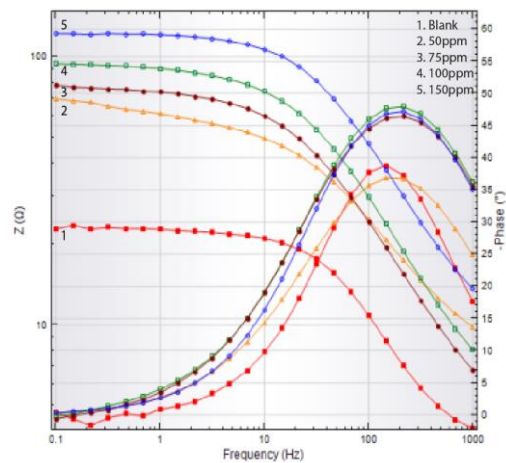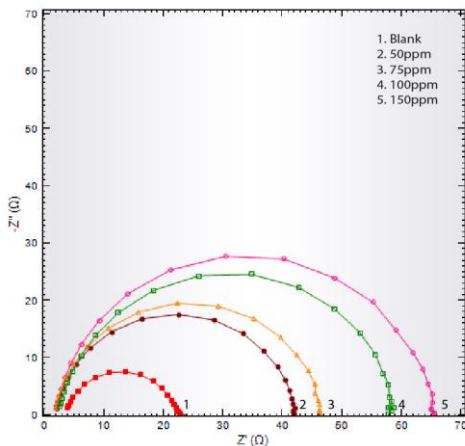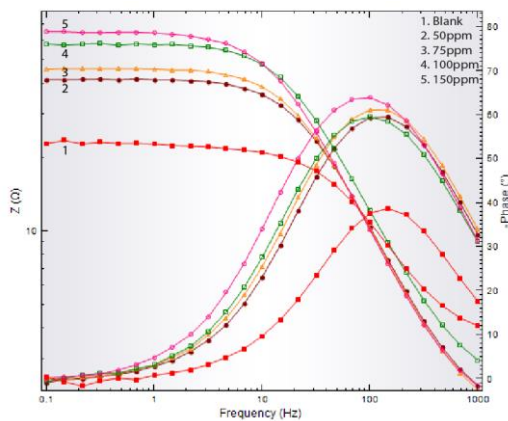**Fig.2.56 Tafel plots of MS in the presence and absence of DHEDTDH in 0.5M H₂SO₄**
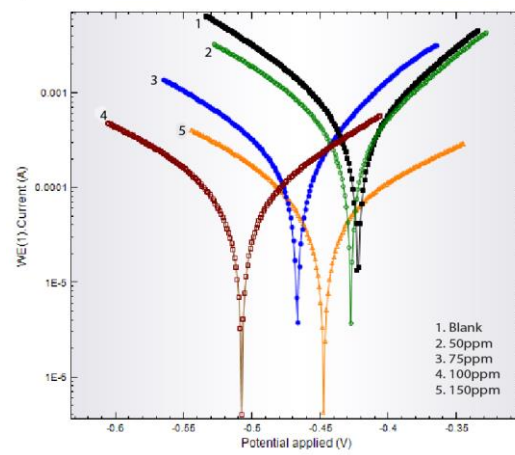
Fig.2.57 Tafel plots of MS in the presence and absence of HEDTDH in 0.5M H₂SO₄
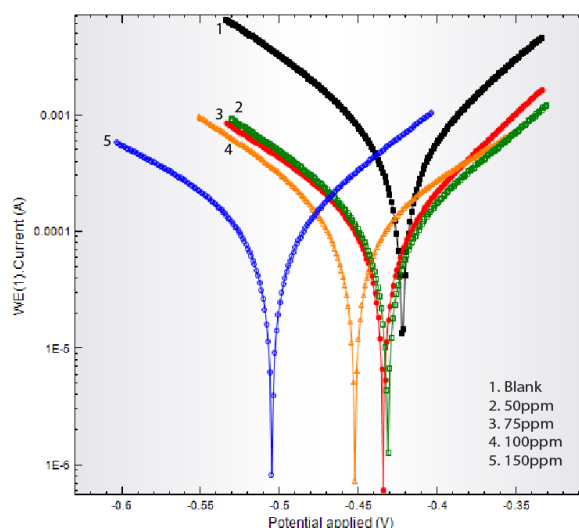
Fig. 2.58 Tafel plots of MS in the presence and absence of TMEDTDH in 0.5M H₂SO₄

Even though the inhibitors DHEDTDH, HEDTDH and TMEDTDH showed extremely poor inhibitive capacity after 24hours as per weight loss measurements, their corrosion inhibition power according to the polarization measurements were much greater than that. The presence of three different hetero atoms, the aromatic rings and the azomethine linkage present in the molecule would result in the enhanced the corrosion inhibition behavior of these Schiff base inhibitors. On close examination of the Tafel slopes, it is evident that these compounds showed much variation in cathodic and anodic Tafel slopes which suggest that they could affect the anodic and cathodic sites of corrosion. The Corrosion potential E_{corr} value also didn't show much variation during the measurements of TEDTDH, NEDTDH and DHEDTDH and hence be called as mixed corrosion inhibitors. The E_{corr} values of HEDTDH and TMEDTDH changed cathodically to a great extent and can be called as cathodic inhibitors. The corrosion inhibition efficiency of the Schiff base indicators followed the order TEDTDH > NEDTDH > DHEDTDH > HEDTDH >

TMEDTDH which is same as the result of EIS measurements. A comparison chart of inhibition efficiencies are presented in Figure 2.59.

Table 2.13 Potentiodynamic polarization parameters in the presence and absence of Schiff base inhibitors in 0.5M H₂SO₄

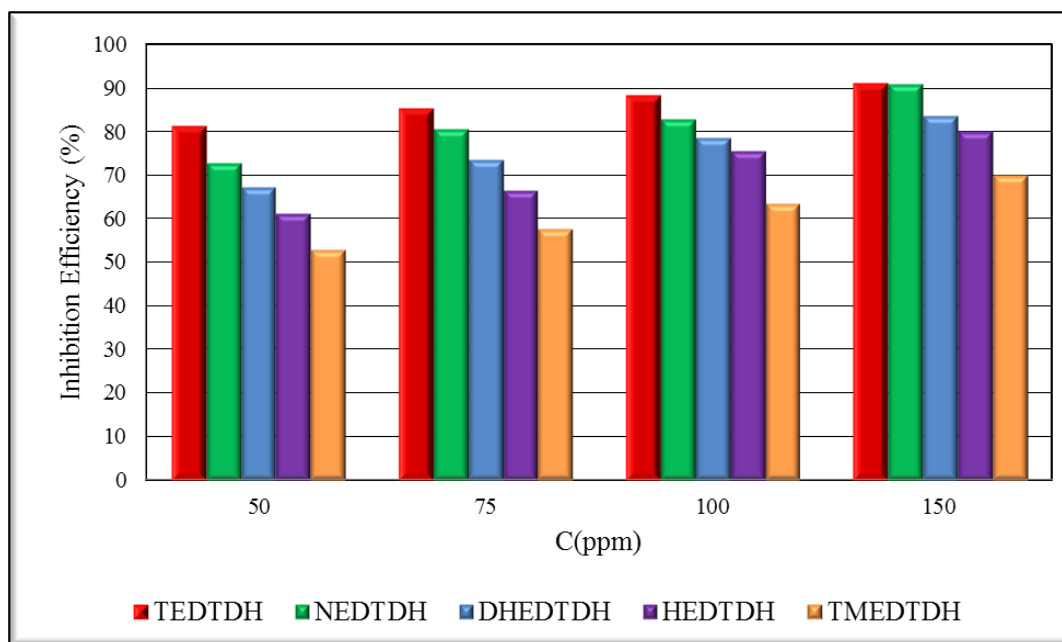| Inhibitor	Concentration	b_a (mV/dec)	b_c (mV/dec)	E_{corr} (V)	j_{corr} (A/cm²)	θ	$\eta_{pol}\%$
	blank	98	124	-0.428	559.8		
TEDTDH	50ppm	75	88	-0.432	113.54	0.7972	79.72
	75ppm	69	78	-0.426	76.595	0.8632	86.32
	100ppm	42	49	-0.448	45.527	0.9187	91.87
	150ppm	36	45	-0.440	33.743	0.9397	93.97
NEDTDH	50ppm	80	59	-0.472	125.81	0.7753	77.53
	75ppm	70	98	-0.452	97.137	0.8265	82.65
	100ppm	41	59	-0.431	50.291	0.9102	91.02
	150ppm	63	72	-0.475	45.911	.918	91.8
DHEDTDH	50ppm	104	102	-0.403	242.73	0.5664	56.64
	75ppm	98	101	-0.45	153.41	0.726	72.6
	100ppm	83	60	-0.472	130.18	0.7675	76.75
	150ppm	81	72	-0.447	58.626	0.8953	89.53
HEDTDH	50ppm	66	92	-0.429	259.32	0.5368	53.68
	75ppm	52	90	-0.465	98.555	0.8239	82.39
	100ppm	89	95	-0.507	69.83	0.8753	87.53
	150ppm	76	107	-0.448	64.052	0.8856	88.56
TMEDTDH	50ppm	105	109	-0.431	130.59	0.7667	76.67
	75ppm	101	92	-0.434	117.87	0.7894	78.94
	100ppm	70	98	-0.452	97.165	0.8264	82.64
	150ppm	61	72	-0.505	74.83	0.8663	86.63
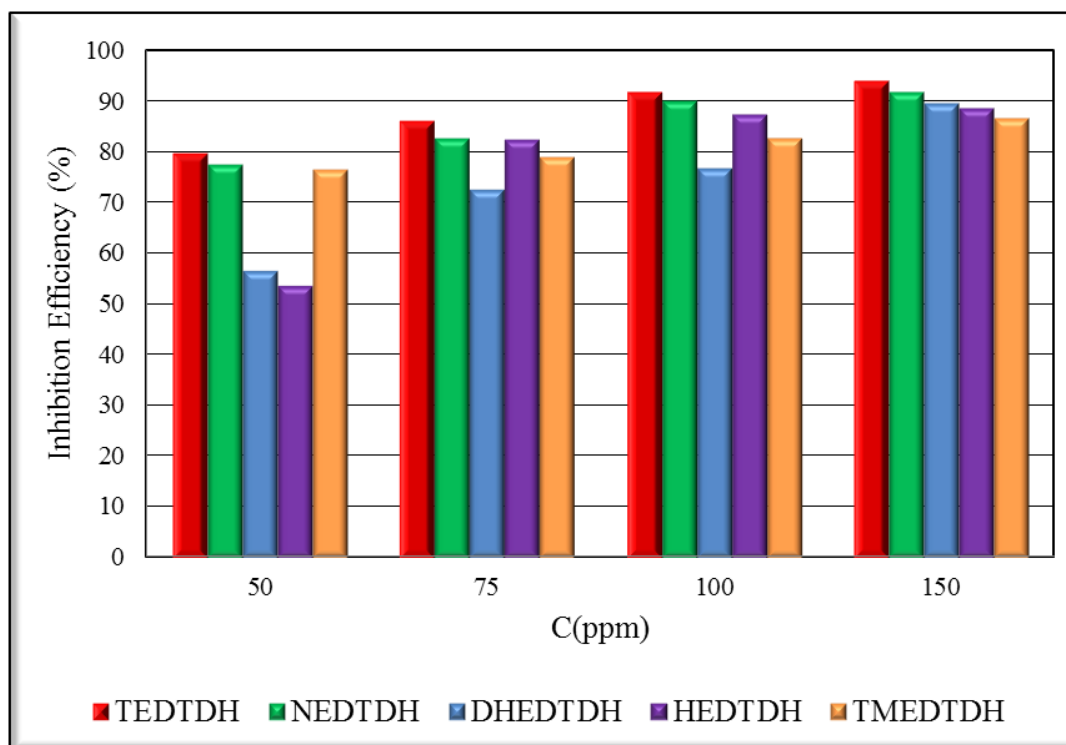
Fig. 2.59 Comparison of corrosion inhibition efficiencies ($\eta_{pol}\%$) of Schiff bases TEDTDH, NEDTDH, DHEDTDH, HEDTDH, and TMEDTDH on MS in 0.5M H_2SO_4

CONCLUSION

The corrosion inhibition efficiencies of newly synthesized Schiff base inhibitors namely 1,14-di(thiophen-2-yl) 5,10-di(thiophen-2-yl)-6,9diazotetradeca 1,5,9,13-tetraene -3,12-dione 4,11-diphenyl-hydrazone [TEDTDH], 1,14-di(2-hydroxy phenyl) 5,10-di(ethylene- 2- hydroxy phenyl)-6,9diazotetradeca 1,5,9,13-tetraene -3,12-dione 4,11-diphenyl-hydrazone [HEDTDH], 1,14-di(2,4-dihydroxy phenyl) 5,10-di(ethylene- 2,4-dihydroxy phenyl)-6,9diazotetradeca 1,5,9,13-tetraene -3,12-dione 4,11-diphenyl-hydrazone [DHEDTDH], 1,14-di(naphthyl) 5,10-di(ethylene-naphthyl)-6,9diazotetradeca 1,5,9,13-tetraene -3,12-dione 4,11-diphenyl-hydrazone [NEDTDH] and 1,14-di(3,4,5-trimethoxy phenyl) 5,10-di(ethylene- 3,4,5-trimethoxy phenyl)-6,9diazotetradeca 1,5,9,13-tetraene -3,12-dione 4,11-diphenyl-hydrazone [TMEDTDH]against MS specimens in 1.0M HCl and 0.5M H_2SO_4 solutions were investigated using conventional weight loss method and electrochemical methods such as electrochemical impedance spectroscopy (EIS) and potentiodynamic polarization methods. It was found that all the Schiff base inhibitors exhibited very good anticorrosive property on mild steel in HCl medium. The inhibitors exhibited poor corrosion inhibition efficiency in H_2SO_4 medium than in HCl medium. Adsorption studies and surface morphological analysis were performed to establish the mode of adsorption of these inhibitors on metal surface. The weight loss studies conducted in HCl medium, ascertained that the inhibition efficiencies increased with the inhibitor concentrations for all the Schiff base compounds. At a maximum concentration of 150ppm, all the studied inhibitors presented 71-89% inhibition efficiencies in the weight loss method. At the electrochemical studies, they performed very potential anticorrosive activity (92-95%) towards MS at 150ppm concentration. The compound TEDTDH exhibited

the highest inhibition capacity against mild steel (95%). By virtue of the electron density on the aromatic rings, the azomethine linkage and highly polarizable sulphur atom, nitrogen atoms and oxygen atoms the molecule exhibited better inhibition efficiency. Adsorption studies revealed that Freundlich isotherm was the best fit isotherm for TEDTDH and DHEDTDH molecules whereas Langmuir isotherm was followed by NEDTDH, HEDTDH and TMEDTDH in 1.0M HCl medium. The thermodynamic parameters obtained suggested that adsorption process was spontaneous and the interaction between the metal and inhibitor molecules involves both the electrostatic and chemisorption. The effect of increased number of electron donating centers in the inhibitory action was proved when the parent compounds of the Schiff base inhibitors were analyzed for their anticorrosive activity. The activities were higher for the Schiff base compounds than their parent compounds.

The electrochemical studies for corrosion on MS in HCl medium were carried out and the order of inhibition capacity of the studied Schiff bases was the same as that got from gravimetric studies, TEDTDH > DHEDTDH > NEDTDH > HEDTDH > TMEDTDH. Potentiodynamic polarization studies performed suggested that all studied inhibitors acted as a mixed type inhibitors in 1.0M HCl except NEDTDH. In general it is observed that the inhibition efficiencies of these Schiff base inhibitors are quite higher in electrochemical studies than those obtained from weight loss studies

In 0.5M sulphuric acid medium, the gravimetric studies furnished another order of corrosion inhibition efficiency for the Schiff base inhibitors, i.e. TEDTDH > NEDTDH >DHEDTDH > HEDTDH > TMEDTDH. A maximum of 76.898% was obtained by TEDTDH at 150ppm concentration. The inhibition efficiencies of all

the compounds were less significant than that in HCl medium, which can be justified by the aggressive nature of the sulphuric acid. Weight loss measurements of Schiff base inhibitors and their corresponding parent compounds in both acidic mediums were performed and compared. Langmuir isotherm was the best fit one for TEDTDH and Freundlich isotherm was the best fit for others. The ΔG^0_{ads} values for all the Schiff base molecules suggested that the adsorption is spontaneous and involved both physisorption and chemisorption.

Electrochemical impedance spectral and potentiodynamic analyses in 0.5M H_2SO_4 medium gave higher corrosion inhibition efficiencies compared to the results obtained from gravimetric studies. Inhibition efficiency greater than 90% was displayed by TEDTDH in both studies. TEDTDH, NEDTDH and DHEDTDH, exhibited much variation in cathodic and anodic slopes which propose that these Schiff base molecules could affect the anodic and cathodic sites on metal surface and can be called as mixed corrosion inhibitors. HEDTDH and TMEDTDH showed pronounced variations in the corrosion potential cathodically and can be called as cathodic inhibitors. These newly synthesized Schiff bases can be used as potent corrosion inhibitors against mild steel corrosion.

CHAPTER III

ANTITUMOUR STUDIES OF SCHIFF BASES DERIVED FROM ARYL AZO DERIVATIVES OF 1,7-DIARYLHEPTA-1,6-DIENE-3,5-DIONES AND THEIR TRANSITION METAL CHELATES WITH CU(II), Zn(II) & Ni(II)

SECTION I

Antitumour studies of Schiff bases derived from aryl azo derivative of 1,7-bis(thiophen-2-yl)-hepta-1,6-diene-3,5-dione and 1,7-bis(3-methyl thiophen-2-yl)- hepta-1,6-diene-3,5-dione with ethylene diamine and their transition metal complexes

This section describes the cytotoxic and antitumour activities of 1,14-di(thiophen-2-yl) 5,10-di(ethylene- thiophen-2-yl)-6,9diazotetradeca 1,5,9,13-tetraene -3,12-dione 4,11-diphenyl-hydrazone [TEDTDH] (1a); 1,14-di(3- methyl-thiophen-2-yl) 5,10-di(ethylene- 3-methyl-thiophen-2-yl)-6,9diazotetradeca 1,5,9,13-tetraene - 3,12-dione 4,11-diphenyl-hydrazone [MTEDTDH] (1b) and their metal chelates Cu(II), Zn(II) & Ni(II) . Invitro cytotoxic activity of the above Schiff bases and their metal complexes against DLA and EAC cell lines were well studied. The invivo antitumour activity of the compounds was assessed by using DLA cell line induced solid tumour and EAC cell line induced ascites tumour model in mice and its comparison with a standard antitumour drug cyclophosphamide.

Invitrocytotoxic activity:

Short term cytotoxic activity of Schiff base compounds TEDTDH (1a); MTEDTDH (1b) and their metal chelates Cu(II), Zn(II) & Ni(II) were analysed by estimating the percentage viability of DLA and EAC cells using Trypan blue dye exclusion method .

Invitro Cytotoxic studies of Schiff base TEDTDH (1a) and their metal complexes [Cu(II),Zn(II) & Ni(II)] towards EAC cells

The Schiff base TEDTDH (1a) and their metal chelates were used for in vitro cytotoxicity study towards EAC cells. All the test compounds were prepared in various concentrations ranging from 10μg/ml to 200μg/ml. The cytotoxicity of the

compounds was determined in terms of percentage cell death produced by them. The analysed results are given in Table 3.1 and represented diagrammatically in Fig.3.1

Table 3.1 Invitro Cytotoxic studies of Schiff base TEDTDH (L1) and their metal complexes towards EAC

Drug Con.	%Cell Death			
µg/ml	L_1	$Cu(L_1)$	$Zn(L_1)$	$Ni(L_1)$
10	6	33	29	23
20	9	49	42	36
50	15	66	57	52
100	29	81	74	67
200	41	93	83	76
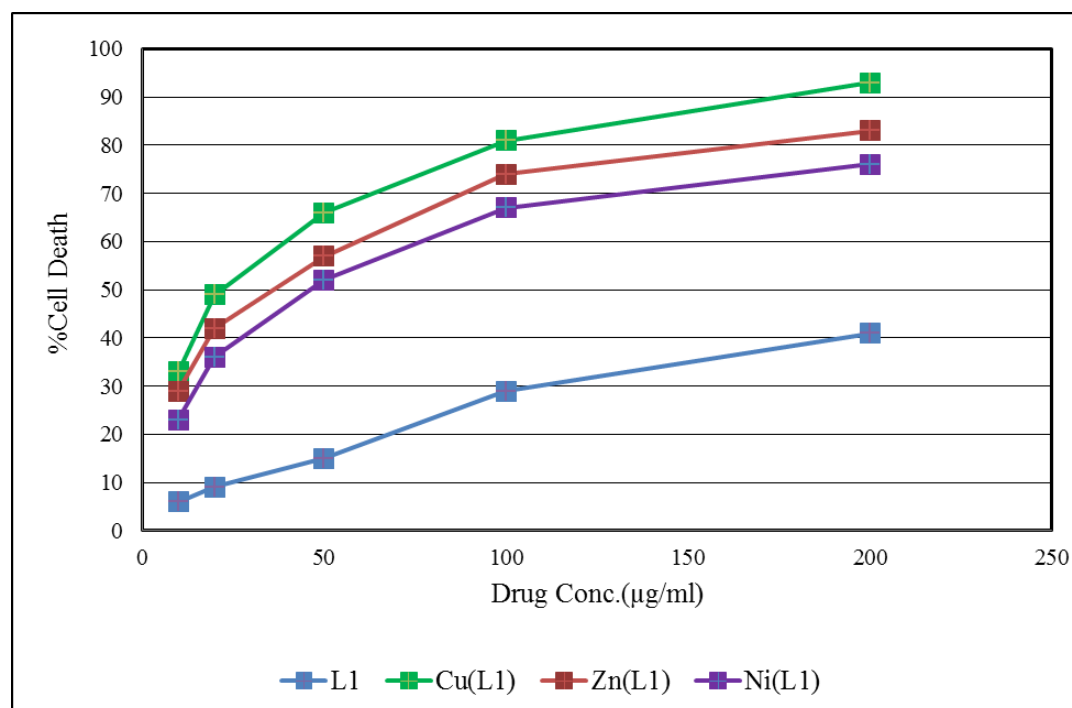
Fig. 3.1 Invitro Cytotoxic studies of Schiff base TEDTDH (L1) and their metal complexes towards EAC

The Schiff base 1a gave 41% cell death towards the EAC cells at a concentration of 200μg/ml. At lower concentrations the activity of the compound was insignificant. All the metal complexes exhibited greater percentage of cell death. They were quite effective even at lower concentrations. As concentration of the drug increased the percentage of cell death also increased. All the metal complexes showed significant cytotoxic activity. The percentage cell death produced by Cu(II),Zn(II) and Ni(II) complexes at 200μg/ml are 93, 83, & 76 % respectively. The Cu(II) complex of Schiff base 2a was very effective by producing a cell death of 93% suggesting its potent cytotoxic nature. The Zn(II) and Ni(II) complexes showed similar cytotoxicity approximately 80% which was twice that of the ligand. The Ni(II)complexes exhibited minimum activity among the complexes, but even then it produced 76% cell death. The results indicated that metal complexation enhances cytotoxicity of Schiff bases to a great extent.

Invitro Cytotoxic studies of Schiff base TEDTDH (1a) and their metal complexes [Cu(II), Zn(II) & Ni(II)] towards DLA cells

The percentage cell death was also calculated with DLA cell lines. The results of the study in terms of percentage cell death is shown in Table 3.2 and represented graphically in Fig. 3.2.

Table.3.2 Invitro Cytotoxic studies of Schiff base TEDTDH (L1) and their metal complexes towards DLA cells

Drug Con. µg/ml	%Cell Death			
	L_1	$Cu(L_1)$	$Zn(L_1)$	$Ni(L_1)$
10	4	32	28	20
20	9	46	41	34
50	14	60	56	46
100	25	76	71	62
200	39	90	81	74

Fig.3.2 Invitro Cytotoxic studies of Schiff base TEDTDH (L1) and their metal complexes towards DLA cells

The results obtained from the cytotoxic analysis indicated that the activity of compound 1a and its metal complexes against DLA cells followed a similar manner as that with EAC cells. The Schiff base as well as their metal complexes exhibited a slight decrease in activity when compared with their activities towards EAC cells. But all the three metal complexes showed improved activity when compared to the Schiff base. The Schiff base 1a produced 39% cell death where as its Cu(II) complex produced 90% cell death. The cytotoxicity of metal complexes followed the order Cu(II)>Zn(II)>Ni(II) and the percentage cell death produced by them were 90,81 and 74 respectively. The values revealed that all the metal complexes possess significant cytotoxic nature.

Invitro Cytotoxic studies of Schiff base MTEDTDH (1b) and their metal complexes [Cu(II),Zn(II)&Ni(II)] towards EAC cells

The invitro cytotoxic analysis were done using Schiff base MTEDTDH (1b) and its metal complexes towards EAC cell lines. The observations are shown in Table 3.3 and diagrammatically in Fig. 3.3. The Schiff base 1b which has a methyl group on the thiophenyl ring in addition on comparison with ligand 1a and exhibited smaller percentage of cell death of EAC cells. All the metal complexes exhibited better cytotoxic activity than ligands. But a comparison of the metal complexes of 1a, with the metal complexes of 1b showed that complexes of 1b exhibited lesser percentage of cell death. The percentage cell death produced by Cu(II) complex of 1b was 81% and was not as much active as Cu(II) complex of 1a. Comparing the Schiff bases and metal complexes, the complexes were twice more active than the Schiff bases.

Table 3.3 Invitro Cytotoxic studies of Schiff base MTEDTDH (L2) and their metal complexes towards EAC

Drug Con.	%Cell Death			
μg/ml	L2	Cu(L2)	Zn(L2)	Ni(L2)
10	4	22	17	12
20	7	37	34	26
50	11	54	47	38
100	26	69	64	53
200	38	81	74	66
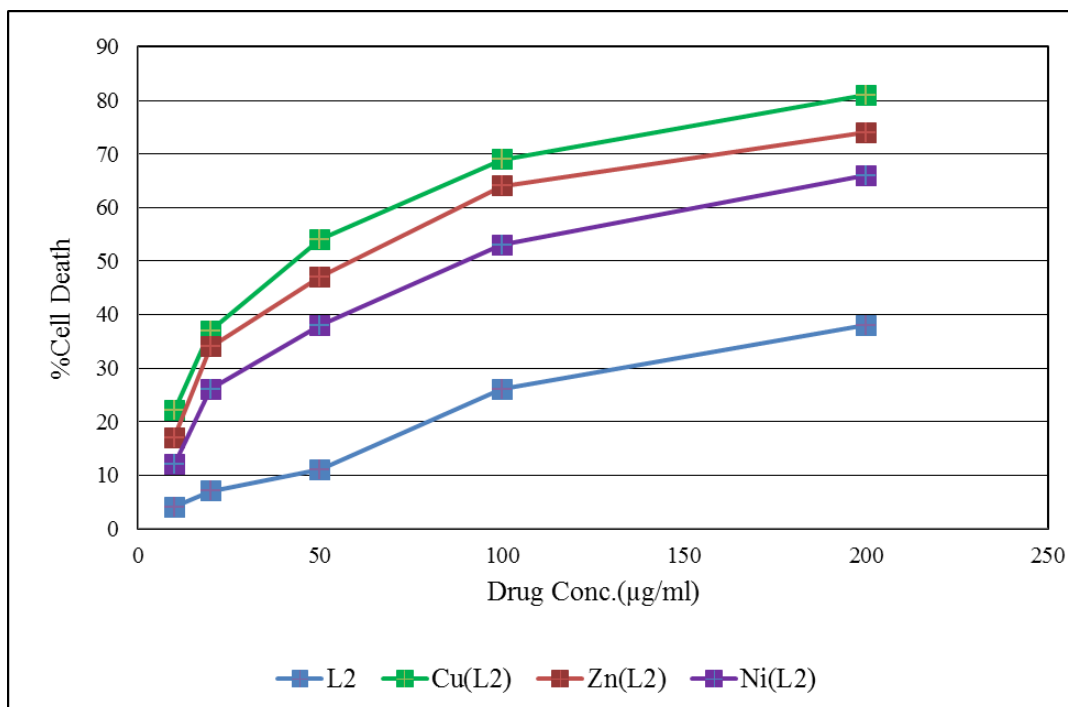
Fig. 3.3 Invitro Cytotoxic studies of Schiff base MTEDTDH (L2) and their metal complexes towards EAC

Invitro Cytotoxic studies of Schiff base MTEDTDH (L2) and their metal complexes towards DLA

The values obtained from the study are given in Table 3.4 and displayed graphically in Fig. 3.4. In the activity against DLA cells the Schiff base 1b and its metal complexes were not as efficient as ligand 1a and its metal complexes. The

results showed that minute activity was found with 10µg/ml. Also it was found that the ligand and complexes at its higher concentrations showed maximum activity towards EAC cells than DLA. Even though all the experimented metals were divalent, better results were observed for complexes formed by Cu(II).

Table 3.4 Invitro Cytotoxic studies of Schiff base MTEDTDH (L2) and their metal complexes towards EAC

Drug Con.	%Cell Death			
µg/ml	L2	Cu(L2)	Zn(L2)	Ni(L2)
10	5	17	15	8
20	7	33	28	22
50	13	40	45	34
100	22	65	58	51
200	36	77	71	62

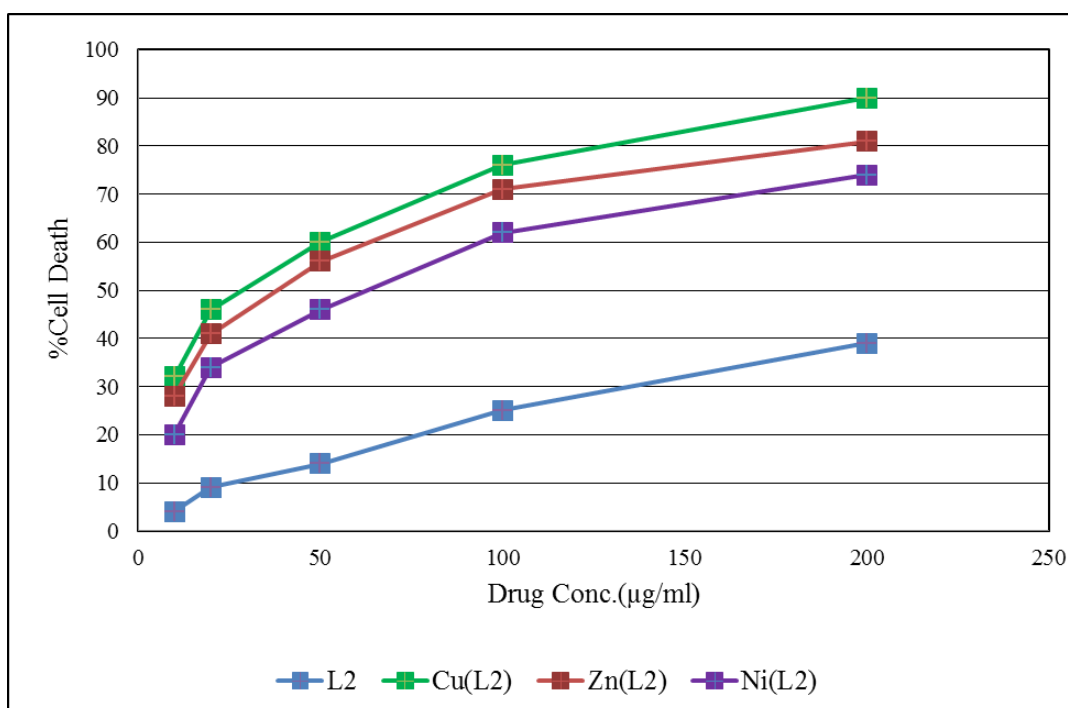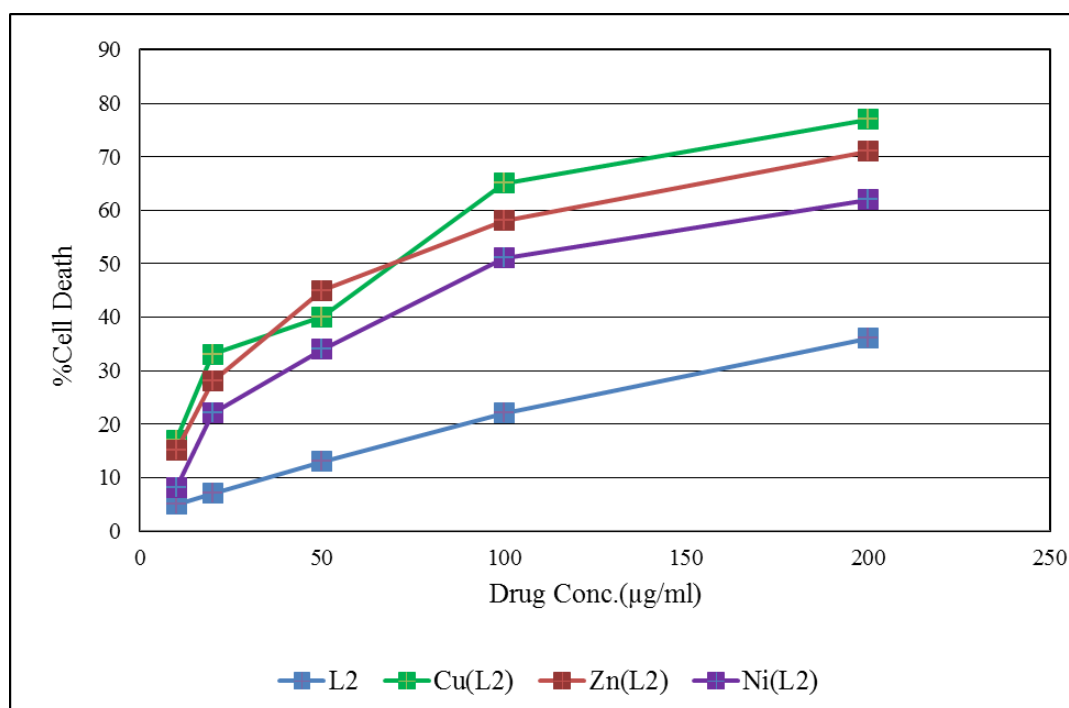**Fig. 3.4 Invitro Cytotoxic studies of Schiff base MTEDTDH (L2) and their metal complexes towards EAC**

Fair results of cytotoxic activity were observed with Schiff base MTEDTDH (1b) and their metal complexes towards percentage cell death of DLA cells. Except copper complex all other metal chelates showed almost similar results, but the values were double the values obtained for Schiff base ligand.

Conclusion

A comparative study of the metal complexes of the Schiff base ligands TEDTDH (1a); MTEDTDH (1b) showed that ligand 1a and its metal complexes gives better results than that of 1b towards both EAC & DLA cell lines. So, out of the two thiophenyl Schiff base ligands, 1a, the unsubstituted thiophene Schiff base and its complexes were more active than methyl group substituted ligand in the invitro studies performed.

Invivo antitumour studies of Schiff bases 1a, 1b and their Cu(II) metal complexes

The effect of Schiff base ligands TEDTDH (1a); MTEDTDH (1b)and their Cu(II) complexes on the life span of animals bearing ascites tumour were studied. Swiss Albino mice (male animals only,6-8 weeks old) weighing 25-30g were divided into 14 groups of 5 animals each. Viable EAC cells in 0.1ml of PBS were injected into the peritoneal cavity of the animals in the 14 groups. Group1 kept as Control group: Oral administration of 0.1 ml of distilled water only/group of animals without drug treatment. Group 2 kept as Standard group: Cyclophosphamide was administered 25mg/kg body weight. Group 3-5: Schiff base, TEDTDH (1a) with concentrations 20μg/ml, 10μg/ml and 5μg/ml was given as drug. Group 6-8 Cu(II) complex of 1a as drug with concentrations 20μg/ml, 10μg/ml & 5μg/ml was administered. Group 9-11: Schiff base, MTEDTDH (1b) with concentrations

20μg/ml, 10μg/ml and 5μg/ml was given as drug. Group 12-14: Cu(II) complex of ligand 1b as drug with concentrations 20μg/ml, 10μg/ml & 5μg/ml was given.

Effect of Schiff base ligand TEDTDH (1a) and the Cu(II) complex on ascites tumour

The test compounds were injected intraperitoneally and their impact in reducing ascites tumour development in mice was assessed. The number of days survived by the control group animals, the animals given standard drug and the animals treated with test compounds and their percentage increase in life span was found and the results are shown in Table 3.5 .

Table 3.5 Effect of Schiff base TEDTDH (L1) and their metal complexes on ascites tumour reduction

Animal groups	Conc. μg/ml	No. of Animals with tumour	No. of days survived	% ILS
Control		5/5	17.3±1.20	
Std. Drug		5/5	31.6±0.245	82.66
L_1	20	5/5	27.7 ±1.3	60.12
L_1	10	5/5	27.1 ±2.3	56.65
L_1	5	5/5	25.6 ±3.2	47.98
$Cu(L_1)$	20	5/5	31.3 ±1.04	80.92
$Cu(L_1)$	10	5/5	31.1 ±1.16	79.77
$Cu(L_1)$	5	5/5	29.4 ±1.27	69.94

The treatment with test compounds namely Schiff base ligand TEDTDH (L1) and its Cu(II) complex at various concentrations like 5, 10, 20μg/ml increased the average life span of tumour bearing mice. The number of days survived by control group was 17.3±1.2 whereas for standard drug cyclophosphamide it was 31.6±0.245. At concentrations 5, 10 and 20μg/ml, the Schiff base 1a increased the

survival rate of animals by 25.6±3.2, 27.1±2.3, 27.7 ± 1.3 days respectively. The Schiff base ligand produced 60% ILS at higher concentration of 20μg/ml. But the Cu(II) complex produced a notable change in life span of 69%,79% and 80% at 5,10, 20μg/ml concentrations respectively. The Cu(II) complex has appreciably increased the life span of ascites tumour bearing animals. The % ILS obtained for Cu(II) complex is comparable with the results obtained for standard drug.
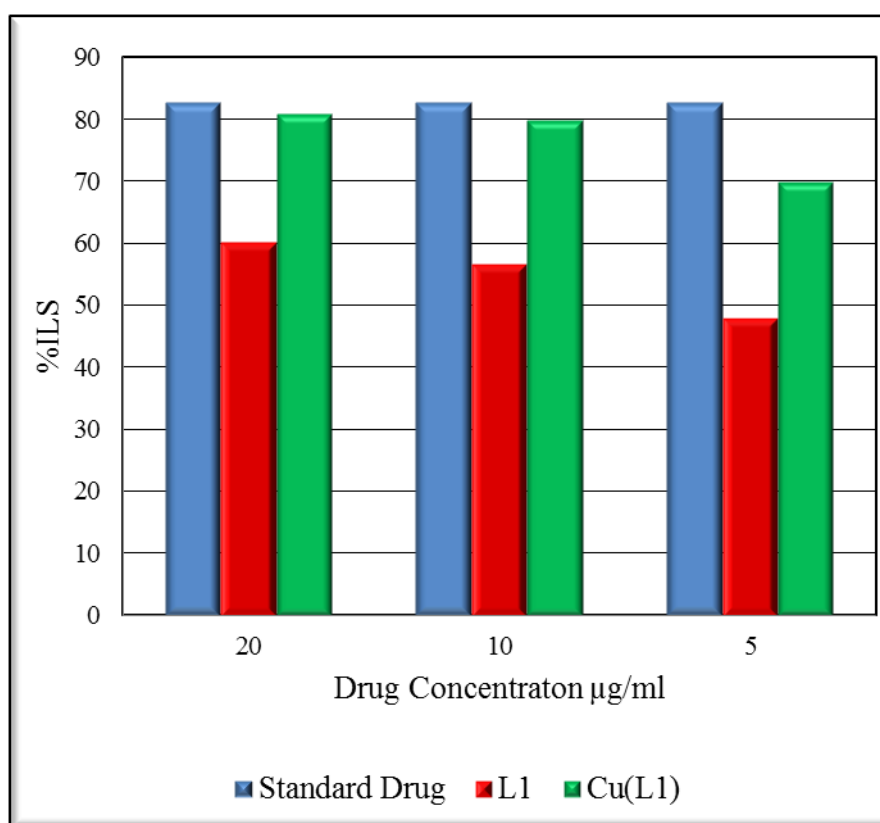
Fig. 3.5 Effect of Schiff base TEDTDH (L1) and their metal complexes on ascites tumour reduction

Effect of Schiff base MTEDTDH (1b) and the Cu(II) complex on ascites tumour

All the test compounds were injected intraperitoneally to the mice and their effect in reducing ascites tumour development in mice was studied. The number of days survived by the control group animals, the animals given standard drug and the

animals treated with test compounds was noted and their percentage increase in life span was found and the values obtained are presented in Table 3.6 and comparison diagram in Fig.3.6

Table 3.6 Effect of Schiff base MTEDTDH (L2) and its Cu(II) complex on ascites tumour reduction

Animal groups	Conc. µg/ml	No. of Animals with tumour	No. of days survived	% ILS
Control		5/5	17.3±1.20	
Std. Drug		5/5	31.6±0.245	82.66
L_2	20	5/5	26.0 ±2.7	50.29
L_2	10	5/5	25.4 ±3.2	46.82
L_2	5	5/5	22.0 ±2.01	27.17
$Cu(L_2)$	20	5/5	30.1 ±1.13	73.99
$Cu(L_2)$	10	5/5	29.8 ±1.16	72.25
$Cu(L_2)$	5	5/5	28.1 ±1.77	62.43

The mice with only EAC induced tumour survived for a period of 17.3±1.20 days. The application of standard drug cyclophosphamide increased the life span to 31.6±0.245days. The %ILS produced by the ligand at 5, 10, 20 µg/ml are 27,46 and 50% respectively but for Cu(II) complex at the same concentrations the %ILS are 62, 72, 73% respectively. All the test compounds exhibited enhanced activity at higher concentrations. Whereas the Cu(II) complex was quite active even at lower concentration. The activity of the copper complex was comparable with the standard drug.
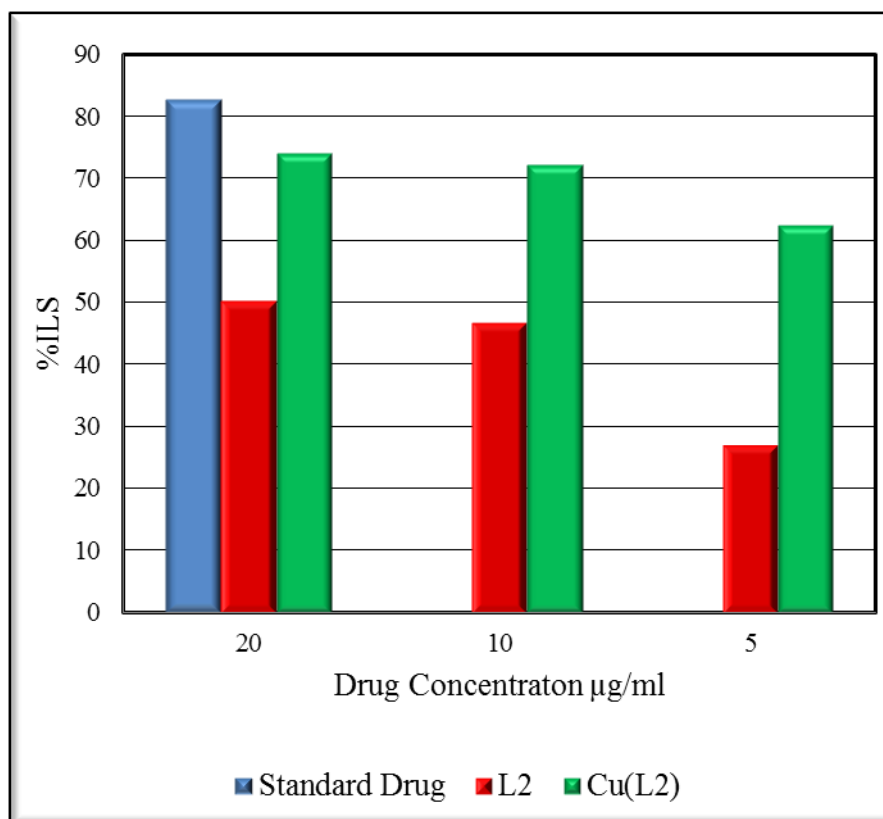
Fig. 3.6 Effect of Schiff base MTEDTDH (L2) and its Cu(II) complex on ascites tumour reduction

Comparing the ligands 1a and 1b and their Cu(II) complexes, the Schiff base ligand MTEDTDH (L2)and its copper complex was not as efficient as 1a and its complex in increasing the life span of the animals. The Cu(II) complex of the Schiff base ligand TEDTDH (L1) was found to be the most active compound in the invivo cytotoxic studies and was very effective in increasing the life span of EAC induced tumour bearing mice.

Invivo cytotoxic study on solid tumour development

Effect of compounds on solid tumour development

The DLA cell lines were injected subcutaneously on the right hind limb of Swiss albino mice to induce solid tumour. The animals were divided into six groups.

Group 1:control group (induced DLA cells, without any drug), Group 2:injected reference drug cyclophosphamide 10mg/kg body weight+ DLA cells, Group 3:schiff base, 1a + DLA cells, Group 4:Cu(II) complex of 1a+ DLA cells, Group 5:schiff base 1b+ DLA cells, Group 6:Cu(II) complex of 1b+ DLA cells. The ligands 1a and 1b and their copper complexes were tested as antitumour drugs, to find their effect on solid tumour growth in mice. The test compounds (200μmol/Kg body weight) were injected for 10 consecutive days after 24hrs of tumour inoculation. The diameter of the tumour developed was measured by vernier calipers every third day for one month and tumour volume was determined. The results are presented Table 3.7 and figured in 3.7

Table 3.7   Effect of Compounds on solid tumour

Compounds	Tumour volume on the 31st day
Control group	4.842 cm^3
1a (L$_1$)	2.03 cm^3
1b (L$_2$)	2.63 cm^3
Cu (L$_1$)	1.95 cm^3
Cu (L$_2$)	2.05 cm^3
Standard group	1.863 cm^3
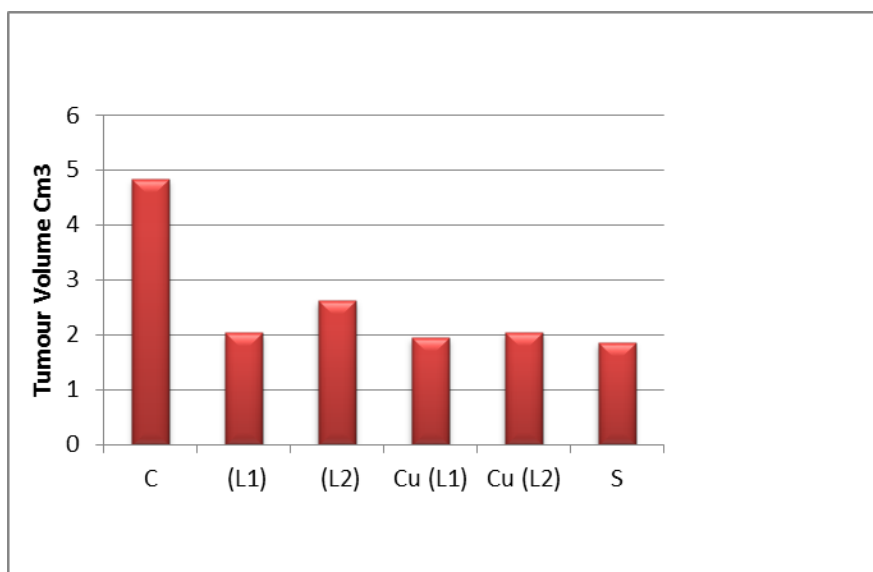
Fig. 3.7 Effect of Compounds on solid tumour

All the ligands and complexes exhibited a considerable reduction of solid tumour volume in mice. In comparison with ligands, relevant Cu(II) chelates were more active in producing   reduction in solid tumour volume. The calculated tumour volume was 4.842 cm^3 for the control group on the 31^{rst} day. The tumour volume of the standard drug treated mice showed a reduction of 1.863 cm^3.The Schiff bases 1a and 1b treated groups notably decreased the tumour volume to 2.03cm^3 and 2.63cm^3 respectively. Comparing with that of the tumour volume of control group, the Schiff bases produced a decrease in tumour volume of 2.812 cm^3 and 2.212 cm^3 respectively. Considering the Schiff bases, 1a was more active than 1b in lessening the tumour volume. The tumour volumes measured on day thirty-one for copper complexes of 1a and 1b were 1.95cm^3 and 2.05 cm^3 respectively. The reduction in tumour volume was 2.892 cm^3 and 2.792 cm^3 respectively with respect to control group. The decrease in tumour volume for standard drug was 2.979 cm^3. The Cu(II) complex of TEDTDH (L1) had shown a prominent effect in reducing tumour volume.

SECTION II

Antitumour studies of Schiff bases derived from aryl azo derivative of 1,7-bis(2-methyl phenyl)-hepta-1,6diene-3,5-dione and 1,7-bis(2-hydroxy phenyl)-hepta-1,6-diene-3,5-dione with ethylene diamine and their transition metal complexes

This section reports the antitumour activities of Schiff bases of mono substituted 1,7-diaryl heptanoids namely 1,14-di(2-methyl phenyl) 5,10-di(ethylene- 2- methyl phenyl)-6,9diazotetradeca 1,5,9,13-tetraene -3,12-dione 4,11-diphenyl-hydrazone [MEDTDH] (2a) ; 1,14-di(2-hydroxy phenyl) 5,10-di(ethylene- 2- hydroxy phenyl)-6,9diazotetradeca 1,5,9,13-tetraene -3,12-dione 4,11-diphenyl-hydrazone [HEDTDH] (2b)and their metal complexes [Cu(II),Zn(II) &Ni(II)]. The cytotoxicity of both ligands and their transition metal chelates were examined by different methods. The different methods adopted were as follows.

1) Invitro cytotoxicity study of the Schiff bases against EAC cells by Trypan blue exclusion method

2) Invitro cytotoxicity study of the Schiff bases against DLA cells by Trypan blue exclusion method

3) Determination of ascites tumour reducing activity in mice (In vivo cytotoxicity study)

4) Determination of the effect of Schiff bases on solid tumour development

Invitro Cytotoxic studies of Schiff base MEDTDH (2a) and its metal complexes [Cu(II),Zn(II)&Ni(II)]

Cytotoxic studies were done using Schiff base MEDTDH (2a) and its metal complexes against tumour bearing cells DLA & EAC using Trypan blue exclusion method. The Schiff base and its metal chelates were dissolved in minimum quantity of solvent DMSO. The test compounds were taken in different concentrations ranging from 10-200 µg/ml and the solutions were diluted with PBS. The cell suspension (0.1 ml stock solution which contains nearly 1 million cells) was added to the tubes containing different concentration of the test compounds. These assay mixtures were incubated for 3 hours at 37^{0}C.Then the mixtures were mixed with 0.1ml of 1% Trypan blue dye and kept for 5 minutes and loaded on a haemocytometer. The dead cells take up the blue colour of Trypan blue while the live cells do not take up the blue dye. The stained and unstained cells were counted and percentage cell death was found. The results of cytotoxic studies are given in Table 3.8

Table 3.8 Invitro Cytotoxic studies of Schiff base MEDTDH (L1) and their metal complexes towards EAC cells

Drug Con.	%Cell Death			
µg/ml	L1	Cu(L1)	Zn(L1)	Ni(L1)
10	3	9	13	6
20	9	14	10	11
50	13	28	19	21
100	20	47	31	32
200	25	64	45	49
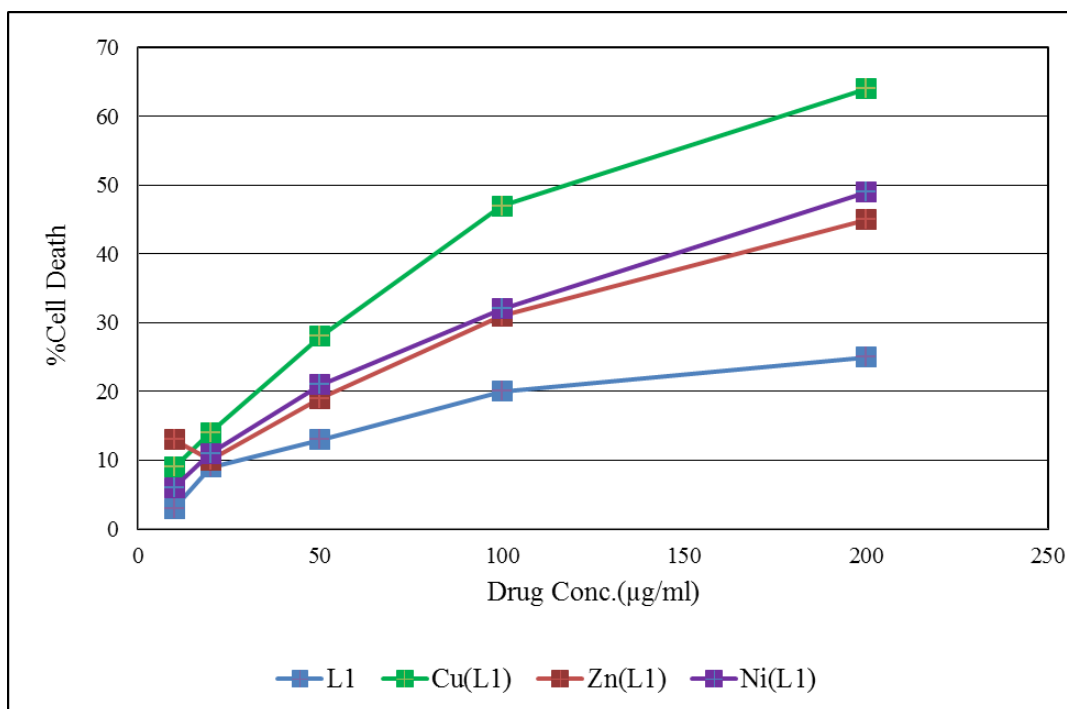
Fig. 3.8 Invitro Cytotoxic studies of Schiff base MEDTDH (L1) and their metal complexes towards EAC cells

On comparing the cytotoxicity activity of ligand (2a) and its metal complexes, it is observed that all metal complexes are more cytotoxic than the ligand. Among the studied metal complexes, Cu(II) complexes showed enhanced cytotoxicity towards EAC cells. All the test compounds exhibited maximum activity at higher concentration of 200 μg/ml. The results showed that the percentage cell death produced increased with the increase in concentration of the Schiff base compound. For a known concentration 200 μg /ml, the % cytotoxicity of ligand and Cu(II),Zn(II) & Ni(II) complexes were 25, 64, 45 and 49% respectively. The Zn and Ni complexes showed comparable cytotoxic effect against EAC cells. The metal complexes followed the order Cu(II)> Ni(II)>Zn(II) for the cytotoxic nature.

The results of invitro cytotoxic studies of 1a and their metal complexes towards DLA are presented in Table.3.9. & Fig.3.9.

Table 3.9 Invitro Cytotoxic studies of Schiff base MEDTDH (L1) and their metal complexes towards DLA

Drug Con.	%Cell Death			
µg/ml	L_1	$Cu(L_1)$	$Zn(L_1)$	$Ni(L_1)$
10	3	10	7	8
20	11	16	13	14
50	19	30	21	26
100	24	51	33	36
200	32	71	48	51
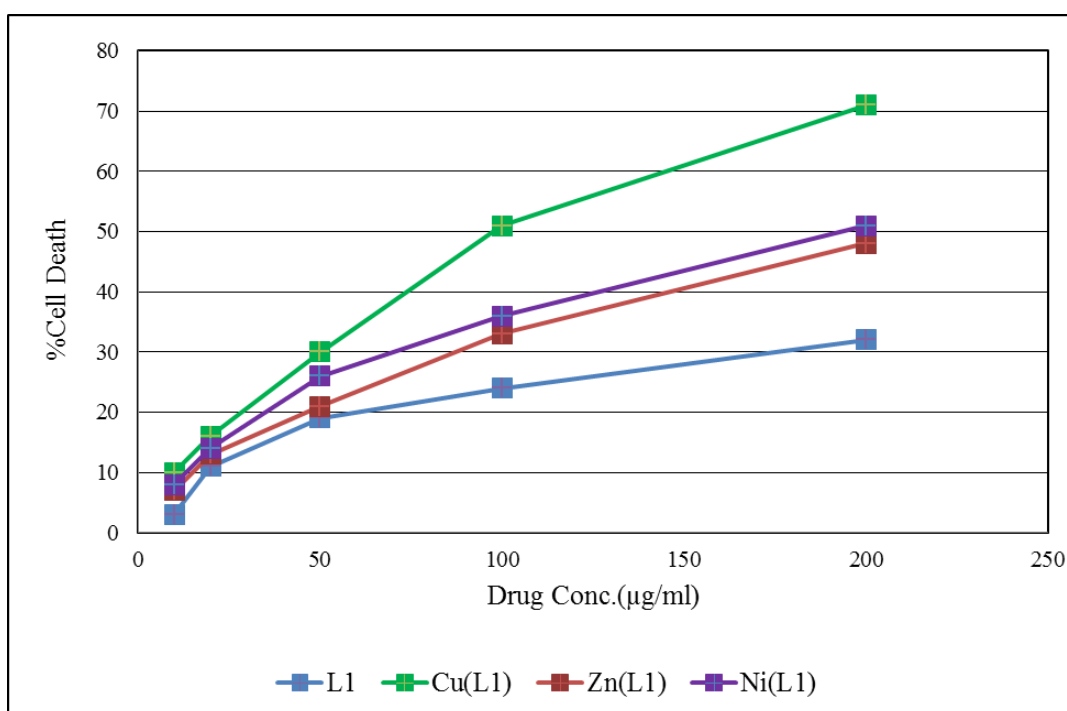
Fig. 3.9 Invitro Cytotoxic studies of Schiff base MEDTDH (L1) and and their metal complexes towards DLA

It is evident from the results in Table 3.9 that ligand (2a) showed better cytotoxicity towards DLA cells compared to EAC cells lines. The ligand showed 32% cytotoxicity against DLA cells at a concentration of 200µg/ml whereas the percentage cytotoxicity towards EAC cells was 25% at that highest concentration. The metal complexes of the ligand also showed an equivalent increase in

percentage cell death similar to the ligand. In this case also metal complexation had increased the cell death. Cu(II) complex exhibited a maximum activity of 71% cell death and its activity was nearly more than twice that of the ligand. Ni(II) complex stood second in activity and Zn(II) complex showed lowest activity. At lower concentration the percentage cell death produced by ligand and complexes was very low.

Invitro Cytotoxic studies of Schiff base HEDTDH (2b) and their metal complexes [Cu(II), Zn(II) & Ni(II)]

Invitro Cytotoxic studies of Schiff base HEDTDH (2b) and their metal complexes were performed using Trypan blue exclusion method against EAC and DLA cells as explained in chapter 1.The results obtained are given in Table 3.10 and Fig. 3.10.

Table 3.10 Invitro Cytotoxic studies of Schiff base HEDTDH (L2) and their metal complexes towards EAC cell lines

Drug Con.	%Cell Death			
μg/ml	L2	Cu(L2)	Zn(L2)	Ni(L2)
10	3	16	5	6
20	5	36	6	7
50	6	48	9	14
100	11	67	21	22
200	21	81	35	39

The hydroxyl group substituted ligand (2b) exhibited cytotoxic activity lower than the ligand (2a) with one methyl group on the phenyl ring. The Cu(II) complex of ligand 2b showed 81% cell death at a concentration 200 μg/ml. The cytotoxic

activity of the Cu(II) complex was about four times greater than that of the ligand. The complex was rather effective in producing cell death. The Zn(II) and Ni(II) complexes showed comparable activities and their cytotoxic behaviour was greater than ligand.
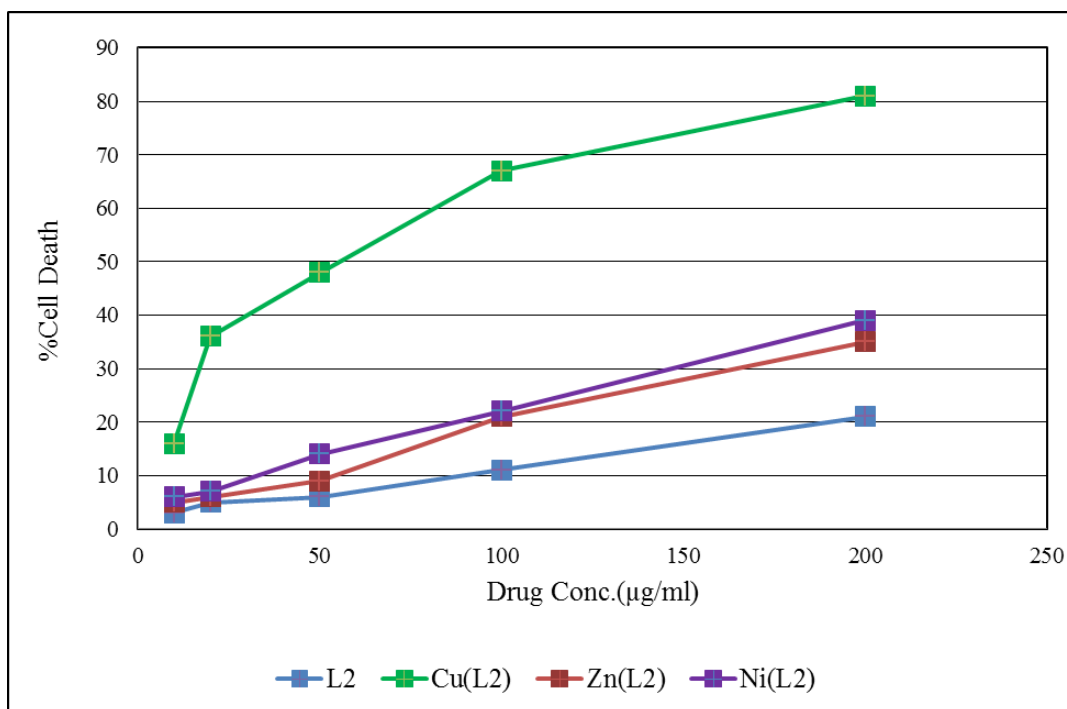
Fig.3.10 Invitro Cytotoxic studies of Schiff base HEDTDH (L2) and their metal complexes towards EAC

Table 3.11 Invitro Cytotoxic studies of Schiff base HEDTDH (L2) and their metal complexes towards DLA

Drug Con.	%Cell Death			
μg/ml	L2	Cu(L2)	Zn(L2)	Ni(L2)
10	3	14	5	6
20	6	33	7	9
50	7	46	14	13
100	11	65	16	19
200	19	79	32	37
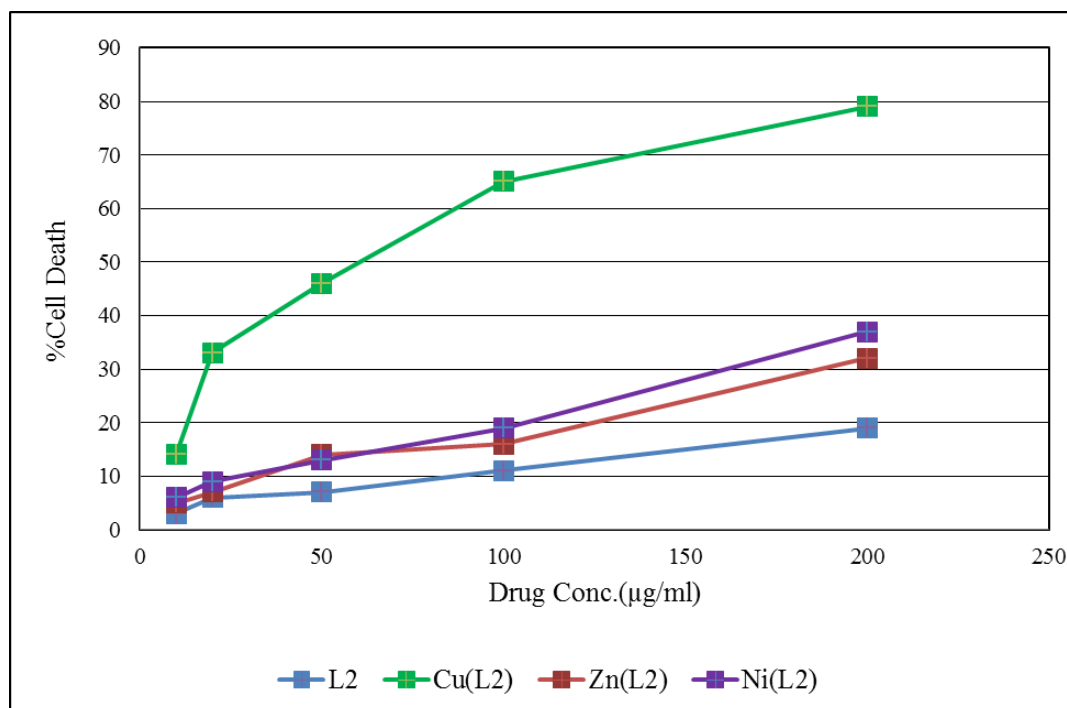
Fig.3.11 Invitro Cytotoxic studies of Schiff base HEDTDH (L2)and their metal complexes towards DLA

The ligand (2b) was not that much effective against DLA cells. The percentage cell death was only 19% for the ligand but for its Cu(II) complex it was found to be 79%. It is evident that the metal copper has an inevitable part in cytotoxicity. All the metal complexes were more efficient in showing cytotoxic activity than the ligands. The Ni(II) complexes showed 37% cytotoxicity which was almost twice that of ligand. The Zn(II) complex showed lowest activity among the complexes.

Invivo antitumour studies of Schiff base HEDTDH and their Cu(II) and Ni(II) metal complexes

The invivo antitumour studies were carried out in Swiss Albino mice with the ligand schiff base HEDTDH (2b) and its Cu(II) & Ni(II) complexes. The Cu(II) &

Ni(II) metal complexes of 2b were found to be effective against DLA and EAC cells in invitro studies performed. So they were chosen for this specific study and the results are shown in Table 3.12. The three compounds were administered to tumour bearing mice quintets (11 groups, each with 5 animals) as drug. The Schiff base and its metal complexes were injected intraperitoneally to the mice and their effectiveness in reducing ascites tumour development in mice were investigated. The numbers of days survived by the control group, the group that given standard drug and the group of animals treated with test compounds noted and calculated their percentage increase in life span. The results are presented in the table below.

Table 3.12 Effect of Schiff base HEDTDH (L2) and their metal complexes on ascites tumour reduction

Animal groups	Conc. µg/ml	No. of Animals with tumour	No. of days survived	% ILS
Control		5/5	17.3±1.20	
Std. Drug		5/5	31.6±0.245	82.66
L2	20	5/5	21.1 ±1.83	21.97
L2	10	5/5	19.8 ±1.85	14.45
L2	5	5/5	18.7 ±2.16	8.09
Cu(L2)	20	5/5	29.5 ±1.08	70.52
Cu(L2)	10	5/5	26.6 ±1.82	53.76
Cu(L2)	5	5/5	22.3 ±1.68	28.9
Ni(L2)	20	5/5	23.6 ±0.62	36.42
Ni(L2)	10	5/5	21.7 ±1.46	25.43
Ni(L2)	5	5/5	20.1 ±1.6	16.18
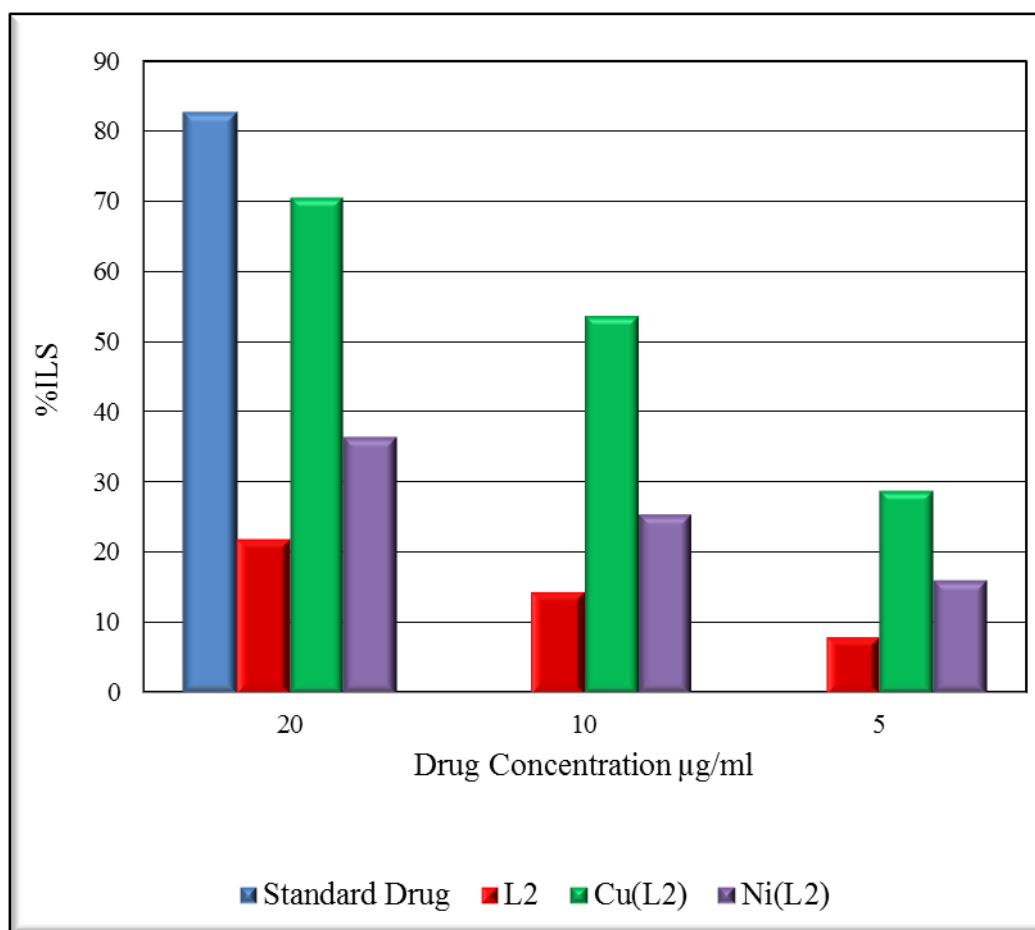
Fig. 3.12 Effect of Schiff base HEDTDH (L2) and their metal complexes on ascites tumour reduction

The Schiff base HEDTDH (L2) and their metal complexes Cu(II) & Ni(II) were given as drug in different concentrations ranging from 5 μg/ml to 20μg/ml. The number of days survived by control group animals was 17.3±1.2 whereas for standard drug cyclophosphamide injected group it was 31.6±0.245. There happened an increase in life span percentage (% ILS) of 82.66% for the animals injected with the standard drug. The Schiff base produced only 21.97% ILS at a concentration of 20μg/ml. But the Cu(II) complex produced an increase in life span of 70.52% at the same concentration 20μg/ml which was nearly four times that of Schiff base. This is comparable with the percentage increase in life span produced

by the standard drug. The animals treated with Ni(II) complex survived for 23.6 days and produced a % ILS of 36.42 at the higher concentration. On comparing the Schiff base, Cu(II) and Ni(II) complexes it was observed that Cu(II) Schiff base complex was most effective drug in increasing the life span of tumour bearing mice.

Invivo cytotoxic study on solid tumour development

Effect of Schiff base MEDTDH (2a); Schiff base HEDTDH (2b) and their
Cu(II) complexes on solid tumour development

The effects of Schiff base ligands 2a, 2b and their copper complexes on solid tumour development in Swiss Albino mice were investigated. Solid tumour was induced in sets of mice by subcutaneous injection of DLA cell lines on the right hind limb of the mice. One group of mice was kept as control, one group was given the standard drug and other groups were gradually injected with the test compounds (200μmol/Kg body weight) for 10 days. Tumour diameter was measured with vernier calipers every third day for one month and tumour volume was determined. The results of the study are presented in the Table 3.13 and represented graphically in Fig. 3.13

Table 3.13 Effect of Compounds on solid tumour

Compounds	Tumour volume on the 31st day
Control group	4.842 cm^3
2a (L$_1$)	3.08 cm^3
2b (L$_2$)	3.68 cm^3
Cu (L$_1$)	2.65 cm^3
Cu (L$_2$)	2.05 cm^3
Standard drug	1.863 cm^3
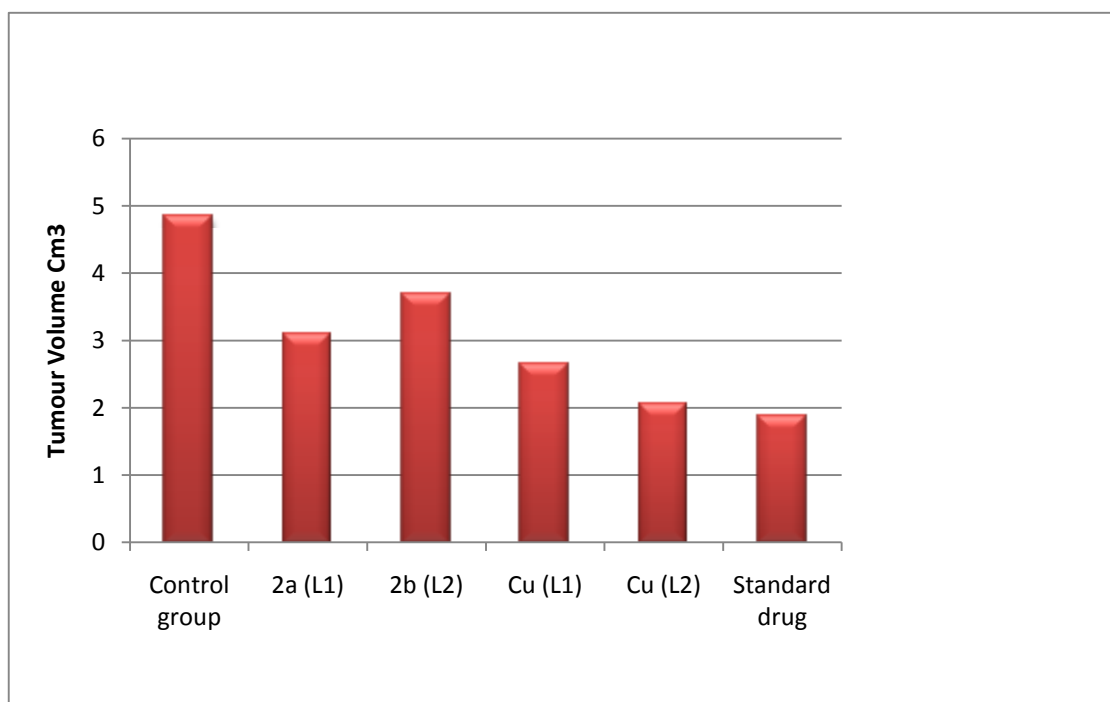
Fig. 3.13 Effect of Compounds on solid tumour

The Schiff bases and their copper complexes made a significant lessening of solid tumour volume in mice. Compared to Schiff bases, their Cu(II) chelates were more efficient in bringing about reduction in solid tumour volume. The calculated tumour volume was 4.842 cm^3 for the control group on the 31^{rst} day and it were 3.08 cm^3 and 3.68 cm^3 for 2a and 2b respectively. Comparing with the tumour volume of the control group, the ligands produced a decrease in tumour volume of 1.762 cm^3 and 1.162 cm^3 respectively. Among the Schiff bases, 2a was more effective in decreasing the tumour volume than 2b. The tumour volume on 31^{rst} day for copper complexes of 2a and 2b were 2.65 cm^3 and 2.05 cm^3 respectively. The decrease in tumour volume for the copper complexes of 2a and 2b was 2.192 cm^3 and 2.792 cm^3 respectively with respect to control group. The copper complex of Schiff base (2b) exhibited a marked effect in reducing tumour volume.

SECTION-III

Antitumour studies of Schiff bases derived from aryl azo derivative of 1,7-bis(3-ethoxy 4-hydroxy phenyl)-hepta-1,6-diene-3,5-dione,1,7-bis(2,4-di hydroxy phenyl)- hepta-1,6-diene-3,5-dione and 1,7-bis(3,4,5-trimethoxy phenyl)- hepta-1,6-diene-3,5-dione with ethylene diamine and their transition metal complexes

Short term cytotoxic study of the Schiff bases 1,14-di(3-ethoxy 4-hydroxy phenyl) 5,10-di(ethylene- 3-ethoxy 4-hydroxy phenyl)-6,9diazotetradeca 1,5,9,13-tetraene -3,12-dione 4,11-diphenyl-hydrazone [EHEDTDH] (3a); 1,14-bis(2,4-dihydroxy phenyl) 5,10-bis(ethylene- 2,4-dihydroxy phenyl)-6,9diazotetradeca 1,5,9,13-tetraene -3,12-dione 4,11-diphenyl-hydrazone [DHEDTDH] (3b); 1,14-di(3,4,5-trimethoxy phenyl) 5,10-di(ethylene- 3,4,5-trimethoxy phenyl)-6,9diazotetradeca 1,5,9,13-tetraene -3,12-dione 4,11-diphenyl-hydrazone [TMEDTDH] (3c) and their Cu, Zn &Ni metal complexes are detailed in this chapter. The activity was examined by determining the percentage viability of DLA and EAC cells using the Trypan blue dye exclusion procedure. The results obtained from the study are given below.

Invitro Cytotoxic studies of Schiff base EHEDTDH (3a) and their metal complexes

Invitro cytotoxic analysis was carried out with Schiff base EHEDTDH (3a) and its different metal complexes. The effect of these compounds against the cell lines of EAC & DLA was found in terms of percentage cell death. The results obtained with EAC cells are described in Table 3.14 and Fig.3.14 and the values obtained with DLA cells are detailed in Table 3.15 and Fig.3.15

Table 3.14 Invitro Cytotoxic studies of Schiff base EHEDTDH (L1) and their metal complexes with EAC cells

Drug Con.	%Cell Death			
µg/ml	L_1	$Cu(L_1)$	$Zn(L_1)$	$Ni(L_1)$
10	1	21	6	2
20	3	42	25	11
50	9	59	41	22
100	13	74	59	32
200	27	83	71	40

Fig.3.14 Invitro Cytotoxic studies of Schiff base EHEDTDH (L1) and their metal complexes with EAC cells

Table 3.15 Invitro Cytotoxic studies of Schiff base EHEDTDH (L1) and their metal complexes with DLA cells

Drug Con.	%Cell Death			
µg/ml	L1	Cu(L1)	Zn(L1)	Ni(L1)
10	3	22	8	3
20	9	46	30	12
50	12	56	43	23
100	20	77	64	32
200	30	87	75	42
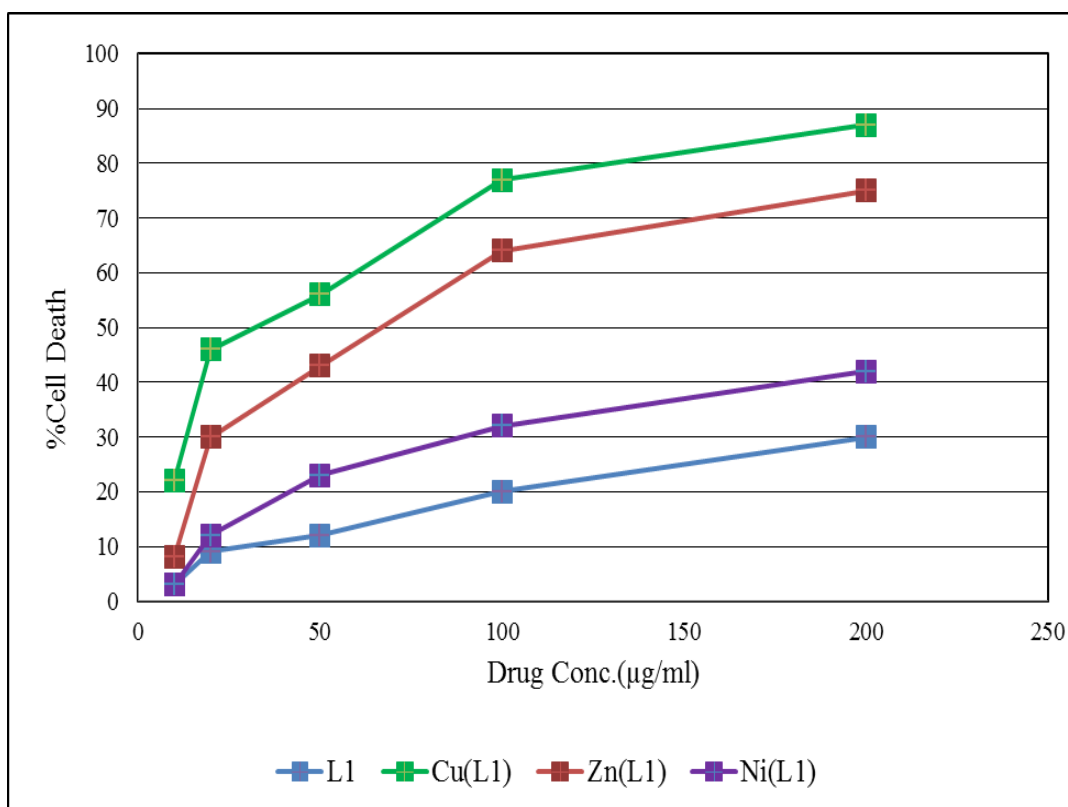
Table 3.15 Invitro Cytotoxic studies of Schiff base EHEDTDH (L1) and their metal complexes with DLA cells

The Schiff base EHEDTDH had shown comparable percentage cell death of EAC and DLA cell lines with 27% and 30 % respectively. The Cu(II) complex of the ligand was found to be significant in their cytotoxic activity with a percentage cell death of 87 % with DLA cells. The cell death occurred was to some extent greater with DLA cells. The Cu(II) complex was almost thrice more active than the ligand. The Zn(II) complex has also produced a percentage cell death in the range 75%.The Ni(II) complex of the Schiff base has offered greater activity than the ligand (42%) but has least activity among the other metal complexes. The cytotoxic behaviour of copper complexes was high. Metal complexation resulted in an enhanced cytotoxic activity of the ligand.

Invitro Cytotoxic studies of Schiff base ligand DHEDTDH (3b) and their metal complexes

Invitro cytotoxic analysis of DHEDTDH (3b) and their metal complexes Cu(II),Zn(II)&Ni(II) were extensively carried out on EAC and DLA cells. All the results obtained are displayed in Table 3.16 & Table 3.17

Table 3.16 Invitro Cytotoxic studies of Schiff base DHEDTDH (L2) and their metal complexes towards EAC

Drug Con.	%Cell Death			
µg/ml	L2	Cu(L2)	Zn(L2)	Ni(L2)
10	0	1	1	1
20	6	11	6	8
50	11	17	9	11
100	16	36	24	19
200	31	53	41	32
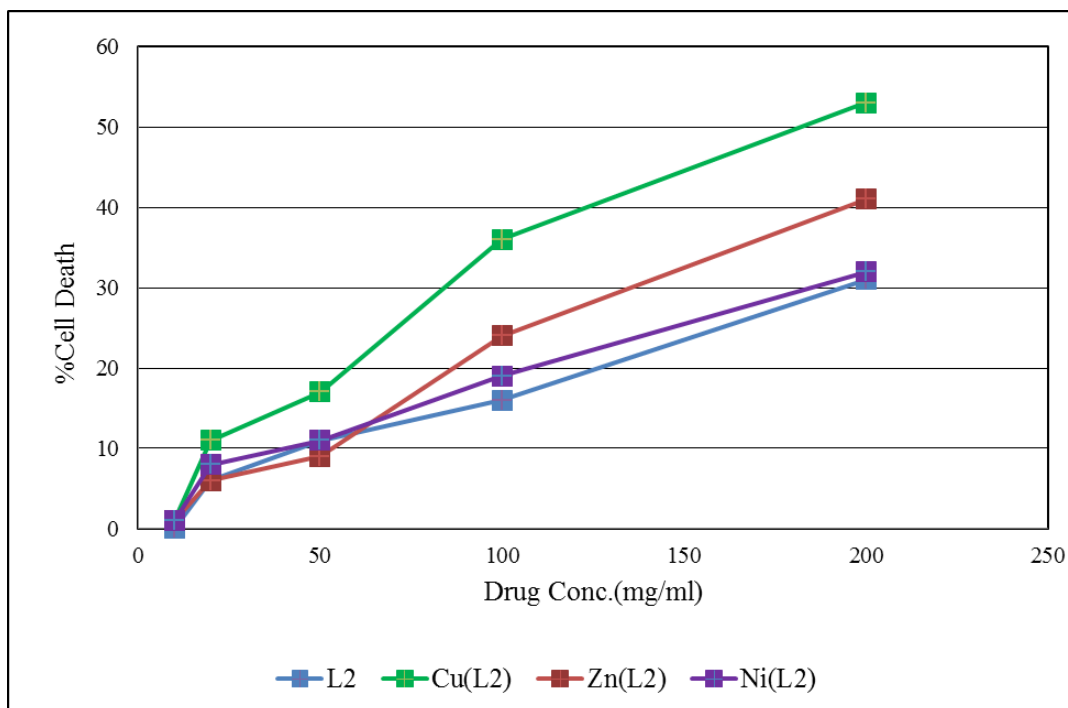
Table 3.16 Invitro Cytotoxic studies of Schiff base DHEDTDH (L2) and their metal complexes towards EAC

Table 3.17 Invitro Cytotoxic studies of Schiff base DHEDTDH (L2) and their metal complexes towards DLA

Drug Con.	%Cell Death			
µg/ml	L2	Cu(L2)	Zn(L2)	Ni(L2)
10	0	0	0	0
20	5	14	10	8
50	11	21	13	11
100	19	39	28	23
200	35	56	45	36
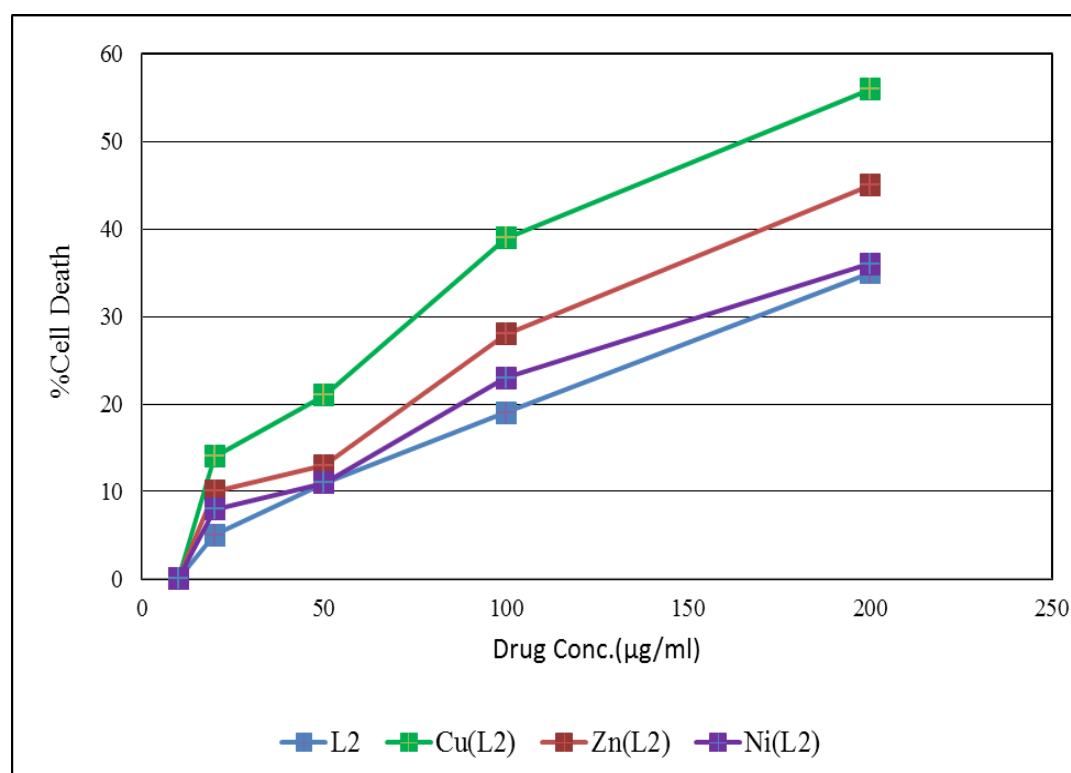
Fig. 3.17 Invitro Cytotoxic studies of Schiff base DHEDTDH (L2) and their metal complexes towards DLA

The Schiff base ligand DHEDTDH (3b) has given a % cell death of 31% at concentration 200 µg/ml. The metal complexation has not increased the activity much. The Cu(II) complex has shown % cell death of 53%. All other metal

complexes have shown very less activity which is less than 50%.The conc. of the metal complexes needed to bring about 50% cell death was 200 µg/ml. The Zn(II) and Ni(II) complexes possess almost comparable activities against cancer cells. The Ni(II) complex had shown almost same activity as that of the ligand. The ligand as well as the metal complexes was not at all active at lower concentrations. Even at a concentration of 50 µg/ml their activity was negligible. The cytotoxic nature has increased only slightly even after metal complexation.

Invitro Cytotoxic studies of Schiff base ligand TMEDTDH (3c) and their metal complexes

In vitro Cytotoxic studies of TMEDTDH (3c) and their metal complexes towards EAC are given in Table 3.18 & Fig.3.18 The cytotoxic activity of the compounds towards DLA cells are given in Table 3.19 & Fig.3.19.

Table 3.18 Invitro Cytotoxic studies of Schiff base TMEDTDH (L3) and their metal complexes towards EAC

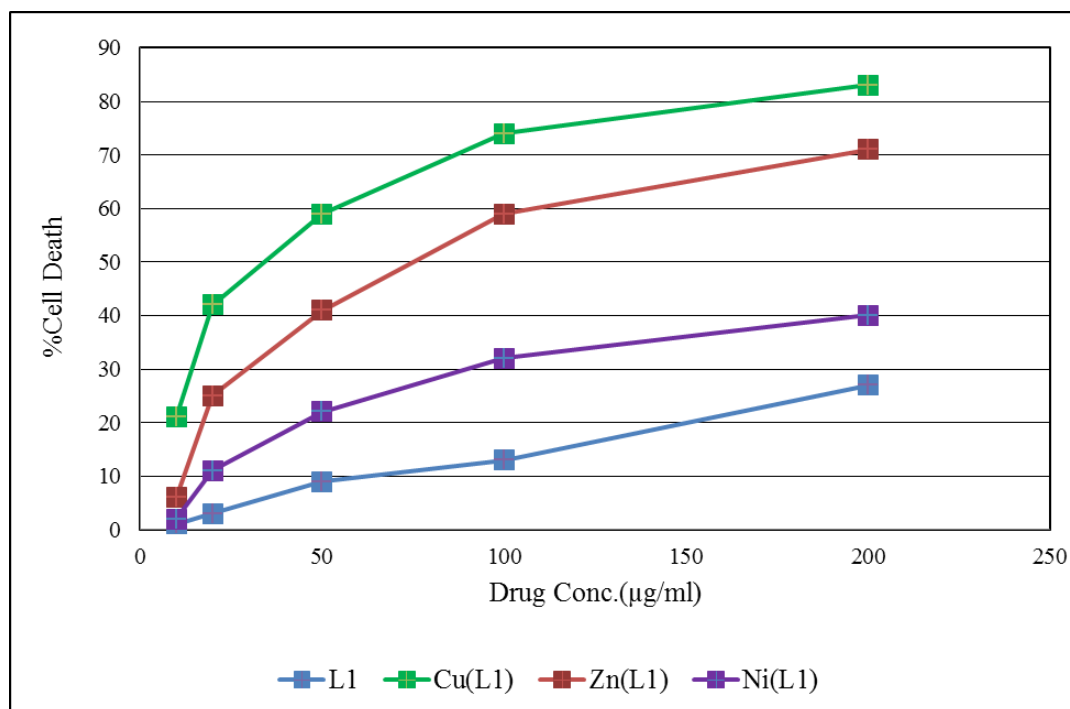| Drug Con.	%Cell Death			
µg/ml	L3	Cu(L3)	Zn(L3)	Ni(L3)
10	10	26	15	12
20	26	47	32	29
50	36	60	44	39
100	58	77	65	62
200	72	92	82	80
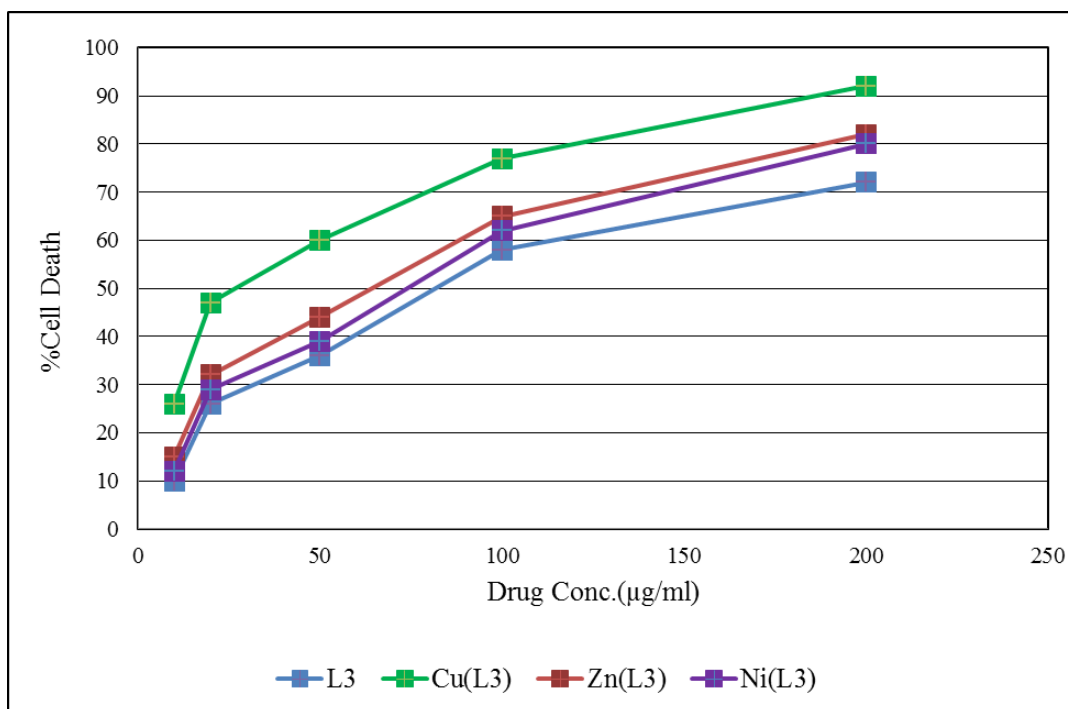
Fig. 3.18 Invitro Cytotoxic studies of Schiff base TMEDTDH (L3) and their metal complexes towards EAC

Table 3.19 Invitro Cytotoxic studies of Schiff base TMEDTDH (L3) and their metal complexes towards DLA

Drug Con. µg/ml	%Cell Death			
	L3	Cu(L3)	Zn(L3)	Ni(L3)
10	12	29	16	15
20	28	50	34	32
50	43	62	50	48
100	61	82	68	67
200	73	93	84	80
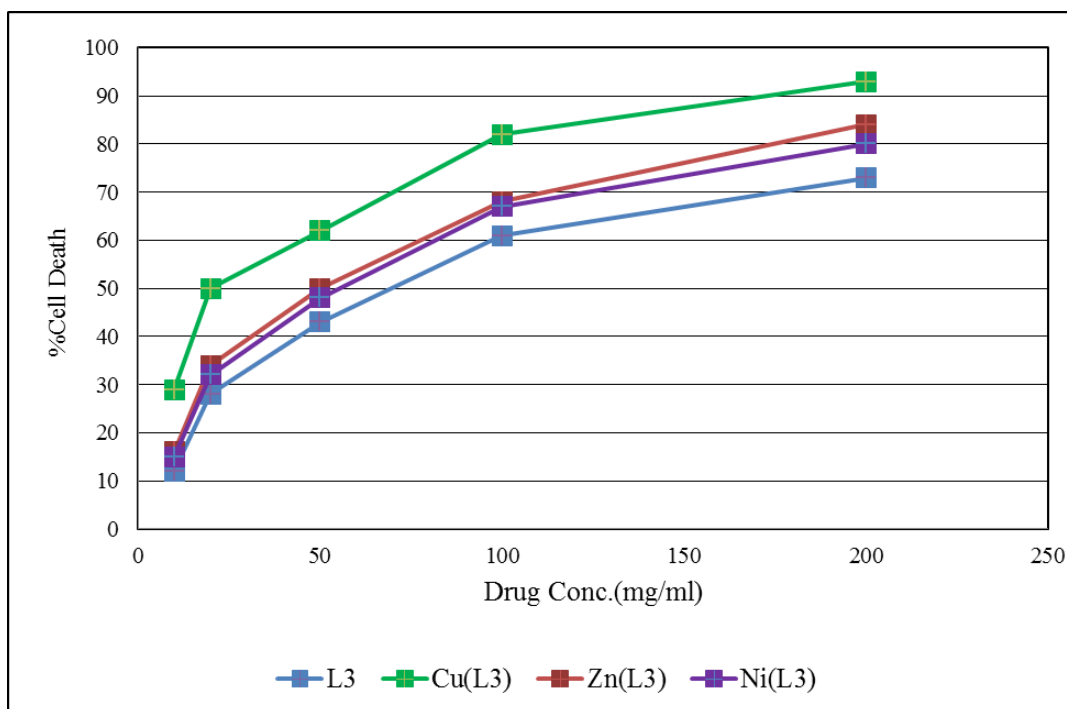
Fig. 3.19 Invitro Cytotoxic studies of Schiff base TMEDTDH (L3) and their metal complexes towards DLA

The data given in tables 3.18 and 3.19 revealed that the Schiff base TMEDTDH (L3) possessed excellent cytotoxic activity against both EAC and DLA cell lines at higher concentrations. All the metal complexes were found to be highly active against cancerous cells. Metal complexation has raised the cytotoxic nature extensively. The metal complexes especially that of Cu and Zinc was quite cytotoxic to both DLA cells and EAC cells. The effect of the studied Schiff bases and metal complexes on both DLA and EAC cells followed the same pattern in results. The complexes exhibited good cytotoxic activity even at smaller concentrations. The cytotoxic activity of the metal complexes was enhanced when compared with the activity of Schiff base ligand. The Cu(II) complex gave almost 93% cell death at higher concentration of 200µg/ml.

Conclusion

In this unit the invitro cytotoxic studies of three Schiff bases 3a, 3b & 3c and their Cu, Zn and Ni complexes have been elaborated. The Schiff bases followed the cytotoxic activity order 3c >3b >3a.The Schiff base with trimethoxy group on phenyl rings was most efficient and the one with hydroxyl functional groups on phenyl ring was moderately effective compared to 3c. The Schiff base with ethoxy and hydroxyl groups substituted phenyl ring reported least activity. On comparing the activities of the metal complexes, the highest activity was seen with the metal Copper. The Cu(II) complex of Schiff base TMEDTDH was revealed as the utmost cytotoxic compound by exhibiting 93% cell death. A comparative pictographic representation of Schiff base and its Cu(II) complex is presented in Fig.3.20
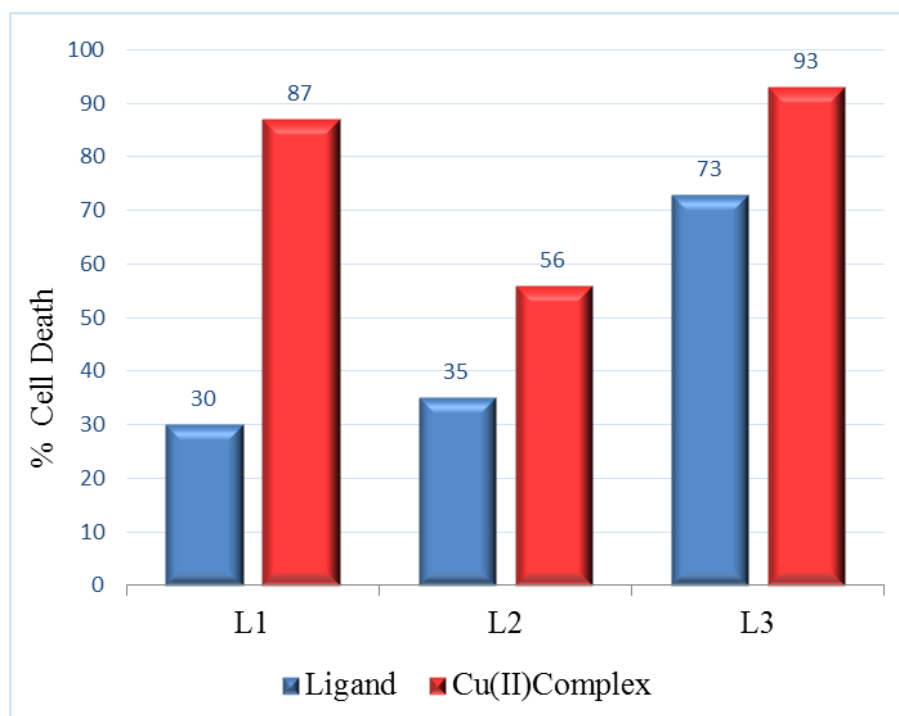
Fig.3.20 Comparative pictographic representation of activity Schiff base and its Cu(II) complex against DLA cells

The invivo antitumour studies of Schiff base EHEDTDH and the Cu(II) complex

Animals (Swiss albino mice) were grouped into 8 units and ascites tumour was induced in them. The Schiff base ligand EHEDTDH and its Cu(II) complex were delivered as drugs to tumour bearing mice in varying concentrations of 20,10 and 5 µg/ml. Anticancer study was performed and the number of days lived by the animals treated with the drugs was observed and the increase in life span of observing animals were found. The denominations of number of days survived are the 'means of five determinations ± ' (SD is the standard deviation).The result obtained from the study are exhibited in Table 3.20

Table 3.20 Effect of Schiff base ligand EHEDTDH (L1) and its Cu(II)complex on ascites tumour reduction

Animal groups	Conc. µg/ml	No. of Animals with tumour	No. of days survived	% ILS
Control		5/5	17.3±1.20	
Std. Drug		5/5	31.6±0.245	82.66
L1	20	5/5	22.0 ±2.4	27.17
L1	10	5/5	20.2 ±1.32	16.76
L1	5	5/5	19.0 ±1.26	9.83
Cu(L1)	20	5/5	25.4±1.19	46.82
Cu(L1)	10	5/5	23.2±0.95	34.1
Cu(L1)	5	5/5	19.8 ±0.86	14.45
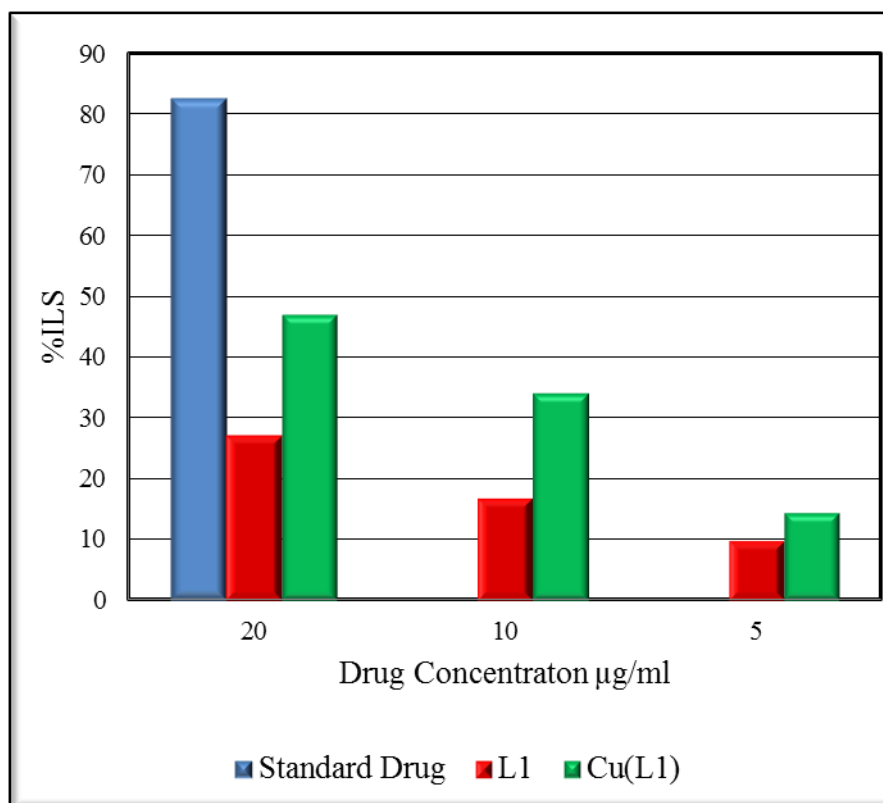
Fig.3.21 Effect of Schiff base ligand EHEDTDH (L1) and its Cu(II)complex on ascites tumour reduction

The percentage increase in life span of the animals carrying ascites tumour was 82% on the treatment with standard drug called cyclophosphamide. Compared with the standard drug the %ILS displayed by the ligand L1 was one third of its value, 27% was exhibited at a concentration of 20µg/ml and that exhibited by its Cu(II) complex was almost nearly half of its value, 46% ILS at concentration 20µg/ml. In case of the copper complex the number of days survived by the animals was 25.4±1.19days. At higher concentrations both the Schiff base and metal complex were more active to a certain extent. The Cu(II) complex was found to be twice more efficient than the ligand in increasing the life span of tumour induced animals.

The invivo antitumour studies of Schiff base TMEDTDH and Cu(II) complex

The compound TMEDTDH (L3) and its Cu(II) complex was given by intraperitoneal injection from the first day of tumour induction as drug to mice groups. The death pattern of animals due to tumour burden was noted and the percentage increase in life span was found. The results were discussed in Table 3.21

Table 3.21 Effect of Schiff base TMEDTDH (L3) and the Cu(II) complex on ascites tumour reduction

Animal groups	Conc. μg/ml	No. of Animals with tumour	No. of days survived	% ILS
Control		5/5	17.3 ±1.20	
Standard Drug		5/5	31.6±0.245	82.66
L3	20	5/5	26.3 ±1.2	65.32
L3	10	5/5	25.2 ±3.2	45.66
L3	5	5/5	19.0 ±2.6	17.34
Cu(L3)	20	5/5	27.8±1.7	81.5
Cu(L3)	10	5/5	26.7±2.1	54.34
Cu(L3)	5	5/5	19.8 ±1.4	31.79

The Schiff base (L3) and its Cu(II) complex when applied intraperitoneally could produce considerable enhancement in the life span of mice bearing ascites tumour. The tumour induced animals of the control group survived for a period of 17.3±1.2 days and those treated with standard drug cyclophosphamide survived for a period of 31.6±0.245days. Cu(II) complex of the Schiff base reported an increase in life span of tumour carrying mice compared with that of the Schiff base ligand. The percentage increase in life span (%ILS) of the tumour bearing mice were 65.32,

45.60 and 17.34% for ligand at various concentrations namely 20,10 and 5µg/ml respectively. In case of the Cu(II) complex, the percentage increase was 81.5 % with a concentration of   20µg/ml. There was an enhancement in the average life span of the cancer induced animals for the Schiff base and its metal complex. However the analysis revealed that Cu(II) complex was very effective in declining the tumour development in mice and improving the life span of the animal. The Cu(II) complex showed significant antitumour activity in invivo studies.
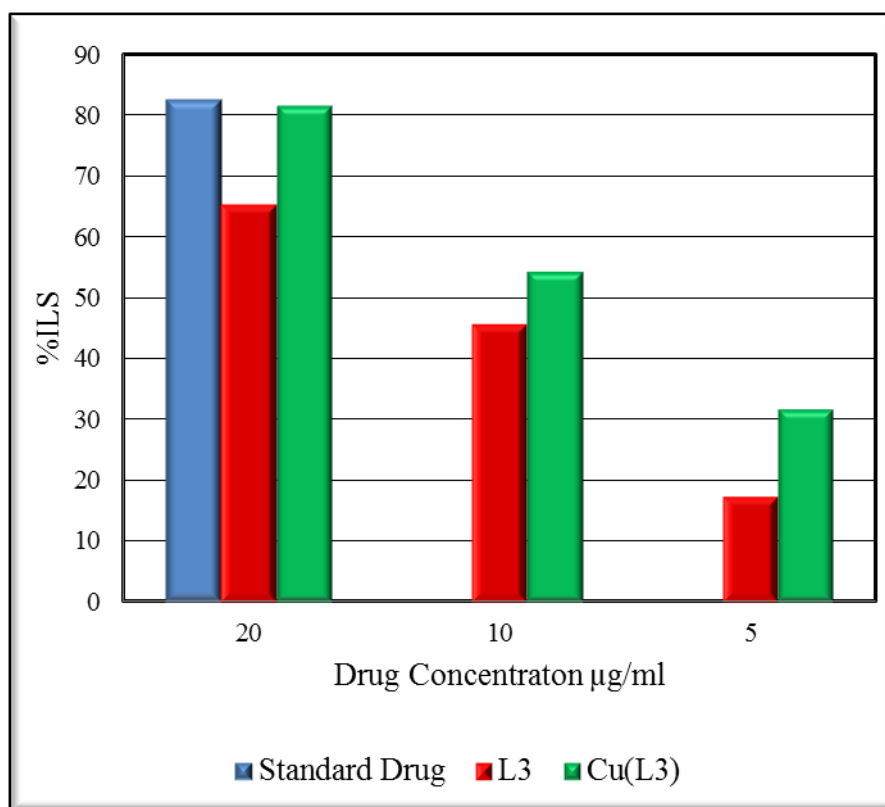
Fig.3.22 Effect of Schiff base TMEDTDH (L3) and the Cu(II) complex on ascites tumour reduction

Effect of Schiff base EHEDTDH (3a); Schiff base TMEDTDH (3c) and their Cu(II) complexes on solid tumour development

The effects of Schiff base ligands 3a, 3c and their copper complexes on solid tumour development in Swiss Albino mice were investigated. Solid tumour was induced in sets of mice by subcutaneous injection of DLA cell lines on the right hind limb of the mice. One group of mice was kept as control, one group was given the standard drug and other groups were gradually injected with the test compounds (200μmol/Kg body weight) for 10 days. Tumour diameter was measured with vernier calipers every third day for one month and tumour volume was determined. The results of the study are presented in the Table 3.22 and represented graphically in Fig. 3.23.

Table 3.22 Effect of Compounds on solid tumour

Compounds	Tumour volume on the 31st day
Control group	4.842 cm^3
3a (L1)	2.732 cm^3
3c (L3)	2.01 cm^3
Cu (L1)	2.35 cm^3
Cu (L3)	1.901 cm^3
Standard drug	1.863 cm^3

The Schiff bases and their copper complexes made a significant lessening of solid tumour volume in mice. Compared to Schiff bases, their Cu(II) chelates were more efficient in bringing about reduction in solid tumour volume. The calculated tumour volume was 4.842 cm^3 for the control group on the 31^{rst} day and it were 2.732 cm^3 and 2.01 cm^3 for 3a and 3c respectively. Comparing with the tumour volume of the control group, the ligands produced a decrease in tumour volume of 2.11 cm^3 and 2.832 cm^3 respectively. Among the Schiff bases, 3c was more effective in decreasing the tumour volume than 3a. The tumour volume on 31^{rst} day for copper complexes of 3a and 3c were 2.35 cm^3 and 1.901 cm^3 respectively. The decrease in tumour volume for the copper complexes of 3a and 3c was 2.492 cm^3 and 2.941 cm^3 respectively with respect to control group. The copper complex of Schiff base (3c) exhibited a marked effect in reducing tumour volume.
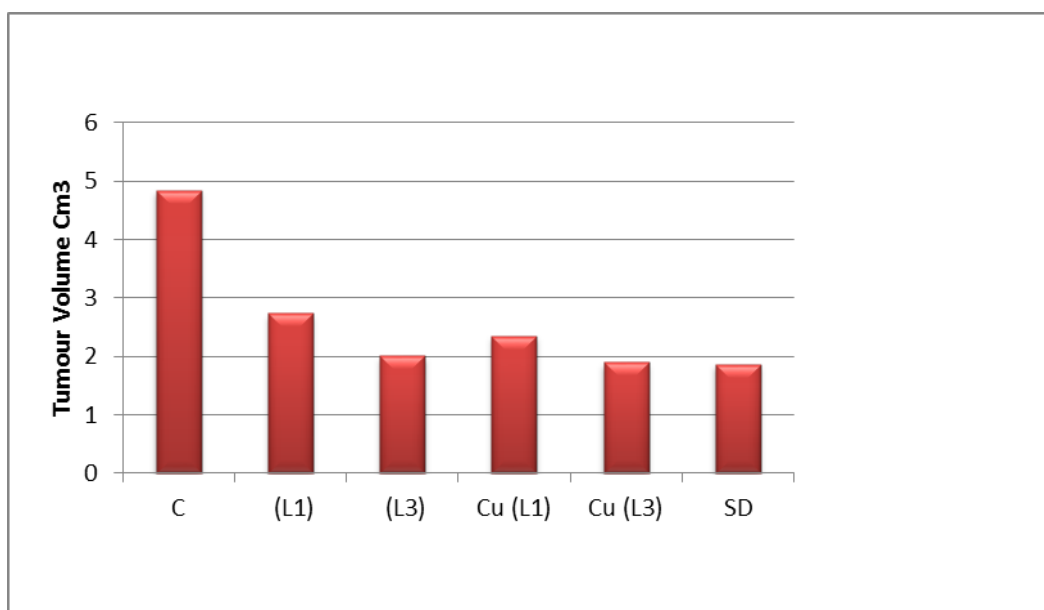
Fig. 3.23 Effect of Compounds on solid tumour

SECTION IV

Antitumour studies of Schiff bases derived from aryl azo derivative of 1,7-bis(naphthyl)-hepta-1,6-diene-3,5-dione,1,7-bis(2-methoxy naphthyl)- hepta-1,6-diene-3,5-dione and 1,7-bis(2-hydroxy naphthyl)- hepta-1,6-diene-3,5-dione with ethylene diamine and their transition metal complexes

In this section, the cytotoxic activity of Schiff bases derived from curcuminoid analogues namely1,14-di(naphthyl) 5,10-di(ethylene- naphthyl)-6,9diazotetradeca 1,5,9,13-tetraene -3,12-dione 4,11-diphenyl-hydrazone [NEDTDH] (4a); 1,14-bis(2-methoxy naphthyl) 5,10-bis(ethylene-2-methoxy naphthyl)-6,9diazotetradeca 1,5,9,13-tetraene -3,12-dione 4,11-diphenyl-hydrazone[MNEDTDH] (4b); 1,14-di(2-hydroxynaphthyl) 5,10-di(ethylene- 2-hydroxy naphthyl)-6,9diazotetradeca 1,5,9,13-tetraene -3,12-dione 4,11-diphenyl-hydrazone [HNEDTDH] (4c) were assessed, by in vitro studies. Their complexes with Cu (II), Zn(II) and Ni(II) also undergone invitro cytotoxicity analysis .The Schiff bases and their complexes were tested for their invitro cytotoxic activity against DLA (Daltons Lymphoma Ascites) and EAC (Ehrlich Ascites Carcinoma) tumour cells. The analysis results are elucidated in this section.

Invitro Cytotoxic studies of Schiff base NEDTDH (4a) and their metal complexes Cu (II), Zn(II) and Ni(II)

Cytotoxic activities of Schiff base NEDTDH (4a) and its metal complexes with Cu (II), Zn(II) and Ni(II) were assessed by finding the percentage viability of DLA and EAC cells by Trypan blue dye exclusion technique. Results obtained from the studies with EAC & DLA are given in Table 3.23 & Table 3.24.respectively.They are also represented graphically in Fig. 3.24 & Fig. 3.25

Table.3.23 Invitro Cytotoxic studies of Schiff base NEDTDH (4a) and their metal complexes towards EAC

Drug Con.	%Cell Death			
μg/ml	L_1	$Cu(L_1)$	$Zn(L_1)$	$Ni(L_1)$
10	4	9	8	5
20	6	17	14	9
50	12	31	26	19
100	21	46	39	34
200	31	73	55	41
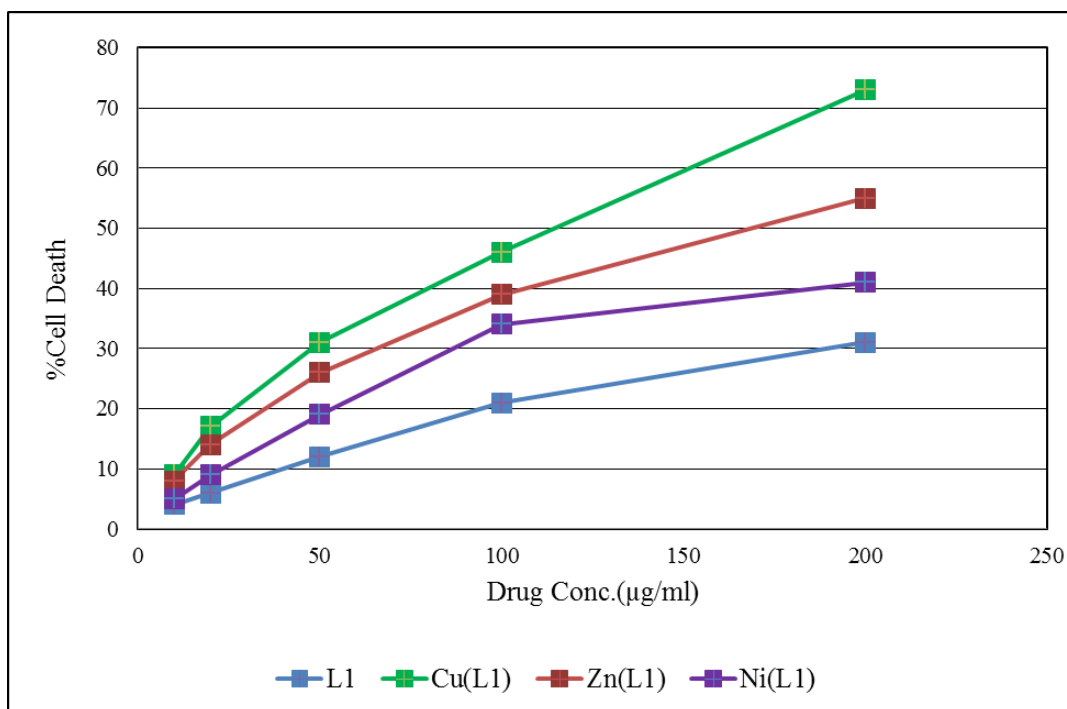
Fig.3.24 Invitro Cytotoxic studies of Schiff base NEDTDH (4a) and their metal complexes towards EAC

The cytotoxic behaviour of all the tested compounds increased with increase in concentration. The Schiff base and its complexes were quite effective at higher

concentration of 200 μg/ml. The metal complexes showed greater% cell death than the ligand. The highest activity was observed for Cu(II) complex(73%)and lowest activity for Ni(II)complex(41%). The metal complexes exhibited the activity in the order Cu(II)>Zn(II)>Ni(II).

Table 3.24 Invitro Cytotoxic studies of Schiff base NEDTDH (4a) and their metal complexes towards DLA

Drug Con.	%Cell Death			
μg/ml	L_1	$Cu(L_1)$	$Zn(L_1)$	$Ni(L_1)$
10	4	7	5	4
20	6	14	9	7
50	11	29	19	19
100	17	44	35	33
200	31	71	51	41
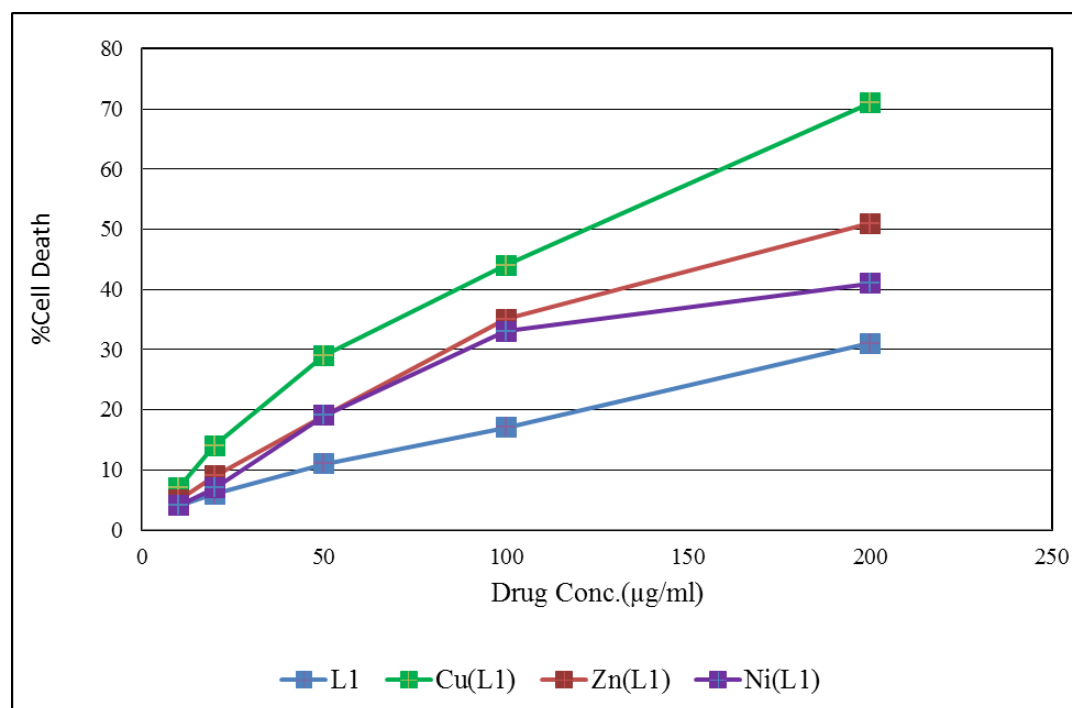
Fig.3.25. Invitro Cytotoxic studies of Schiff base NEDTDH (4a) and their metal complexes towards DLA

Invitro Cytotoxic studies of Schiff base MNEDTDH (4b) and their metal complexes Cu (II), Zn(II) and Ni(II)

In vitro Cytotoxic studies of Schiff base NEDTDH (4b) and their transition metal chelates were studied and the analysis results with DLA and EAC cells are presented in following Tables.

Table 3.25 Invitro Cytotoxic studies of Schiff base MNEDTDH (4b) and their metal complexes towards EAC

Drug Con.	%Cell Death			
µg/ml	L2	Cu(L2)	Zn(L2)	Ni(L2)
10	5	17	11	8
20	7	24	18	13
50	12	39	28	23
100	23	54	43	37
200	37	81	59	45
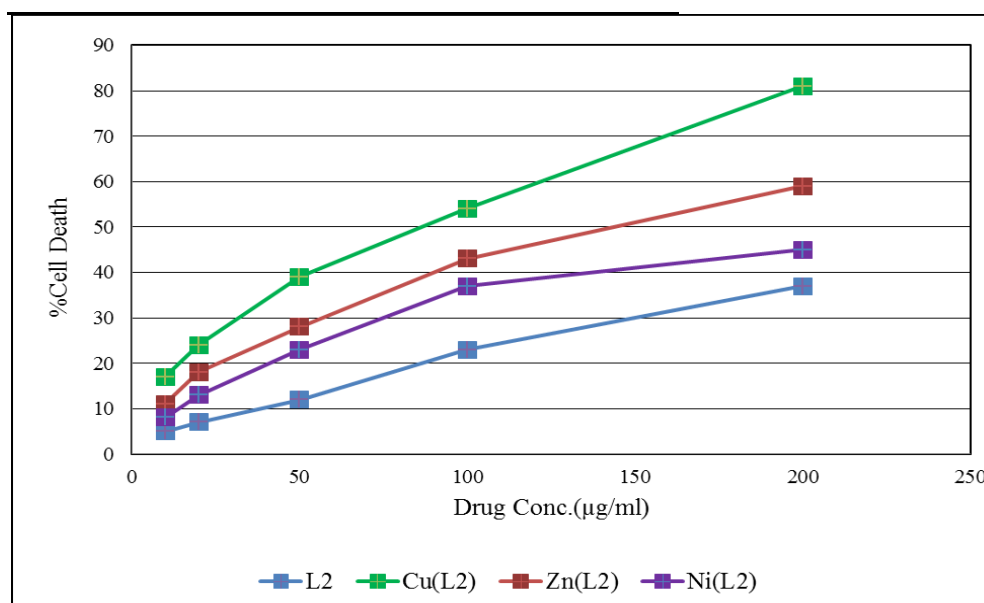
Fig.3.26 Invitro Cytotoxic studies of Schiff base MNEDTDH (4b) and their metal complexes towards EAC

The Schiff base with a methoxy group on naphthyl ring was a little more effective against cancer cells than the Schiff base ligand with naphthyl rings. At lower concentrations, the efficiency of the Schiff base as well as the metal complexes was very low. The Schiff base gave 37% cell death at a concentration of 200 μg/ml. The Cu(II) complex of the ligand exhibited notable cytotoxic activity to both the DLA and EAC cell lines. It showed the largest activity of 81%.The Zn(II) complex also exhibited comparable cell death. The cytotoxic behaviour of different metal complexes and the ligand are as follows: Cu(II) > Zn(II) > Ni(II) > ligand.

Table 3.26 Invitro Cytotoxic studies of Schiff base MNEDTDH (4b) and their metal complexes towards DLA

Drug Con.	%Cell Death			
μg/ml	L2	Cu(L2)	Zn(L2)	Ni(L2)
10	4	15	9	6
20	7	22	17	11
50	12	37	26	22
100	19	52	40	36
200	35	79	59	44
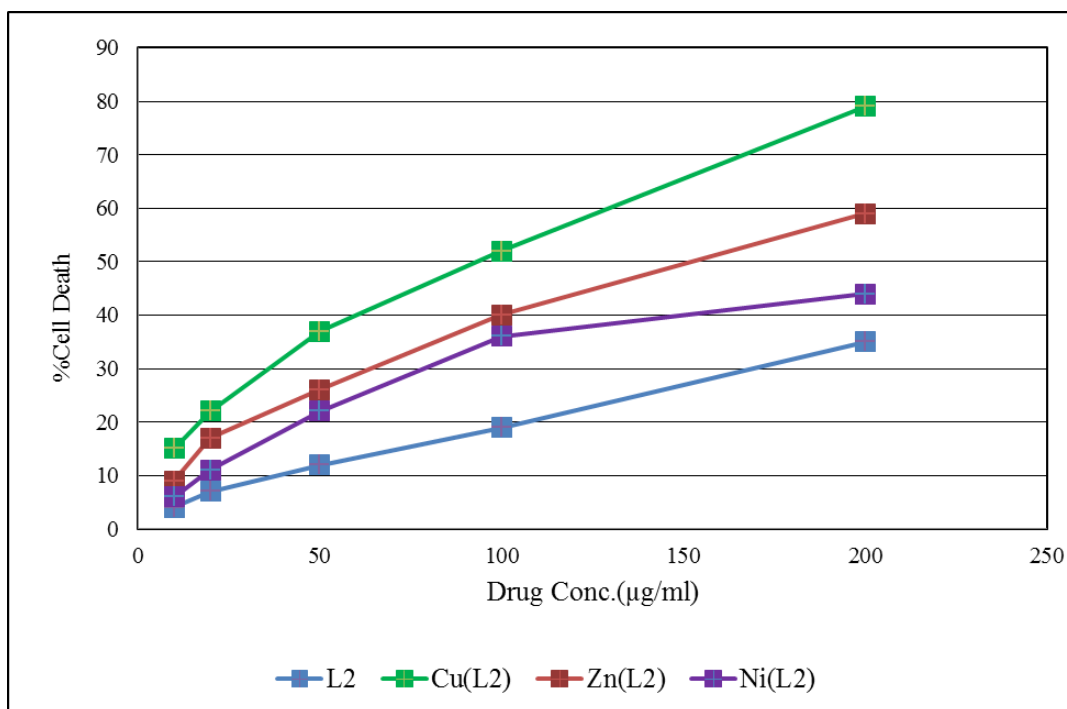
Fig.3.27 Invitro Cytotoxic studies of Schiff base MNEDTDH (4b) and their metal complexes towards DLA

Almost similar results were obtained for the cytotoxic activity of the compounds towards DLA cells. The % cell death produced by them is comparable with that towards EAC cells. All the compounds were less cytotoxic with DLA cells than EAC cells. The activity of ligands and their metal complexes reveals that metal complexation increases activity.

Invitro Cytotoxic studies of Schiff base HNEDTDH (4c) and their metal complexes Cu(II), Zn(II)&Ni(II)

Schiff base HNEDTDH (4c) and its metal complexes were taken for the analysis of their invitro cytotoxic nature. The observations are displayed in Table 3.27 and Table 3.28

Table 3.27 Invitro Cytotoxic studies of Schiff base HNEDTDH (4c) and their metal complexes towards EAC

Drug Con.	%Cell Death			
µg/ml	L3	Cu(L3)	Zn(L3)	Ni(L3)
10	8	16	14	11
20	11	29	21	17
50	17	51	37	23
100	28	77	52	34
200	43	86	72	50
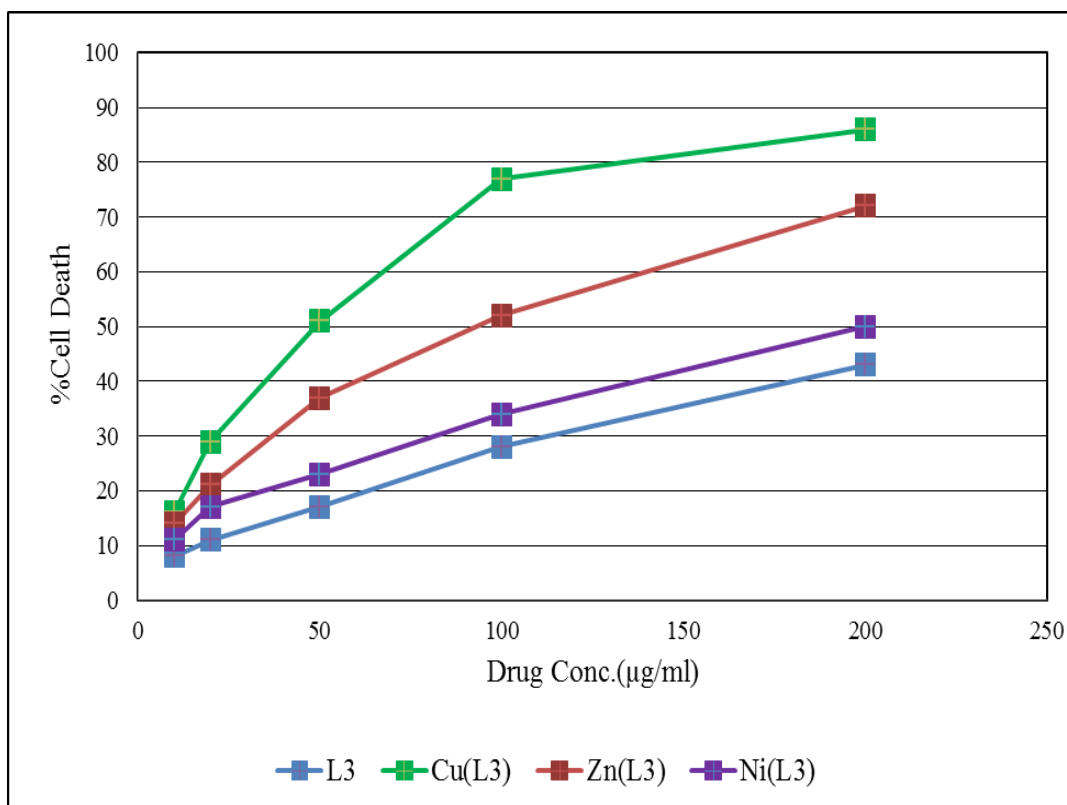
Fig.3.28 Invitro Cytotoxic studies of Schiff base HNEDTDH (4c) and their metal complexes towards EAC

Table.3.28 Invitro Cytotoxic studies of Schiff base HNEDTDH (4c) and their metal complexes towards DLA

| Drug Con.	%Cell Death			
µg/ml	L3	Cu(L3)	Zn(L3)	Ni(L3)
10	5	14	10	7
20	9	22	15	11
50	17	45	30	20
100	25	73	49	32
200	41	84	66	46
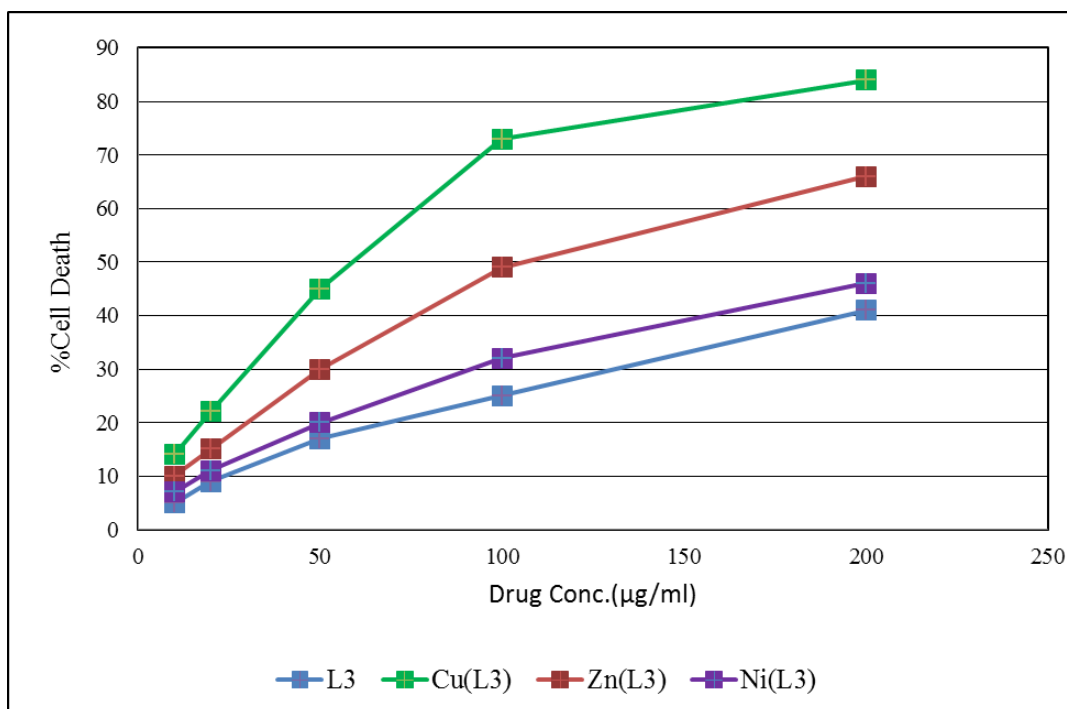
Fig.3.29 Invitro Cytotoxic studies of Schiff base HNEDTDH (4c) and their metal complexes towards DLA

The Schiff base with hydroxyl group on naphthyl rings was most efficient in exhibiting cytotoxic behaviour among the Schiff bases discussed in this section. The Schiff base exhibited 43% cell death at 200 µg/ml. The present study reported

that Cu(II)complex of the Schiff base could considerably impede both DLA and EAC cells to a great extent. The copper complex presented a cell death % of almost 86%.The IC50 value(the concentration which needs to produce 50% of cell death) of Cu(II) complex was 50 μg/ml, whereas for Zn(II)complex the value is 100 μg/ml. The Cu complex of the Schiff base was efficient even at smaller concentrations. The Zinc complex too was very effective against the cancerous cells and they produced approximately 72% of cell death. The Ni(II) complex was somewhat more efficient than the Schiff base ,but while considering the metal complexes it owned minimum cytotoxicity. The Schiff base as well as the metal complexes showed more activity towards EAC cells than with DLA cells.

The invivo antitumour studies of Schiff bases of aryl azo derivatives of curcuminoid analogues with substituted naphthyl ring and their Cu(II) complexes

Compounds exhibiting good cytotoxicity towards tumour cells are preferred for the antitumour studies in animals (Ruby et al ,1995)[163].So here the Schiff bases MNEDTDH (4b);HNEDTDH (4c) and their Cu(II) complexes which aroused quite active in the invitro cytotoxic studies completed before, were preferred. The current study was carried out to assess the invivo antitumour efficiency of the selected compounds against EAC cancer cell lines using ascites tumour bearing animal models. Viable EAC cells were administered into the peritoneal cavity of mice and developed tumours in its body.

Table 3.29 Effect of Schiff base MNEDTDH (4b) and its Cu(II) complex on ascites tumour reduction

Animal groups	Conc. µg/ml	No. of Animals with tumour	No. of days survived	% ILS
Control		5/5	17.3±1.20	
Std. Drug		5/5	31.6±0.245	82.66
L	20	5/5	26.7 ±1.2	54.34
L	10	5/5	25.3 ±2.4	46.24
L	5	5/5	19.8 ±2.5	14.45
Cu(L)	20	5/5	29.2±3.2	68.79
Cu(L)	10	5/5	27.0±1.4	56.07
Cu(L)	5	5/5	20.7 ±2.5	19.65

Drugs (4b, 4c and their Cu(II) complexes) were given as intraperitoneal injection at different concentrations such as 20,10 and 5 µg/ml for 10 days after tumour development. The death date of tumour infected animals was noticed and the percentage increase in average life span of the mice was calculated. The No. of days persisted by the animals are the means of five determinations $\pm SD$ (standard deviation).The results obtained with MNEDTDH (4b) and its Cu(II) complex are shown in Table 3.29.
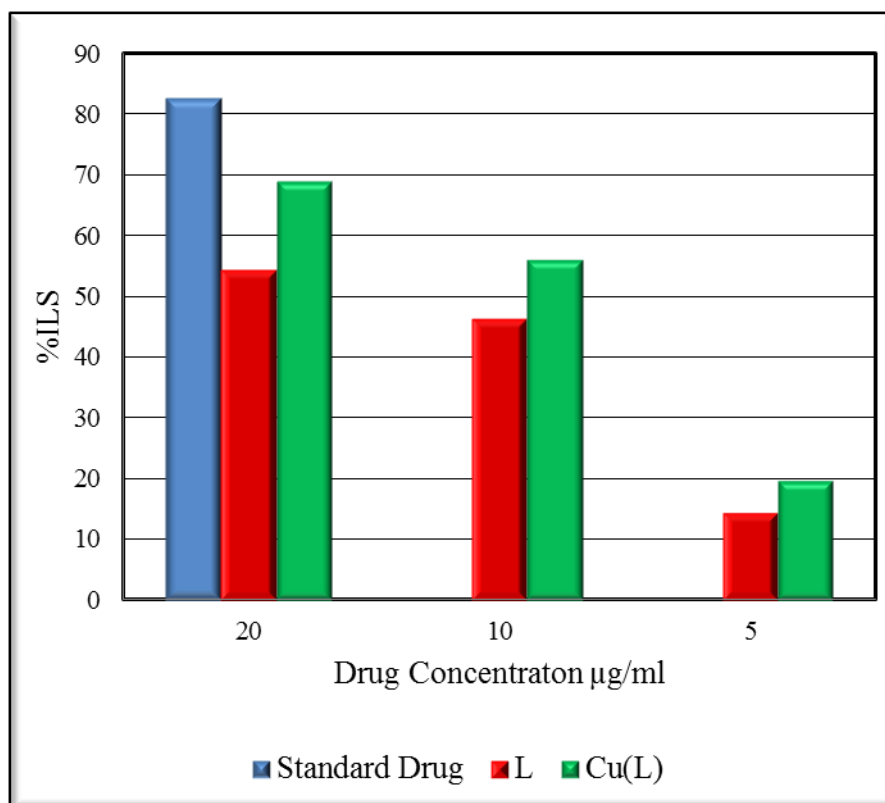
Fig. 3.30 Effect of Schiff base MNEDTDH (4b) and its Cu(II) complex on ascites tumour reduction

The mice carrying DLA induced tumour stayed alive for a span of 17.3 ± 1.2 days. The administration of the standard drug cyclophosphamide to the mice increased the life span of mice to 31.6 ± 0.245 days. The Schiff base at 20,10 and 5 µg/ml enhanced the average life span of animals to 26.7 ± 1.2, 25.3 ± 2.4, 19.8 ± 2.50 days respectively. Compared with the drug cyclophosphamide the % ILS exhibited by the Schiff base ligand L was 54% at a concentration 20µg/ml and that shown by its Cu(II) complex was 68% at a concentration of 20µg/ml. Both the Schiff base ligand and its metal complex were highly active at higher concentrations. The Cu(II) complex exhibited more activity than the ligand in lifting up the life span of tumour carrying animals

The invivo antitumour studies of Schiff base HNEDTDH (4c) & Cu(II) complex

The Schiff base HNEDTDH (4c) and its Cu(II) complex was delivered to the animals by intraperitoneal injection from the next day to the tumour induction as drugs to the mice. The death date of animals due to tumour infection was observed and the percentage increase in the life span of animals were determined .The results are detailed in Table 3.30

The schiff base and its Cu(II) complex when administered intraperitoneally as drugs could produce significant increase in the life span of mice bearing EAC cell lines. The animals of control group stayed for a period of 17.3 ± 1.2 days and those treated with drug cyclophosphamide (standard) for a span of 31.6 ± 0.245 days. Cu(II) complex of the Schiff base produced an increase in the life span of the tumour bearing animals in comparison with that of the Schiff base ligand. The percentage increase in the life span (%ILS) of the tumour bearing mice were 57.05, 52.6 and 14.45 % for the Schiff base at different concentrations such as 20,10 and 5µg/ml respectively. For the Cu(II) complex, the percentage increase (%ILS) was about 74.57 % at a concentration of   20µg/ml. An increase in the average life span of animals for both the ligand and the metal complex were seen. Certainly the studies revealed that Cu(II) complex is very efficient in inhibiting the tumour development in mice and increasing the life span of the tumour bearing animal. The Cu(II) complex exhibited substantial antitumour activity in in-vivo studies.

Table 3.30 Effect of Schiff base HNEDTDH (4c) and its Cu(II) complex on ascites tumour reduction

Animal groups	Conc. µg/ml	No. of Animals with tumour	No. of days survived	% ILS
Control		5/5	17.3±1.20	
Std. Drug		5/5	31.6±0.245	82.66
L	20	5/5	27 ±2.5	57.05
L	10	5/5	26.4 ±2.6	52.6
L	5	5/5	19.8 ±1.6	14.45
Cu(L)	20	5/5	30.2±0.9	74.57
Cu(L)	10	5/5	29±2.5	67.63
Cu(L)	5	5/5	21.7 ±1.6	25.43
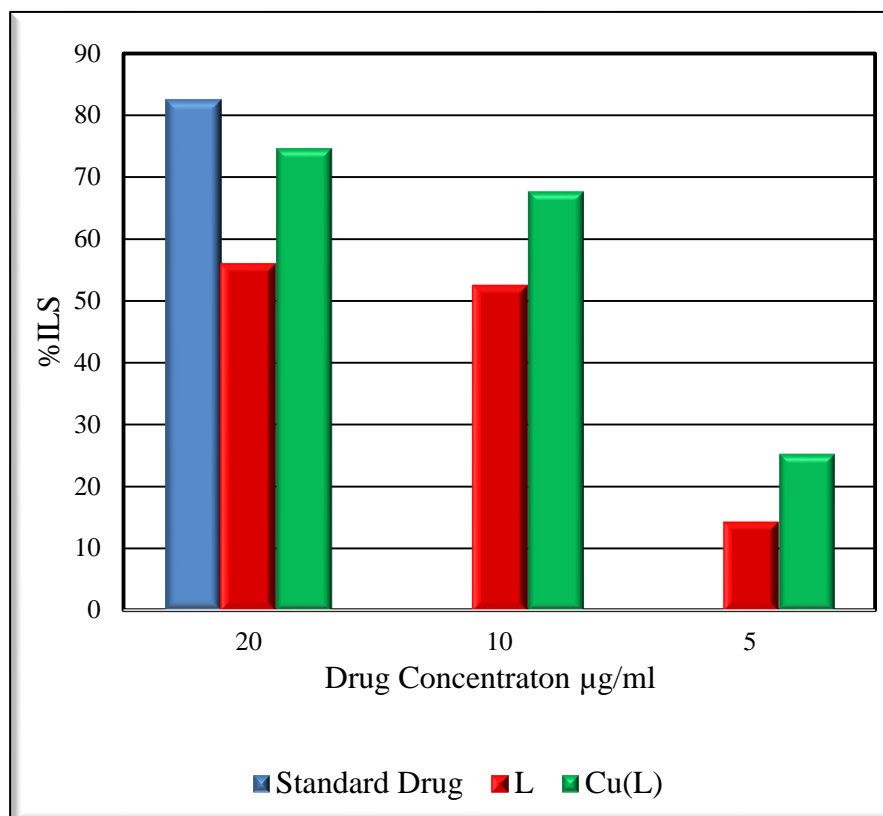
Fig. 3.31 Effect of Schiff base HNEDTDH (4c) and its Cu(II) complex on ascites tumour reduction

CONCLUSION

Invitro cytotoxicity study

Invitro cytotoxicity studies were performed using Schiff bases derived from aryl azo derivatives of 1,7-diaryl heptanoids & metal complexes with different concentrations like 200, 100, 50, 20 & 10 μg/ml against the tumour cells (DLA & EAC). The cytotoxic nature of the Schiff base compounds was found in terms of the percentage cell death produced by them. All the Schiff base compounds produced greater percentage cell death at an optimum concentration of 200 μg/ml. Schiff base ligands with methyl substituted phenyl rings showed nominal activity. A comparison study of the cytotoxic nature of the ligands has shown that the most active Schiff base is 3c with trimethoxy phenyl ring which gave 70 % cell death. All the Schiff base ligands except 3c required more than 200 μg/ml concentration for 50% cell death. The compounds with heterocyclic thiophenyl ring and hydroxyl substituted naphthyl ring were also very active against cancer cells producing 40% cell death. It may be concluded that 1a, 3c & 4c are better candidates for in vitro cytotoxic studies towards EAC & DLA. The activities of the ligands are compared and presented in Fig.3.32.
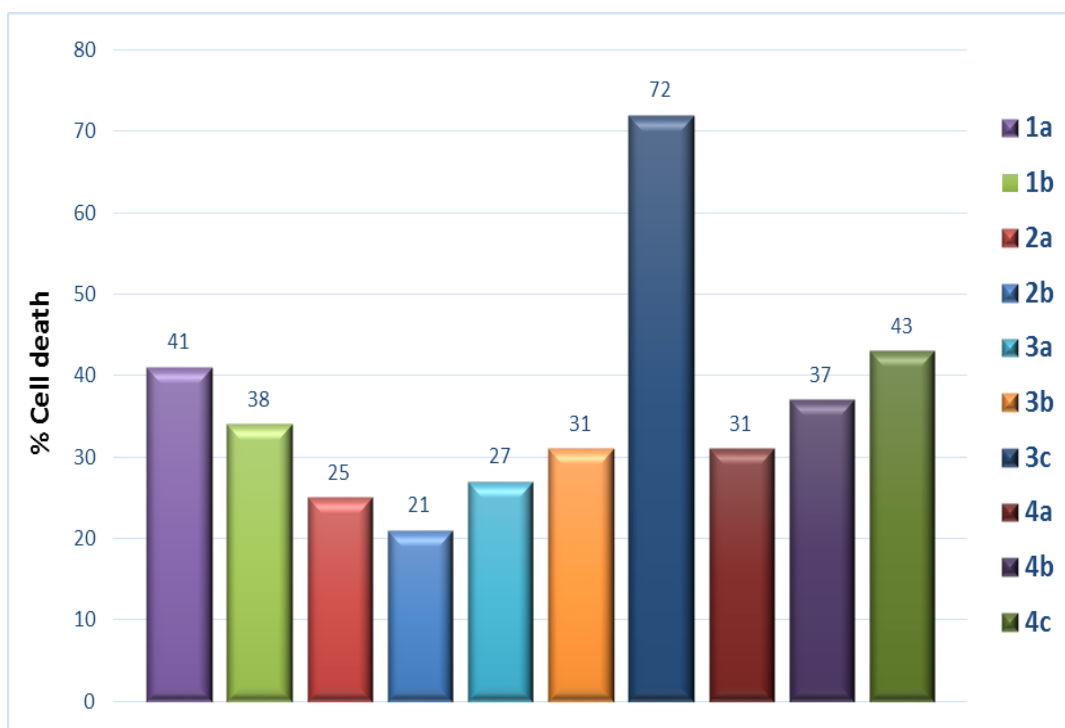
Fig.3.32 % cell death for ligands towards EAC at concentration 200µg/ml

In vitro cytotoxicity studies were performed using the metal chelates, with Cu(II), Zn(II) and Ni(II) .Out of the different metal complexes, Cu(II) complexes possess maximum cytotoxic activity. The most active compound is Cu(II) complex of 1a with thiophenyl rings with 93% cell death. The Cu(II) complex of 3c also gave 92% cell death. It is noted that metal chelation boosts the cytotoxic nature considerably. The cytotoxic activities of Cu(II) complexes and Zn(II) complexes are compared and given in Fig.3.33 &3.34 respectively.
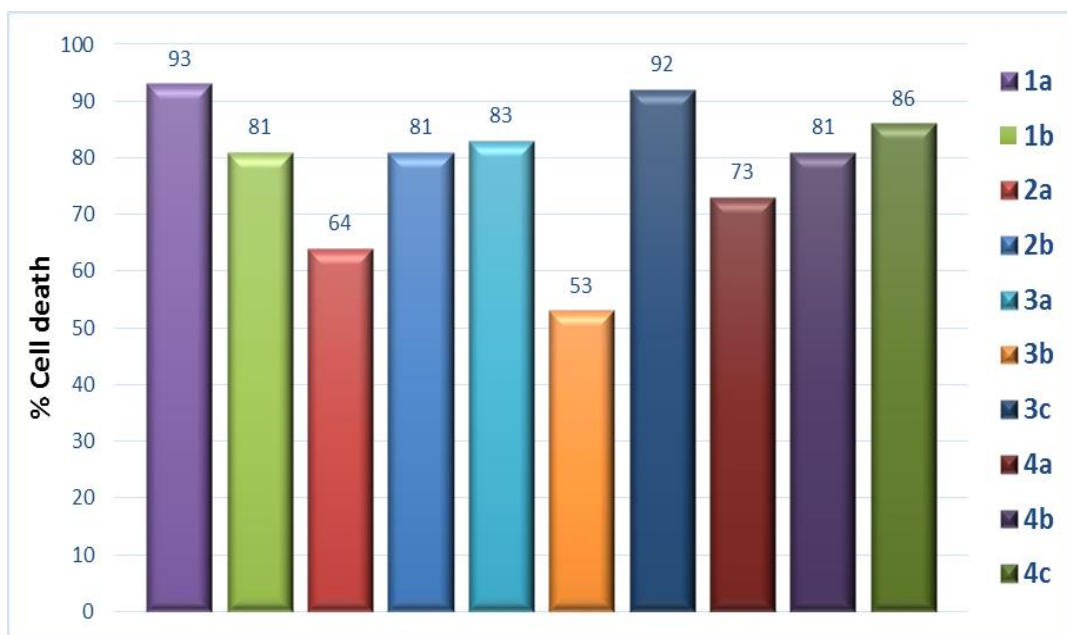
Fig.3.33 % cell death for Cu(II) complexes of ligands towards EAC at concentration 200µg/ml
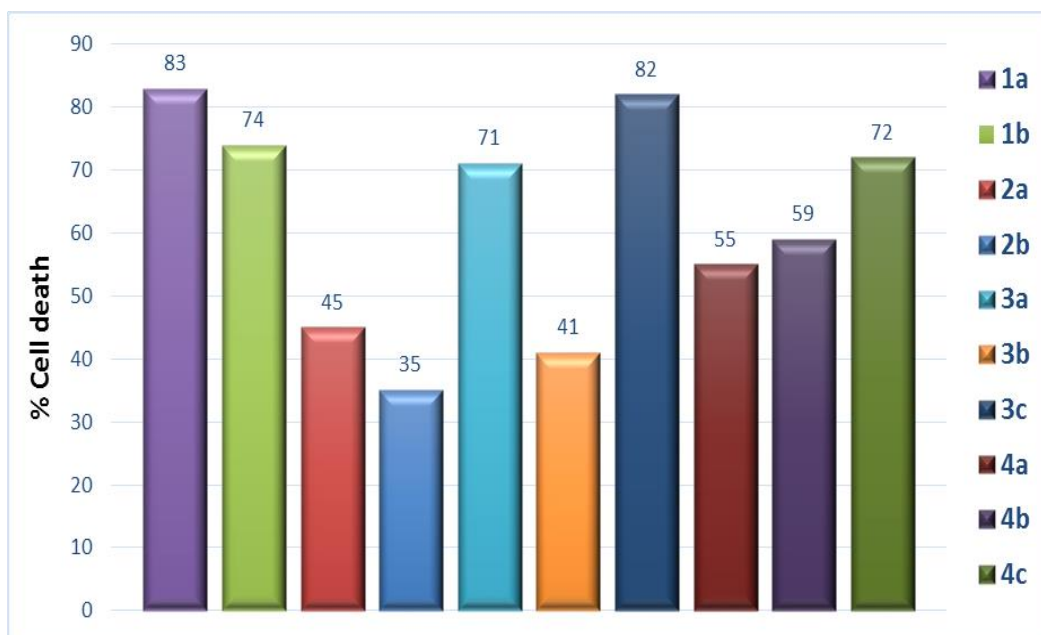
Fig.3.34 % cell death for Zn(II) complexes of ligands towards EAC at concentration 200µg/ml

Invivo antitumour studies

The invivo antitumour experiments were carried with tumour bearing mice using EAC cells. Selected Schiff base ligands and metal complexes were given to the animals as drugs with concentrations of 20μg/ml, 10μg/ml and 5μg/ml. The percentage increase in the life span of the tumour bearing mice were noted and compared with that of the standard drug. Schiff base ligands which were highly active in the invitro studies conducted were selected for the invivo studies. Maximum good results were obtained with a concentration of 20μg/ml. Out of the ligands, 3c gave maximum results. The percentage ILS shown by tri methoxy substituted Schiff base 3c was 65.32 against 82.66% for the standard drug. The % ILS shown was 60.12% for the Schiff base ligand with thiophenyl ring (1a).
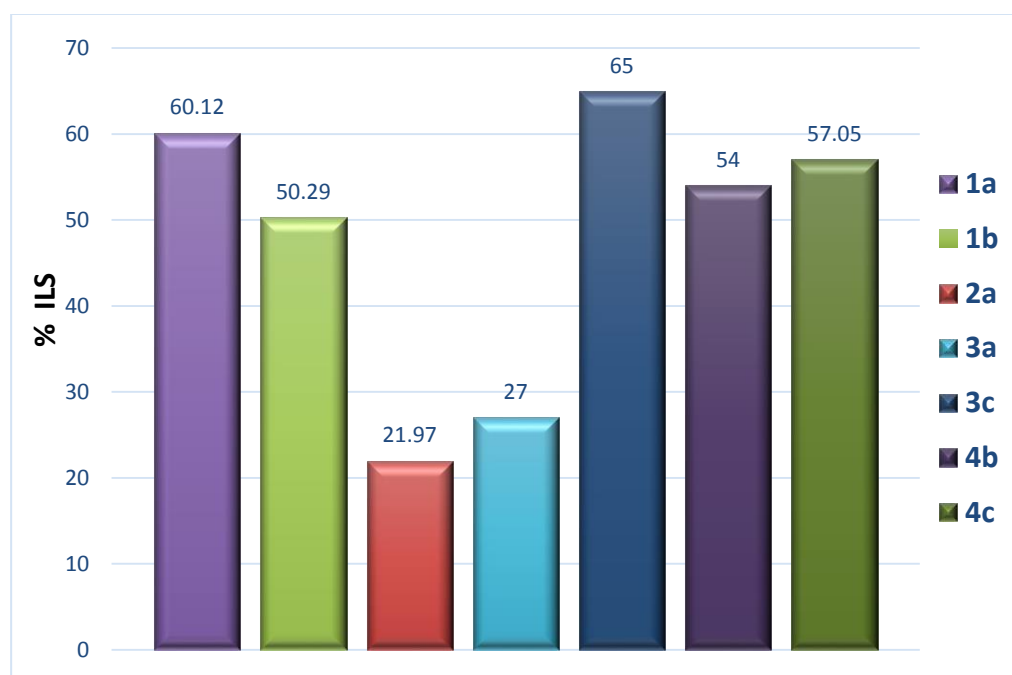
Fig.3.35 % ILS of tumour bearing mice by the administration of Schiff base ligands.

The metal complexes particularly Cu(II) and Ni(II) gave a maximum value of % ILS(Increase in life span) compared to that of Schiff base ligands. Among the different concentrations of metal complexes administered and the maximum result was attained with con.20 μg/ml. The %ILS for Cu(II) complex of 3c is 81% and of 1a is 80.92% which is comparable with that of standard drug. A comparative study of percentage increase in life span for Schiff base ligands and their Copper complexes are presented in Fig.3.35 &3.36 respectively
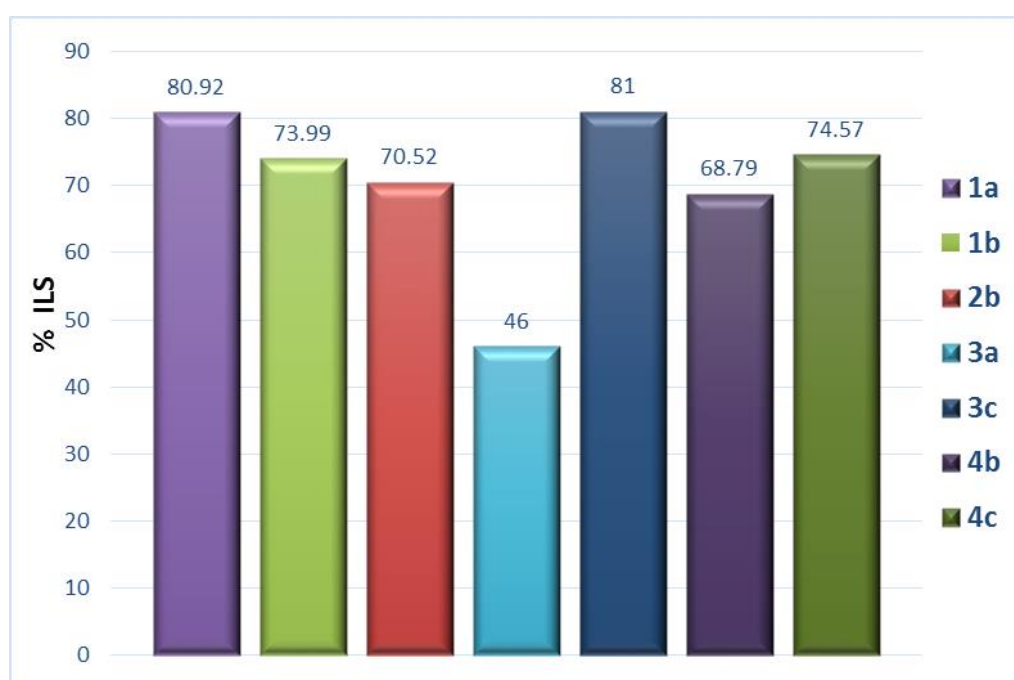
Fig.3.36 % ILS of tumour bearing mice by the administration of copper complexes of   ligands

Effect of compounds on solid tumour development

The effect of Schiff base compounds on solid tumour development was analysed with ligands 1a, 1b, 2a, 2b, 3a and 3c and their Cu(II) complexes .The results obtained are comparable with the results of the invivo studies carried out in tumour bearing mice. The Schiff base ligand 3c and its Cu(II) complex was very effective in reducing the solid tumour volume developed in mice. The Schiff base compound

treated group and metal complex treated group considerably decreased the tumour volume to 2.01 and 1.901 cm^3. The standard drug treated animal group showed a reduced tumour volume 1.863cm^3 when compared with the control group animals with tumour volume 4.842cm^3. For ligand 1a treated group, the tumour volume was 2.03cm^3 and for the metal complex treated group the volume was 1.95cm^3.So the Schiff base ligand 1a with thiophenyl ring and its Cu(II) complex was also efficient in reducing the solid tumour volume. The synthesized Schiff bases and their metal complexes can be used as effective antitumour drugs.

REFERENCES

1.   Joshi, J., Joshi, B. S., Duchaniya, Y. & Kumari, T. Applications of Schiff ' s Bases Metallorganic Derivatives − A Review. *IJETSR* 2, 99–115 (2015).

2.   Danyi, W. E. I., Ning, L. I., Gui, L. U. & Kemin, Y. A. O. Synthesis , catalytic and biological activity of novel dinuclear copper complex with Schiff base. *Sci. China* 49, 225–229 (2006).

3.   Chinnasamy, R. P. Synthesis , characterization , and analgesic activity of novel schiff base of isatin derivatives. *J. Adv. Pharm. Technol. Res.* 1, 342–347 (2010).

4.   Ali, S. M. M. *et al.* In vivo anticancer activity of vanillin semicarbazone. *Asian Pac. J. Trop. Biomed.* 2, 438–442 (2012).

5.   Krishnamohan Sharma, C. V. Crystal Engineering-Where Do We Go from Here? *Cryst. Growth Des.* 2, 465–474 (2002).

6.   Duran, B. & Yurt, A. Schiff bases as corrosion inhibitor for aluminium in HCl solution. *Corros. Sci.* 54, 251–259 (2012).

7.   Gouda, P., Kumar, C. H. V., Patil, S. A., Shivananda, K. N. & Nagaraju, C. European Journal of Medicinal Chemistry Synthesis , spectral characterization , in-vitro microbiological evaluation and cytotoxic activities of novel macrocyclic bis hydrazone. *Eur. J. Med. Chem.* 44, 3552–3559 (2009).

8.   Mounika, K., Anupama, B., Pragathi, J. & Gyanakumari, C. Synthesis¸ Characterization and Biological Activity of a Schiff Base Derived from 3-Ethoxy Salicylaldehyde and 2-Amino Benzoic acid and its Transition Metal

Complexes. *J. Sci. Res.* 2, 513–524 (2010).

9.   Miri, R. & Razzaghi-asl, N. QM study and conformational analysis of an isatin Schiff base as a potential cytotoxic agent. *J Mol Model* 19, 727–735 (2013).

10. Abu-dief, A. M. & Mohamed, I. M. A. A review on versatile applications of transition metal complexes incorporating Schiff bases. *Beni-Suef Univ. J. Basic Appl. Sci.* (2015). doi:10.1016/j.bjbas.2015.05.004

11. Zoubi, W. Al. Biological Activities of Schiff Bases and Their Complexes : A Review of Recent Works. *Int. J. Org. Chem.* 3, 73–95 (2013).

12. Yurt, A. & Aykın, Ö. Diphenolic Schiff bases as corrosion inhibitors for aluminium in 0 . 1 M HCl : Potentiodynamic polarisation and EQCM investigations. *Corros. Sci.* 53, 3725–3732 (2011).

13. Soliman, S. A., Metwally, M. S., Selim, S. R., Bedair, M. A. & Abbas, M. A. Corrosion inhibition and adsorption behavior of new Schiff base surfactant on steel in acidic environment: Experimental and theoretical studies. *J. Ind. Eng. Chem.* 20, 4311–4320 (2014).

14. Sondhi, S. M., Singh, N., Kumar, A. & Meijer, L. Synthesis, anti-inflammatory, analgesic and kinase (CDK-1, CDK-5 and GSK-3) inhibition activity evaluation of benzimidazole/benzoxazole derivatives and some Schiff's bases. *Bioorganic Med. Chem.* 14, 3758–3765 (2006).

15. Verma, M., Pandeya, S. N., Singh, K. N. & Stables, J. P. Anticonvulsant activity of Schiff bases of isatin derivatives. *Acta Pharm.* 54, 49–56 (2004).

16. Aboui-fadl, T., Mohammed, F. A. & Hassan, E. A. Synthesis , Antitubercular Activity and Pharmacokinetic Studies of Some Schiff Bases

Derived from 1- Alkylisatin and Isonicotinic Acid Hydrazide (INH). *Arch. Pharm. Res.* 26, 778–784 (2003).

17. Chainani-wu Nita, D.M.D., M.P.H., M. . Safety and Anti-Inflammatory Activity of Curcumin : *J. Altern. Complement. Med.* 9, 161–168 (2003).

18. Shishodia, S., Sethi, G. & Aggarwal, B. B. Curcumin: Getting back to the roots. *Ann. N. Y. Acad. Sci.* 1056, 206–217 (2005).

19. Al-Hujaily, E. M. *et al.* PAC, a novel curcumin analogue, has anti-breast cancer properties with higher efficiency on ER-negative cells. *Breast Cancer Res. Treat.* 128, 97–107 (2011).

20. Cicek, Volkan, and B. A.-N. . *Corrosion Chemistry,.* (Wiley, 2012, 2011).

21. Cicek, V. . *Corrosion Engineering,.* (John Wiley & Sons 2014).

22. C . G . Munger. Corrosion Prevention by Protective Coatings. (1999).

23. M. Behpour, S. M. Ghoreish, A. Gandomi, N. Niasar, N. Soltani, M. Niasari M, J. *Mater. Sci.,.* (44 (2009) 2444).

24. Sastri, V. S. Green Corrosion Inhibitors : Theory and Practice,. (2011).

25. Hassan, H. H. Inhibition of mild steel corrosion in hydrochloric acid solution by triazole derivatives Part II : Time and temperature effects and thermodynamic treatments. 53, 1722–1730 (2007).

26. Cruz, J. & Mart, R. Experimental and theoretical study of 1- (2-ethylamino) -2-methylimidazoline as an inhibitor of carbon steel corrosion in acid media. 566, 111–121 (2004).

27. Joseph, B., John, S., Joseph, A. & Narayana, B. Imidazolidine-2-thione as corrosion inhibitor for mild steel in hydrochloric acid. *Indian J. Chem.*

Technol. 17, 366–374 (2010).

28. Desai, M. N., Talati, J. D. & Shah, N. K. Schiff bases of ethylenediamine/triethylenetetramine with benzaldehyde/cinnamic aldehyde/salicylaldehyde as corrosion inhibitors of zinc in sulphuric acid. *Anti-Corrosion Methods Mater.* 55, 27–37 (2008).

29. Lee, J. H. *et al.* Dietary phytochemicals and cancer prevention: Nrf2 signaling, epigenetics, and cell death mechanisms in blocking cancer initiation and progression. *Pharmacol. Ther.* 137, 153–171 (2013).

30. Azuine, M. A. & Bhide, S. V. Chemopreventive effect of turmeric against stomach and skin tumors induced by chemical carcinogens in Swiss mice. *Nutr. Cancer* 17, 77–83 (1992).

31. Leu, T.-H. & Maa, M.-C. The molecular mechanisms for the antitumorigenic effect of curcumin. *Curr. Med. Chem. - Anti-Cancer Agents* 2, 357–370 (2002).

32. Chuang, S. E., Cheng, A. L., Lin, J. K. & Kuo, M. L. Inhibition by curcumin of diethylnitrosamine-induced hepatic hyperplasia, inflammation, cellular gene products and cell-cycle-related proteins in rats. *Food Chem. Toxicol.* 38, 991–995 (2000).

33. Huang, M., Lou, Y., Ma, W., Newmark, L. & Reuhl, R. Inhibitory Effects of Dietary Curcumin on Forestomach , Duodenal , and Colon Carcinogenesis in Mice Inhibitory Effects of Dietary Curcumin on Forestomach , Duodenal , and Colon Carcinogenesis in Mice '. *Cancer Res.* 54, 5841–5847 (1994).

34. Lee, S. L., Huang, W. J., Lin, W. W., Lee, S. S. & Chen, C. H. Preparation and anti-inflammatory activities of diarylheptanoid and diarylheptylamine

analogs. *Bioorganic Med. Chem.* 13, 6175–6181 (2005).

35. Kuttan, R., Bhanumathy, P., Nirmala, K. & George, M. C. Potential anticancer activity of turmeric (Curcuma longa). *Cancer Lett.* 29, 197–202 (1985).

36. Singh, S. V. *et al.* Mechanism of inhibition of benzo[a]pyrene-induced forestomach cancer in mice by dietary curcumin. *Carcinogenesis* 19, 1357–1360 (1998).

37. Huang, M., Smart, R. C., Wong, C. & Conney, A. H. Inhibitory Effect of Curcumin , Chlorogenic Acid , Caffeic Acid , and Ferulic Acid on Tumor Promotion in Mouse Skin by 12- O Inhibitory Effect of Curcumin , Chlorogenic Acid , Caffeic Acid , and Ferulic Acid on Tumor Promotion in Mouse Skin by 12-O-Tetrad. *Cancer Res.* 48, 5941–5946 (1988).

38. Hanif, R., Qiao, L., Shiff, S. J. & Rigas, B. Curcumin, a natural plant phenolic food additive, inhibits cell proliferation and induces cell cycle changes in colon adenocarcinoma cell lines by a prostaglandin-independent pathway. *J. Lab. Clin. Med.* 130, 576–84 (1997).

39. Mohandas, K. M. & Desai, D. C. Epidemiology of digestive tract cancers in India. V. Large and small bowel. *Indian journal of gastroenterology* 18, 118–121 (1999).

40. Kawamori, T. *et al.* Chemopreventive Effect of Curcumin , a Naturally Occurring Anti-Inflammatory Agent , during the Promotion / Progression Stages of Colon Cancer Chemopreventive Effect of Curcumin , a Naturally Occurring Anti-Inflammatory Agent , during the Promotion / Prog. *Cancer Res.* 59, 597–601 (1999).

41.   Dorai, T., Cao, Y., Dorai, B., Buttyan, R. & Katz, A. E. Therapeutic Potential of Curcumin in Human Prostate Cancer . III . Curcumin Inhibits Proliferation , Induces Apoptosis , and Inhibits Angiogenesis of LNCaP Prostate Cancer Cells InVivo. *Prostate* 47, 293–303 (2001).

42.   Liu, J. Y., Lin, S. J. & Lin, J. K. Inhibitory effects of curcumin on protein kinase C activity induced by 12-O-tetradecanoyl-phorbol-13-acetate in NIH 3T3 cells. *Carcinogenesis* 14, 857–861 (1993).

43.   Zhang, F., Altorki, N. K., Mestre, J. R., Subbaramaiah, K. & Dannenberg, A. J. Curcumin inhibits cyclooxygenase-2 transcription in bile acid- and phorbol ester-treated human gastrointestinal epithelial cells. *Carcinogenesis* 20, 445–51 (1999).

44.   Chen, H.-W. & Huang, H.-C. Effect of curcumin on cell cycle progression and apoptosis in vascular smooth muscle cells. *Br. J. Pharmacol.* 124, 1029–1040 (1998).

45.   Wilken, R., Veena, M. S., Wang, M. B. & Srivatsan, E. S. Curcumin: A review of anti-cancer properties and therapeutic activity in head and neck squamous cell carcinoma. *Mol. Cancer* 10, 10–12 (2011).

46.   Mosley, C. A., Liotta, D. C. & Snyder, J. P. Highly active anticancer curcumin analogues. *Adv. Exp. Med. Biol.* 595, 77–103 (2007).

47.   Liang, G. *et al.* Synthesis and anti-bacterial properties of mono-carbonyl analogues of curcumin. *Chem. Pharm. Bull. (Tokyo).* 56, 162–167 (2008).

48.   Liang, G. *et al.* Synthesis, crystal structure and anti-inflammatory properties of curcumin analogues. *Eur. J. Med. Chem.* 44, 915–919 (2009).

49.   Poma, P. *et al.* The antitumor activities of curcumin and of its isoxazole

analogue are not affected by multiple gene expression changes in an MDR model of the MCF-7 breast cancer cell line: analysis of the possible molecular basis. *Int J Mol Med* 20, 329–335 (2007).

50. Ahmed, M. *et al.* Synthesis, characterization, biological activities and molecular modeling of Schiff bases of benzene sulfonamides bearing curcumin scaffold. *Arab. J. Chem.* (2016). doi:10.1016/j.arabjc.2016.11.017

51. Padhye, S. *et al.* New difluoro knoevenagel condensates of curcumin, their schiff bases and copper complexes as proteasome inhibitors and apoptosis inducers in cancer cells. *Pharm. Res.* 26, 1874–1880 (2009).

52. Flora, S. J. S. & Pachauri, V. Chelation in metal intoxication. *Int. J. Environ. Res. Public Health* 7, 2745–2788 (2010).

53. Daniel, S., Limson, J. L., Dairam, A., Watkins, G. M. & Daya, S. Through metal binding, curcumin protects against lead- and cadmium-induced lipid peroxidation in rat brain homogenates and against lead-induced tissue damage in rat brain. *J. Inorg. Biochem.* 98, 266–275 (2004).

54. Zebib, B., Mouloungui, Z. & Noirot, V. Stabilization of curcumin by complexation with divalent cations in glycerol/water system. *Bioinorg. Chem. Appl.* 2010, (2010).

55. Baum, L. & Ng, A. Curcumin interaction with copper and iron suggests one possible mechanism of action in Alzheimer ' s disease animal models. *J. Alzheimer's Dis.* 6, 367–377 (2004).

56. Valentini, A. *et al.* Synthesis, oxidant properties, and antitumoral effects of a heteroleptic palladium(II) complex of curcumin on human prostate cancer cells. *J. Med. Chem.* 52, 484–491 (2009).

57. Jiang, T., Zhi, X. L., Zhang, Y. H., Pan, L. F. & Zhou, P. Inhibitory effect of curcumin on the Al(III)-induced Aβ42 aggregation and neurotoxicity in vitro. *Biochim. Biophys. Acta - Mol. Basis Dis.* 1822, 1207–1215 (2012).

58. Song, Y.-M. *et al.* Syntheses, characterization and biological activities of rare earth metal complexes with curcumin and 1,10-phenanthroline-5,6-dione. *J. Inorg. Biochem.* 103, 396–400 (2009).

59. Barik, A. *et al.* Evaluation of a new copper(II)-curcumin complex as superoxide dismutase mimic and its free radical reactions. *Free Radic. Biol. Med.* 39, 811–822 (2005).

60. Caruso, F. *et al.* Ruthenium−Arene Complexes of Curcumin: X-Ray and Density Functional Theory Structure, Synthesis, and Spectroscopic Characterization, in Vitro Antitumor Activity, and DNA Docking Studies of (p -Cymene)Ru(curcuminato)chloro. *J. Med. Chem.* 55, 1072–1081 (2012).

61. Santini, C. *et al.* Advances in copper complexes as anticancer agents. *Chemical Reviews* 114, (2014).

62. Joseph, J. & Boomadevi Janaki, G. Synthesis, structural characterization and biological studies of copper complexes with 2-aminobenzothiazole derivatives. *J. Mol. Struct.* 1063, 160–169 (2014).

63. González-Vílchez, F. & Vilaplana, R. in *Metallotherapeutic Drugs and Metal-Based Diagnostic Agents* 219–236 (John Wiley & Sons, Ltd, 2005). doi:10.1002/0470864052.ch12

64. Schiff, H. Mittheilungen aus dem Universit??tslaboratorium in Pisa: Eine neue Reihe organischer Basen. *Justus Liebigs Ann. Chem.* 131, 118–119 (1864).

65. Cimerman, Z., Miljanić, S. & Galić, N. Schiff Bases Derived from Aminopyridines as Spectrofluorimetric Analytical Reagents. *Croat. Chem. Acta* 73, 81–95 (2000).

66. Kupchan, s. M., raymond, doskotc, w., peter & vanevenhov, w. *Organic Syntheses*. 53, (1964).

67. Zheng, Y. *et al.* One pot synthesis of imines from aromatic nitro compounds with a novel Ni/SiO$_2$ magnetic catalyst. *Catal. Letters* 128, 465–474 (2009).

68. Love, B. E. & Ren, J. Synthesis of Sterically Hindered Imines. *J. Org. Chem.* 58, 5556–5557 (1993).

69. Look, G. C., Murphy, M. M., Campbell, D. A. & Gallop, M. A. Trimethylorthoformate: A mild and effective dehydrating reagent for solution and solid phase imine formation. *Tetrahedron Lett.* 36, 2937–2940 (1995).

70. Chakraborti, A. K., Bhagat, S. & Rudrawar, S. Magnesium perchlorate as an efficient catalyst for the synthesis of imines and phenylhydrazones. *Tetrahedron Lett.* 45, 7641–7644 (2004).

71. Cellosolve, M., Korczynski, A., Bischoff, C. & Bardach, B. Reduction of Schiff Bases . 11 . Benzhydrylamines and Structurally Related. *J. Org. Chem.* 23, 535–539 (1958).

72. Kulkarni, A., Patil, S. A. & Badami, P. S. Synthesis, characterization, DNA cleavage and in vitro antimicrobial studies of La(III), Th(IV) and VO(IV) complexes with Schiff bases of coumarin derivatives. *Eur. J. Med. Chem.* 44, 2904–2912 (2009).

73. Varma, R. S., Dahiya, R. & Kumar, S. Clay catalyzed synthesis of imines

and enamines under solvent-free conditions using microwave irradiation. *Tetrahedron Lett.* 38, 2039–2042 (1997).

74. Guzen, k. P.; Guarezemini, A. S.; Orfao, A. T. G.; Cella, R.; Pereira, C. M. P. . S. H. A. Eco-Friendly Synthesis of Imines by Ultrasound Irradiation. *Tetrahedron Lett.* 48, 1845–1848 (2007).

75. Xavier, A. & Srividhya, N. Synthesis and Study of Schiff base Ligands. *IOSR J. Appl. Chem.* 7, 6–15 (2014).

76. Ghose, B. N. Synthesis of some schiff bases. *J. Chem. Eng. Data* 29, 237 (1984).

77. Hussain, Z., Yousif, E., Ahmed, A. & Altaie, A. Synthesis and characterization of Schiff's bases of sulfamethoxazole. *Org. Med. Chem. Lett.* 4, (2014).

78. Ashassi-Sorkhabi, H., Shaabani, B. & Seifzadeh, D. Corrosion inhibition of mild steel by some schiff base compounds in hydrochloric acid. *Appl. Surf. Sci.* 239, 154–164 (2005).

79. Agrawal, Y. K., Talati, J. D., Shah, M. D., Desai, M. N. & Shah, N. K. Schiff bases of ethylenediamine as corrosion inhibitors of zinc in sulphuric acid. *Corros. Sci.* 46, 633–651 (2004).

80. Iyer, M. A. Q. M. W. M. A. S. M. and S. V. Influence of some thiazole derivatives on the corrosion of mild steel in hydrochloric acid. *Anti-Corrosion Methods Mater.* 43, 5–8 (1996).

81. Sadeghi Erami, R., Amirnasr, M., Raeissi, K., Momeni, M. M. & Meghdadi, S. Multidentate Schiff bases as new and effective corrosion inhibitors for mild steel in hydrochloric acid solution: An electrochemical and quantum

chemical assessment. *J. Iran. Chem. Soc.* 12, 2185–2197 (2015).

82.   Neelima, Poonia, K., Siddiqui, S., Arshad, M. & Kumar, D. In vitro anticancer activities of Schiff base and its lanthanum complex. *Spectrochim. Acta - Part A Mol. Biomol. Spectrosc.* 155, 146–154 (2016).

83.   Nair, M. S., Arish, D. & Joseyphus, R. S. Synthesis, characterization, antifungal, antibacterial and DNA cleavage studies of some heterocyclic Schiff base metal complexes. *J. Saudi Chem. Soc.* 16, 83–88 (2012).

84.   Hung, H. C. *et al.* Fruit and vegetable intake and risk of major chronic disease. *J. Natl. Cancer Inst.* 96, 1577–1584 (2004).

85.   Halliwell, B. Dietary polyphenols: Good, bad, or indifferent for your health? *Cardiovasc. Res.* 73, 341–347 (2007).

86.   Manach C, Scalbert A, Morand C, et al. Polyphenols: Food sources andBioavailability. *Am. J. Clin. Nutr.* 79, 727–747 (2004).

87.   M.L. Dhar, M. M. D. et al; Screening of Indian Plants for Biological Activity. *Indian J. Exp. Biol.* 6, 232–247 (1968).

88.   Ammon, H. P. & Wahl, M. A. Pharmacology of Curcuma longa. *Planta Med.* 57, (1991).

89.   Araújo, C. C. & Leon, L. L. Biological activities of Curcuma longa L. *Mem. Inst. Oswaldo Cruz* 96, 723–728 (2001).

90.   Shrishail, D., Handral Harish, K., Ravichandra, H., Tulsianand, G. & Shruthi, S. D. Turmeric: Nature's precious medicine. *Asian J. Pharm. Clin. Res.* 6, 10–16 (2013).

91.   Sidhu, G. S. *et al.* Enhancement of wound healing by curcumin in animals.

Wound Repair Regen. 6, 167–177 (1998).

92.   S.D.Deodhar, R. S. and R. . S. Preliminary study on antirheumatic activity of curcumin(diferuloyl methane). *Indian J. Med. Res.* 632–634 (1980). doi:10.1016/j.phrs.2009.12.004

93.   Funk, J. L. *et al.* Turmeric extracts containing curcuminoids prevent experimental rheumatoid arthritis. *J. Nat. Prod.* 69, 351–355 (2006).

94.   Mayer, F. Natural Organic Colouring Matters. *Nature* 156, (1945).

95.   Selvam, R., Subramanian, L., Gayathri, R. & Angayarkanni, N. The anti-oxidant activity of turmeric (Curcuma longa). *J. Ethnopharmacol.* 47, 59–67 (1995).

96.   Naz, S., Ilyas, S., Parveen, Z. & Javed, S. Chemical Analysis of Essential Oils from Turmeric (Curcuma longa) Rhizome Through GC-MS. *Asian J. Chem.* 22, 3153–3158 (2010).

97.   Leach, A. E. The composition of turmeric. *J. Am. Chem. Soc.* 26, 1210–1211 (1904).

98.   Goud, V. K., Polasa, K. & Krishnaswamy, K. Effect of turmeric on xenobiotic metabolising enzymes Introduction Diet contains many inhibitors of chemical carcinogens such as phenols , indoles , aromatic isothiocyanates , flavones , vitamin C , E and other by the S . typhimurium assay of Ames . The a. *Plant Foods Hum. Nutr.* 44, 87–92 (1993).

99.   Iqbal, M., Sharma, S. D., Okazaki, Y., Fujisawa, M. & Okada, S. Dietary supplementation of curcumin enhances antioxidant and phase II metabolizing enzymes in ddY male mice: possible role in protection against chemical carcinogenesis and toxicity. *Pharmacol. Toxicol.* 92, 33–38 (2003).

100. Lampe, V. & Milobedzka, J. Studien uber Curcumin. *Berichte der Dtsch. Chem. Gesellschaft* 46, 2235–2240 (1913).

101. Miiobedzka, J. *et al.* Zur Kenntnis des Curcumins. *Berichte der Dtsch. Chem. Gesellschaft* 43, 2163–2170 (1910).

102. Weber, W. M., Hunsaker, L. A., Abcouwer, S. F., Deck, L. M. & Vander Jagt, D. L. Anti-oxidant activities of curcumin and related enones. *Bioorganic Med. Chem.* 13, 3811–3820 (2005).

103. Priyadarsini, K. I. *et al.* Role of phenolic O-H and methylene hydrogen on the free radical reactions and antioxidant activity of curcumin. *Free Radic. Biol. Med.* 35, 475–484 (2003).

104. Lampe, V. Synthese von Curcumin. *Berichte der Dtsch. Chem. Gesellschaft* 51, 1347–1355 (1918).

105. Pabon, H. J. J. A synthesis of curcumin and related compounds. *Recl. des Trav. Chim. des Pay* 83, 379–386 (1964).

106. Bhagat, S., Sharma, N. & Chundawat, T. S. Synthesis of some salicylaldehyde-based schiff bases in aqueous media. *J. Chem.* (2013). doi:10.1155/2013/909217

107. Ahmed, M. *et al.* Synthesis, characterization, biological activities and molecular modeling of Schiff bases of benzene sulfonamides bearing curcumin scaffold. *Arab. J. Chem.* (2016). doi:10.1016/j.arabjc.2016.11.017

108. Krishnankutty, K., Basheer, M. & Kamalakshy, D. Arylazo derivatives of some fluorinated β-diketones and their metal complexes. *J. Iran. Chem. Res.* 2, 111–119 (2009).

109. A. Fadda, A. & M. Elattar, K. Synthesis of Novel Azo Disperse dyes Derived from 4-Aminoantipyrine and their Applications to Polyester Fabrics. *Am. J. Org. Chem.* 2, 52–57 (2012).

110. Zhang, Q. *et al.* Synthesis and preliminary evaluation of curcumin analogues as cytotoxic agents. *Bioorganic Med. Chem. Lett.* 21, 1010–1014 (2011).

111. Saha, S. K., Dutta, A., Ghosh, P., Sukul, D. & Banerjee, P. Novel Schiff-base molecules as efficient corrosion inhibitors for mild steel surface in 1 M HCl medium: experimental and theoretical approach. *Phys. Chem. Chem. Phys.* 18, 17898–17911 (2016).

112. Ahamad, I., Prasad, R. & Quraishi, M. A. Thermodynamic, electrochemical and quantum chemical investigation of some Schiff bases as corrosion inhibitors for mild steel in hydrochloric acid solutions. *Corros. Sci.* 52, 933–942 (2010).

113. El-lateef, H. M. A. Experimental and Computational Investigation on the Corrosion Inhibition Characteristics of mild steel by some novel synthesized imines in Hydrochloric acid Solutions. *Corros. Sci.* (2014). doi:10.1016/j.corsci.2014.11.040

114. Bedair, M. A., Soliman, S. A. & Metwally, M. S. Synthesis and characterization of some nonionic surfactants as corrosion inhibitors for steel in 1.0 M HCl. *J. Ind. Eng. Chem.* doi:10.101, (2016).

115. Sı, G. & Erbil, M. Assessment of the inhibition efficiency of 3 , 4-diaminobenzonitrile against the corrosion of steel. 102, 437–445 (2016).

116. Hosseini, M. G., Ehteshamzadeh, M. & Shahrabi, T. Protection of mild steel corrosion with Schiff bases in 0 . 5 M H $_2$ SO $_4$ solution. *Electrochim. Acta*

52, 3680–3685 (2007).

117. Ansari, K. R. & Quraishi, M. A. Bis-Schiff bases of isatin as new and environmentally benign corrosion inhibitor for mild steel. *J. Ind. Eng. Chem.* 20, (2014).

118. Kamal vashih. B. Naik. Synthesis Sy nthesis of Novel Schiff Base B ase and Azetidinone D erivatives and their Antibacterial A ctivity. *E-Journal Chem.* 1, 272–276 (2004).

119. Bhattacharya, A., Purohit, V. C. & Rinaldi, F. Environmentally friendly solvent-free processes: Novel dual catalyst system in Henry reaction. *Org. Process Res. Dev.* 7, 254–258 (2003).

120. S. Parveen and F. Arjmand. Interaction of calf thymus DNA with new asymmetric copper (II) N , N-ethane. *Indian J. Chem.* 44, 1151–1158 (2005).

121. Kannappan, R., Tanase, S., Mutikainen, I., Turpeinen, U. & Reedijk, J. Low-spin iron(III) Schiff-base complexes with symmetric hexadentate ligands: Synthesis, crystal structure, spectroscopic and magnetic properties. *Polyhedron* 25, 1646–1654 (2006).

122. Sivasubramanian, V. K., Ganesan, M., Rajagopal, S. & Ramaraj, R. Iron(III)-salen complexes as enzyme models: Mechanistic study of oxo(salen)iron complexes oxygenation of organic sulfides. *J. Org. Chem.* 67, 1506–1514 (2002).

123. Butler, A. & Walker, J. V. Marine Haloperoxidases. *Chem. Rev.* 93, 1937–1944 (1993).

124. Shechter, Y., Goldwaser, I., Mironchik, M., Fridkin, M. & Gefel, D. Historic

perspective and recent developments on the insulin-like actions of vanadium; toward developing vanadium-based drugs for diabetes. *Coord. Chem. Rev.* 237, 3–11 (2003).

125. Thompson, K. H., McNeill, J. H. & Orvig, C. Vanadium Compounds as Insulin Mimics. *Chem. Rev.* 99, 2561–2572 (1999).

126. Eady, R. R. Current status of structure function relationships of vanadium nitrogenase. *Coord. Chem. Rev.* 237, 23–30 (2003).

127. Grivani, G., Delkhosh, S., Fejfarová, K., Dušek, M. & Khalaji, A. D. Polynuclear oxovanadium(IV) Schiff base complex [VOL2]n(L = (5-bromo-2-hydroxybenzyl-2-furylmethyl)imine): Synthesis, characterization, crystal structure, catalytic properties and thermal decomposition into V2O5nano-particles. *Inorg. Chem. Commun.* 27, 82–87 (2013).

128. Chohan, Z. H., Praveen, M. & Ghaffar, A. Structural and biological behaviour of Co(II), Cu(II) and Ni(II) metal complexes of some amino acid derived Schiff-bases. *Met. Based. Drugs* 4, 267–272 (1997).

129. Ershad, S., Sagathforoush, L. A., Karim-Nezhad, G. & Kangari, S. Electrochemical behavior of N2SO Schiff-base Co(II) complexes in non-aqueous media at the surface of solid electrodes. *Int. J. Electrochem. Sci.* 4, 846–854 (2009).

130. Yousif, E. *et al.* Metal complexes of Schiff base: Preparation, characterization and antibacterial activity. *Arab. J. Chem.* 10, S1639–S1644 (2017).

131. Selwin Joseyphus Shiju, C., Joseph, J., Justin Dhanaraj, C., Bright, K.C., R. Synthesis and characterization of Schiff base metal complexes derived from

imidazole-2-carboxaldehyde with L-phenylalanine. *Der Pharma Chem.* 7, 6–12 (2015).

132. Saghatforoush, L. A., Aminkhani, A. & Chalabian, F. Iron(III) Schiff base complexes with asymmetric tetradentate ligands: Synthesis, spectroscopy, and antimicrobial properties. *Transit. Met. Chem.* 34, 899–904 (2009).

133. Morad, F. M., El, M. M. & Gweirif, S. Ben. Preparation , Physical Characterization and Antibacterial Activity of Ni (II) Schiff Base Complex. *J. Sci. Its Appl.* 1, 72–78 (2007).

134. Boghaei, D. M. & Lashanizadegan, M. Metal complexes of non-symmetric tetradentate Schiff bases derived from n-(1-hydroxy-2-acetonaphthone)-1-amino-2-phenyleneimine. *Synth. React. Inorg. Met. Chem.* 30, 1393–1404 (2000).

135. Ammar, R. A. A. & Alaghaz, A. M. A. Synthesis , Spectroscopic Characterization and Potentiometric Studies of a Tetradentate [N 2 O 2] Schiff Base , N , N -bis (2- hydroxybenzylidene) -1 , 1-diaminoethane and Its Co (II), Ni (II), Cu (II) and Zn (II) Complexes . *Int. J. Electrochem. Sci.* 8, 8686–8699 (2013).

136. Gaballa, A. S., Asker, M. S., Barakat, A. S. & Teleb, S. M. Synthesis, characterization and biological activity of some platinum(II) complexes with Schiff bases derived from salicylaldehyde, 2-furaldehyde and phenylenediamine. *Spectrochim. Acta - Part A Mol. Biomol. Spectrosc.* 67, 114–121 (2007).

137. Ejidike, I. P. & Ajibade, P. A. Synthesis, Characterization, Anticancer, and Antioxidant Studies of Ru(III) Complexes ofMonobasic Tridentate Schiff

Bases Ikechukwu. *Bioinorg. Chem. Appl.* (2016). doi:10.1155/2016/9672451

138. Toyota, E., Sekizaki, H., Takahashi, Y., Itoh, K. & Tanizawa, K. Amidino-containing Schiff base copper (II) and iron (III) chelates as a thrombin inhibitor. *Chem. Pharm. Bull.* 53, 22–26 (2005).

139. Parashar, R. K., Sharma, R. C. & Mohan, G. Biological activity of some Schiff bases and their metal complexes. *Biol. Trace Elem. Res.* 23, 145–50 (1990).

140. Kumar, S. & Durga Nath Dhar and P N saxena. Applications of metal complexes of Schiff bases- A review. *J. Sci. Ind. Res.* 68, 181–187 (2009).

141. Zhang, N. *et al.* Syntheses , crystal structures and anticancer activities of three novel transition metal complexes with Schiff base derived from 2-acetylpyridine and l-tryptophan. *Inorg. Chem. Commun.* 22, 68–72 (2012).

142. Elkacimi, Y., Achnin, M., Aouine, Y., Touhami, M. E. & Alami, A. Inhibition of Mild Steel Corrosion by some Phenyltetrazole Substituted Compounds in Hydrochloric Acid. *Port. Electrochim. ACTA* 30, 53–65 (2012).

143. P.Manjula, S. Manonmani, P. jayaram, S. R. Corrosion behaviour of carbon steel in the presence of N-cetyl-N , N , N- trimethylammonium bromide, Zinc and Calcium gluconate. *Anti-Corrosion Methods Mater.* 48, 319–324 (2001).

144. M Bouklah, N Benchat, B Hammouti, A Aouniti, S. K. Thermodynamic characterisation of steel corrosion and inhibitor adsorption of pyridazine compounds in 0.5 M H_2SO_4. *Mater. Lett.* 60, 1901–1905 (2006).

145. J. O'M. Bockris, A. K. N. R. *'Modern Electrochemistry-2',*. (Plenum Press,

New York, (1970)).

146. Jones, D. A. *, 'Principles and Prevention of Corrosion',.* (Macmillam publishing, New York, (1992).).

147. E. Barsoukov, J. R. M. *, 'Impedance Spectroscopy, Theory, Experiment and Applications',.* (Wiley Interscience publications, New York, 2nd Ed., (2005).).

148. Mansfield, F. *, Electrochim. Acta,.* (35 (1990) 1533F).

149. M. Kendig, J. Scully, J. *Electrochem. Soc.,.* (141 (1994) 1823).

150. G. Reinhard, U. R. *Corrosion,.* (15 (1984)).

151. T. Strivens, C. T. *Mater. Chem.,.* (7 (1982) 199.).

152. F. Mansfeld, M. K. *'Evaluvation of Protective Coatings with Impedance measurements',.* (International Congress on Metallic corrosion, 3 (1984) 74.).

153. MacDonald, D. D. *, 'Transient Techniques in Electrochemistry',.* (Plenum press. New York, (1977).).

154. Singh, A., Avyaya, J. N. & Quraishi, M. A. Schiff ' s base derived from the pharmaceutical drug Dapsone (DS) as a new and effective corrosion inhibitor for mild steel in hydrochloric acid. (2012). doi:10.1007/s11164-012-0577-y

155. Belghiti, M. E. *et al.* Anti-corrosive properties of 4-amino-3,5-bis(disubstituted)-1,2,4-triazole derivatives on mild steel corrosion in 2 M H_3PO_4 solution: Experimental and theoretical studies. *J. Mol. Liq.* 216, 874–886 (2016).

156. Manivel, A., Ramkumar, S., Wu, J. J., Asiri, A. M. & Anandan, S. Journal of Environmental Chemical Engineering corrosion inhibitor for mild steel in acidic media. *Biochem. Pharmacol.* 2, 463–470 (2014).

157. Yurt, A., Balaban, A., Kandemir, S. U., Bereket, G. & Erk, B. Investigation on some Schiff bases as HCl corrosion inhibitors for carbon steel. *Mater. Chem. Phys.* 85, 420–426 (2004).

158. Hassan, H. H., Abdelghani, E. & Amin, M. A. Inhibition of mild steel corrosion in hydrochloric acid solution by triazole derivatives Part I . Polarization and EIS studies. 52, 6359–6366 (2007).

159. T. Badea, M. Nicola, I. D. Vaireanu, I. Maior, A. C. *'Electrochimie si Coroziune, Matrixrom, Bucuresti', (2005) 150.*

160. M. G. Fontana, N. D. G. *'Corrosion Engineering', .* (McGraw-Hill, New York, (1978)).

161. Rosenfield, I. L. *, 'Corrosion Inhibitors', McGraw-Hill, New York, (1981) 66.*

162. John, V. D. & Krishnankutty, K. Antitumour activity of synthetic curcuminoid analogues (1,7-diaryl-1,6-heptadiene-3,5-diones) and their copper complexes. *Appl. Organomet. Chem.* 20, 477–482 (2006).

163. Ruby, A. J., Kuttan, G., Dinesh Babu, K., Rajasekharan, K. N. & Kuttan, R. Anti-tumour and antioxidant activity of natural curcuminoids. *Cancer Lett.* 94, 79–83 (1995).

164. Likhanova, N. V *et al.* The effect of ionic liquids with imidazolium and pyridinium cations on the corrosion inhibition of mild steel in acidic environment. *Corros. Sci.* 52, 2088–2097 (2010).

165. Bouanis, M. *et al.* Applied Surface Science Corrosion inhibition performance of HCl solution : Gravimetric , electrochemical and XPS studies. *Appl. Surf. Sci.* 389, 952–966 (2016).

166. Mazumder, M. A. J., Al-Muallem, H. A., Faiz, M. & Ali, S. A. Design and synthesis of a novel class of inhibitors for mild steel corrosion in acidic and carbon dioxide-saturated saline media. *Corros. Sci.* 87, 187–198 (2014).

LIST OF PUBLICATIONS

1. Raina Jose Cherappanath, Dr. John V D, "Synthesis, Characterization, Anti-corrosive/Antitumour Applications of a New Type Arylazo Compound 1,7-Bis(2-Hydroxy Phenyl)-4-(Phenyl Hydrazono)-Hepta-1,6-Diene-3,5-Dione". *Journal of Bio-and Tribo-Corrosion (2018), 4:66, September/2018. Springer Publications.*

2. Raina Jose Cherappanath, Delmy Davis, Dr. John V D, "The Synthesis, Characterization, Cytotoxic and Antitumour activities of Schiff Bases of curcuminoid analogues and their copper complexes" *Heterocyclic Letters, Vol. 7/ No.4/ /Aug-Oct/2017*

CONFERENCE PAPERS

1. Raina Jose Cherappanath and Dr. John V D, "The Synthesis and Characterization of Schiff bases derived from Curcuminoid analogues and their metal complexes" UGC sponsored National Seminar on Modern Trends in Chemistry,organized by St.Aloysius College Thrissur, January 2014.(poster)

2. Raina Jose Cherappanath and Dr. John V D "The Synthesis, Characterization and Antitumour studies of Schiff Bases and their complexes" proceedings of Chemical research Society of India, CRSI, Symposium in chemistry, organised by NIT Triruchirappalli. July 2015

3. Raina Jose Cherappanath and Dr. John V D, "The Synthesis, Characterization and Anti Corrosive activity of a newly synthesized Schiff Base" UGC sponsored National Seminar on Organic Synthesis, organized by St. Joseph's College Irinjalakkuda. January 2016

4. Raina Jose Cherappanath and Dr. John V D, "Anti Corrosive study of a newly synthesized Schiff base 1,7 bis(anthracenyl)-4-(phenyl-hydrazono)-hepta-1,6diene-3,5-dione" proceedings of a UGC sponsored National Seminar on Emerging trends in chemical research, organized by Christ College Irinjalakkuda. February 2017

5. Raina Jose Cherappanath and Dr. John V D, "Anti Corrosive study of a newly synthesized Schiff base 1,7 bis(thiophenyl)-4-(phenyl-hydrazono)-hepta-1,6diene-3,5-dione" proceedings of a UGC sponsored National Seminar on Nano materials for medical applications, organized by Little Flower College Guruvayoor.July 2017.

CrossMark

Synthesis, Characterization, Anti-corrosive/Anti-tumor Applications of a New Type Arylazo Compound 1,7-Bis(2-Hydroxy Phenyl)-4-(Phenyl Hydrazono)-Hepta-1,6-Diene-3,5-Dione

Raina Jose Cherappanath[1] · V. D. John[1]

Abstract

The purpose of the study is to synthesize and characterize a new arylazo compound 1,7-bis(2-hydroxyphenyl)-4-(phenylhydrazono)hepta-1,6-diene-3,5-dione (HPHDD) . The corrosion inhibition behavior of the compound on mild steel in 1 M HCl was investigated using weight loss method, electrochemical impedance spectroscopy, and potentiodynamic measurements. The results revealed that this arylazo compound effectively inhibited the corrosion reaction in HCl medium. The surface analysis indicated that this inhibitor was strongly adsorbed on the metal surface. The electrochemical studies at different temperatures showed the thermal stability of the inhibitor. Quantum chemical studies were performed using DFT at the B3LYP/6-31G (d, p)basis set. Contrary to the carcinogenic property of usual anti-corrosive substances, the in vitro cytotoxic studies of the newly synthesized arylazo derivative against Dalton lymphoma ascites cells confirm the anti-tumor properties of the compound.

1 Introduction

Corrosion which deteriorates the oil or gas pipelines or oil tanks affects the national economy and also has severe adverse effects on the ecosystem. One of the methods of combating corrosion is the use of effective non-toxic corrosion inhibitors [1, 2]. The use of corrosion inhibitors is a vital method of prevention of corrosion particularly in hydrochloric acid and sulfuric acid mediums, which are used for the pickling of aluminum and electrochemical etching. The major industries where corrosion inhibitors are used are petroleum refining, oil and gas exploration, chemical production, and water treatment plants. Anti-corrosive agents are also used in the sterilization of medical endoscopes. Many organic compounds are widely studied as corrosion inhibitors against mild steel (MS) corrosion in acid medium [3, 4]. The high inhibition efficiency of organic molecules is strictly related with its molecular structure, presence of

electronegative atoms (such as N, S, and O), unsaturated bonds, electronic properties as well as corrosive environment [5–12]. Corrosion control could be enhanced with more efficient corrosion inhibitors containing more heteroatoms. Recent studies have shown that the anti-corrosive agents used in the industry are highly toxic and carcinogenic [13, 14]. In these circumstances, there is necessity for developing effective low-cost, low-toxic, green organic corrosion inhibitor compounds.

The synthesis involves the preparation of 1,7-diaryl heptanoids using Pabon method and consequent coupling with benzene diazonium salt to form arylazo compound. The presence of electron donating centers and the C=N group in the synthesized compound prompted us to do the corrosion studies. The purpose of the present work is to investigate the corrosion inhibition efficiency of the synthesized compound for MS in IM hydrochloric acid using weight loss method, electrochemical impedance spectroscopy, and potentiodynamic measurements. The synthesized arylazo compound 1,7-bis(2-hydroxyphenyl)-4-(phenylhydrazono) hepta-1,6-diene-3,5-dione (HPHDD) molecule due to the presence of β diketo group may bind directly with DNA [15] and trigger DNA damage and also inhibit expression of DNA repair proteins in cancer cells [16] and so can be used

✉ V. D. John
   rainajc@gmail.com

1   Research and PG Department of Chemistry, Christ College, Irinjalakkuda, India

🌀 Springer

in medical field also. This instigated us to do the cytotoxic study of the newly synthesized compound.

2 Experimental Details

2.1 Materials

The MS of the following composition was used for the studies (0.2% C, 1% Mn, 0.3% P, 0.2% S, and the rest Iron). MS coupons of 1.5 cm × 1.5 cm × 1 mm were used (1 cm² exposed area). The coupons were cut and abraded with different grades of emery paper and washed with deionized water. They were then degreased with acetone to remove the possible residues of polishing and dried in air.

2.2 Test Solutions

Aggressive 1 M HCl solution was prepared by diluting analytical grade 37% HCl with deionized water. The test solutions of different concentrations of inhibitor 50 ppm, 75 ppm, 100 ppm, and 150 ppm were prepared.

2.3 Preparation of Inhibitor

2.3.1 Synthesis of 1,7-Bis(2-Hydroxyphenyl) Hepta-1,6-Diene-3,5-Dione

Acetyl acetone (0.005 mol, 0.5 g) and boric oxide (0.0035 mol, 0.25 g) were stirred about 1 h to obtain acetyl acetone–boron complex. To the reaction mixture, the salicylaldehyde (0.01 mol) dissolved in dry ethyl acetate (7.5 ml) and tri(sec-butyl) borate (0.02 mol, 5.4 ml) were added and the reaction mixture was stirred and the temperature was kept above 80 °C. While stirring, n-butyl amine (0.1 ml dissolved in 1 ml dry ethyl acetate) was added dropwise

for about 40 min. Stirring was continued for an additional period of ~ 4 h and the mixture was kept aside overnight. Hot (~ 60 °C) HCl (0.4 M, 7.5 ml) was added and then the mixture was again stirred for ~ 1 h. Two layers were separated and the top organic layer was extracted with 5 ml ethyl acetate. The extracts were allowed to evaporate and the residue material was stirred with concentrated HCl (10 ml) for ~ 1 h. The solid product separated was washed with water and dried in vacuum. A mixture of 1,7-diaryl heptanoid and 6-aryl hexanoid was obtained. The products obtained were quantitatively separated by column chromatography using silica gel (60–120 mesh) (Pabon method) [17]. The product was purified by column chromatography over silica gel (60–120 mesh) using 2:1 (v/v) chloroform:acetone mixture as the eluent and recrystallized twice from hot benzene to get pure crystalline material.

2.3.2 Synthesis of HPHDD

The arylazo derivative (HPHDD) was synthesized by the coupling of benzene diazonium salt with β-diketone [18]. Benzene diazonium salt (0.01 mol) was prepared and it was added drop by drop to a solution of the β-diketone (0.01 mol) kept below 0 °C with constant stirring. The precipitated compound was filtered, washed with water, and recrystallized from ethanol to get chromatographically pure (TLC) material; arylazo compound 91% was obtained (Scheme 1).

2.4 Weight Loss Measurements

The experiments were carried out in blank 1 M HCl and in the test solutions containing inhibitor concentrations ranging from 50 ppm to 150 ppm. The pre-weighed MS coupons were suspended in different concentrations of inhibitor in 1 M HCl solution at 28 °C using glass hooks in the absence and presence of inhibitor in aerated condition. Test coupons

Scheme 1 Synthetic route of the studied arylazo compound
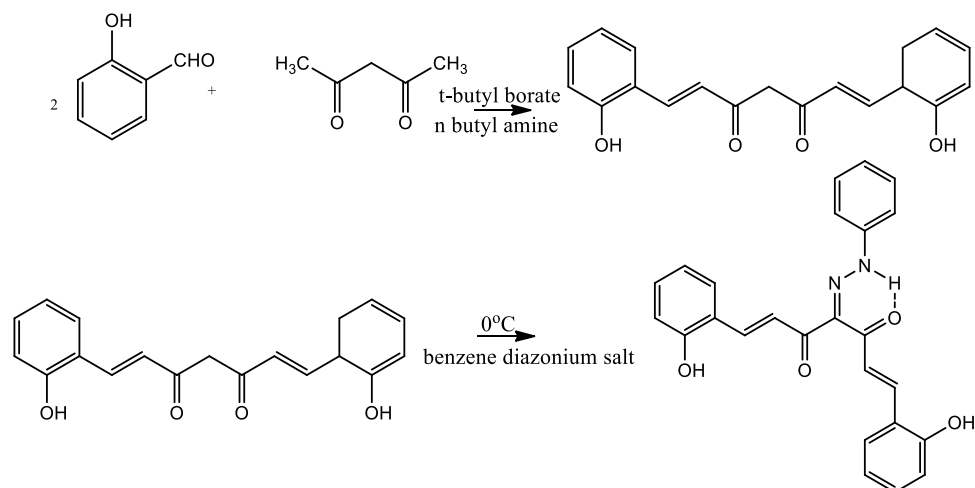
were taken out and reweighed after 24 h. The difference between the initial and final weights of the coupons gave the weight loss.

2.5 Electrochemical Measurements

Electrochemical measurements were realized using computer-controlled Metrohm Autolab PGSTAT 50519. The EIS measurements were carried out using a classical three-electrode corrosion cell. A three-electrode system was used to determine the potential across electrochemical interface accurately. Saturated calomel electrode was used as the reference electrode, MS coupons with exposed surface area 1 cm^2 were used as the working electrode, and the Platinum electrode was used as the counter electrode. 50 ml of 1 M HCl solutions with and without inhibitor was used for the studies. After keeping the solutions for 1 h for stabilizing OCP, the values were measured. Nova Software was used to collect the experimental data. The electrochemical impedance measurements were carried out in frequency ranging from 100,000 Hz to 10^{-1} Hz with an amplitude of 10 mV at the open circuit potential by applying AC signal. To investigate the anti-corrosive behavior of the HPHDD at different temperatures, the impedance study of the test solutions was carried out at different temperatures also. The temperature was controlled by an aqueous thermostat. The potentiodynamic measurements were carried out for cathodic and anodic part with a scan rate of 1 mV/s.

2.6 Surface Analysis

Scanning electron microscopic (SEM) analysis was carried out on SEM Jeol JSM-4500 instrument. Micrographs of the MS surface before and after 3 days immersion in 1 M HCl with and without corrosion inhibitor were taken. The energy of the acceleration beam was 20 kV and the given results are of 1000× magnitudes. EDX spectra were taken using BRUKER XFlash 6/10 instrument. The energy of the beam used was 30 MeV. AFM analysis was done using Bruker dimension edge model instrument in non-contact mode.

2.7 Quantum Chemical Studies

Quantum mechanical calculations were done on the inhibitor molecule by DFT method using B3LYP/6-31G (d, p) basis set. The structure of the inhibitor molecule for the optimization process was drawn using Gauss view 5.0. According to Koopmans' theorem, the energy of highest occupied molecular orbital (E_{HOMO}) and the energy of the lowest unoccupied molecular orbital (E_{LUMO}) of the molecule are related to ionization potential (I) and the electron affinity (A) by the relations, $I = -E_{HOMO}$ and $A = -E_{LUMO}$. Several other Quantum chemical descriptors are to be considered in order to correlate the predicted inhibition efficiency with the experimentally determined. Absolute electronegativity (χ) is the measure of power of the atom to attract the electrons towards it. Absolute hardness (η) is the measure of resistance of an atom to charge transfer. Stability of the molecule is given by (σ). Electrophilicity index (ω) and the change in the number of electrons transferred (ΔN) can be calculated from I and A values. All the above parameters can be calculated using the following equations:

$$\chi = \frac{(I + A)}{2} \tag{1}$$

$$\eta = \frac{(I - A)}{2} \tag{2}$$

$$\sigma = \frac{1}{\eta} \tag{3}$$

$$\omega = \frac{\chi^2}{2\eta} \tag{4}$$

$$\Delta N = \frac{\chi_{Fe} - \chi_{inh}}{2(\eta_{Fe} - \eta_{inh})}, \tag{5}$$

where χ_{Fe} and χ_{inh} denote the absolute electronegativity of iron and inhibitor molecule. The η_{Fe} and η_{inh} represent absolute hardness of iron and the inhibitor molecule. The values of χ_{Fe} and χ_{inh} are taken as 7 eV mol^{-1} and 0 eV mol^{-1}, respectively, by assuming that for a metallic bulk $I = A$.

2.8 In vitro Cytotoxicity Studies

In vitro cytotoxicity studies were carried out using the arylazo compound dissolved in minimum quantity of DMSO at Amala Cancer Research Centre, Thrissur, Kerala. The Dalton lymphoma ascites (DLA) tumor cells were aspirated from the peritoneal cavity of tumor-bearing mice. The cells were washed with phosphate-buffered saline (PBS) and centrifuged for 15 min at 1500 rpm. Viability of the cells was determined by trypan blue exclusion method [19]. Viable cells (1×10^6 cells on 0.1 ml) were added to tubes containing various concentrations of the inhibitor compound and the volume was made up to 1 ml using PBS. Control tube contains only cell suspension. Then these mixtures were incubated for 3 h at 37 °C. Further, cell suspension was mixed with 0.1 mol of 1% trypan blue and kept for 2–3 min and loaded on a hemocytometer. The number of stained (dead)

and unstained (live) cells were counted and percentage cytotoxicity was evaluated.

3 Results and Discussions

3.1 Structural Characterization

Structural characterization of the inhibitor molecule was done using C, H, N elemental analysis IR and mass spectra. The structure of the compound is shown in Fig. 1.

3.1.1 FTIR Spectrum

The IR spectrum (Fig. 2) of the synthesized compound showed the following absorption bands at 1590 cm^{-1} (C=N), 1708 cm^{-1} (free C=O). The bands are listed in Table 1.

3.1.2 ^{1}H NMR Spectrum

^{1}H NMR (CDCl$_3$) showed different bands at $\partial = 9.953$ ppm (s, 1H, phenolic); $\partial = 8.671$ ppm (s, 1H, NH) [20];

Table 1 IR bands of synthesized arylazo compound

Assignment	Wave number (cm^{-1})
(C=N)	1590
Chelated (C=O)	1655
Free (C=O)	1708
Hydrogen bonded OH group	3277

$\partial = 7.359–7.465$ (m, aryl protons); and $\partial = 6.853–7.801$(d, alkenyl protons). The ^{1}H NMR data confirmed the expected hydrogen proton distribution in the synthesized arylazo compound.

3.1.3 Mass Spectrum

The mass spectrum (Fig. 3) of the synthesized inhibitor illustrated a (M + 1) peak at m/z 413(4%) and base peak at 69 (100% [NH=N–C=C=O]$^+$) together with other significant peaks. The mass spectrum confirmed the structure of the inhibitor molecule.

3.1.4 C, H, and N Elemental Analysis

C, H, and N elemental analysis shows that the theoretical and experimental data are close approximately. This indicates the purity of synthesized inhibitor .The results obtained C (71.98%), H (4.4%), N (6.6%) are summarized in Table 2.
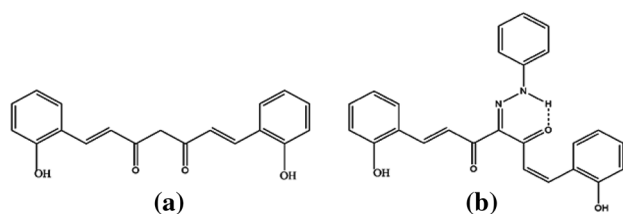

Fig. 1 The molecular structure of **a** 1,7-bis(2-hydroxyphenyl)hepta-1,6-diene-3,5-dione and **b** the inhibitor HPHDD

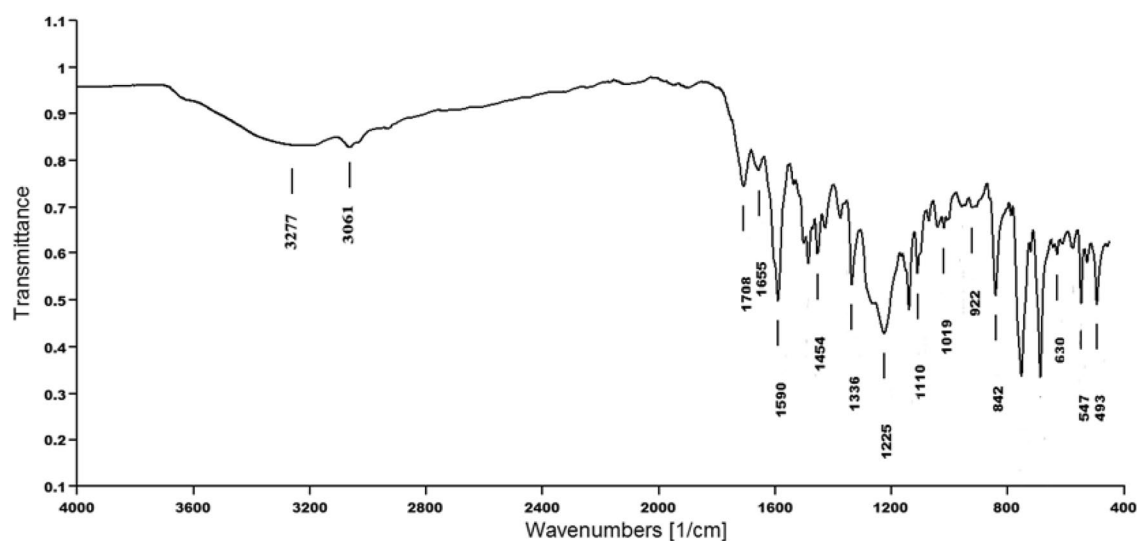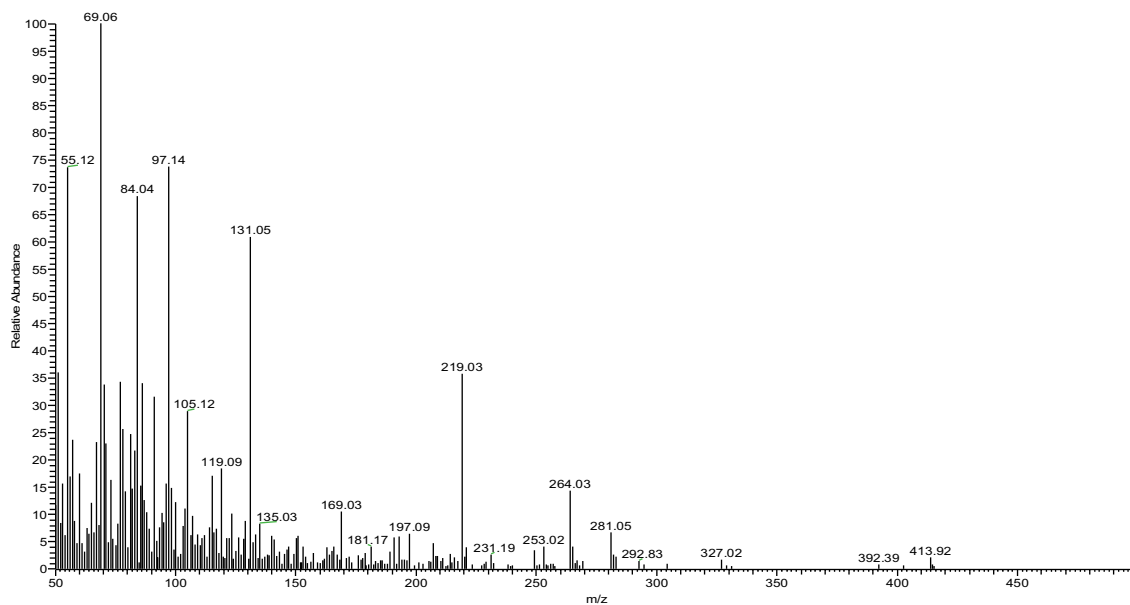**Fig. 2** IR spectrum of the synthesized inhibitor

Fig. 3 Mass spectra of the inhibitor molecule

Table 2 C, H, N elemental analysis of the synthesized arylazo compound

Element %	C %	H %	N %
Found	71.98	4.4	6.6
Calculated	72.00	4.8	6.7

Table 3 Weight loss data for MS in 1 M HCl without and with different concentrations of HPHDD at 28 °C

Conc.	Arylazo (K)	η_w%	Diketone (K)	η_w%
Blank	4.401			
50 ppm	1.197	72.8	2.11	52.06
75 ppm	0.825	81.25	1.83	58.41
100 ppm	0.599	86.38	1.45	67.05
150 ppm	0.483	89.03	0.972	77.91

3.2 Weight Loss Measurements

The values of corrosion rate, inhibition efficiency (η_w), and the degree of surface coverage (θ) for MS immersed in 1 M HCl in the absence and presence of different concentrations of HPHDD from the weight loss method are shown in Table 3. The results show that the corrosion rate (k) decreases in the presence of inhibitor and the percentage of inhibition increases with increasing concentration of the inhibitor, which is due to the increased adsorption of the HPHDD on the metal surface. The corrosion rate (k) in mg cm^{-2} h^{-1} was calculated by the following equation [7, 21]:

$$k = \frac{\Delta W}{S \times t},\tag{6}$$

where ΔW is the weight loss of coupon (mg), S is the total area of the coupon (cm^2), and t is the time of treatment (h).The degree of surface coverage (θ) and the inhibition efficiency η_w [22–24] were calculated using Eqs. 7, 8, respectively.

$$(\theta) = \frac{K_o - K}{K_o}\tag{7}$$

$$\eta_w = \frac{K_o - K}{K_o} \times 100\tag{8}$$

where K_o and K are the values of the corrosion rate without and with inhibitor, respectively. From the results (Table 3) it is clear that inhibition efficiency increases with increase in the concentration of the inhibitor. The maximum inhibition efficiency indicates that the inhibitor adsorbed effectively on MS surface and led to the formation of a strong metal–inhibitor interaction and also it decreases the chloride ion attack on MS surface.

3.3 Comparison of Inhibition Efficiency of Arylazo Compound with Parent Diketone

The inhibition efficiencies of arylazo compound and parent diketo compound were compared using weight loss measurements of MS specimens in 1 M HCl at 28 °C. The analysis (Table 3) revealed that the inhibition efficiency of the arylazo compound is greater than the parent compound. The presence of the (C=N) group enhanced the corrosion
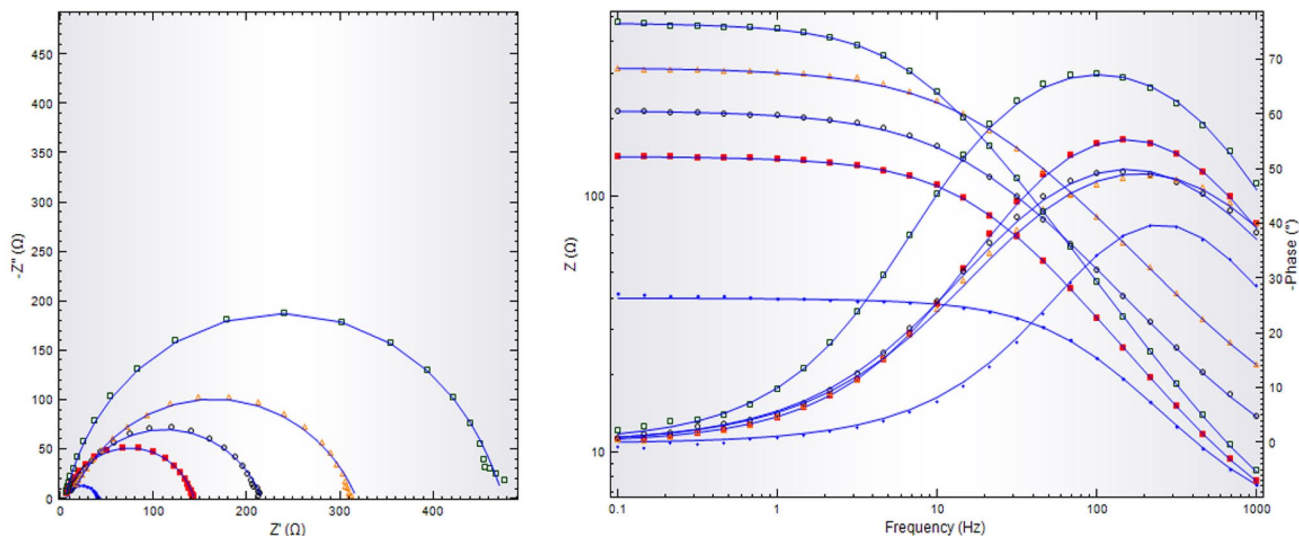
Fig. 4 EIS results of MS in 1 M HCl solution (blue-filled circle) and containing 50 ppm (red-filled square), 75 ppm (open circle), 100 ppm (yellow-filled triangle), 150 ppm (open square) of the inhibitor and the Bode plots. (Color figure online)

Table 4 The parameters obtained from fitting the EIS data in 1 M HCl test solution, for the absence and presence of inhibitor

Conc.	R_{ct} (Ω cm^2)	CPE (μS cm^{-2})	$\eta\%$
Blank	34.9	164	
50 ppm	139	150	74.89
75 ppm	209	143	83.3
100 ppm	308	96.3	88.67
150 ppm	438	32.6	92.03

Fig. 5 Circuit diagram for EIS measurements (Randles circuit)

inhibition behavior of the arylazo compound. The more number of heteroatoms (electron donating centers) in the arylazo compound helps the compound to actively participate in corrosion inhibition mechanism.

3.4 Electrochemical Measurements

3.4.1 Electrochemical Impedance Spectroscopic Measurements

The behavior of the metal/solution interface was studied using electrochemical impedance spectroscopic technique. The plot of the real part of impedance against the imaginary part gives a Nyquist plot. The Nyquist plots of MS in 1 M HCl solution in the absence and presence of different concentrations of HPHDD are shown in Fig. 4. In the Nyquist plots, a depressed single capacitive loop was obtained in each case, i.e., the center of the each semicircle is depressed by an angle of $(1 - n) = 90°$. The parameters associated with impedance analysis and the percentage efficiency calculated are given in Table 4.
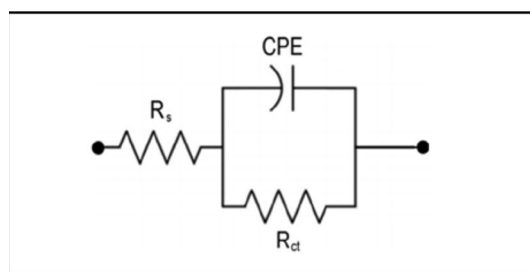
Electrochemical equivalent circuit model for the corrosion studies is shown in Fig. 5. The Randles circuit is one of the simplest cell models. It is used to model corrosion processes. The R_{ct} is the charge transfer resistance and R_s is the solution resistance [25]. Modeling an electrochemical phenomenon with an ideal capacitor assumes that the surface under investigation is homogenous which normally not the case is. Since the interface is not ideal, a constant phase element is used instead of pure capacitance. CPE is the constant Phase element. This non-ideal behavior can be explained with the electrical double layer theory. There exists two capacitors in serial, one between the metal and outer Helm Holtz plane and another through the Gouy Chapman diffuse layer, and as a consequence a differential capacitance behavior occurs [26]. The impedance of the CPE could be expressed as follows [27, 28]:

$$z_{CPE} = \left[Y_o (j\omega)^n \right]^{-1}, \tag{9}$$

where Y_o is the admittance of an ideal capacitance; $j^2 = -1$ is the imaginary number; ω is the angular frequency; and n

is an empirical constant ranging from 0 to 1. The n values are connected to the deviation of ideal capacitance behavior. For ideal electrodes, the value of n is equal to one and for a pure resistor n is equal to zero. The inhibition efficiency was calculated using the following equation [29, 30]:

$$\eta\% = \frac{R'_{ct} - R_{ct}}{R'_{ct}} \times 100 \tag{10}$$

where R_{ct} and R'_{ct} are the charge transfer resistances obtained in the solutions without and with inhibitor, respectively. It is evident that the R_{ct} values are increasing with increase in the concentration of the inhibitor. In case of uninhibited solution, the R_{ct} obtained was only 34.9 Ω cm^2, whereas in the case of inhibitor solution, the R_{ct} obtained (139 Ω cm^2) was relatively larger when compared to the blank solution. This shows that the inhibitor molecule adsorbed on the MS surface decreases the area available for H$^+$ ion reduction. At the same time, the value of CPE decreases with the concentration of inhibitor as the inhibitor displaces the other ions originally adsorbed on the surface. The results show that the protective adsorption layer formed by the inhibitor molecules on metal surface provides an effective barrier to the corrosion media. The formation of a surface film by HPHDD on the MS either decreases the local dielectric constant and/or increases the thickness of electrical double layer. The $\eta\%$ value is maximum (92%) for 150 ppm of the inhibitor. The results of EIS studies are in accordance with the results obtained from weight loss method. The absolute value of impedance and phase shifts are plotted as a function of frequency in two different plots giving a Bode plot as shown in Fig. 4. This is the more complete way of presenting the data. The Bode plots show that the break point frequency shifted gradually to lower values as the concentration of the inhibitor increases. The Bode plots show a slightly broadened maximum which may account for the formation of a protective layer after 1 h of immersion time.

3.4.2 Polarization Measurements

The potentiodynamic polarization curves of the MS in 1 M HCl and at different concentrations of HPHDD are shown in Fig. 6. Using the Nova Software, the cathodic and anodic slopes of Tafel plots were determined. The corresponding corrosion potential (E_{corr}) and current density (I_{corr}) obtained are given in Table 5. The Tafel plots show that the addition of HPHDD has a pronounced inhibitive effect on the anodic and cathodic part of the curves, while the corrosion potential (E_{corr}) is only slightly shifted. In the inhibited solution, the E_{corr} has shifted to more negative direction than the uninhibited solution. This negative shift of E_{corr} indicates that this Schiff base has the ability
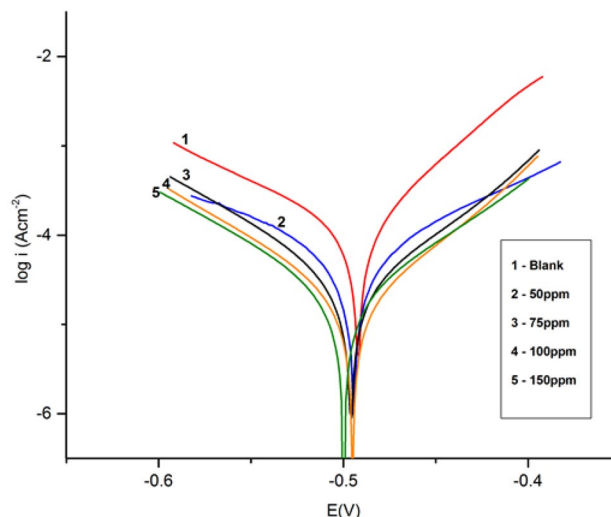

Fig. 6 Potentiodynamic polarization curves for mild steel in 1 M HCl solution at different concentrations of the inhibitor

to inhibit the acid corrosion of MS. The literature suggests that if the corrosion potential displacement on addition of inhibitor is greater than 85 mV, the inhibitor can be classified as cathodic or anodic type and if it is less than 85 mV, then the inhibitor can be considered as a mixed type of inhibitor [31]. Hence HPHDD can be considered as a mixed type inhibitor.

The polarization curves show that the cathodic and anodic current densities are decreasing gradually with increasing concentrations of the inhibitor. The values of the slopes β_a and β_b of the Tafel plots are decreasing which confirms that the inhibitor is not influencing the corrosion reactions; instead HPHDD is forming a barrier film on metal surface creating a substantial resistance against the charge transfer at the interface [32]. A more pronounced decrease in cathodic part indicates that the inhibitor affects the cathodic branch of corrosion process in a significant manner. This is due to a greater suppression of the cathodic hydrogen evolution than the anodic metal dissolution. The results (Table 5) indicate a significant lowering in the values of I_{corr} with the increasing concentration of HPHDD. The inhibition efficiencies were calculated from polarization measurements according to the relation [33].

$$\eta\% = \frac{I^*_{corr} - I_{corr}}{I^*_{corr}} \times 100 \tag{11}$$

where I^*_{corr} and I_{corr} are the corrosion current densities without and with inhibitor, respectively. The results show that the inhibition efficiency increased considerably with increase in the concentration of inhibitor, reaching a maximum of 93.98% for 150 ppm of inhibitor. The potentiodynamic

measurements reveal that HPHDD is a good corrosion inhibitor for MS against 1 M HCl solution.

3.4.3 Effect of Temperature

The EIS measurements were also realized in temperature range from 28 to 50 °C to study the thermal stability of the inhibitor molecule. The EIS results obtained for 1 M HCl solution in the absence and presence of 100 ppm of inhibitor at different temperatures were studied (Figs. 7, 8). The charge transfer resistance, CPE, and efficiency calculated are listed in Table 6. The R_{ct} values decreased and CPE values increased gradually with temperature. At 50 °C, the R_{ct} values of blank and 100 ppm of inhibitor are 22.5 Ω cm^2 and 106 Ω cm^2 respectively. At 50 °C, an efficiency of 78% is observed. The decrease may be due to the desorption of the inhibitor molecules from the adsorption sites at high temperature.

3.5 Adsorption Isotherms

Adsorption isotherms provide information about the mechanism of adsorption and surface behavior of adsorbed species.

Attempts were made to fit the data from polarization curves to most common adsorption isotherms. The Langmuir isotherm (Fig. 9) was found to fit best for HPHDD which confirms the adsorption of inhibitor molecules on the metal surface. The Langmuir isotherm for monolayer adsorption can be formulated as

$$\frac{C_{inh}}{\theta} = \frac{1}{K_{ads}} + C_{inh}, \tag{12}$$

where C_{inh} is the concentration of the inhibitor; θ is the fractional surface coverage; and K is the adsorption equilibrium constant. The intercept of the plot gives the value of K_{ads}. This value was calculated as 1.5321×10^4 M^{-1}, which indicates that a high proportion of HPHDD is adsorbed on steel surface [34, 35]. The K_{ads} and ΔG^o are related by the equation

$$\Delta G° = -RT \ln\left(55.5\, K_{ads}\right), \tag{13}$$

where R is the universal gas constant and T is the temperature in kelvin.

The calculated value of $\Delta G°_{ads}$ is − 34.17 kJ/mol. The negative values of $\Delta G°_{ads}$ indicate that the adsorption of

Table 5 Electrochemical parameters for MS in 1 M HCl solution containing different concentrations of the inhibitor

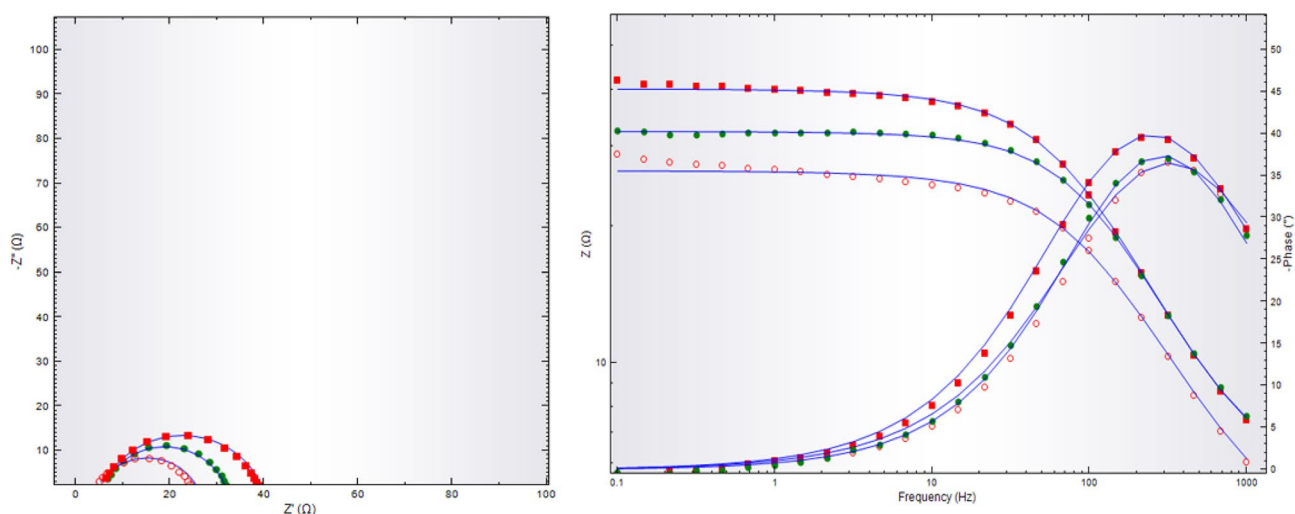| Conc. (ppm)	β_a (mV/dec)	$-\beta_c$ (mV/dec)	E_{corr} vs. SCE (V)	j_{corr} (µA/cm^2)	θ	$\eta\%$
Blank	75	112	− 0.493	209.95		
50 ppm	76	92	− 0.494	38.947	0.8145	81.45
75 ppm	74	88	− 0.496	34.236	0.8369	83.69
100 ppm	68	82	− 0.495	20.318	0.9032	90.32
150 ppm	72	87	− 0.499	12.629	0.9398	93.98

Fig. 7 EIS results of MS in 1 M HCl at different temperatures (red-filled square) 28 °C, (green-filled circle) 40 °C, (red open circle) 50 °C. (Color figure online)
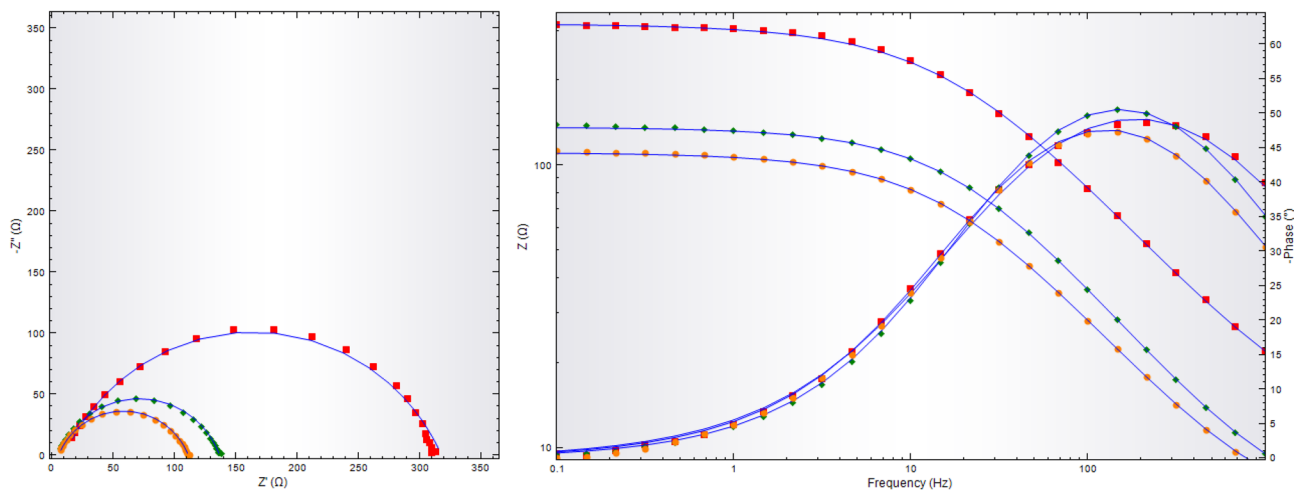
Fig. 8 EIS results of MS in 100 ppm of the inhibitor at different temperatures (red-filled square) 28 °C, (green-filled diamond) 40 °C, (yellow-filled circle) 50 °C. (Color figure online)

Table 6 The parameters obtained from fitting the EIS data in 1 M HCl test solution and in the presence of 100 ppm of inhibitor at different temperatures

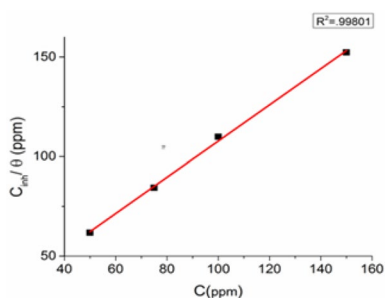| Temperature (°C)	R_{ct} (Ω cm^2) Blank	CPE (μS cm^{-2}) Blank	R_{ct} (Ω cm^2) Inhibitor	CPE (μS cm^{-2}) Inhibitor	$\eta\%$
28	34.9	164	308	96.3	88.67
40	26.8	179	131	168	84.05
50	22.5	226	106	253	78.77

Fig. 9 Langmuir adsorption isotherm for MS in 1 M HCl solution containing different concentrations of the inhibitor

HPHDD on the metal surface is a spontaneous process. The studies reveal that the value of ΔG°_{ads} up to -20 kJ/mol or lower is consistent with electrostatic interactions between the charged inhibitor molecule and charged metal which indicates a process of physisorption. The ΔG°_{ads} value around -40 kJ/mol or higher is considered as evidence for coordinate covalent bonding of molecules on metal surface (chemisorption) [36, 37]. The obtained ΔG°_{ads} value -34.17 kJ/mol suggests that the HPHDD adsorption on MS is not merely physisorption or chemisorption but includes a comprehensive adsorption of both.

3.6 Surface Analysis

SEM images recorded were used to study the surface morphology of MS specimen in acidic solution. Figure 10a–c shows the 1000 times magnified images of polished MS, the corroded MS in HCl solution, and the surface of MS immersed in 1 M HCl solution containing 150 ppm inhibitor for 3 days, respectively. A number of pits and cracks are seen in the SEM image of MS immersed in HCl solution (Fig. 10b). These are the results of aggressive action of HCl on MS Surface. In the presence of inhibitor (Fig. 10c), the surface is free from the pits and cracks except polishing line. This is due to the formation of a barrier film by the inhibitor. The inhibitor prevents the metal dissolution and protects the MS from corrosion. The protective film formed may be decreasing the surface area available for the reduction of H$^+$ ions and thereby acting as a strong barrier to further anodic metal dissolution.

Energy dispersive X-ray (EDX) spectra were used to determine the elements present on the MS surface before and after exposure to the inhibitor solution. Figure 11 shows the EDX spectra of the MS surface in the absence and the presence of inhibitor solution. In uninhibited solution, only the peaks for iron and oxygen are present on the sample. In the spectra of the inhibited solution, there is a peak for nitrogen and a more enhanced peak for oxygen. The data
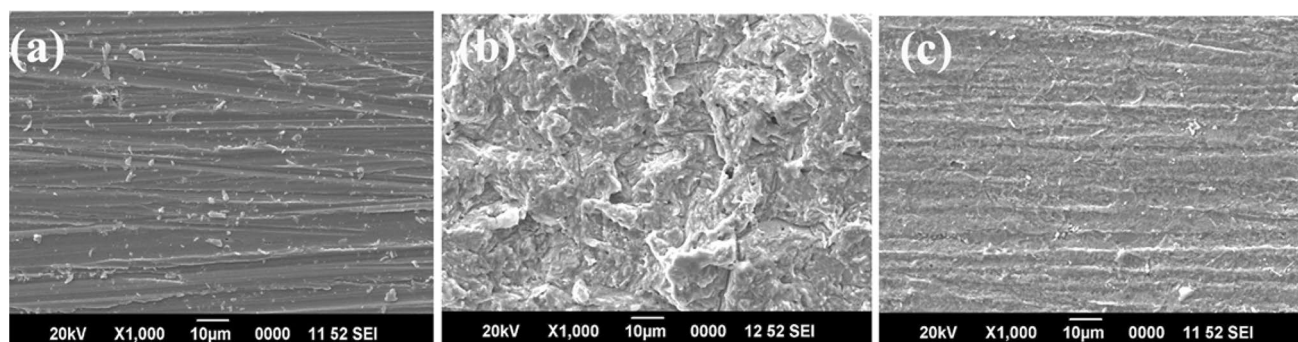
Fig. 10 SEM images of polished MS (**a**), MS in the absence (**b**) and the presence of 150 ppm of the inhibitor (**c**) after 3 days of immersion time
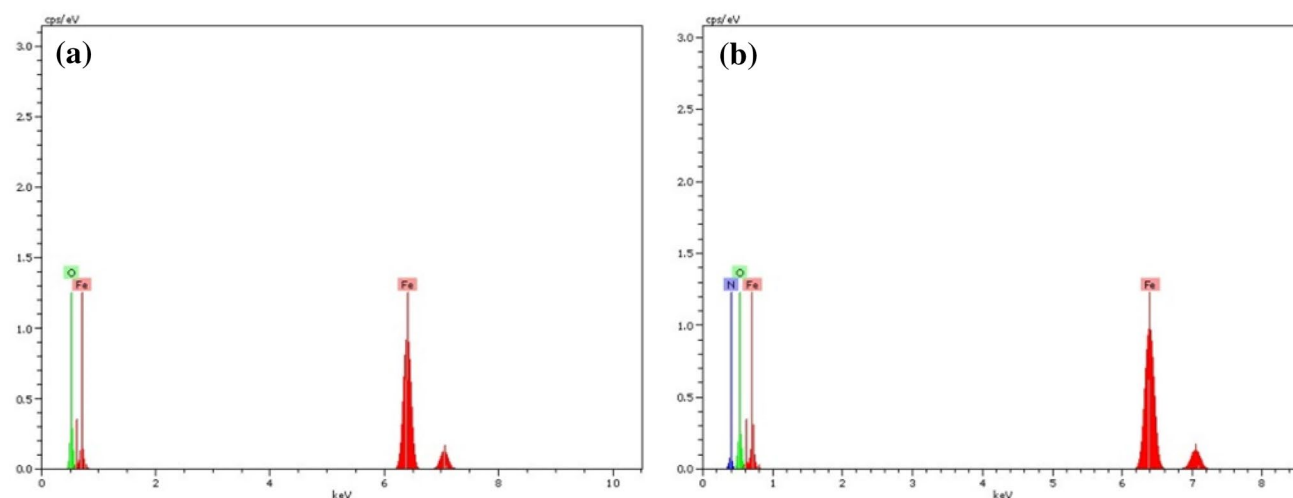

Fig. 11 EDX spectra of MS in the absence (**a**) and presence of 150 ppm of the inhibitor (**b**)

reveal the presence of an organic compound containing oxygen and nitrogen on sample surface. The higher electron density on the functional groups leads to the formation of a surface film through greater adsorption and consequently higher inhibition.

AFM is the most versatile and powerful microscopy technology for studying the surface morphology of samples at nano to microscale. The two-dimensional and three-dimensional AFM images of the MS surface exposed to 1 M HCl solution and with 100 ppm of HPHDD for 72 h are given in Fig. 12. The AFM images of MS in 1 M HCl (Fig. 12a, b) show the presence of many narrow pits of few micrometer ranges. The metal in the pit dissolves along with the reduction of oxygen. The rapid dissolution of metal in the pit results in a build-up of excessive positive charge in the pit followed by the migration of chloride ion into the pits to maintain the electroneutrality condition. Thus, high concentration of chloride ions, along

with low solution pH values, strongly favors the process of corrosion. Fig. 12c, d shows the MS surface exposed to 100 ppm of the inhibitor for 72 h which shows the presence of a uniform inhibitor layer over the MS surface due to the adsorption of the inhibitor on the MS surface. The protective barrier film formed prevents the pitting process thereby increasing the inhibition efficiency.

3.7 Quantum Chemical Studies

Quantum chemical calculations (using DFT method) were performed to investigate the effect of different physiochemical parameters such as chemical structure, charge density at the active centers (heteroatoms) of the molecule, and the mode of adsorption on the inhibition efficiency of the inhibitor. The optimized molecular structure and their calculated HOMO and LUMO levels of corrosion inhibitor HPHDD are shown in Fig. 13. Quantum chemical parameters obtained such as
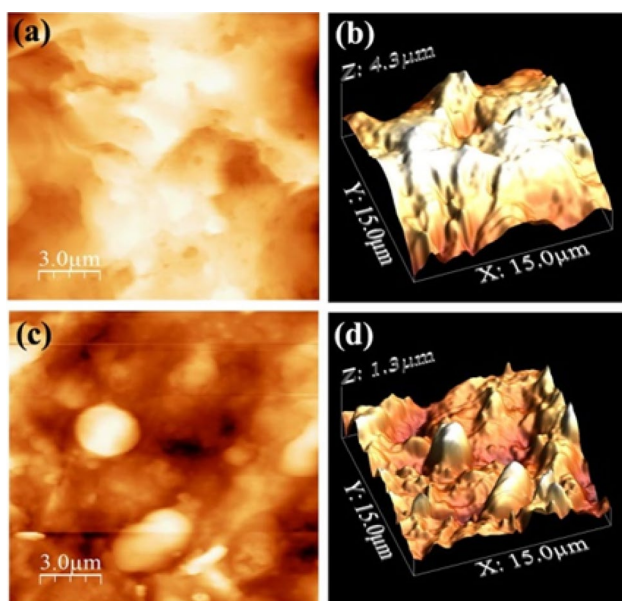
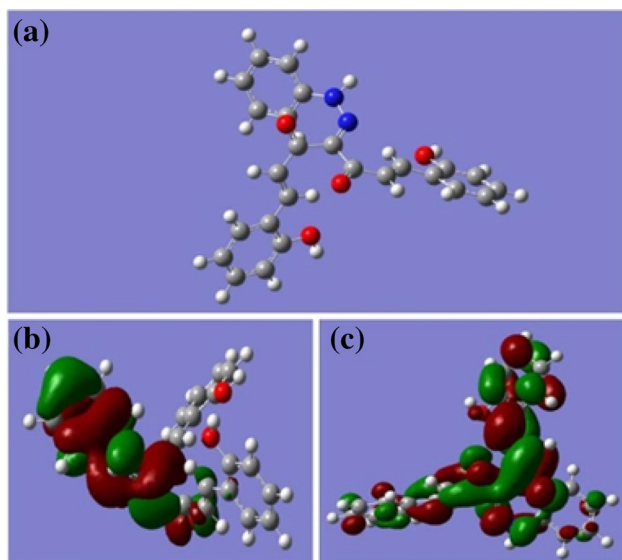**Fig. 12** AFM images of MS in the absence (**a, b**) and presence of 150 ppm of the inhibitor (**c, d**)

Fig. 13 The optimized molecular structure (**a**) and their calculated HOMO (**b**) and LUMO (**c**) levels of corrosion inhibitor HPHDD using DFT at the B3LYP/6-31G (d, p)basis set

the energy of highest occupied molecular orbital (E_{HOMO}), the energy of the lowest unoccupied molecular orbital (E_{LUMO}), and the dipole moment (μ) of the molecule obtained are given in Table 7. Different parameters are used to explain the electron transfer mechanism between inhibitor molecule and the metal surface. The ionization potential (I), the electron affinity (A), absolute electronegativity (χ), absolute hardness (η), stability of the molecule (σ), electrophilicity index (ω), and the change in the number of electrons transferred (ΔN) are the important parameters used to reveal the electron transfer mechanism between inhibitor molecule and the metal surface which are calculated and collected in Table 7. The high value of E_{HOMO} indicates the tendency to donate electrons and the lower value of E_{LUMO} shows the ability of the molecule to accept electrons. The energy values obtained suggest the better inhibition efficiency of the compound. The lower energy gap (ΔE) shows the higher reactive nature of the molecule which in turn increases the inhibition efficiency. From the earlier studies it is clear that if the ΔN value is less than 3.6 ($\Delta N < 3.6$), the inhibition efficiency of the inhibitor enhances by increasing the electron donation to the metal surface. The ΔN value obtained in the study proves that the synthesized compound is a good inhibitor. Mulliken charges on heteroatoms determined by optimization process are presented in Table 8.

The two types of adsorption responsible for the formation of protective layer are physisorption and chemisorption. The calculations show that there is more than one active center in the inhibitor molecule and all the active centers (heteroatoms) carry a high value of negative charge. These negatively charged heteroatoms can easily donate the electrons to the vacant d orbitals of the metal which results in the physisorption. Chemisorption can be better explained as the aromatic ring moiety of the inhibitor donates the π electrons and the heteroatoms donate the lone pair of electrons to the metal surface. A molecule with more planarity may be considered as a good inhibitor rather than a molecule with less planarity. The optimized structure clearly shows the planarity of the aromatic rings. This again correlates with high inhibition efficiency of the mixed type inhibitor HPHDD.

3.8 Mechanism of Inhibition

The arylazo molecule exists as protonated through nitrogen atoms in HCl solutions and the protonated inhibitor molecule

Table 7 Quantum chemical parameters for the inhibitor with the DFT at the B3LYP/6-31G (d, p)basis set

E_{HOMO}	E_{LUMO}	ΔE	I	A	μ	χ	σ	ω	ΔN
− 5.684	− 1.852	3.833 eV	5.684 eV	1.852 eV	7.974 D	3.768 eV	0.522	3.704	0.8433

Table 8 Calculated Mulliken atomic charges for heteroatoms of the inhibitor using DFT at the B3LYP/6-31G (d, p) basis set

| Atoms	Mulliken charges
15 O	-0.4959
18 N	-0.2933
19 N	-0.4238
33 O	-0.4719
37 O	-0.5578
50 O	-0.5572

could be assorted on the metal surface via chloride ions. This will cause an electrostatic attraction between the protonated inhibitor molecules and the metal surface. After the first electrostatic adsorption of the inhibitor molecules, via, formerly adsorbed chloride ions, the inhibitor molecule would directly be adsorbed on to the metal surface. The anodic sites on metal surface have vacant d orbitals of Fe^{2+} ions, which interact with the electrons of the inhibitor and adsorb the inhibitor leading to the formation of a strong barrier film on metal surface. The presence of π electrons and the non-bonded electrons of sulfur, nitrogen, and oxygen contributes to the strong metal inhibitor interaction. Besides, the double bonds present in the inhibitor molecule allow the back donation of metal d electrons to the π* orbital. Moreover, the adsorption of the inhibitors containing aromatic rings occurs mostly normal to the surface thereby inhibiting the corrosion by geometric blocking of the available cathodic and anodic sites on the metal surface.

3.9 Invitro Cytotoxicity

The results of invitro cytotoxicity studies of HPHDD towards DLA cells are shown in Fig. 11. The test compound was prepared in various concentrations ranging from 10 μg/ml to 200 μg/ml. The cytotoxicity of the compounds was determined in terms of percentage cell death produced by them. The cell death of DLA at the highest quantities of the inhibitor (200 μg/ml) was 80%. This indicates that the synthesized arylazo compound shows high degree of anti-tumor activity and is completely non-toxic and the inhibitor can be considered as an anti-tumor agent. The cytotoxic activity of the HPHDD is due to its unique structure which is similar to the 1,7-di aryl heptanoids (curcuminoids), the bioactive compounds with strong medicinal properties found in turmeric (Table 9; Fig. 14).

Table 9 Invitro cytotoxic studies of inhibitor HPHDD towards DLA

Drug con. (μg/ml)	10	20	50	100	200
% Cell death	11	23	43	65	80
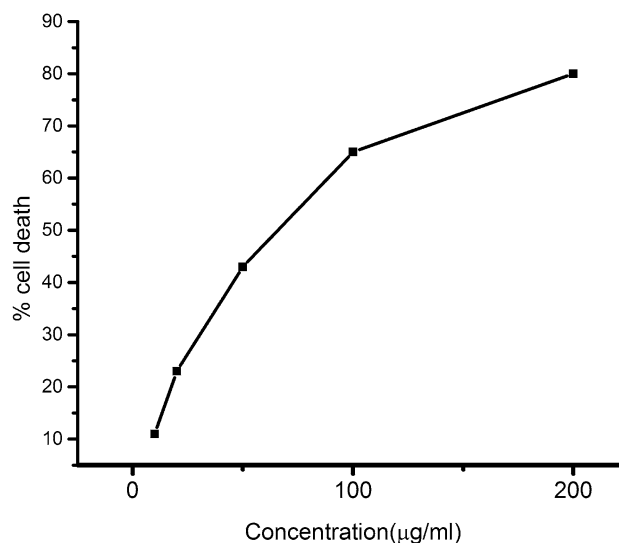
Fig. 14 The results of invitro cytotoxicity studies of HPHDD towards DLA

4 Conclusions

The inhibition efficiency of synthesized arylazo compound HPHDD has been investigated for MS corrosion in 1 M HCl solution. The electrochemical and non-electro chemical methods were made use of for the studies. The HPHDD is found to be a good anti-corrosive agent for MS against 1 M HCl corrosion. The inhibition efficiency increased with increasing inhibitor concentration. An efficiency of 93.98% was obtained by using 150 ppm of HPHDD. The anti-corrosive activity is mainly due to the adsorption of HPHDD on the MS surface. Reasonably good agreement exists between the values obtained from weight loss method, electrochemical impedance method, and Tafel extrapolation method. The synthesized compound is found to be a mixed type inhibitor affecting both cathodic and anodic sites. The EIS studies conducted at different temperatures revealed the efficiency of HPHDD at high temperatures. The adsorption obeyed Langmuir adsorption isotherm and regarded as a combined effect of both physical and chemical adsorption. The SEM images, the EDX spectra, and the AFM analysis confirm the formation of an inhibitor layer on MS surface. From the cytotoxic studies, the synthesized arylazo compound is assigned as good anti-cancerous compound.

References

1. Akrout H, Maximovitch S, Bousselmi L, Triki E, Dalard F (2007) Evaluation of corrosion non toxic inhibitor adsorption for steel in near neutral solution: L (+) ascorbic acid. Mater Corros 58:202–206

2. Akrout H, Bousselmi L, Triki E, Maximovitch S, Dalard F (2005) Adsorption mechanism of non-toxic organic inhibitors on steel in solutions at pH 8 determined by electrochemical quartz crystal microbalance measurements. Mater Corros 56:185–191

3. Hosseini MG, Ehteshamzadeh M, Shahrabi T (2007) Protection of mild steel corrosion with Schiff bases in 0.5 M H_2SO_4 solution. Electrochim Acta 52:3680–3685

4. Emregül KC, Atakol O (2004) Corrosion inhibition of iron in 1 M HCl solution with Schiff base compounds and derivatives. Mater Chem Phys 83:373–379

5. Aysel Yurt ÖA (2011) Diphenolic Schiff bases as corrosion inhibitors for aluminium in 0.1 M HCl: potentiodynamic polarisation and EQCM investigations. Corros Sci 53:3725–3732

6. Erbil M, Tüken T, Demir F, Kıcır N, Sıg G (2012) Inhibition effect of 1-ethyl-3-methylimidazolium dicyanamide against steel corrosion. Corros Sci 59:110–118

7. Soliman SA, Metwally MS, Selim SR, Bedair MA, Abbas MA (2014) Corrosion inhibition and adsorption behavior of new Schiff base surfactant on steel in acidic environment: experimental and theoretical studies. J Ind Eng Chem 20:4311–4320

8. Arab ST, Noor EAA (1993) Inhibition of acid corrosion of steel by some S-alkylisothiouronium Iodides. Corrosion 49:122–129

9. Elmsellem H, Harit T, Aouniti A, Malek F (2015) Adsorption properties and inhibition of mild steel corrosion in 1 M HCl solution by some bipyrazolic derivatives: experimental and theoretical investigations. Prot Met Phys Chem Surf 51:873–884

10. Chen S, Kar T (2012) Theoretical investigation of inhibition efficiencies of some schiff bases as corrosion inhibitors of aluminum. Int J Electrochem Sci 7:6265–6275

11. Belghiti ME et al (2016) Anti-corrosive properties of 4-amino-3,5-bis(disubstituted)-1,2,4-triazole derivatives on mild steel corrosion in 2 M H_3PO_4 solution: experimental and theoretical studies. J Mol Liq 216:874–886

12. Agrawal YK, Talati JD, Shah MD, Desai MN, Shah NK (2004) Schiff bases of ethylenediamine as corrosion inhibitors of zinc in sulphuric acid. Corros Sci 46:633–651

13. Oguzie EE (2005) Corrosion inhibition of mild steel in hydrochloric acid solution by methylene blue dye. Mater Lett 59:1076–1079

14. Zucchi F, Trabanelli G, Brunoro G (1992) The influence of the chromium content on the inhibitive efficiency of some organic compounds. Corros Sci 33:1135–1139

15. Noor Hasima, Bharat B, Aggarwal (2012) Cancer-linked targets modulated by Curcumin. Int J Biochem Mol Biol 3:328–351

16. Mark R, Kelley D, Logden, Mellssa L, Fishell (2014) Targetting DNA repair pathways for cancer treatment: what's new. Future Oncol 10:1215–1237

17. Krishnankutty K, John VD (2003) Synthesis, characterization, and antitumour studies of metal chelates of some synthetic curcuminoids. Synth React Inorg Met Org Chem 33:343–358

18. Krishnankutty K, Basheer M, Kamalakshy D (2009) Arylazo derivatives of some fluorinated β-diketones and their metal complexes. J Iran Chem Res 2:111–119

19. John VD, Ummathur MB, Krishnankutty K (2013) Synthesis, characterization, and antitumour studies of some curcuminoid analogues and their aluminum complexes. J Coord Chem 66:1508–1518

20. Tan SF, Ang KP, How GF (1991) Intermolecular and intramolecular hydrogen bonding in 5-pyridylmethylenehydantoins: IR and NMR study. J Phys Org Chem 4, 170–176

21. Li X, Deng S, Xie X (2014) Inhibition effect of tetradecylpyridinium bromide on the corrosion of cold rolled steel in 7.0 M H_3PO_4. Arab J Chem. https://doi.org/10.1016/j.arabjc.2014.05.004

22. Elkacimi Y, Achnin M, Aouine Y, Touhami ME, Alami A (2012) Inhibition of mild steel corrosion by some phenyltetrazole substituted compounds in hydrochloric acid. Port Electrochim Acta 30:53–65

23. Manjula P, Manonmani S, Jayaram P, S. R (2001) Corrosion behaviour of carbon steel in the presence of N-cetyl-N, N, N-trimethylammonium bromide, zinc and calcium gluconate. Anti-Corros Methods Mater 48:319–324

24. Bedair MA, Soliman SA, Metwally MS (2016) Synthesis and characterization of some nonionic surfactants as corrosion inhibitors for steel in 1.0 M HCl. J Ind Eng Chem 41:10–22

25. Singh A, Avyaya JN, Quraishi MA (2012) Schiff' s base derived from the pharmaceutical drug Dapsone (DS) as a new and effective corrosion inhibitor for mild steel in hydrochloric acid. Res Chem Intermed. https://doi.org/10.1007/s11164-012-0577-y

26. Gokmen SI, Erbil M (2016) Assessment of the inhibition efficiency of 3, 4-diaminobenzonitrile against the corrosion of steel. Corros Sci 102, 437–445

27. Manivel A, Ramkumar S, Wu JJ, Asiri AM, Anandan S (2014) Exploration of (S)-4, 5, 6, 7-tetrahydrobenzo [d] thiazole-2, 6-diamine as feasible corrosion inhibitor for mild steel in acidic media. J Environ Chem Eng 2:463–470

28. Hassan HH (2007) Inhibition of mild steel corrosion in hydrochloric acid solution by triazole derivatives. Part II: time and temperature effects and thermodynamic treatments. Electochim Acta 53:1722–1730

29. Yurt A, Balaban A, Kandemir SU, Bereket G, Erk B (2004) Investigation on some Schiff bases as HCl corrosion inhibitors for carbon steel. Mater Chem Phys 85:420–426

30. Hassan HH, Abdelghani E, Amin MA (2007) Inhibition of mild steel corrosion in hydrochloric acid solution by triazole derivatives Part I. Polarization and EIS studies. Electochim Acta 52:6359–6366

31. Bouanis M et al (2016) Corrosion inhibition performance of HCl solution: gravimetric, electrochemical and XPS studies. Appl Surf Sci 389:952–966

32. Mazumder MAJ, Al-Muallem HA, Faiz M, Ali SA (2014) Design and synthesis of a novel class of inhibitors for mild steel corrosion in acidic and carbon dioxide-saturated saline media. Corros Sci 87:187–198

33. Solmaz R, Kardas G (2008) Investigation of adsorption and inhibitive effect of 2-mercaptothiazoline on corrosion of mild steel in hydrochloric acid media. Electochim Acta 53:5941–5952

34. Xu B, Liu Y, Yin X, Yang W, Chen Y (2013) Experimental and theoretical study of corrosion inhibition of 3-pyridinecarbozalde thiosemicarbazone for mild steel in hydrochloric acid. Corros Sci 74:206–213

35. Zhou X, Yang H, Wang F (2011) Electrochimica Acta [BMIM] BF 4 ionic liquids as effective inhibitor for carbon steel in alkaline chloride solution. Electrochim Acta 56:4268–4275

36. Likhanova NV et al (2010) The effect of ionic liquids with imidazolium and pyridinium cations on the corrosion inhibition of mild steel in acidic environment. Corros Sci 52:2088–2097

37. El-lateef HMA (2014) Experimental and computational Investigation on the corrosion inhibition characteristics of mild steel by some novel synthesized imines in hydrochloric acid solutions. Corros Sci. https://doi.org/10.1016/j.corsci.2014.11.040

SYNTHESIS,CHARACTERIZATION, CYTOTOXIC& ANTITUMOUR ACTIVITIES OF SCHIFF BASES OF CURCUMINOID ANALOGUES AND THEIR COPPER COMPLEXES

Raina Jose Cherappanath*, Delmy Davis, Dr.V D John

Department of Chemistry, Christ College Autonomous (Affiliated to University of Calicut), Irinjalakuda, Kerala India
rainajc@gmail.com

Abstract
Synthesizedand characterized Schiff bases of four curcuminoidanalogues and their copper(II) complexes of ML_2 stoichiometry. In vitro cytotoxic studies of the synthesized Schiff bases and their copper complexes were done against Daltons Lymphoma Ascites cells usingTrypan blue exclusion method. Compound I**a**and the corresponding copper complex were found to be more active towards increase in life span of tumour-bearing mice and reducing thesolid tumour(ErlichAscites Carcinoma cells) volume in mice.
Keywords: Curcuminoids;IR; NMR; mass spectra; cytotoxicity;antitumour.

Introduction
        Curcuminis a naturalpolyphenolic compound which is responsible for the yellow colour of the turmeric, possess potent antiinflammatory[i-iii], antifungal, antiproliferative, antioxidant [iv] and anticancer activities[v-xi]. Turmericcontains three different kinds of curcuminoids namely curcumin,demethoxycurcumin and bisdemethoxycurcumin.Structurally they are linear 1,7-diaryl-1,6-heptadiene-3,5-diones which exist in rapid equilibrium with its tautomericenol form. The synthesized curcuminoid analogues retain the α,β unsaturated 1,3-diketo moiety of the natural curcuminbut the aryl ringsare modified.The poor bioavailability of the curcumin can be improved by the use of structural analogues of curcumin.
Curcuminoidsform metal complexes in the same manner as 1,3-diketones do.The curcuminoids and their metal complexes possess remarkable biochemical activities[xii]. The anticarcinogenic activity of curcumin is due to the direct antioxidant and free radical scavenging properties as well as their ability to indirectly increase glutathione levels, thereby assisting in detoxification of mutagens and carcinogens.Curcuminoids are powerful chelating agents and can be used in therapy. Chelation therapy is a medical procedure that involves the administration of chelating agents to remove heavy metals from the body[xiii,xiv]. These ligands bind to heavy metals such as cadmium and lead, thereby reducing the toxicity of these heavy metals.The metal chelating abilities of curcuminoids is through the β diketogroup[xv,xvi]which in turn forms new structural entities with modified biochemical activities. The physicochemical features such as the planarity, hydrophobicity and size and nature of the

ligand, as well as the coordinationgeometry of the metal complex all haveimportant roles in determining the binding/intercalating mode of copper complexes to DNA. According to these observations, a large number of copper complexes has been and is still being tested as anticancer drug.

In the present study,as continuation of our work we synthesized and characterized Schiff bases of four curcuminoid analogues and their copper complexes.We have focused on the cytotoxic effects of curcuminoids onErlichAscites Carcinoma cells(EAC) and Daltons Lymphoma Ascites(DLA)tumour cell lines.

Experimental
Materials
The chemicals required were procuredfrom Sigma Aldrich chemical suppliers and were of analytical reagent grade. Daltons Lymphoma Ascites cells and ErlichAscites Carcinoma cells were obtained from the Adayar Cancer Research Institute, Chennai, India and maintained as transplantable tumours in Swiss albino mice by injecting a suspension of cells intraperitoneally(ip). Swiss albino mice for the experiments were purchased from Vetenary College, Thrissur, Kerala, India.The animals were fed with normal mouse chow (Lipton India) and water *ad libitum*.

Synthesis of 1,7-di aryl-hepta-1,6diene-3,5-diones.
The curcuminoid analogues wereprepared by the condensation of aromatic aldehydeswithacetyl acetone-boric oxide complex in ethyl acetate medium in the presence of tributyl borate and n-butylamine as reported earlier (Pabons Method)[xvii].The product was purified by column chromatography over silica gel (60-120 mesh) using 2:1 (v/v) chloroform: acetone mixture as the eluent and recrystallized twice from hot benzene to get pure crystalline material

Synthesis of Schiff Bases
The Schiff bases were synthesized by the coupling of benzene diazonium salt with β-diketones[xviii]. Benzene diazonium salt was prepared and added drop by drop to a solution of the β-diketone kept below 0^0c with constant stirring. The precipitated compound was filtered, washed with water and recrystallized from ethanol to get chromatographically pure (TLC) material.

Synthesis of metal complexes
The Cu (II) complexes were prepared by adding a methanolic solution of copper (II) acetate (25 ml, 0.001mol) to a solution of curcuminoidanalogue (25 ml, 0.002mol) in methanol and refluxed gently for 3 hrs. After reducing the volume to half, the solution was cooled to room temperature. The precipitated complex was filtered, washed with 1:1, methanol: water mixture and recrystallized from hot methanol.

Antitumor Experiments
In vitro cytotoxicity studies
In vitro cytotoxicity studies were carried out using the Schiff bases and their Cu(II) complexes dissolved in minimum quantity of DMSO. The tumour cells aspirated from the peritoneal cavity of tumour bearing mice were washed with PBS (Phosphate Buffered Saline) and centrifuged for 15minutes at 1500 rpm. Cell viability was determined usingTrypan blue exclusion method. ViableDLA cells (1×10^6 cells in 0.1 ml) were added to tubes containing various concentrations of the test compounds and the volume was made up to 1ml using PBS. Control tube contained only cell suspension. These mixtures were incubated for 3hrs at 37^oC.

Further, cell suspension was mixed with 0.1ml of 1% trypan blue and kept for 2-3 minutes and loaded on a haemocytometer. The number of stained (dead) and unstained (live) cells were counted and percentage cytotoxicity was evaluated by Trypan blue exclusion method[xix].

$$\% \, cytotoxicity = \left(\frac{No.of \; dead \; cells}{No.of \; dead \; cells + No.of \; live \; cells} \right) \times 100 \qquad (1)$$

Determination of tumour reducing activity
The animals (male mice, 6-8 weeks old) weighing 20-25g were divided into groups of 5 animals each. EACcells (1×10^6cells per animal) were injected into the peritoneal cavity of mice. One group of animals was kept as control, without injecting any test compound. The other groups were injected with different concentrations (20μg/ml, 10μg/ml and 5μg/ml) of the test compounds afterthe tumour formation and injections were continued for ten days. The mortality rate of animals due to tumour burden was noted and the percentage increase in life span (ILS) was calculated using the given formula.

$$\% ILS = \left(\frac{T-C}{C} \right) \times 100 \qquad (2)$$

Where, T and C are mean survival time of treated and control mice respectively in days[19].

Determination of effects of compounds on solid tumourdevelopment
The Swiss albino mice were used to study the effect of the synthesized compounds on solid tumourvolume reduction.Since the synthesized Schiff bases and their copper complexes are found to be more cytotoxic to DLA celllines, they were used to study its potential to reduce solid tumour induced by DLA cell lines in mice. The animals were divided into groups of six.Viable DLA cells (1×10^6cells per animal) were transplanted subcutaneously into the right hind limb of the mice. Drugs (50 and 100mg /kg of body weight) were injected to the animals on alternate days for two weeks. The group that received only DLA cells served as the control. The tumour development on animals was determined by measuring the diameter of the tumour growth in two perpendicular phases using vernier calipers, every third day for one month.The tumour volume was calculated using the formula given,

$$V = \frac{4}{3} \pi r_1 r_2^2 \qquad (3)$$

Where, r_1 and r_2 are the minor and major radii respectively[xx].

Analytical instruments
Carbon and hydrogen percentages were determined by microanalysis (Heraeus Elemental analyzer) and metal content by AAS (Perkin Elmer 2380). The electronic spectra were recorded on a Shimadzu UV-VIS-1601 Spectrophotometer. IR spectra were recorded on Perkin Elmer FTIR spectrophotometer. The ^{1}H NMR spectra were recorded on a FT-NMR spectrophotometer. The FAB mass spectra were recorded on a Joel SX–102 mass spectrophotometer from CDRI, Lucknow, India.

Results and Discussion
Structural characterization of 1,7-di aryl-hepta-1,6diene-3,5-diones
The synthesized curcuminoid analogues were characterized by CHN analysis, UV, IR, ^{1}H NMR and Mass spectral data (Table I). The UV spectra of the compounds in methanol show two absorption maxima corresponding to n→ π* and π→ π* transitions. The values at 260-300nm are due to $\pi \rightarrow \pi *$ transition and at 300-460nm are due to n→ $\pi *$ transitions of fully conjugated systems based on earlier reports. The presence of α, β unsaturation shifts the wavelength for the carbonyl absorption to a higher value.

Table I : Spectral data of synthesized 1,7-di aryl-hepta-1,6diene-3,5-diones

Compound	UV data λ_{max}(nm)	IR data cm^{-1} (Chelated C=O)	^{1}H NMR spectral data Chemical shift (ppm)			Mass spectral data (m/z)
			NH	Phenyl	Alkenyl	
HL^1	278,354	1629	9.695	7.233-7.438	6.856-7.734	561,367,145,105,77
HL^2	280,356	1626	9.936	7.359-7.565	6.78-7.85	413,264,131,105,77,69
HL^3	273,349	1615	9.607	7.365-7.430	7.157-7.415	513,333,179,131,105,77
HL^4	266,353	1621	9.036	7.371-7.837	6.983-7.954	582,377,204,105,77

IR spectra of synthesized ligands are characterized by the presence of three strong bands in the region 1590 cm^{-1} to 1710 cm^{-1} respectively due to the stretching of free carbonyl, intramolecularly hydrogen bonded carbonyl and C=N stretching vibrations . This shows that the compound exist in the intra-molecularly hydrogen bonded hydrazone-keto form. In the spectra, the strong intra-molecular hydrogen bonding shows a broad band in the region 2550-3600 cm^{-1}. There are a number of medium intensity vibrations observed in the region 1550-1600 cm^{-1} due to various stretching vibrations of the phenyl group, alkenyl& chelate ring. The band in the region 979 cm^{-1} and 974 cm^{-1} is assigned to the trans CH=CH vibration. The ^{1}H NMR spectra of synthesized curcuminoids also support the hydrazone-keto structure of the compound. The peaks corresponding to NH proton, alkenyl, and phenyl groups can be observed in the spectrum. Ligands displayed a one proton singlet at δ ~ 9.4ppm assignable to strong intra-molecularly hydrogen bonded NH proton[xxi]. The aryl protons show signals in the region 7.1 – 7.5ppm and the alkenyl protons show signals in the region of 6.5 – 8.0ppm. The mass spectra give an idea about the various fragmentation modes of the compounds. The mass spectra of the synthesized Schiff bases showed intense molecular ion peaks. Important peaks appeared in the spectra of compounds can be accounted by the fragmentation pattern. The peaks for [M+1] ion, [NH=N-C=C=O]$^+$ion together with other significant peaks are observed in mass spectra of synthesized Schiff bases. The remaining important peaks are that due to the fragment ions.
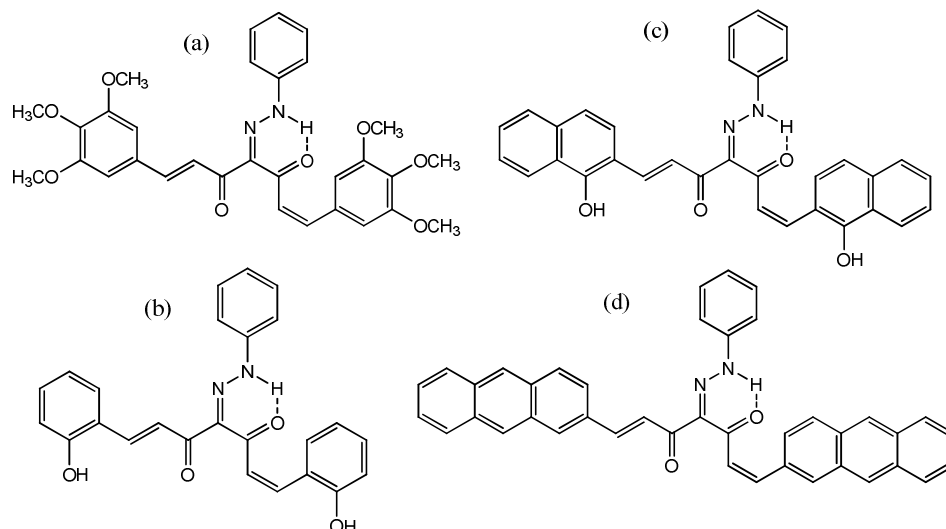
Fig.I. The structure of curcuminoid analogues
(a) 1,7-bis(3,4,5 tri methoxy phenyl)-4-(phenyl-hydrazono)-hepta-1,6diene-3,5-dione,(HL[1]);
(b)1,7-bis(2 hydroxy phenyl)-4-(phenyl-hydrazono)-hepta-1,6diene-3,5-dione,(HL[2]);
 (c)1,7-bis(2hydroxynaphthyl)-4-(phenyl-hydrazono)-hepta-1,6diene-3,5-dione,(HL[3]);
(d)1,7-bis(anthracenyl)-4-(phenyl-hydrazono)-hepta-1,6diene-3,5-dione,(HL[4]).

Structural characterization of copper complexes
The complexes have absorption maxima relatively same as that of ligands indicating that the structure of the ligands remains almost unaltered in complexes. There is a slight bathochromic shift of absorption maxima of complexes which shows the involvement of the carbonyl moiety in chelate formation. In the IR spectra of metal chelates, the band at ~1626 cm^{-1} due to intra molecularly hydrogen bonded carbonyl function disappeared and instead a strong band assignable to stretching of the metal coordinated carbonyl moiety appeared at ~1554 cm^{-1}. Additional bands appeared at ~405cm^{-1} to ~420 cm^{-1} are assignable to ν (M–O) vibrations. The replacement of NH proton by a metal ion is also evident from the absence of the broad band in the region of 2600 -3500 cm^{-1}which was present in the ligand.
Table II: Spectral data of the Cu (II) complexes

Compound	Elemental found(calculated) %			Analysis: IR data cm^{-1}		Mass spectral data (m/z)
	C	H	Cu	ν C=O	ν M-O	
[M(L^1)$_2$]	62.82(62.96)	5.43(5.28)	5.31(5.37)	1559	417,407	1182,834,740,274,198,169
[M(L^2)$_2$]	67.78(67.70)	4.42(4.5)	7.24(7.16)	1554	422,405	886,685,603,275,199,172
[M(L^3)$_2$]	72.82(72.95)	4.36(4.26)	5.74(5.84)	1557	418,410	1086,786,692,212,181,105
[M(L^4)$_2$]	80.21(80.40)	4.58(4.60)	5.11(5.18)	1554	420,408	1224,856,762,274,197,170

The main feature of NMR spectra of metal complex is the absence of singlet signal at δ ~ 9.4ppm which was due to the NH proton in the ligands. This indicates the replacement of NH proton by metal atom in metal complexes. The phenyl and alkenyl protons are not altered much since they are not involved in metal complexation. Thus the spectra of ligand and complexes are much similar except those of NH proton. In the mass spectra of complexes, all the compounds showed relatively intense peaks at m/z corresponding to ML$_2$ stoichiometry, where M is metal and L is ligand. Mass spectral fragmentation pattern plays an important role

in elucidating the structure of metal complexes. It was found that some fragment ions undergo rearrangement to form stable species. The mass spectral data shows that stepwise removal of aryl groups is the characteristic feature of all complexes.Smaller species such as O, OH, CH etc. are also eliminated. In all the cases $[ML_2]^+$ ion is the most intense peak.. Peaks due to $[ML_2]^+$, $[ML]^+$, L^+ and fragments of L^+ are also detected in the spectrum.
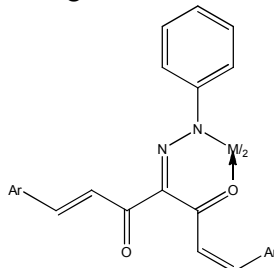

Fig.II.The structure of metal complex of curcuminoid analogue

In vitro cytotoxicity
*Invitro*cytotoxicity studies towards DLA cells revealed that both ligands and complexes exhibited greater %cell death at higher concentrations i.e., 200μg/ml.As concentration of drug compound increases from10μg/ml to 200μg/ml the %cell death increases.Comparing the ligands,$HL^1$with three methoxygroups was found to be more cytotoxic than other three ligands.All the metal complexes showed significant increase in %cell death than the ligands which shows that metal chelation enhances cytotoxicity of compounds considerably. Among the metal complexes the activity follows the order $[M(L^1)_2]> [M(L^2)_2])> [M(L^3)_2]>[M(L^4)_2]$. The copper complex of 1,7-bis(3,4,5 tri methoxyphenyl)-4-(phenyl-hydrazono)-hepta-1,6diene-3,5-dionewas found to be very effective and produced 98%cell death.The results of *in vitro* cytotoxicity of ligands and their copper complexes towards DLA cells are given in Table**.** III.

Table III: Percentage cytotoxicity towards DLA cells for curcuminoid analogues and Cu(II) chelates

Compounds	% cell death at different concentrations				
	10μg/ml	20μg/ml	50μg/ml	100μg/ml	200μg/ml
HL^1	13	22	52	65	90
HL^2	11	22	43	65	80
HL^3	11	20	40	63	78
HL^4	9	17	35	59	76
$[M(L^1)_2]$	20	34	58	77	98
$[M(L^2)_2]$	18	31	53	76	95
$[M(L^3)_2]$	17	27	55	71	90
$[M(L^4)_2]$	15	25	49	65	80

Effect of compounds on ascites tumour reduction (*in vivo*)
The animals of the tumour control group inoculated with Ehrlich ascites tumour cells survived for a period 16.6±1.49 days (Table IV). The group of animals which were given the drug 1,7-bis(3,4,5 tri methoxy phenyl)-4-(phenyl-hydrazono)-hepta-1,6diene-3,5-dione

survived for 26.3±1.5 days with the concentration 20μg/ml. The increase in life span for corresponding copper complex was maximum (86.7%) with 20μg/ml concentration. Effect of synthesized compounds (concentration 20μg/ml) on ascites tumour reduction is presented in Table IV. The effect of copper complexes of curcuminoid analogues on Ascites tumour reduction are shown in Fig.III.

TableIV: Effect of synthesized compounds (of concentration 20μg/ml) on ascites tumour reduction

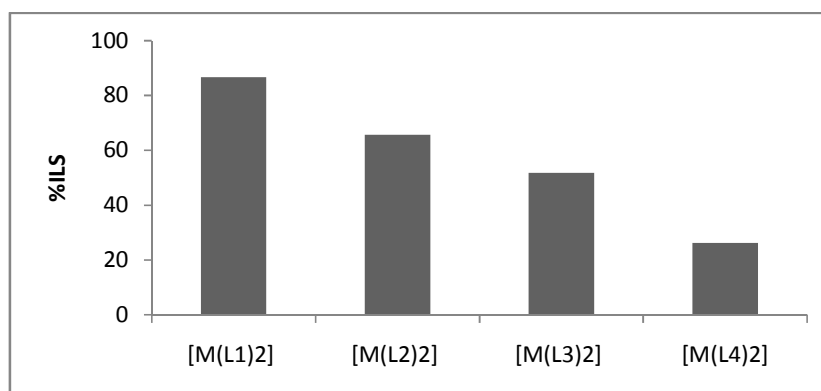| Sl. No.	Animal groups	No. of animals with tumour	No. of days survived	Percent ILS
1	control	5/5	16.6±1.49	
2	HL^1	5/5	26.3±1.5	58.4
3	HL^2	5/5	25.2±2.7	51.8
4	HL^3	5/5	24.3 ± 1.9	46.4
5	HL^4	5/5	18.4 ± 1.9	10.8
6	$[M(L^1)_2]$	5/5	31.0±1.7	86.7
7	$[M(L^2)_2]$	5/5	27.5±1.3	65.6
8	$[M(L^3)_2]$	5/5	25.2±2.63	51.8
9	$[M(L^4)_2]$	5/5	22.5 ± 1.8	26.2

Fig.III. Effect of copper complexes of curcuminoid analogues on Ascites tumour reduction

Solid tumourreduction(*in vivo*)
Inhibitory effect of compounds on tumour growth in mice by the intraperitoneal administration of compounds is shown graphically in Fig.IV. The graphs show that the curcuminoids and their complexes reduce the tumour volume in a good manner. The copper complexes are found to be more efficient in reducing tumour volume than their corresponding ligands.Tumour volumes on the thirtieth day for HL^1, HL^2, HL^3,HL^4 and control are $1.675cm^3$, $2.023cm^3$, $2.210cm^3$ $2.329cm^3$and $3.624cm^3$ respectively and for their copper complexesare $0.940cm^3$, $1.093cm^3$, $1.182cm^3$ and $1.203cm^3$ respectively. Copper complexes have been shown to possess a broader spectrum of activity and a lower toxicity

than the platinum drugs and are suggested to be able to overcome inherited and/or acquired resistance to cisplatin.
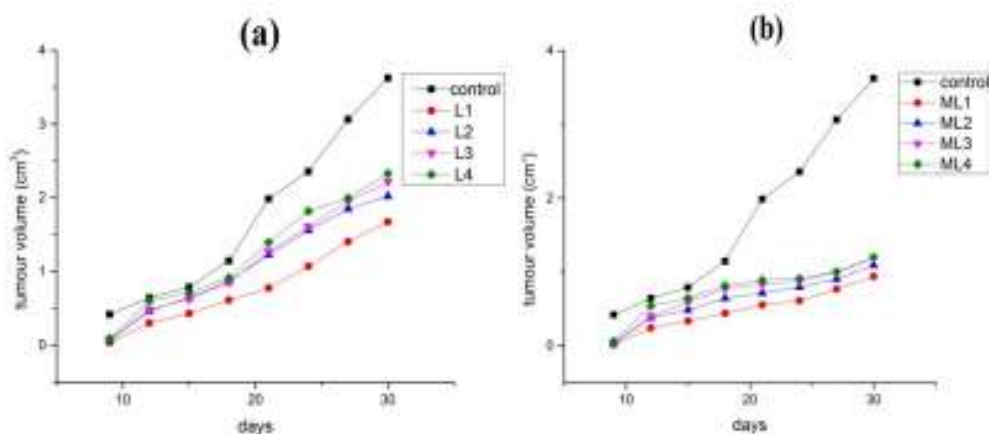

Fig.IV: Effect of curcuminoid analogues on solid tumour development(a), metal complexes on solid tumour development (b).

Conclusion
The newlysynthesized four Schiff bases of curcuminoid analogues and their copper complexes were characterized using different spectral techniques and investigated for their possible cytotoxic and anticancer activities. All the metal complexes exhibited enhanced cytotoxicand antitumouractivities than their ligands. Theinvitro cytotoxicity studiesreveal that metal chelation considerably increases the cytotoxicity of the Schiff bases towards DLA cells. The Cu(II) complex of1,7-bis(3,4,5 tri methoxy phenyl)-4-(phenyl-hydrazono)-hepta-1,6diene-3,5-dione was found to be the most active compound by producing 80% cell death. HL[4] with unsubstitutedanthracenyl ring is the least active compound compared to the other compounds.The antitumour studies (in vivo) on mice show that the hydroxyl and methoxy derivatives of diketones and their metal complexes havegreaterinhibitory effect on EAC and DLA cells. HL[1]and the corresponding copper complex were found to be more active towards increase in life span of tumour-bearing mice and reducing the solid tumour(EAC cells) volume in mice. The copper complexes possess maximum activity which is comparable with a standard anticancerous drug. The studies reveal that chelation remarkably enhanced the in vitro and in vivoantitumour activities.

Acknowledgement
The authors are grateful to University Grant Commission for the funding for FDP, P.G and research Department of Chemistry, Christ College Irinjalakkuda, Calicut University, National Institute of Technology, Trivandrum, CUSAT Cochin and Dr.RamdasanKuttan, ProfessorAmala Cancer Research CentreThrissur, India for the antitumour studies.

References
i.   Chainani-wu, N. Safety and Anti-Inflammatory Activity of Curcumin : *J. Altern. Complement. Med.***9,** 161–168 (1999).
ii.   Holt, P. R., Katz, S. & Kirshoff, R. Curcumin therapy in inflammatory bowel disease: A pilot study. *Dig. Dis. Sci.***50,** 2191–2193 (2005).
iii.   Shishodia, S., Sethi, G. & Aggarwal, B. B. Curcumin: Getting back to the roots. *Ann.*

*N. Y. Acad. Sci.***1056,** 206–217 (2005).

iv.   Ak, T. Chemico-Biological Interactions Antioxidant and radical scavenging properties of curcumin. **174,** 27–37 (2008).

v.   Iqbal, M., Sharma, S. D., Okazaki, Y., Fujisawa, M. & Okada, S. Dietary supplementation of curcumin enhances antioxidant and phase II metabolizing enzymes in ddY male mice: possible role in protection against chemical carcinogenesis and toxicity. *Pharmacol. Toxicol.***92,** 33–38 (2003).

vi.   Kuo, M. L., Huang, T. S. & Lin, J. K. Curcumin, an antioxidant and anti-tumor promoter, induces apoptosis in human leukemia cells. *Biochim. Biophys. Acta - Mol. Basis Dis.***1317,** 95–100 (1996).

vii. Subramanian, M., Sreejayan, Devasagayam, T. P. A. & Singh, B. B. Diminution of singlet oxygen-induced DNA damage by curcmin and related antioxidants. *Mutat. Res. Regul. Pap.***311,** 249–255 (1994).

viii. Azuine, M. A. & Bhide, S. V. Chemopreventive effect of turmeric against stomach and skin tumors induced by chemical carcinogens in Swiss mice. *Nutr. Cancer***17,** 77–83 (1992).

ix.   Leu, T.-H. & Maa, M.-C. The molecular mechanisms for the antitumorigenic effect of curcumin. *Curr. Med. Chem. - Anti-Cancer Agents***2,** 357–370 (2002).

x.   Al-Hujaily, E. M. *et al.* PAC, a novel curcumin analogue, has anti-breast cancer properties with higher efficiency on ER-negative cells. *Breast Cancer Res. Treat.***128,** 97–107 (2011).

xi.   Wilken, R., Veena, M. S., Wang, M. B. & Srivatsan, E. S. Curcumin: A review of anti-cancer properties and therapeutic activity in head and neck squamous cell carcinoma. *Mol. Cancer***10,** 12 (2011).

xii. John, V. D. & Ummathur, M. B. and antitumour studies of some curcuminoid analogues and their aluminum complexes. 37–41 (2013). doi:10.1080/00958972.2013.784281

xiii. Flora, S. J. S. & Pachauri, V. Chelation in metal intoxication. *Int. J. Environ. Res. Public Health***7,** 2745–2788 (2010).

xiv. Daniel, S., Limson, J. L., Dairam, A., Watkins, G. M. & Daya, S. Through metal binding, curcumin protects against lead- and cadmium-induced lipid peroxidation in rat brain homogenates and against lead-induced tissue damage in rat brain. *J. Inorg. Biochem.***98,** 266–275 (2004).

xv.   Ravindran, J., Subbaraju, G. V, Ramani, M. V, Sung, B. & Aggarwal, B. B. Bisdemethylcurcumin and structurally related hispolon analogues of curcumin exhibit enhanced prooxidant , anti-proliferative and anti-inflammatory activities in vitro. *Biochem. Pharmacol.***79,** 1658–1666 (2010).

xvi. Nichols, C. E., Youssef, D., Harris, R. G. & Jha, A. Microwave-assisted synthesis of curcumin analogs. **2006,** 64–72 (2006).

xvii. Pabon, H. J. J. A synthesis of curcumin and related compounds. *Recl. des Trav. Chim. des Pays***83,** 379–386 (1964).

xviii. Krishnankutty, K., Ummathur, M. B., Kamalakshy, D. & Philip, P. M. Ar ch ive. **2,** 111–119 (2009).

xix. John, V. D. & Krishnankutty, K. Antitumour Studies of Aluminium Complexes of Synthetic Curcuminoids.

xx.   Ruby, A. J., Kuttan, G., Dinesh Babu, K., Rajasekharan, K. N. & Kuttan, R. Anti-tumour and antioxidant activity of natural curcuminoids. *Cancer Lett.***94,** 79–83 (1995).

xxi. SAU-FUN TAN, KOK-PENG ANG AND GEE-FUNG HOW, Intermolecular and

intramolecular hydrogen bonding in 5-pyridylmethylenehydantoins: IR and NMR study. *J. Phys. Org. Chem.* **4,** 170–176 (1991).

Received on August 26, 2017.